THE EFFECTS OF MOLECULAR ORIENTATION ON THE PHYSICAL AGING BEHAVIOR OF ORIENTED GLASSY AMORPHOUS POLYMERS

by

MARCUS D. SHELBY

Dissertation submitted to the Faculty of the

Virginia Polytechnic Institute and State University

in partial fulfillment of the requirements for the degree of

DOCTOR OF PHILOSOPHY

in

Chemical Engineering

APPROVED:

G. L. Wilkes, Chairman

R. M. Davis

H. L. Marand

D. A. Dillard

T. C. Ward

December, 1996
Blacksburg, Virginia

Keywords: polycarbonate, polystyrene, dilatometry, positron annihilation, permeability

THE EFFECTS OF MOLECULAR ORIENTATION ON THE PHYSICAL AGING BEHAVIOR OF ORIENTED GLASSY AMORPHOUS POLYMERS

by

Marcus D. Shelby

Chairman: G. L. Wilkes
Department of Chemical Engineering

(ABSTRACT)

The objective of this study was to determine whether molecular orientation has an effect on the rate of physical aging in amorphous glassy polymers. There is already a large body of literature concerning the phenomenon of physical aging, although the vast majority has been directed toward isotropic, unoriented systems. The importance of this study is therefore twofold: first, from a theoretical standpoint, a better understanding of physical aging in oriented systems will help to elucidate the physics of glassy relaxation which is important since the exact mechanism behind physical aging are still unknown. Second, from an engineering standpoint, a knowledge of the orientation aging relationship will help the designer/engineer with product development since many commercially produced plastic items have some degree of orientation present as a result of the processing methods involved.

To measure the aging behavior, samples of bisphenol A polycarbonate and atactic polystyrene were hot drawn (i.e. stretched above T_g) to varying stretch ratios and the degree of orientation quantified using birefringence and the Herman's orientation function, f. Physical aging rates were determined as a function of f using volume and linear dilatometry, mechanical creep measurements, DSC, and tensile properties. The molecular state, including the free volume, of the oriented polymers was quantified using Positron

Annihilation Lifetime Spectroscopy (PALS), oxygen permeability/diffusion measurements, dynamic mechanical analysis, DSC, and density measurements. The data indicate that physical aging rates are influenced by orientation but the degree varies with the method of testing. Volume relaxation rates were approximately 50% higher for the oriented samples, however, mechanical shift rates determined from the creep data showed a slight decrease with orientation. Further analysis shows that the effective relaxation/retardation times decrease significantly with orientation even though the free volume--as determined by density and PALS measurements--also decreases. This implies a serious deficiency in the free volume theory for molecular mobility. Implications for these findings and possible explanations for this behavior are discussed.

ACKNOWLEDGMENTS

A large number of people have been involved with this work in one form or another, all of whom I would like to thank. First, I would like to express my greatest appreciation to Dr. Wilkes. If it were not for the excellent short course he taught at Eastman in 1991, I would probably never have made it back to graduate school. Working with Dr. Wilkes has been both a pleasureable and rewarding experience.

I would also like to thank my committee members: Professors Davis, Dillard, Marand and Ward, for their help and guidance along the way. In addition to providing insight into the physical aging problem at hand, their respective courses provided the necessary tools for performing many of the analyses described in this text.

Many people in the Chemical Engineering Department at VPI also played crucial roles in my graduate work. I would first like to thank all of the members of the department staff, but in particular, Sandy Simpkins, Diane Canaday, and Judy Coleman since they had to put up with me on almost a daily basis. I would also like to thank Billy Williams and Wendell Brown for their help with equipment construction. Members of Dr. Wilkes lab including Kurt, Watson, Rob, Chris, Jianye, Ta-Hua, Don, Hongyi, Bryan, Jim, Don, and Varun have all been tremendously helpful in showing me equipment procedures, providing suggestions, and for just keeping laboratory life bearable. I would also like to thank Andy Mellick and Frans Van Damme of the Chemistry Glass Shop for their help and suggestions with constructing the necessary glassware for the dilatometry.

Many people at Eastman Chemical have also played a role in helping me with my graduate studies. I would like to thank Delane Richardson and Phil Griswold for supporting my decision to go back to school, and for helping me to secure financial backing while on leave, Mike Knight for allowing me to use the labs during summers and semester breaks to perform some of my research, and Arved Harding for helpful discussions on statistical analysis.

All of the members of the past and present Packaging Research Lab also deserve a lot of credit for their help and camaraderie over the years. In particular I would like to thank Derek Farmer for his help with the die swell studies during the summer of 1993; Terrill McGee, Charlie Henry, David Jessee, Ron Shelton and Randy Millhorn for all of their help with processing and supplying materials; Ron Light for his help with data analysis, sample testing and interesting technical discussions; Johnny Shadden for being able to handle every possible administrative problem that came up with my educational leave; Jeff Zawada, Danny Glover, and Steve Weinhold for their help with the permeability studies and interpretation of the data, and Bill Lane for his all of his helpful suggestions over the years.

A number of people in the Polymer Evaluation Laboratory at Eastman also deserve a special thanks. First I would like to thank Brad Snow, John Griggs and Vicki Long for allowing me to process and test samples in the lab. Special thanks goes out to Donna Hardy for stretching film samples on numerous occasions on the T.M. Long; to Brenda McClellan and Connie Nichols for their help with tensile testing; to Shirlene Musick for help with permeability measurements, to Ellen Yeary for help with density measurements and to Edgar Gamble for his help with refractive index measurements.

Two fundamental parts of this project would not have been possible without outside help. First, I would like to thank Dr. Anita Hill of METSS (and CSIRO) and Dr. Marty Tant (Eastman) for performing and funding the positron annihilation testing of the samples and for helpful discussions concerning data interpretation. Also, thanks go out to Dr. T. J. Bastow (CSIRO) for running the SS-NMR experiments and to Dr Jerry Jean of the University of Missouri-KC for his help with running the 2-D ACAR measurements. I would also like to thank Dr. Greg McKenna at NIST for the numerous helpful suggestions he provided with regard to dilatometric testing. Without this help, the dilatometers probably would have never worked.

Finally, I would like to thank Patty Pierce, for her support, understanding, and patience, while writing this dissertation.

TABLE OF CONTENTS

LIST OF TABLES

LIST OF FIGURES

1.0 INTRODUCTION

Physical aging is a process in which many of the structural and physical properties of a glassy polymer change with time. It is also commonly referred to as free volume relaxation. The property changes occur because the glass is not in a true equilibrium state. Unlike the rubbery state, where molecular mobility is high and the polymer is essentially at equilibrium, the glassy state chains are much less mobile and require a longer time to reach equilibrium (in some cases, near infinite time is required). It is this long, gradual relaxation toward equilibrium which manifests itself as physical aging. The actual rate of this aging process depends on the proximity of the annealing temperature to the glass transition temperature (T_g) in addition to various structural factors. Glassy polymers are not the only substance known to show time dependent aging. In fact, other materials such as inorganic glasses, low molecular weight organic glasses, semicrystalline polymers (the amorphous phase only), and glassy metals may exhibit this behavior.[1,2]

Sample properties that show considerable change with aging time include—but are not limited to—mechanical properties such as creep compliance, yield stress, and impact strength; dielectric properties such as the magnitude and location or shape of loss peaks; volumetric or density changes; thermal changes such as apparent shifting of T_g and an increase in the enthalpy of relaxation; and barrier properties such as solubility and diffusion coefficients.[1,2] It is emphasized that chemical changes that may occur in the system such as crosslinking and chain scission do not constitute true physical aging. Instead, physical aging occurs because of the **reversible** approach of thermodynamic variables such as free volume, enthalpy, and entropy toward their equilibrium values. This changes result in a corresponding decrease in molecular mobility which is responsible for the property changes described above. Likewise, the rate of physical aging is also dependent on the molecular mobility. Consequently, as the mobility decreases with physical aging, the rate of aging also decreases resulting in a self-limiting process.

1.1 Research Objectives

The objective of this work is to determine whether or not molecular orientation has an effect on the physical aging behavior of glassy amorphous polymers. Physical aging has already been studied extensively as described in various review papers and books[1,2,3] but most of the focus has been on isotropic, unoriented systems. Only a few papers have dealt with oriented systems, but these systems are generally cold drawn (i.e. stretched below T_g). Studies on cold-drawn polycarbonate have already shown a significant increase in physical aging rate over isotropic samples although this effect may be due more to residual stresses than actual chain orientation.[4,5] The work presented here represents an extension of these aging studies to include amorphous, glassy polymers which are oriented in the melt and then quenched into the glassy state. Melt drawing minimizes the presence of residual stresses while controlling the level of molecular orientation. It is speculated that molecular orientation might alter in some way the shape, size, and/or distribution of free volume in the system since the polymer chains themselves become realigned. This change in free volume distribution, if it indeed occurs, might then modify the characteristic aging behavior of the material. The current study is aimed at determining whether or not this is true.

Studying the orientation-aging relationship not only has benefits for the theorist interested in a better understanding of condensed matter physics, but also for the engineer/designer. A more thorough understanding of the orientation-aging relationship should help the designer since the majority of end-use plastic products have some orientation due to the fabrication process. Physical aging is already a serious problem when designing with glassy polymers. An initially ductile glassy polymer, can become brittle in a matter of days or months, making it unusable for a given design. In addition, oriented amorphous regions are highly prone to stress cracking making the design process even more difficult. If it is found that orientation increases the rate of physical aging, one might wonder whether this (hypothetical) enhanced aging plays a role in the stress cracking mechanism.

1.2 Overview of the Dissertation

The present study is divided into four main sections. First a general literature review is provided covering pertinent topics in physical aging, orientation, and various aging related measurement techniques. This is followed by the experimental section consisting of three "stand-alone" chapters covering various aspects of the testing and analysis. Some overlap occurs between chapters and, additionally, some of the data in the literature review is repeated in the individual chapters (where necessary) for clarity.

The first of these experimental chapters (Chapter 3.0) involves a combined dilatometric and mechanical creep study of both oriented atactic polystyrene and bisphenol-A polycarbonate. Here samples of each polymer were hot-stretched to various draw ratios and aging rates determined as a function of orientation. For all parts of this study, the orientation is characterized by the Hermans' orientation function, f. In Chapter 4.0, a detailed thermodynamic analysis of the oriented (unaged) state of bisphenol-A polycarbonate is performed in order to understand how orientation affects molecular changes such as free volume, interatomic spacing, mobility, etc. Results are compared and contrasted with various theories of the glass transition temperature along with predictions of thermodynamic rubber elasticity. From this, some predictions could be made regarding the changes taking place in the stucture and mobility during orientation. Chapter 5.0 is the result of a collaboration with Dr. Anita Hill of CSIRO (Australia). In this chapter, Positron Annihilation Lifetime Spectroscopy (PALS) measurements were performed as a function of f on the unaged polycarbonate samples. PALS is one of the few techniques available which can measure the free volume directly although there is still some controversy as to the validity of the data interpretation. Because of this controversy, oxygen permeability/diffusivity measurements were also employed since they too are sensitive to mobility and free volume. Interesting correlations were found between the aging behavior, the PALS results, and the diffusivity. It is noted that PALS was also performed on the oriented samples as a function of aging time although the results were suspect and will not be reported here. Finally, following Chapter 5.0, a summary is

provided which brings all of the findings together in an effort to understand the underlying physics. Recommendations are made from a design standpoint as to how to account for orientation in product lifetime determination. Suggestions for future work are also provided.

1.3. References

1 M. R. Tant and G. L. Wilkes, *Polym. Engr. Sci. 21*, 874-894 (1981).

2 L. C. E. Struik, *Physical Aging in Amorphous Polymers and Other Materials*, Elsevier, New York, 1978.

3 I. M. Hodge, *Journal of Non-Crystalline Solids 169*, 211-266 (1994).

4 R. Pixa, B. Grisoni, T. Gay, and D. Froelich, *Polymer Bulletin 16*, 381-387 (1986).

5 J. Bartos, J. Muller, and J. H. Wendorff, *Polymer 31*, 1678 (1990).

2.0 LITERATURE REVIEW

Physical aging is a phenomenon which is directly related to the glass transition. This complicates its understanding since the glass transition is still incompletely understood. This can be seen in the diversity of theories developed to describe it, none of which are completely adequate. It appears that physical aging and the glass transition are so closely coupled that once a foolproof theory is developed for the glass transition, a successful theory for physical aging will likely follow. Because of this interrelation, various aspects of the vitrification process will be discussed first. Much of this part of the review is drawn from the excellent works on glassy behavior by McKenna[1] and general non-equilibrium behavior by Tant and Wilkes.[2,3] This will be followed by a detailed summary of the general physical aging literature, a review of the concepts behind polymer orientation, and finally, a discussion of previous aging studies on cold drawn polymers.

2.1 The Glass Transition

The glass transition is generally defined as the temperature where the volume-temperature curve changes slope (i.e. the thermal expansion coefficient undergoes a step change).[4,5,6] The exact temperature depends on the rate of cooling as faster cooling will yield a higher T_g. When specifying the glass transition temperature for a given polymer, it is essential that the test method and procedure also be specified since the T_g can vary considerably for different test methods. Other methods commonly used to measure T_g include dynamic mechanical,[4] dielectric,[4,7] and calorimetric techniques.[8,9] In every case, there is a rate effect involved which will alter the location of T_g.

Theories of the glass transition fall into two main categories: free volume (and associated kinetic theories), and thermodynamic. A major question that exists is whether or not the glass transition is a manifestation of an equilibrium thermodynamic transition or wholly a kinetic phenomenon.[1] There is no doubt that there is a time dependent effect involved. This is clearly evident from the high sensitivity of the measured T_g to the time

frame of measurement. Supporters of the thermodynamic theories contend that there is a true equilibrium glass transition but it is not directly measureable because of the kinetic limitations imposed by the glassy state. The free volume theories avoid this argument all together and concentrate on the mobility and rheological aspects of the polymer in order to predict quasi-static thermodynamic properties.[1]

Ehrenfest[10] has defined a first-order transition as one in which the free energy (G) is a continuous function of any state variables--pressure (P), temperature (T), or volume (V)--but is discontinuous in the first partial derivative of G with respect to any of these state variables. Likewise, a second-order transition is one in which the first partials are continuous but now the second partial derivatives with respect to any of the state variables are discontinuous. These derivative relationships are [11]

$$\left[\frac{\partial G}{\partial T}\right]_P = -S$$
$$\left[\frac{\partial G}{\partial P}\right]_T = V \qquad (2.1\text{-}1)$$
$$\left[\frac{\partial (G/T)}{\partial (1/T)}\right]_P = H$$

and for the second partials,

$$\left[\frac{\partial^2 G}{\partial T^2}\right]_P = -\left[\frac{\partial S}{\partial T}\right]_P = -\frac{C_P}{T}$$
$$\left[\frac{\partial^2 G}{\partial P^2}\right]_T = \left[\frac{\partial V}{\partial P}\right]_T = -\kappa V$$
$$\left[\frac{\partial}{\partial T}\left[\frac{\partial (G/T)}{\partial (1/T)}\right]_P\right]_P = \left[\frac{\partial H}{\partial T}\right]_P = C_P \qquad (2.1\text{-}2)$$
$$\left[\frac{\partial}{\partial T}\left[\frac{\partial G}{\partial P}\right]_T\right]_P = \left[\frac{\partial V}{\partial T}\right]_P = \alpha V$$

where S is the entropy, H is the enthalpy, C_p is the heat capacity at contstant pressure, κ is the compressibility, and α is the isobaric thermal expansion coefficient. Vaporization and fusion are examples of first-order transitions. Well known examples of second-order transitions include the Curie temperature and the onset of superconductivity.[7,12,13] Sample plots are shown in Figure 2.1-1. Note that C_p, α, and κ are discontinuous in both the first and second-order transition although the nature of the discontinuity is different. If the same data is plotted for a glass in the vicinity of T_g, (see Figure 2.1-1), it is clear that the glass transition behaves similarly to a second-order transition since V, H, and S (i.e. the first partials with respect to G) are continuous functions of temperature across the transition.

One important consequence of any thermodynamic development of the glass transition is the resolution of Kauzmann's paradox.[1,4,14] Kauzmann found that when the equilibrium entropy of some supercooled glass-forming liquids (i.e. typically only so called "fragile" glasses) are extrapolated to low temperatures, the resulting entropy may become less than the entropy of the crystalline solid (see Figure 2.1-2). This is physically meaningless. The only way to resolve this paradox is for an additional transition to occur which would slow the rapidly decreasing entropy function. Kauzmann believed that there was no thermodynamic glass transition and opted for a kinetic description instead. He envisioned the formation of small "crystallites" forming in the glassy phase at low enough temperature, now known to be incorrect. The thermodynamic theory of Gibbs and DiMarzio[15,16,17] was shown to resolve the Kauzmann's paradox by way of a second-order transition (compare the change in slope at the glass transition for the entropy plots in Figure 2.1-2). At this transition to the glass, the configurational entropy reaches and maintains a value of zero. This theory will now be described in more detail.

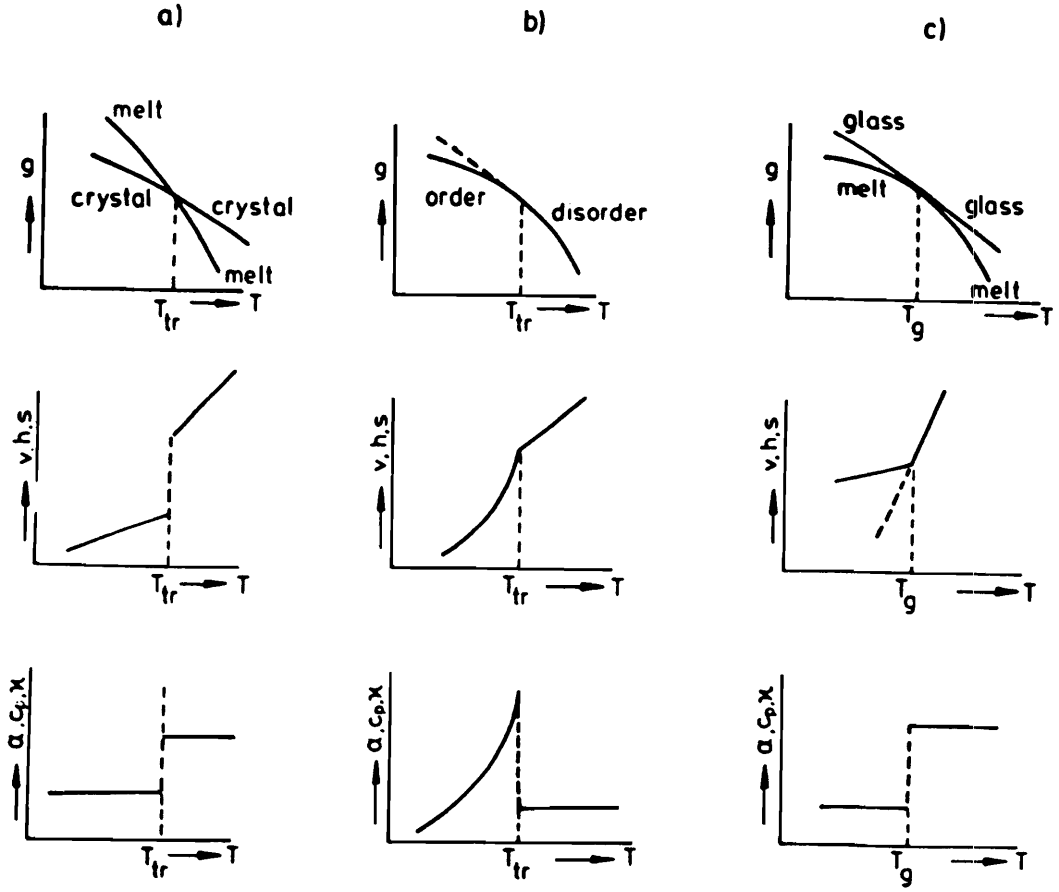

Figure 2.1-1. Thermodynamic parameters for a (a) first order transition, (b) second order transition and (c) the glass transition (after G. Rehage and W. Borchard in "The Physics of Glassy Polymers," R. N. Hayward, Ed., New York, 74, 1973).

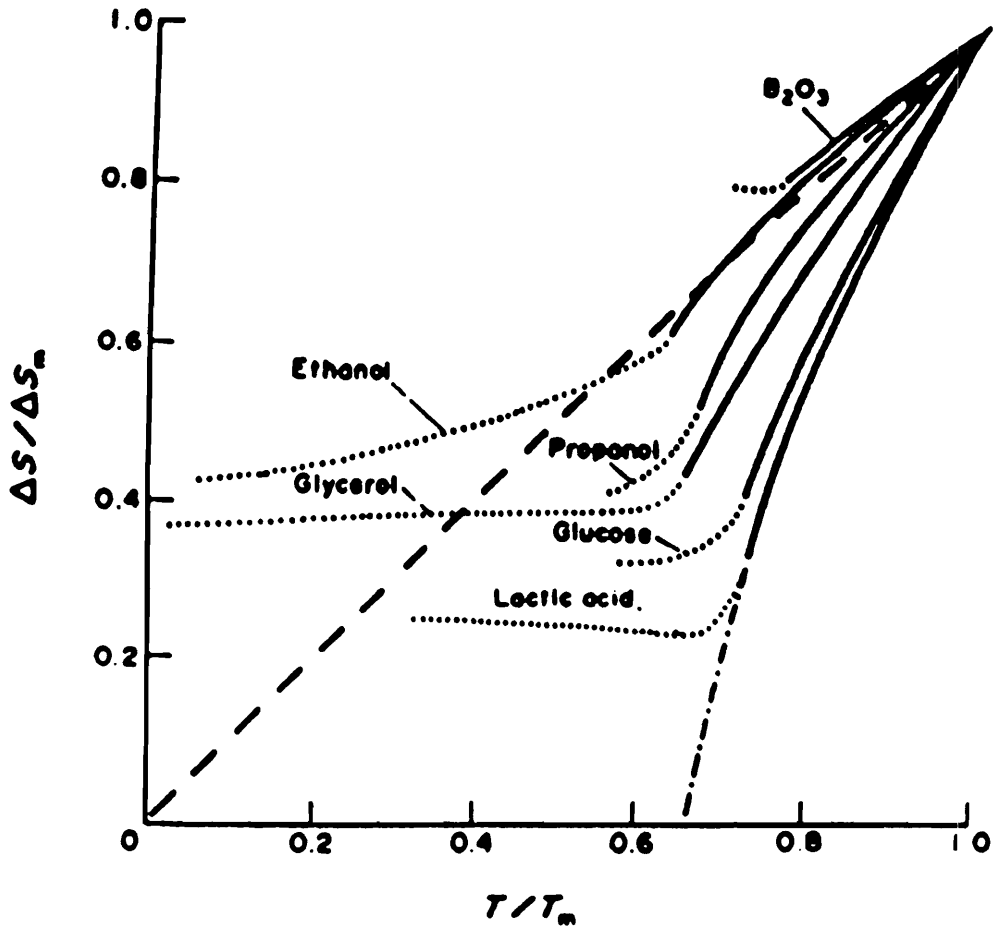

Figure 2.1-2. Schematic representation of Kauzman's paradox for various glass forming substances. $\Delta S/\Delta S_m$ is the difference in entropy between the supercooled liquid and crystalline phases normalized with respect to the entropy of fusion (from W. Kauzmann, *Chem. Rev. 43*, 219 (1948)).

2.1.1 Thermodynamic Theories

The theory of Gibbs and DiMarzio[15,16,17] is based on a Flory-Huggins[18,19] lattice model of the polymer chain. Within the lattice are allowed the introduction of a number, n_o, of "holes" representing the vacancies or free volume in the polymer. The energy associated with this hole formation is proportional to the number of van der Waals bonds broken by the introduction of the hole. In addition, each polymer segment is allowed to be in one of two conformations separated by an energy $\Delta\varepsilon$. The fraction of bonds which are in the higher energy state is denoted by f_b.

From the associated partition function, an equilibrium, second-order transition temperature is predicted which has been associated with an equilibrium glass transition. The temperature of this transition is defined as T_2 in order to distinguish it from the experimentally measured T_g. This temperature corresponds to the point at which the configurational entropy--a combination of entropy terms from the permutations of holes and chain conformational states--becomes zero. The plateauing of the entropy brought about by the transition resolves the Kauzmann's paradox. Nowhere in the analysis is any mention made of kinetic effects; rather it is purely an equilibrium calculation. The transition T_2 is therefore the same as T_g for infinitely slow cooling times. For finite cooling times, the measured T_g is significantly higher, typically about 50°C higher for standard experimental methods. The experimentally measured T_g therefore represents a kinetically driven transition into the glassy state. It is not the true second-order transition, just a non-equilibrium reflection of one.

The Gibbs-DiMarzio model has been used successfully to predict the influence of molecular weight,[20,21,22] crosslinking,[23,24] and composition[25,26,27] on T_g. In addition, it accurately predicts the change in heat capacity at the glass transition.[28] Of particular interest is the application of Gibbs-DiMarzio theory to the effect of deformation on T_g. Qualitatively, the model predicts an increase in the glass transition temperature with increasing elongation. This results from the decreased entropy due to the orientation of the polymer chains. Quantitatively, the model predicts for uniaxial extension,[29]

$$\frac{T_g(\lambda)}{T_g(1)} = \exp\left[\frac{G}{2\Delta C_p T_o}(I_1 - 3)\right] \qquad (2.1\text{-}3)$$

where λ is the stretch ratio, G is the shear modulus measured at temperature T_0, and I_1 is the first strain invariant ($I_1=\lambda_1^2+\lambda_2^2+\lambda_3^2$ in general and $I_1=\lambda^2+2\lambda$ for uniaxial extension). Data from Gee *et al.*[30] shows general agreement with this finding. There have been other studies which are in agreement with these findings as well as those which are in disagreement.[31,32,33] Data for a few different rubber systems are shown in Figure 2.1-3 along with the Gibbs-DiMarzio predictions. Adams and Gibbs[34] and Matsuoka[35] have extended these theories to include the concept of cooperative motions. In each case, segments are no longer allowed to move independently of one another at lower temperatures. This "cooperative motion" becomes more extensive as the temperature drops and results in a decreasing configurational entropy of the system. In keeping with the Gibbs-DiMarzio theory, this entropy goes to zero at T_2. Likewise, at very high temperatures there is no cooperativity as each segment is able to move independently of the others. Matsuoka[35] assumes that the onset temperature for segmental independence occurs around 500°C for most polymers. The assumption of cooperativity leads to the following form for the relaxation time equation,

$$\tau = \tau_o \exp\left(\frac{B}{T - T_2}\right) \qquad (2.1\text{-}4)$$

where B is a constant and τ_o is the relaxation time at high temperatures where no cooperativity is occuring. This equation will be found to be remarkably similar to many of the free volume theory results and is also referred to as the Vogel-Fulcher-Tammann-Hesse (VFTH) equation.[36,37,38]

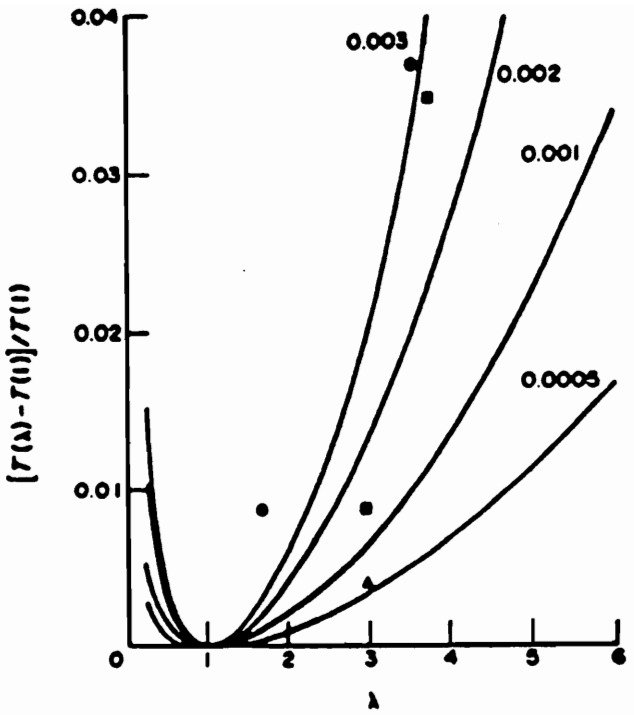

Figure 2.1-3. Predictions based on Gibbs-DiMarzio for the relative change in Tg versus stretch ratio for various values of $Y=G/2\Delta C_pT(1)$. Experimental data from Gee and coworkers [30]. Circles are for natural rubber, squares are for GRS rubber, and the triangle is for Hycar (after E. A. DiMarzio, *J. Res. Natl. Bur. Stand. 68A*, 611 (1964).)

2.1.2 Free Volume Theories

From a conceptual standpoint, the free volume is the extra volume above and beyond that actually occupied by the molecules. This extra volume provides space for the molecules to move within thereby enhancing mobility and diffusion. In a simpler sense, it can be thought of as the voids and holes brought about by incomplete packing of the polymer chains. There are a number of different "quantitative" definitions for the free volume which often leads to some confusion. To further complicate matters, the term "free volume" is often used in the literature without proper definition.[39] The difference in the various free volume definitions is in how the extra void space is measured. Following the descriptions given by Haward[39] and Bondi,[40] the first of these free volume definitions is that of the "empty volume" denoted as v_e, where

$$v_e = v - v_w \qquad (2.1\text{-}5)$$

Here v is the actual volume at some temperature T and v_w is the van der Waals volume as obtained from X-ray diffraction methods or kinetic collision cross-sections. Another less common free volume definition is the "fluctuation volume" which is defined as

$$v_{fl} = N_a V_q \qquad (2.1\text{-}6)$$

where N_a is Avogodro's number and V_q is the volume swept out by the center of gravity of one molecule during thermal vibrations. The last and most commonly used definition is that of the "expansion volume." It is defined as

$$v_f = v - v_o \qquad (2.1\text{-}7)$$

where v_O is the volume occupied by the molecules at 0 K in a close-packed crystalline state (i.e. the occupied volume which includes some interstitial sites). Note that the expansion volume is always less than the empty volume since v_w is smaller than v_o. In some instances, the occupied volume is taken at the close-packed volume at the temperature of the sample. An example of this is shown in Figure 2.1-4 where the occupied volume is found to increase with temperature. This produces a measure of free

volume which is in between that of the "expansion volume" and the "empty volume." It is currently uncertain which of the free volume measures is best for relating mobility and physical aging. This is partially the reason why so many different definitions are applied. Unless otherwise noted, "free volume" will imply the "expansion volume" (although in most of the relations to be described, the various free volume measures can be used interchangeably).

The free volume can be put in terms of the fractional free volume $ffv = v_f/v$, by,

$$ffv = ffv_g + \alpha_f (T - T_g) \qquad (2.1\text{-}8)$$

where ffv_g is the free volume fraction at T_g and α_f is the thermal expansion coefficient for the free volume. The value of α_f is often approximated by

$$\alpha_f = \alpha_l - \alpha_g \qquad (2.1\text{-}9)$$

where the subscripts *l* and *g* refer to the liquid and glassy states respectively. Generally, the free volume is assumed to be approximately constant below T_g. This is not completely true since physical aging leads to a gradual free volume relaxation below T_g, although the magnitude is small compared with the free volume changes in the rubbery state. Additionally, the thermal expansion coefficient changes slightly with temperature in the glassy state—particularly at secondary transitions—and this is likely to have a perturbing effect on the free volume.

Free volume concepts first came into being in the description of viscosity relations for simple liquids by way of the Doolittle equation,

$$\eta = A \exp\left(\frac{b}{f}\right) \qquad (2.1\text{-}10)$$

where η is the viscosity and A and b are constants. If we define a shift factor a_T, as the ratio of the viscosity (or relaxation time τ) at T to the viscosity at some reference temperature T_S,

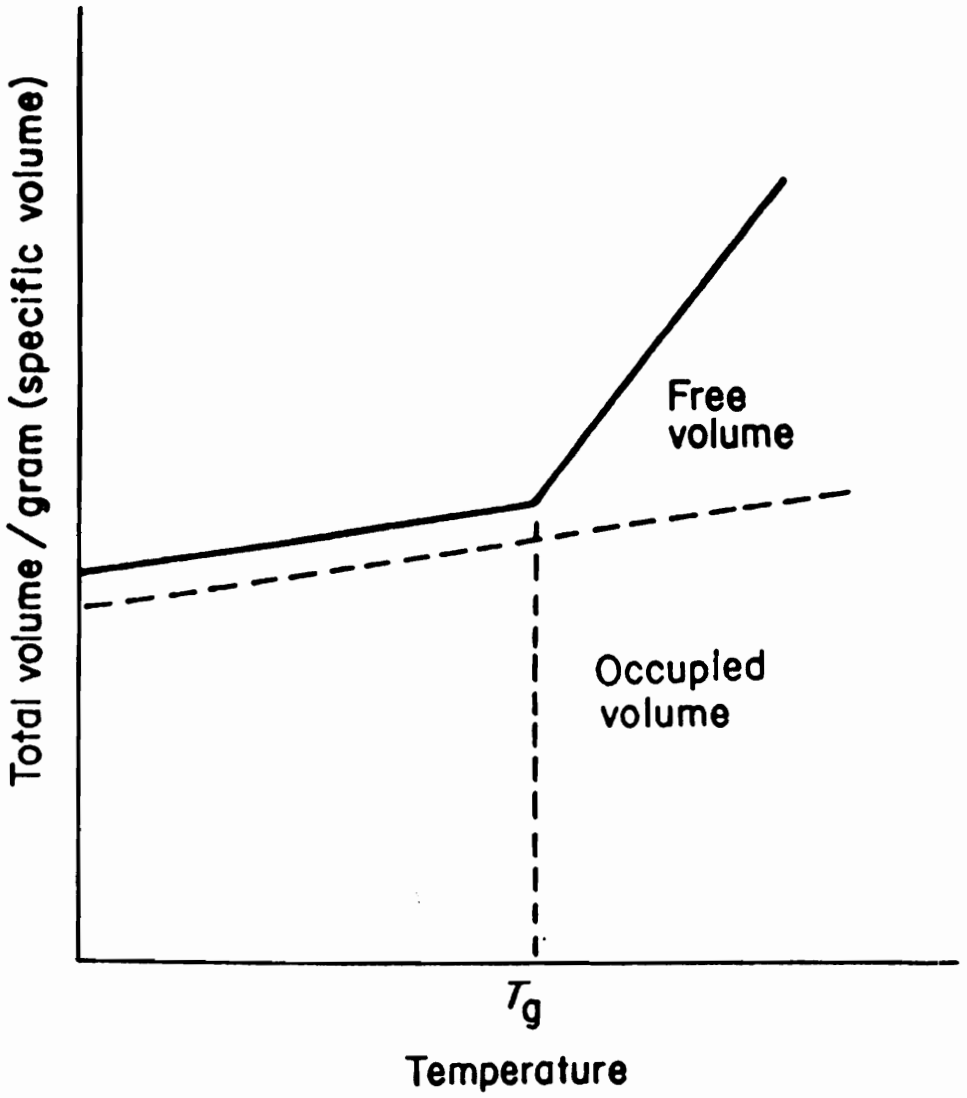

Figure 2.1-4. Typical free volume versus temperature behavior (after I. M. Ward, "Mechanical Properties of Solid Polymers," Wiley, New York, 150, 1983).

$$a_T = \frac{\eta(T)}{\eta(T_s)} = \frac{\tau(T)}{\tau(T_s)} \qquad \text{(2.1- 11)}$$

then we can combine this with (2.1-10) to produce

$$\ln(a_T) = b\left(\frac{1}{f} - \frac{1}{f_g}\right) \qquad \text{(2.1- 12)}$$

where the reference temperature is chosen as T_g. If we substitute (2.1-8) into (2.1-12), we obtain

$$\log(a_T) = -\frac{(b / 2.303 f_g)(T - T_g)}{f_g / \alpha_f + (T - T_g)} \qquad \text{(2.1- 13)}$$

or by defining constants C_1 and C_2 such that

$$\begin{aligned} C_1 &= -b / 2.303 f_g \\ C_2 &= f_g / \alpha_f \end{aligned} \qquad \text{(2.1- 14)}$$

leading to

$$\log(a_T) = \frac{C_1(T - T_g)}{C_2 + (T - T_g)} \qquad \text{(2.1- 15)}$$

which is commonly known as the WLF (Williams-Landel-Ferry) equation. Constants C_1 and C_2 are often treated as nearly universal having values of -17.44 and 51.6 respectively. These universal values accurately predict the shifting behavior for a number of polymers in the rubbery region up to about T_g+ 100°C. For a temperature $T=T_g$-51.6, the denominator goes to zero and the viscosity becomes infinite. Note that this occurs at approximately the same temperature as T_2 from the Gibbs-DiMarzio theory.

Cohen and Turnbull[41,42] modified this approach slightly such that T_β, the secondary relaxation temperature is the reference point. The free volume v_f, is redefined as that portion of the free volume which can be redistributed without a change in energy. This, in

effect, defines a critical free volume hole size such that, for holes below this size, the mobility is unaffected. These assumptions lead to

$$\eta = A \exp\left(\frac{B'}{(T - T_\beta)}\right)$$
$$\tau = \tau_o \exp\left(\frac{B'}{(T - T_\beta)}\right) \qquad (2.1\text{-}16)$$

where A and B' are constants. By letting $T_\beta = T_g$-51.6 °C, the WLF equation is regained (note, however, that T_β is not necessarily 51.6°C below T_g for most polymers). This is also identical to the Adams-Gibbs result (2.1-4) if T_2 is taken as T_β.

Another model which has received some attention is the hole model of Simha and Somcynsky.[43,44] While this model has been highly successful in describing the PVT behavior of polymer melts and glasses, it will only briefly be discussed here since it is a more complex model and provides little additional conceptual information on free volume. This model is based on a cell model for the polymer liquid where the repeat units are confined to each cell. Empty cells are allowed in order to simulate holes. In addition, a Lennard-Jones cell potential is applied to account for segmental interactions. The resulting canonical partition function is then determined from which the Helmholtz free energy can be directly calculated. Free volumes are determined quantitatively with the model and excellent agreement is found with experimental data. Also, no assumptions are made about the constancy of the free volume below T_g unlike the other free volume models. The biggest drawback with the model is the fact that the glass transition cannot be predicted *a priori* but instead, must come from a kinetic interpretation of the results.[1]

As with the thermodynamic models, the free volume theories are also able to successfully predict features such as the influence of molecular weight,[45,46] crosslinking,[47,48] and composition[47,49] on T_g. Where the free volume theory differs dramatically with the Gibbs-DiMarzio theory is in the treatment of deformation. The free volume theory predicts that mobility will increase with increasing free volume, other factors being equal. During most modes of deformation, dilatation will occur causing an

increase in the sample volume and therefore an increase in free volume. The exceptions to this are pure shear where the volume change is zero, and compression where a decrease in volume will occur. Consequently, the free volume theory predicts a lowering of T_g with orientation. This is not generally found to be the case; although, as mentioned earlier, there are data supporting both theories.[1]

Although the free volume theories are generally the more universally applied theories—particularly when explaining physical aging—there are a number of strong arguments against them. Williams,[50] for example, has shown for PMMA that the temperature dependence of the dielectric β-relaxation is similar under both constant pressure and constant volume conditions. The same also holds true for polypropylene oxide. Free volume is expected to increase with temperature under isobaric heating but remain constant under isochoric heating. Therefore, if mobility is indeed connected to the amount of free volume, then isochoric heating should produce little or no change in mobility, and consequently, no temperature shifting of the β-transition. In contrast, the isobarically heated samples, which should show an increase in mobility with temperature, are expected to exhibit a significant temperature dependent shift in the β-relaxation (which is observed experimentally). It was concluded that the dielectric relaxation time was not a unique function of volume and the relations described earlier such as (2.1-15) should be based on more fundamental quantities than the free volume.[5] Struik also provides an assessment of the free volume concept, particularly where it relates to physical aging.[51] He arrives at similar conclusions stating that the inadequacies of the free volume models come about due to the oversimplifying assumptions made in their application and derivation. In particular, the use of only the average free volume with no accounting for the hole distribution provides a poor relation to the system mobility.

2.2 Physical Aging

This section will focus on the various aspects of physical aging including a discussion of some of the more common methods of measuring aging such as dilatometry, mechanical property measurements, and calorimetry. Other more indirect methods will be discussed where applicable. A review of positron annihilation is also included because of its application to this study.

2.2.1 General Aspects of Physical Aging

Physical aging is the physical manifestation of a non-equilibrium glass transition. As the sample gradually moves toward its equilibrium glassy state, properties change with time reflecting the effects of decreased free volume and reduced molecular mobility. It is these time dependent changes which constitute "physical aging." For a better understanding of the physical aging process, the reader is referred to Figure 2.2-1. Here, both free volume and the relaxation time τ, are plotted versus temperature for a sample quenched from a temperature above T_g (denoted as T_o) to an annealing/aging temperature T_a which is below T_g.[52] Above T_g, the relaxation time and free volume follow the predictions of the WLF equation (and related equations) described earlier. However, as the sample is quenched through T_g a noticeable change occurs. In the glassy state, the free volume is frozen in at a nearly constant value. Consequently, the amount of free volume changes only slightly with temperature. If the sample is annealed (in the glass) at a temperature T_a, a further decrease in free volume will occur over time. This gradual decrease is essentially the physical aging process. Aging is relatively slow because of the low mobility of the glassy phase. Therefore, the change in free volume brought about by physical aging is small in comparison with the change in free volume from, for example, a 10°C temperature change in the rubbery state. Although the free volume change during aging is small, it can still have a significant effect on the molecular mobility. This is represented by the increase in relaxation times portrayed in Figure 2.2-1. These relaxation

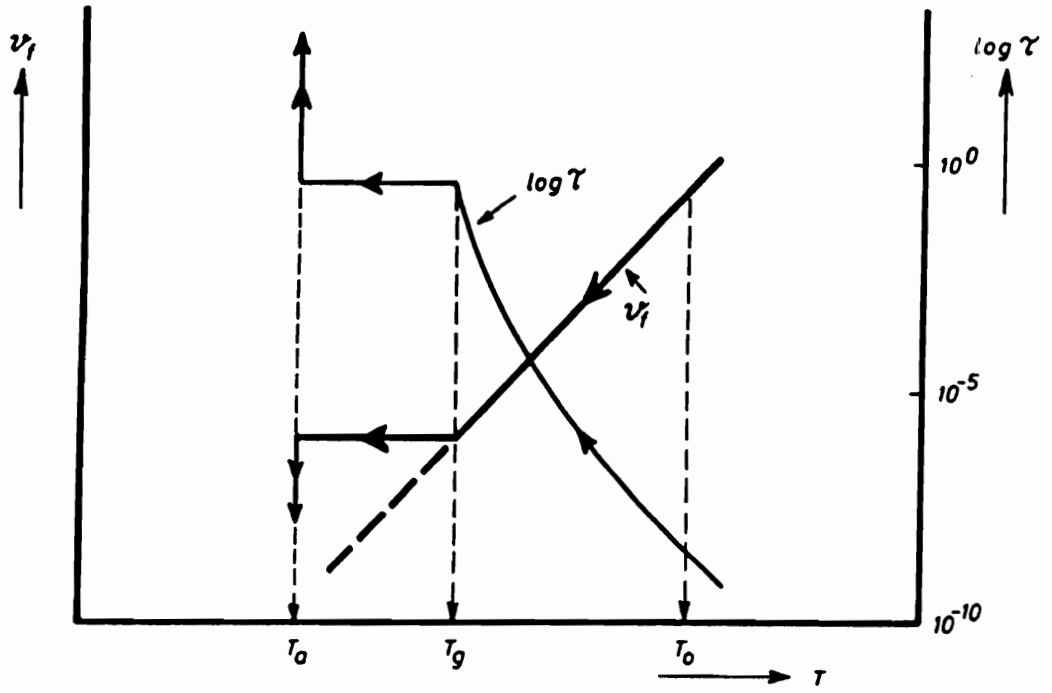

Figure 2.2-1. Free volume and relaxation time dependence for cooling through Tg (from J. G. Rider and E. Hargreaves, *J. Phys. D: Appl. Phys. 3*, 993 (1970)).

time shifts (i.e. decreases in mobility) can lead to the often dramatic changes in various physical properties seen with physical aging such as the ductile-brittle transition.

The rate at which free volume relaxation occurs is very much dependent on the temperature of aging, particularly its proximity to T_g. Generally higher temperatures will result in faster aging than lower temperatures but there are exceptions. For temperatures very close to T_g (within 5 to 10°C), there is actually a decrease in effective aging since the sample is already very close to equilibrium.[51] For very low temperatures—in particular below the secondary transition T_β—the aging rate begins to decrease as well. Segmental mobility decreases considerably below T_β due to a lack of sufficient free volume. Even though secondary transitions may still persist below T_β, they do not cause significant polymer aging since they apparently do not cause a change in free volume and/or relaxation behavior.[2,53]

Another factor alluded to in Figure 2.2-1 is the relation between free volume and molecular mobility (or relaxation time) in the glassy state. Molecular mobility is nothing more than the inverse of the relaxation time τ. The most general relation between the free volume fraction *ffv*, and mobility *M*, as described by Struik,[53] is

$$\ln M = A - \frac{B(T)}{ffv^{\gamma}} + \varphi(T) \qquad (2.2\text{-}1)$$

where *A* is a constant, *B* and ϕ are temperature dependent functions, and γ is a positive exponent. This equation can be reduced into a number of more common forms with the proper choice of constants. For instance, if *B*(T) and ϕ(T) are taken as constants, and γ = 1, one obtains the Turnbull-Cohen-Doolittle-WLF models. If instead, ϕ(T) is taken as -*H/RT* where *H* is an activation energy, one obtains the Litovitz-Macedo model.[54] Finally, if ϕ(T) and *B*(T) are both taken as constants but γ is equal to 2, one obtains the Bueche model.[55,56]

Another concept important to the understanding of physical aging is that of the self-limiting process. As described earlier, mobility decreases with decreasing free volume. Struik has suggested an inverse relationship between the mobility and aging time t_e,[53]

$$M \sim \frac{K}{t_e} \qquad (2.2\text{-}2)$$

where K is a proportionality constant. Note that this equation is not valid near equilibrium. With this in mind, the rate at which the free volume relaxes depends on the instantaneous mobility of the system. Accordingly, as free volume relaxation proceeds, the rate at which it changes continues to diminish. This is what is meant by a self-limiting process. Consequently, it will take near infinite times in most cases for the system to ever reach equilibrium. However, a recent study by Wimberger-Friedl and de Bruin[57] indicates that self-limitation may be finite. Volumetric measurements of bisphenol-A polycarbonate showed that relaxation rates actually began to increase again after 10^7 seconds at room temperature--possibly the result of passing through the α-relaxation. This finding has extremely important consequences for the understanding of the physical aging mechanism and will require further investigation.

Unlike chemical aging, physical aging is a reversible process. All that is needed to erase the current level of aging in a system is to heat it above its glass transition. The high mobility in the rubbery state disrupts the previous free volume relaxation producing an "unaged" sample. Another way to effectively remove any prior aging history is to mechanically deform the sample with a sufficiently large strain.[53,58,59] It is believed that the resulting dilatation is, in a sense, related to an increase in free volume and therefore an increase in mobility (see the free volume and Gibbs-DiMarzio theories discussed previously). However, these results do not always follow intuition. For example, it has been observed that uniaxial compression, shear deformation and tensile deformation all wholly or partially erase the previous physical aging. This is understandable for tensile deformation where dilatation naturally occurs. However, shear deformation is a constant-volume process so no increase in free volume is expected. Likewise, hydrostatic

compression would be expected to reduce the free volume resulting in less mobility. Struik has suggested that the mechanical deformations in conjunction with segmental motion are what generate the free volume.[53] This is irrespective of the type of stress field. Matsuoka and Bair performed experiments with polycarbonate and saw an increase in enthalpy with shearing deformation.[59] They attributed this to the formation of free volume. Matsuoka and coworkers proposed a model relating the free volume fraction to the tensile strain ε, and the Poisson's ratio μ,[58]

$$ffv = ffv_o + \varepsilon(1 - 2\mu) \qquad (2.2\text{-}3)$$

and found that the magnitude of shift with strain using this equation and the WLF equation, agreed with experimental data. Because a further discussion of this rejuvenation process requires an understanding of the methods of creep testing and data shifting, it will be postponed until the section on mechanical testing.

2.2.2 Dilatometric Studies

Dilatometric studies provide the most direct method for studying the changes in free volume. Generally the procedure involves either linear or volumetric dilatometry depending on the type of sample and required temperature range. Both are similar in accuracy although they differ in ease of use and applicability. There are a number of papers available which describe the detailed methodology involved.[53, 60, 61, 62] Volumetric studies usually fall into one of four categories: pressure-volume-temperature (PVT) plots where the specific volume is monitored as a function of temperature and/or pressure, isothermal free volume relaxation experiments, "T-jump" experiments where different combinations of annealing time and temperature are incorporated, and finally, studies involving combined dilatometry and mechanical deformation. A discussion of the deformational-dilatometry will be included in the section on mechanical testing.

2.2.2.1 Pressure-Volume-Temperature Studies

PVT measurements have generally been most useful in the study of the glass transition, particularly when studying the effects of cooling rate and pressure on T_g.[63,64,65,66,67] These measurements, while only indirectly related to physical aging, still provide some relevant information. For example, Figure 2.2-2 shows the effect of cooling rate on the measured glass transition in addition to showing the presence of an equilibrium volume line in glasses.[68] Dilatometric PVT measurements have also been used by Greiner and Scharzl to detect secondary transitions in a number of glassy polymers.[69] Figure 2.2-3 shows a typical plot of specific volume as a function of temperature for polycarbonate. From this data, thermal expansion coefficents can be determined which can then be related to the free volume expansion coefficent.

2.2.2.2 Isothermal Volumetric Studies

Isothermal studies of free volume relaxation are probably the most common and easiest methods for studying physical aging. Here, the sample is usually quenched from above T_g to different temperatures in the glassy regime, and the volume relaxation monitored as a function of aging time. Figure 2.2-4 shows volume relaxation data for polystyrene (Tg = 100°C) at various aging temperatures. Note the logarithmic time scale and the fact that the data is referenced to v_∞, the equilibrium volume at the given aging temperature. The equilibrium volume can be measured experimentally only for small values of $T-T_g$ (~30°C or less). For larger values, the time to reach equilibrium becomes prohibitively large. Another much easier approach is to extrapolate the specific volume curve from the rubbery phase into the glass. In this case, the extrapolated rubbery volume is the equilibrium volume v_∞. Often the data is referenced to the initial volume at the start of annealing instead. Regardless, the data is very close to linear on this semi-log plot. For this reason, a volume relaxation rate β, is defined as[52]

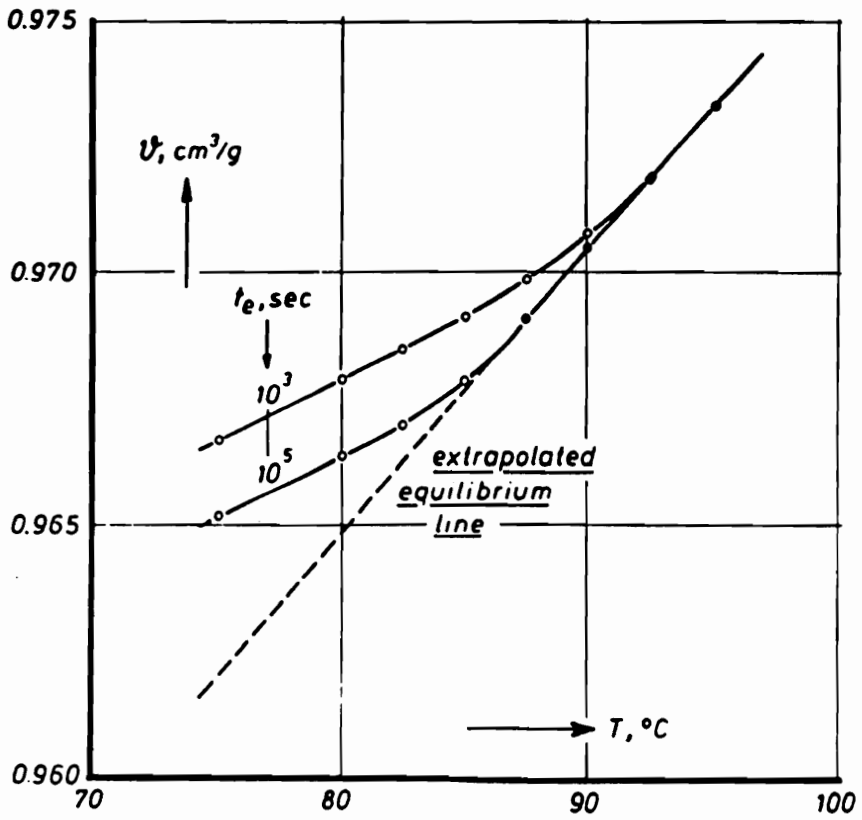

Figure 2.2-2. Specific volume versus temperature for different elapsed annealing times (from [52]).

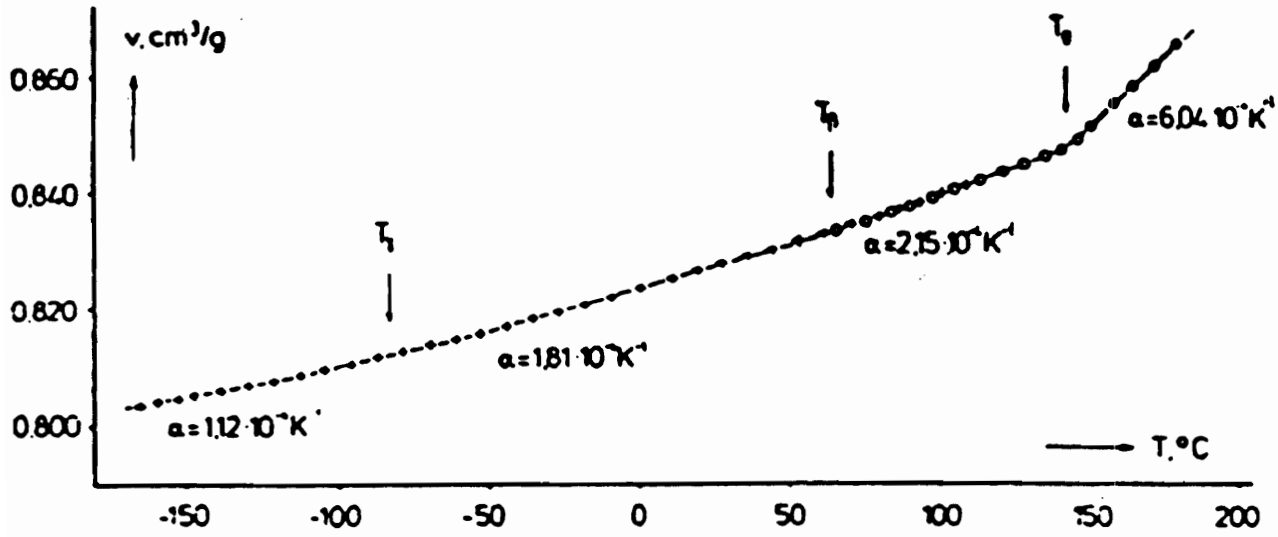

Figure 2.2-3. Volume-temperature curve for polycarbonate (from [69]).

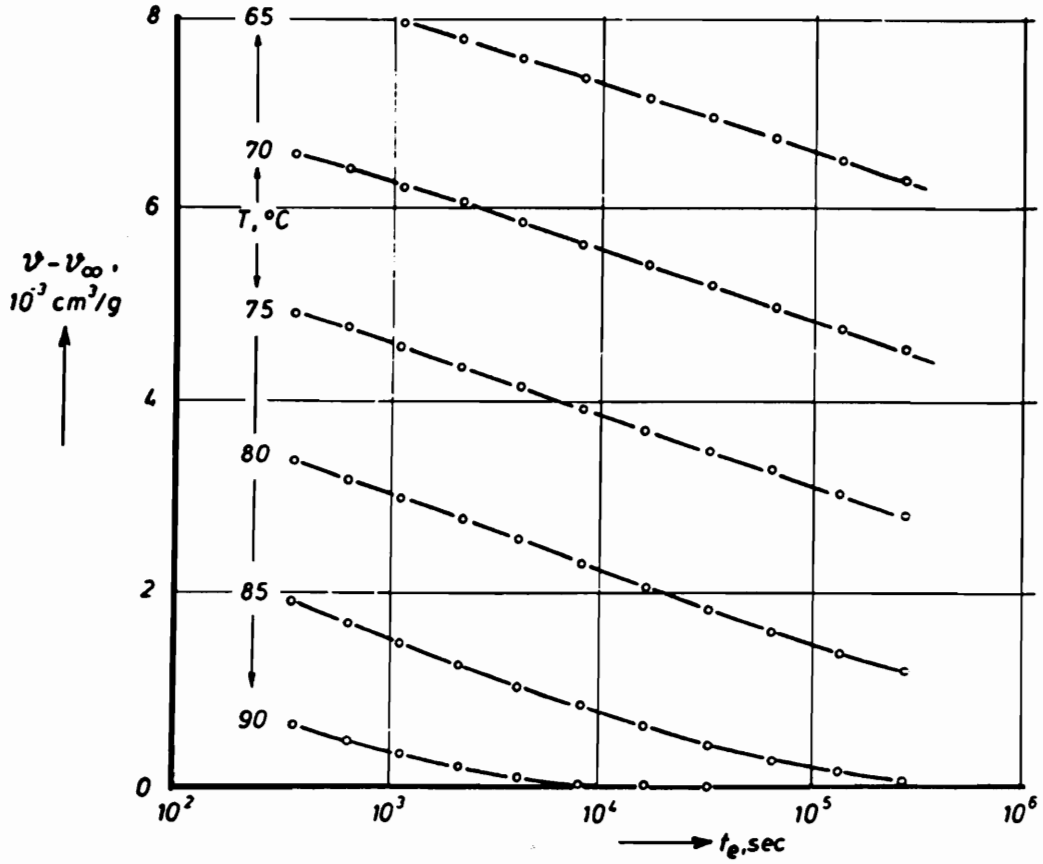

Figure 2.2-4. Volume relaxation of polystyrene as a function of aging time and aging temperature (from [52]).

$$\beta = -\frac{1}{v}\frac{dv}{d\log t_e} = -\frac{3}{l}\frac{dl}{d\log t_e} \qquad (2.2\text{-}4)$$

where l is the length of the sample in the case of length dilatometry (note that this relationship is valid only for unoriented, isotropic samples). Typical values for β range from $1x10^{-4}$ to $9x10^{-4}$. Sample values of β for different polymers as a function of aging temperature are shown in Figure 2.2-5. Note the drop off in relaxation rate within about 10°C of Tg. Also note the unusual behavior of PMMA. PMMA exhibits a secondary, side-chain transition (as opposed to a backbone or main-chain motion) near room temperature which manifests itself as a bump in the β versus temperature plot. For PC, the drop in β with decreasing temperature at 90°C correlates with what is believed to be a secondary *main-chain* transition. The same holds true for PS around 20 to 50°C. In both cases, β decreases monotonically with decreasing temperature below this transtion, unlike the trend observed with the side-chain motion of PMMA. This seems to indicate that main chain mobility, as opposed to side-chain mobility, is the dominant factor controlling the volume relaxation rate.

A comparison of the β values for polystyrene, as obtained by different experimenters, is shown in Figure 2.2-6. The difference in methodology between tests is in the aging time at which point the β slope was determined. Struik's work[53] involved measurements out to only 1 day, whereas Kovacs[67] extended his measurements to 5 days and Greiner and Schwarzl[69] to 12 days. The 5 and 12 day measurements are in close agreement. The 1 day measurements show lower β values at the lower temperatures with the difference being quite significant at room temperature. Greiner and Schwarzl provide an explanation for this behavior which is later reemphasized by Struik.[68] Apparently, at the lower aging temperatures the molecular mobility is low enough such that the sample takes longer to reach its maximum aging rate. This "onset" time gets larger with decreasing temperature. This would explain why Struik's 1-day measurements are yielding lower β values since the sample has not yet reached the faster rate of relaxation. This is further illustrated in Figure

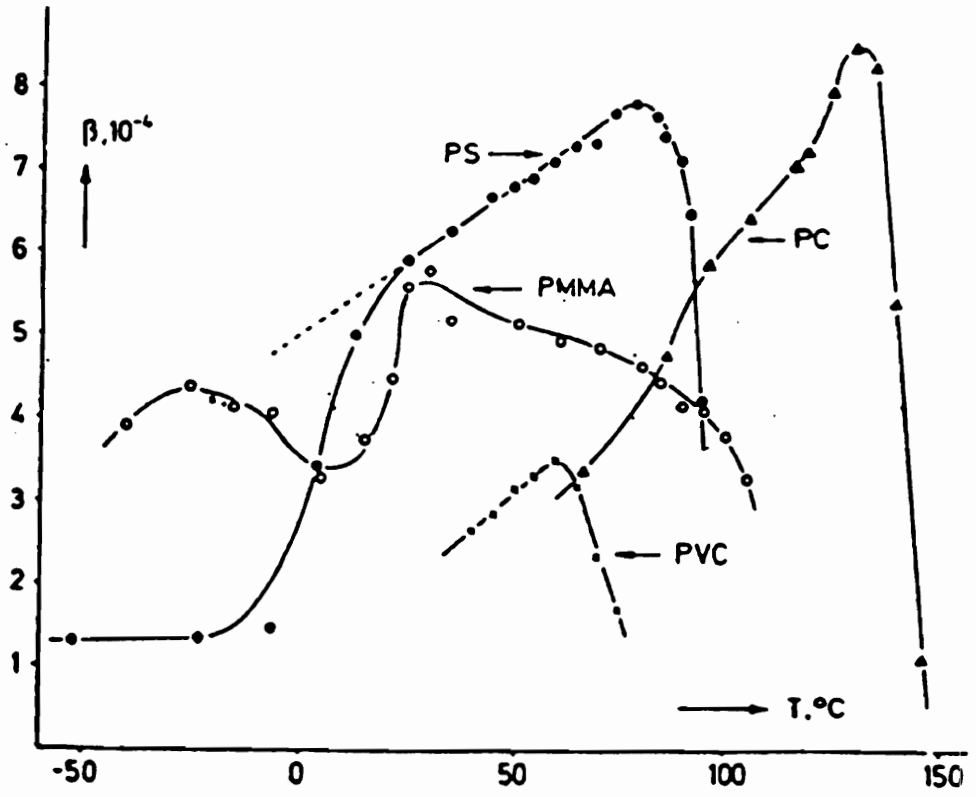

Figure 2.2-5. Volume relaxation rates for various polymers as a function of aging temperature. Values are determined at an aging time of 12 days. (from [69]).

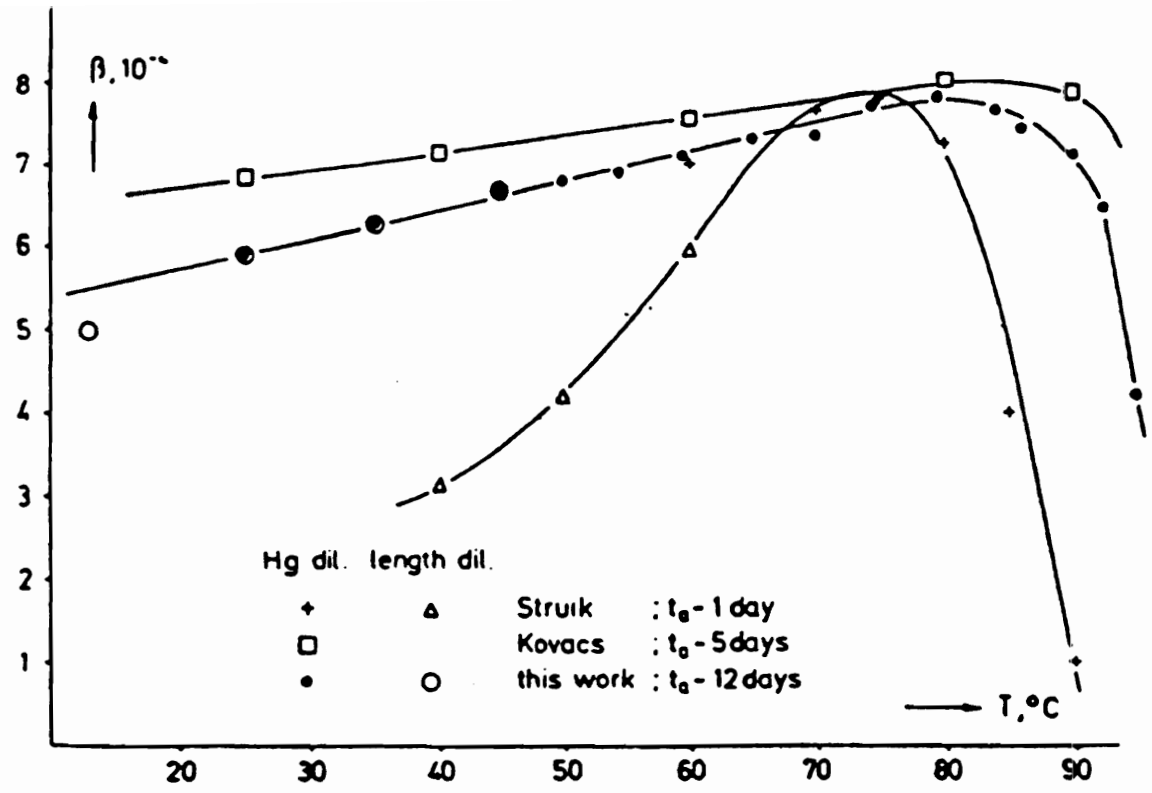

Figure 2.2-6. Volume relaxation data for PS. Data is obtained by different experimenters for different aging times (from [69]).

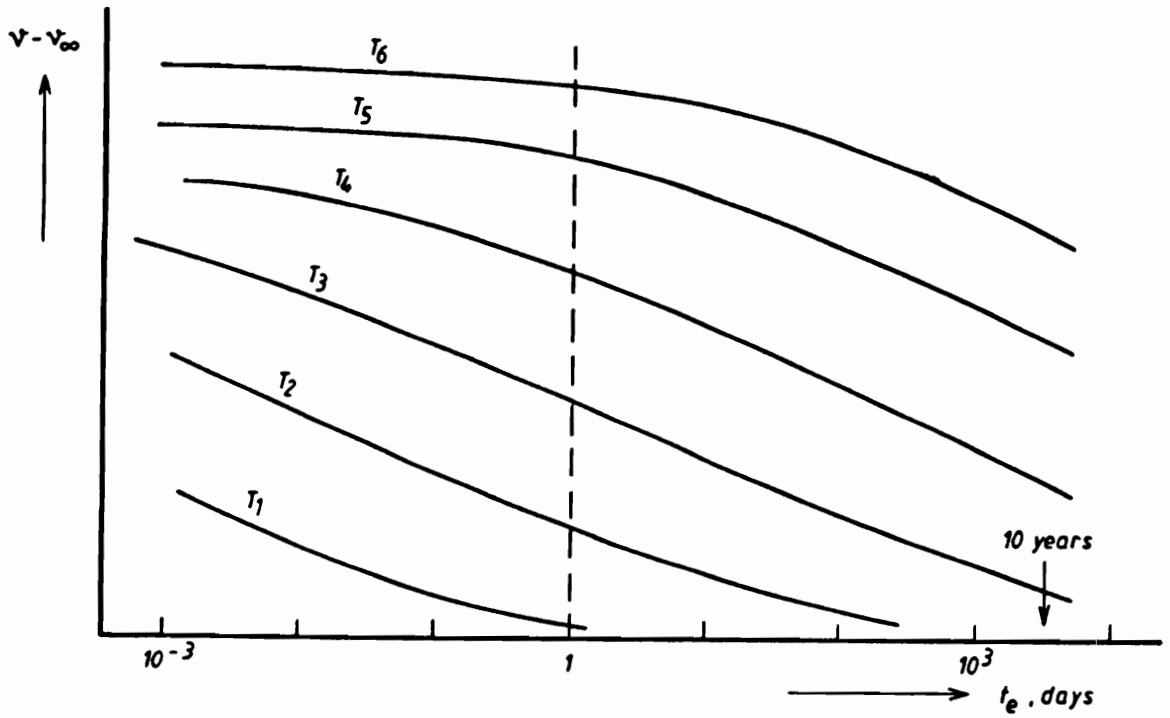

Figure 2.2-7 Typical volume relaxation data as a function of aging time for different annealing temperatures (from [52]).

2.2-7. Here the volume relaxation is plotted for a typical polymer at different aging temperatures. The dashed line represents Struik's 1-day aging time. Note how the lower aging temperatures have not yet attained their maximum relaxation rates. With this in mind, it is clear that care must be taken when making and interpreting dilatometric measurements at lower temperatures (particularly in light of de Bruin's recent report of enhanced aging rates in PC at aging times greater than 10^7 seconds.[57])

2.2.2.3 Temperature Jump Experiments

Temperature jump (T-jump) experiments typically involve annealing a sample at a given temperature for a certain amount of time and then quickly heating/cooling the sample to another (glassy) temperature where it is further annealed. Volumetric measurements made on the second annealing show unusual, highly non-linear behavior in the relaxation response.[53] Figure 2.2-8 from Struik[53] displays specific volume (left) and mechanical (right) relaxation data for polystyrene undergoing different thermal histories. All of the curves represent aging at 85°C, only the prior thermal histories are different. Curve 7 is the reference curve for a standard isothermal relaxation test; the sample was quenched directly from 100°C (above Tg) to 85°C and held throughout. This produces the standard monotonically decreasing volume which is expected with an isothermal test. Curves 3 through 6 involve quenching the sample from 100°C to temperatures of 70°C, 65°C, 60°C, and 50°C respectively, holding the sample for 96 hours, and then reheating to 85° C at which point volumetric measurements were made. The non-equilibrium behavior is clearly present as the volume goes through a maxima (often referred to as "breathing"). Note also how, after sufficient time, the volume relaxation curves eventually overlap the isothermally aged sample (curve 7). In each case, 96 hours is insufficient time for the sample to reach equilibrium. The lowest dashed curve (curve 1), on the other hand, represents a sample annealed at 80°C for long enough time such that the sample has

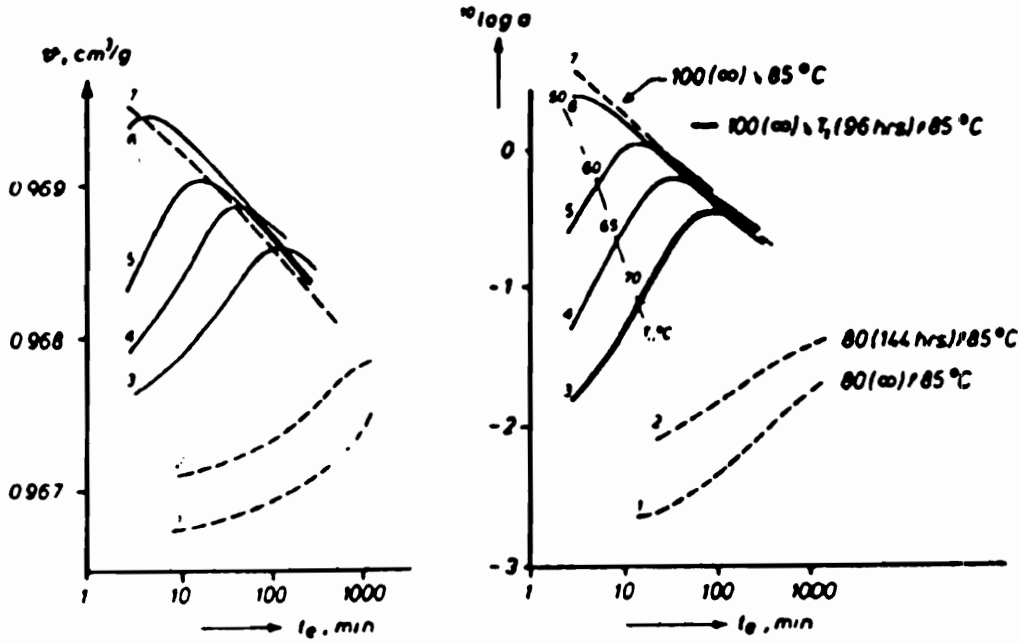

Figure 2.2-8. Volume and mechanical shift factors for polystyrene aged at 85°C with varying thermal histories. See text for curve descriptions (from [53]).

reached equilibrium. When this sample is then upquenched to 85°C as seen in the figure, the volume monotonically increases toward the 85° C equilibrium volume. Clearly the presence of the maxima involves an initial annealed state which was not at equilibrium. The height of the maxima is also an indicator of the distance from equilibrium at the start of the upquench. Struik has explained this breathing behavior using mechanical analogies.[53] His model shows that for breathing to occur, the volume relaxation process must involve a distribution of relaxation times. In addition, the aging time after the first quench must fall between the shortest and longest relaxation times. In other words, if the first annealing is too short or too long, no maximum will occur.

Because of the relatively high maximum that can occur during these quench-anneal-upquench experiments, it is possible to use this process as a sub-T_g method for partially erasing aging. By heating an aged sample to a higher temperature and holding for the proper amount of time, the free volume can be increased significantly. Obviously, if the sample is held too long, the sample will pass through the maximum in the volume-time curve and the volume will decrease again.

Although the data in the previous description emphasized "upquenching" the sample to the final annealing temperature, "downquenching" from a higher temperature is also important. This test method was pioneered by Kovacs using poly(vinyl acetate). First it is necessary to define an effective retardation time, also originating from Kovacs,[70,71,72] as

$$\tau_{eff}^{-1} = -\frac{1}{\delta}\frac{d\delta}{dt} \qquad (2.2\text{-}5)$$

where δ is defined as

$$\delta = \frac{V(t) - V_\infty}{V_\infty} \qquad (2.2\text{-}6)$$

for volumetric measurements but can also be written in terms of enthalpy. Figure 2.2-9 shows the relaxation data for poly(vinyl acetate) aged at 35°C. The curves represent different starting temperatures for the sample prior to their final annealing at 35°C.

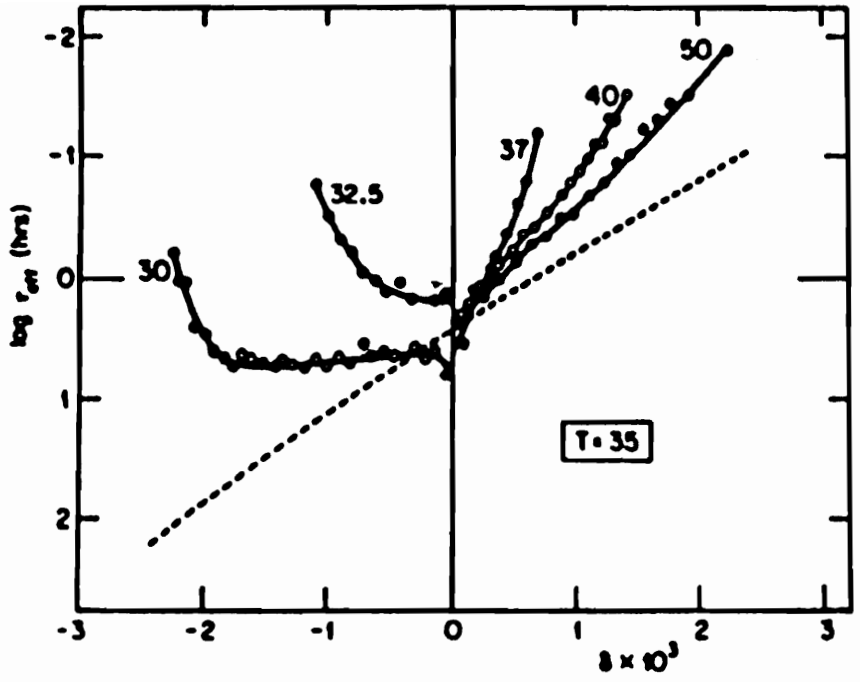

Figure 2.2-9. Relaxation data for poly(vinyl acetate) aged at 35°C and subjected to down and up-quench from various temperatures (from [70]).

Samples were at their equilibrium volume prior to the temperature jump. Kovacs coined these experiments as "simple approach" experiments. Data for these experiments is plotted characteristically as $\log(\tau_{eff})$ versus δ. Upon inspection of Figure 2.2-9, it is clear that the relaxation behavior toward equilibrium ($\delta = 0$) is different depending on whether the approach is from below or above the final aging temperature. The downquench samples converge to the same equilibrium τ_{eff} for different initial temperatures while the upquenched samples do not. Also, the rate of approach clearly varies for the different experiments.

Much effort has been devoted to the prediction and modeling of this behavior. In fact, being able to properly model the nonlinear, non-converging approach for both the up and downquench has been a nearly insurmountable task. The first kinetic theories were of the single parameter type developed by Kovacs.[70] These theories assumed a single relaxation time τ which is a changing function of temperature and aging state (i.e. free volume). For generalized aging, the equation becomes

$$\frac{d\delta}{dt} = -\frac{\delta}{\tau(T, v_f)} + \Delta\alpha q \qquad (2.2\text{-}7)$$

The second term on the right hand side was added to account for temperature changes; q is the heating/cooling rate and $\Delta\alpha$ is the differential thermal expansion between liquid and glass. The above rate equation has been further generalized by way of the multi-parameter models. Instead of only one relaxation time, a series of relaxation times are assumed, each having to satisfy the above equation in addition to

$$\delta = \sum \delta_i \qquad (2.2\text{-}8)$$

where the subscript i refers to the i'th relaxation time. It still remains to define how τ varies with temperature and degree of aging. This is where the various theories diverge. It is generally assumed in most of the theories that the aging behavior is thermorheologically simple. That is, aging's only effect is to shift the relaxation times in

time and not to alter the shape or magnitude of the distribution. Experimentally, this seems to be a reasonably good assumption. In practice, however, small degrees of vertical shifting are often required which imply some, albeit small, distortion of the relaxation time distribution. Generally, the relaxation time distribution can take on many different forms. However, Ng and Aklonis looked at a variety of distributions including the box, double-box, Gaussian, ramp and stretched exponential (KWW) distributions and found that none were completely adequate for describing the non-linear, T-jump, approach behavior.[73] This has been a major limitation of the theory.

There are various expressions in use to describe the effects of aging state and temperature on the shifting behavior of the relaxation time.[74] The first is of the Tool [75,76] and Narayanaswamy [77,78] form and is written as

$$\tau = A \exp[x\Delta h / RT + (1 - x)\Delta h / RT_f] \qquad (2.2\text{-}9)$$

This Arrhenius-type equation consists of two components, one accounting for the effect of aging and one for temperature. The relative weighting between them is parameterized by x which can vary between 0 and 1. The activation energy is denoted by Δh and A is a constant. Hodge has related the Adam-Gibbs configurational entropy expression to the Narayanaswamy parameters and has shown correlations that occur between the parameters.[79] The parameter T_f is denoted as the fictive temperature and is a measure of the departure from equilibrium. It was first introduced by Tool.[75,76] The fictive temperature is defined as that temperature at which the sample would be at equilibrium if cooled or heated very rapidly to it. If a sample is above Tg, then the fictive temperature will equal the actual temperature. Likewise, if a sample is at equilibrium in the glassy state, then the fictive temperature will also be equal to the actual temperature. The quantity T_f-T is essentially a measure of the departure from equilibrium.

Another expression relating τ to the temperature and free volume is based on the free volume concept and has been used by Macedo and Litovitz[80] and Mazurin.[81] It is of the form,

$$\tau = A \exp\{B / [R(T_f - T_2)] + E / RT\} \qquad (2.2\text{-}10)$$

where A, B and E are constants. The quantity T_2 is the temperature of zero free volume. In a similar fashion, an expression for the relaxation time based on configurational entropy (Adam-Gibbs) is

$$\tau = A \exp\left\{ B / RT \left[\int_{T_2}^{T_f} (\Delta C_p / T) dT \right] \right\} \qquad (2.2\text{-}11)$$

except T_2 is now the second order transition temperature of Gibbs-DiMarzio and ΔC_p is the heat capacity difference between rubber and glass.. This expression has been applied by Howell,[82] Plazek,[83] Scherer, [84] Matsuoka,[85] and Hodge.[86]

As to which of these models is the best for predicting T-jump behavior has been debated considerably in the literature.[74, 87, 88, 89] As described by Mijovic, the Tool-Narayanaswamy is the most frequently used because it is easy to manipulate but is often criticized for its rather empirical nature, the unusually large values of Δh, and the fact that it reduces to the Arrhenius form at equilibrium as opposed to the WLF form.[74] The configurational entropy equation has received some criticism because of its dependence on ΔC_p as a measure of structural relaxation. Goldstein has challenged this notion saying that part of the ΔC_p is due to contributions from anharmonic vibrations and secondary relaxations which should not be applicable to structural relaxations.[90] All of the models are able to adequately describe most of the important behavior of volume relaxation behavior. However, as described before, the prediction of the non-linear approach behavior is not entirely correct with any of the models. In particular, the difference in τ_{eff} between down and upquench experiments is not seen with any of the model assumptions.

2.2.3 Mechanical Studies

Mechanical studies of physical aging can incorporate a wide variety of tests including creep, stress relaxation, dynamic mechanical, standard tensile testing, impact, etc. In addition, due to the tensorial nature of stress and strain, the loading can take on varying ranges of complexity from simple shear or tension all the way up to three dimensional stress states. In general, small strain creep and/or stress relaxation tests are the most useful since they are non-destructive in nature and can provide excellent relaxation/retardation data on the material.

Struik[53] has provided an excellent summary of the various aspects of creep/stress relaxation testing and the consequent data reduction. In general, one sample can be used throughout the physical aging test as long as the stress level remains low (less than 10 MPa or 0.3% strain). In addition, subsequent creep loadings at these low stress levels will not alter the aged state so one does not have to requench the sample for every creep test. A typical loading procedure which capitalizes on these features is shown in Figure 2.2-10. The sample is stressed at increasing time intervals and creep compliances measured. The time of testing at each loading must be small compared with the aging time or else the aging will distort the compliance curve. Typically the creep time is taken as one or two-tenths of the current aging time. Separation between creep measurements should be far enough apart to allow for full relaxation of the unloaded creep sample but not so far apart as to make data shifting difficult. A sample set of creep curves is shown in Figure 2.2-11 for rigid PVC at various aging times. It is apparent that the curves can be superimposed by simply shifting them horizontally along the time axis. This implies that the only effect of aging is to shift the relaxation time spectrum. This is the same as the assumption of thermorheological simplicity described earlier for the kinetic models. The general procedure is to chose a reference time and then shift each curve to that reference time. If the amount of horizontal shift a, i.e. the shift factor, is plotted on a doubly logarithmic plot

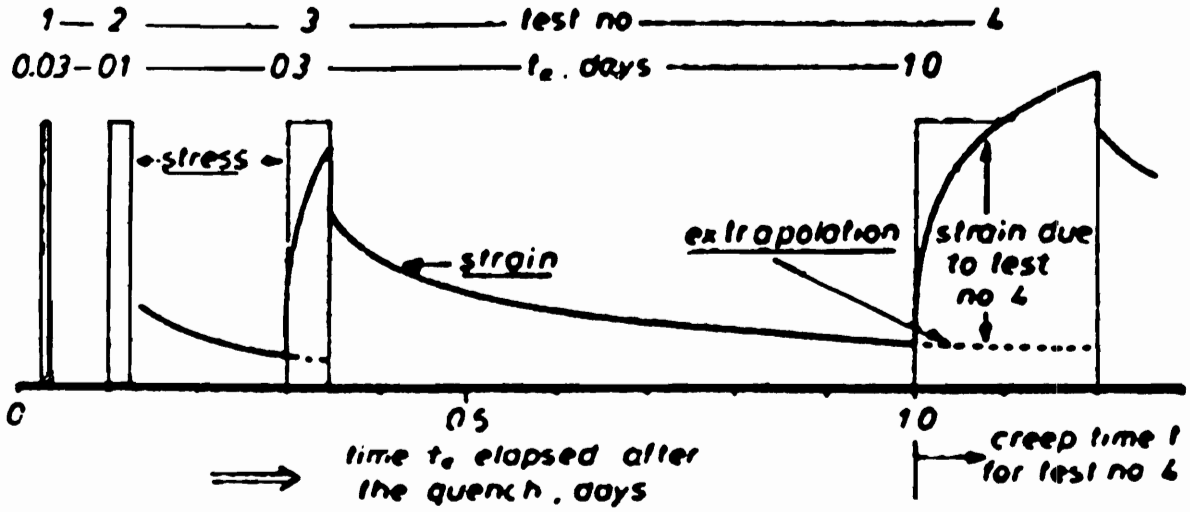

Figure 2.2-10. Typical stress history for aging study (from [53]).

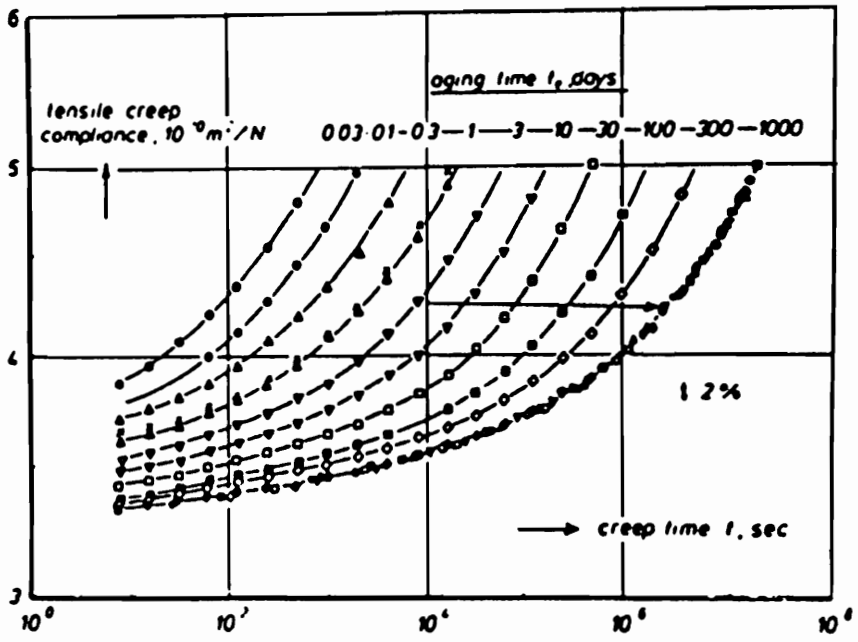

Figure 2.2-11. Creep curves for rigid PVC at various aging times (from L. C. E. Struik, *Physical Aging in Amorphous Polymers and Other Materials,* Elsevier, New York, 1978).

versus the aging time, the data is found to lie along a straight line with a slope of μ. This shift rate is defined as

$$\mu = \frac{d \log a}{d \log t_e} \qquad (2.2\text{-}12)$$

For most glassy polymers μ has a value of approximately 1 over a wide temperature range. This is true as long as the glass is far from equilibrium. Values of μ for a number of different polymers are shown in Figure 2.2-12. Polycarbonate is unusual in that its maximum shift rate is slightly higher (~1.20) as compared with the other glasses. As the temperature approaches T_g, the shift rate falls off considerably. This can be attributed to the closeness to equilibrium at which point the above relation is invalid. Also, at lower temperatures the shift rate decreases. This "roll-off" usually occurs near the secondary relaxation if that relaxation is a main chain and not a side chain relaxation. The behavior is similar to the volume relaxation described earlier. Compare and contrast the mechanical μ data with the β volumetric data described previously. Although most of the trends are similar, there are some differences in the rate at which the various parameters decrease with decreasing temperature. For this, a new parameter S, known as the volume sensitivity, is defined as

$$S = 2.303 \frac{\mu}{\beta} \qquad (2.2\text{-}13)$$

Sensitivity data for a variety of polymers are plotted in Figure 2.2-13. The importance of S is in its relation to the mobility. Struik[53] has shown how Eqn. 2.2-13 can be related to another definition for S,

$$S = \left[\frac{\partial \ln M}{\partial (ffv)} \right]_T \qquad (2.2\text{-}14)$$

where M is the mobility and *ffv* is the free volume fraction. The strong increase in S with decreasing T is important to recognize. It means that a polymer can still undergo

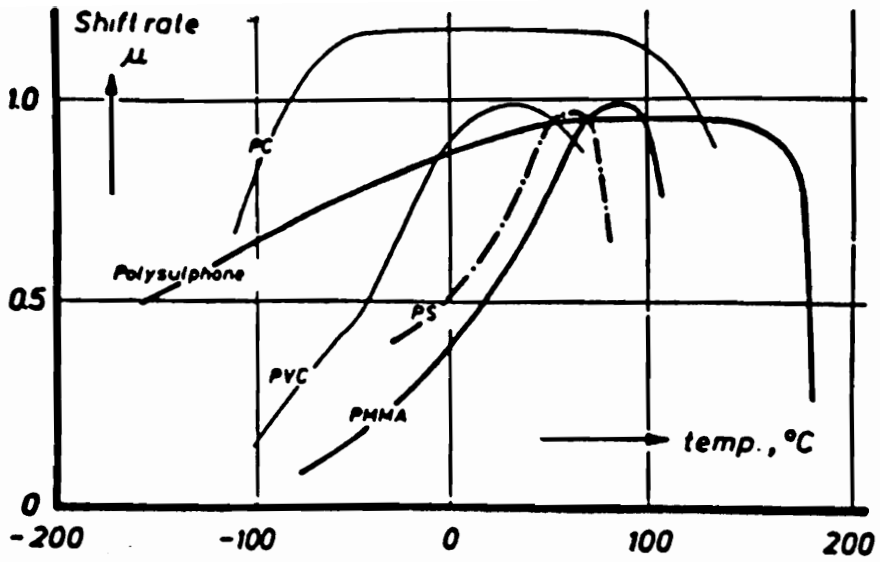

Figure 2.2-12. Mechanical shift rates for various polymers as a function of isothermal aging temperature (from [53]).

significant changes in mechanical mobility at low temperatures even though the specific volume is changing only very little with time. This strong increase in S is also not in line with the predictions of the free volume models such as the WLF equation. While the trend is in the right direction, the magnitudes of shifting for a given change in free volume do not coincide. Apparently this is due to the inaccuracy of applying the free volume equations below Tg where the free volume distribution is no longer an equilibrium distribution. [53]

Read has performed a thorough series of creep tests on PC, PBT, PVC, and HDPE over a very broad time range (10^{-8} to 10^{6} seconds) which encompasses both the secondary (β) and primary (α) relaxations.[91,92,93] A combination of both static and dynamic tests was used to obtain the broad time range. For short-term, small stress creep, the compliance was accurately modeled as the summation of the compliance contributions from the primary and secondary relaxations

$$D(t) = D_{U\beta} + D_{\beta}(t) + D_{\alpha}(t) \qquad (2.2\text{-}15)$$

where D_{u_β} is the unrelaxed compliance at short times and $D_{\alpha}(t)$ and $D_{\beta}(t)$ are the contributions from the α and β relaxations respectively. For the β relaxation,

$$D_{\beta}(t) = \Delta D_{\beta} \Psi_{\beta}(t) \qquad (2.2\text{-}16)$$

where

$$\Delta D_{\beta} = D_{R\beta} - D_{U\beta} \qquad (2.2\text{-}17)$$

and

$$\Psi_{\beta}(t) = \frac{(t / \tau_{\beta})^{n}[(t / \tau_{\beta})^{n} + \cos(n\pi / 2)]}{1 + 2(t / \tau_{\beta})^{n} \cos(n\pi / 2) + (t / \tau_{\beta})^{2n}} \qquad (2.2\text{-}18)$$

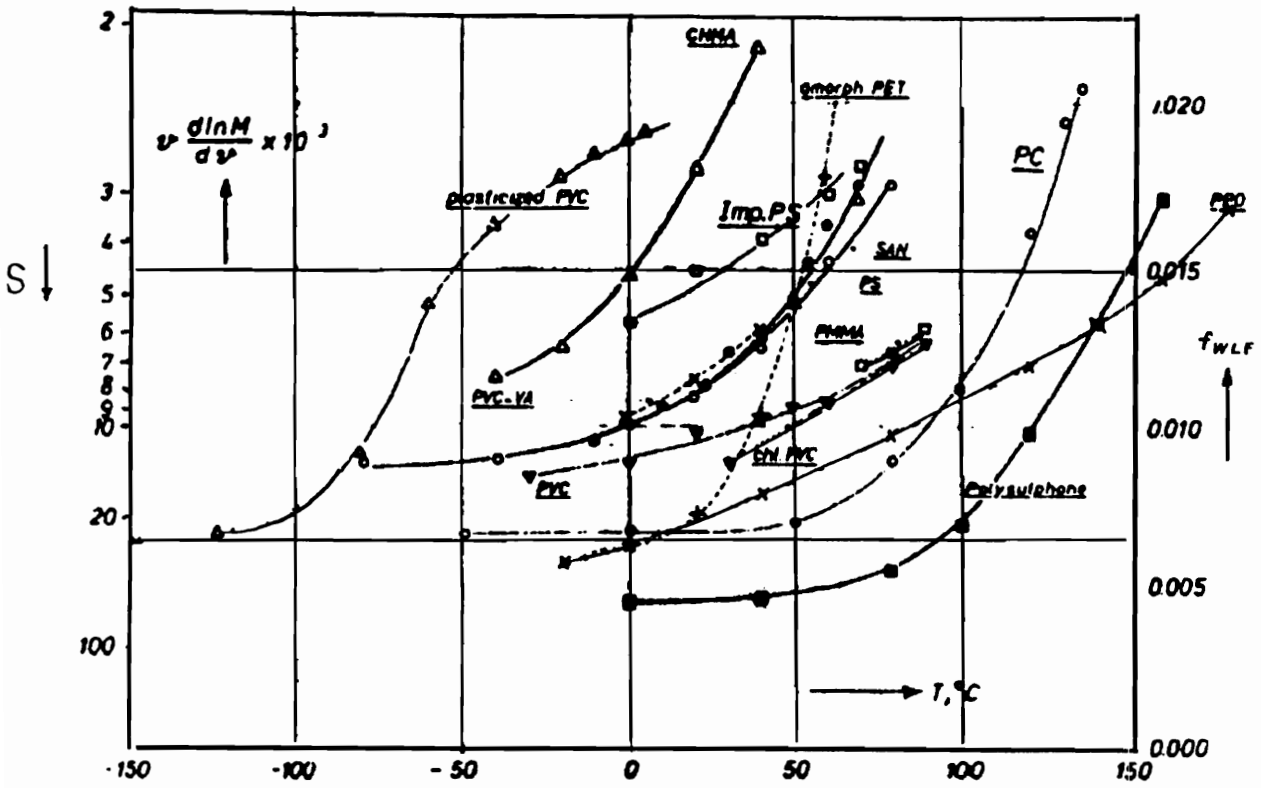

Figure 2.2-13. Mechanical sensitivity data for various polymers. Note that the sensitivity S increases in the downward direction (from [53]).

which is known as the Cole-Cole equation. D_{R_β} is the relaxed compliance. For the α contribution, $D_\alpha(t)$ can be approximated as

$$D_\alpha(t) = D_{R\beta}\Psi_\alpha(t) = D_{R\beta}\exp(t / \tau_o)^\gamma \qquad (2.2\text{-}19)$$

where the exponential term is the same as the Kolrausch-Williams-Watts (KWW) equation. The parameter τ_o is a characteristic relaxation time and γ is the exponentiality parameter (this parameter is denoted as β elsewhere but is denoted as γ here to avoid confusion with the β relaxation). During aging, τ_o is found to increase for the α contribution whereas ΔD_β decreases with aging time for the β relaxation.

The issue of mechanical enhancement of physical aging is an important one but it has generated some confusion. By enhancement it is meant that the application of a high enough stress--regardless of the mode of deformation--will increase the rate of physical aging during consequent annealing. It has already been shown that a stress of sufficient magnitude will erase previous aging (i.e. rejuvenation), either wholly or partly, which seems to be in contradiction to the previous statement. Struik originally showed how high stresses during the creep-aging tests leads to reduced shift factors.[53] This is further illustrated in Figure 2.2-14. Here he assumes the same multiple testing protocol discussed earlier (see Figure 2.2-10). The effect of the higher stress is clearly to reduce the shifting and therefore to reduce μ which leads one to believe that the higher stresses erase physical aging, not enhance it. Prompted by claims from Sternstein[94,95,96] that high stresses did indeed enhance aging, Struik revisited the problem in another report.[97] Struik looked at high stress loadings but followed two different loading patterns. In the first pattern, samples were loaded following the protocol in Figure 2.2-10 (Type 1). In the second pattern, each sample was aged up to the desired time and a only one creep test performed (Type 2). The results are shown in Figure 2.2-15. At low stresses, the two loading

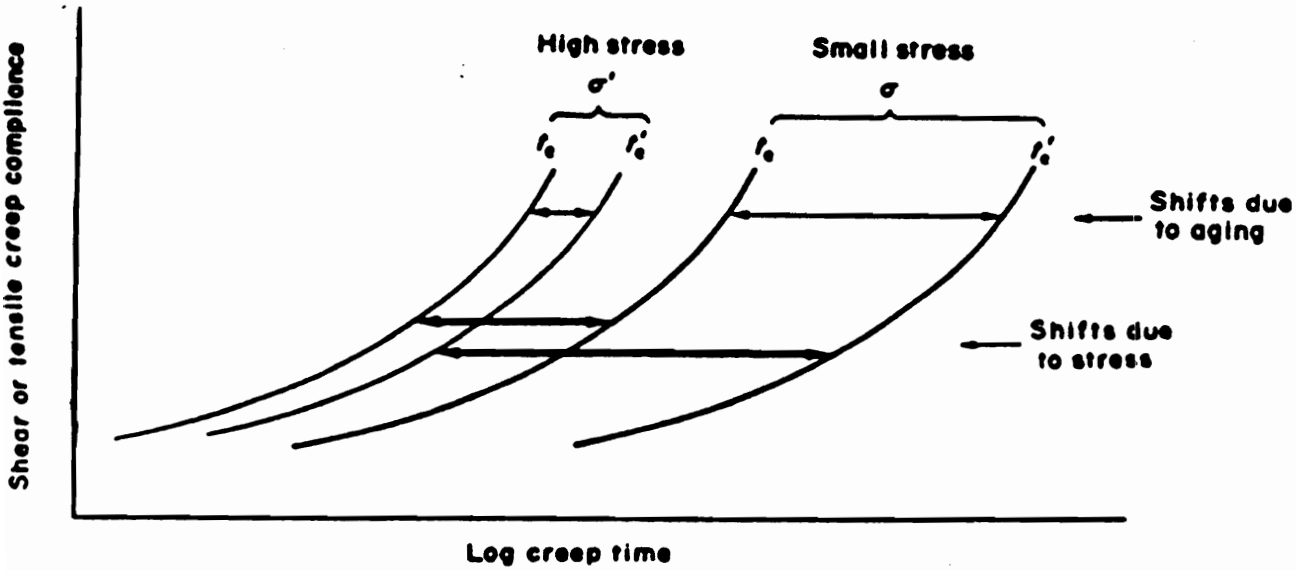

Figure 2.2-14. Effect of high stresses on the mechanical shift behavior (from [53]).

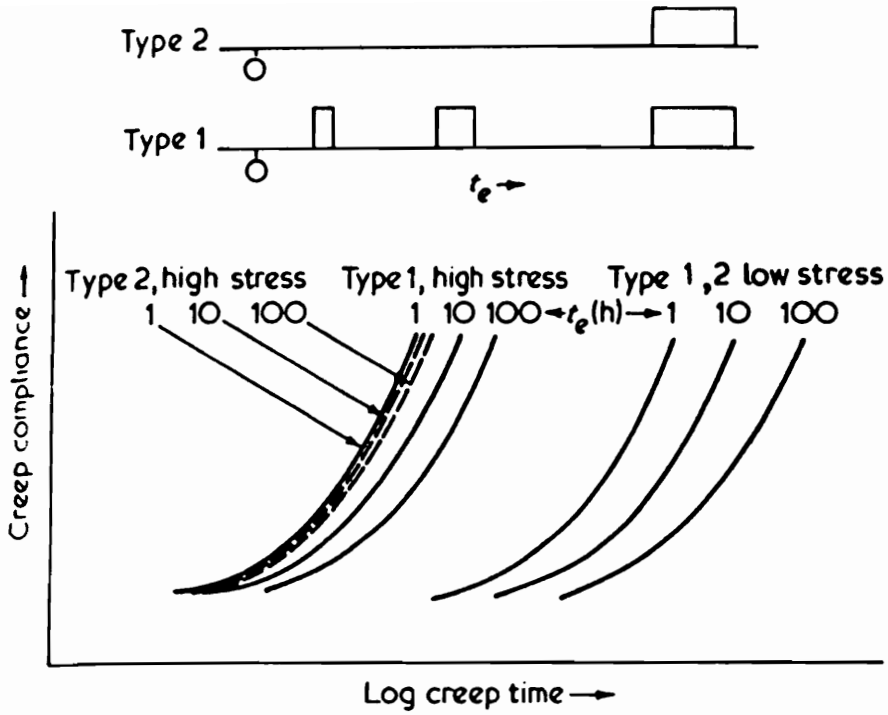

Figure 2.2-15. Effect of high stress on the mechanical shift behavior. Two different loading protocols are shown. See text for further description (from [97]).

protocols give identical results as expected. At higher stresses, the behavior is quite different. Type 1 samples give similar results as in Figure 2.2-14 with a reduction in μ as compared with the low stress samples. The Type 2 samples, on the other hand, show an even smaller shifting. The results might be interpreted as follows (this is this author's interpretation of Struik's results). The process of actually applying the high stress acts to partially erase the previous physical aging. For the Type 2 samples, this means that each sample will behave during the rest of the current creep test as if it were freshly quenched (or at least "less aged"). For the Type 1 samples, the same applies. However, after the creep test is completed, the sample is further aged and then another creep test performed. The interim aging period is is where enhancement enters the picture. The sample will age at a faster rate after the first loading is completed due to the high stress effect. At the next creep loading, the aging will again be partially erased; but, there is a higher residual degree of aging than before. This results in a greater μ as compared with the Type 2 samples. As to why high stresses enhance aging rates may be closely related to the issue of why cold-drawing enhances physical aging. It is likely that the plastic deformation and residual stresses present in the sample are at least partially responsible.

The issue of rejuvenation has also come under question in recent years based on work by McKenna and coworkers using a torsional dilatometer.[98,99,100,101] The torsional dilatometer allows for simultaneous measurements of mechanical and volumetric relaxation during aging. Mechanical shift factors for an epoxy glass aged very close to its Tg are shown in Figure 2.2-16 as a function of different stress levels. The slopes of the curves, which are equal to μ, are gradually decreasing with increasing stress as expected. Note however that t^*, the time to reach equilibrium, is constant for all of the stress levels. This indicates that the glassy structure is somehow decoupled from the applied stress field. One would expect, in the event of rejuvenation, that t^* would change since the aged structure is also supposed to be changing. Dilatometric measurements have also been performed which discredit the concept of rejuvenation. A volumetric plot of an epoxy sample being aged in the torsional dilatometer is shown in Figure 2.2-17. The sample was

loaded periodically with a large torsional strain following the same loading protocol described earlier. The torsion strains, which show up as spikes on the plot, were large enough to cause a change in the mechanical shift rate data (i.e. rejuvenation by the old definition). A baseline for a non-loaded sample is shown as a solid line in the figure. Note that with each loading and unloading, the volume increases tremendously and then quickly relaxes back down to the unloaded baseline. The baseline volumetric response appears to be insensitive to any mechanical loading further supporting the idea that the mechanical and volumetric fields are decoupled. In addition, it was shown that the time scales for evolution of the volume response and the mechanical response were clearly different. An additional set of data which further supports the decoupling idea is shown in Figure 2.2-18. Here the mechanical shift factor is plotted as a function of δ for an up-jump aging experiment. The data shows that the mechanical shifting still proceeds even after the sample has reached volumetric equilibrium. The idea that free volume alone is a measure of the aging state appears to be incorrect based on these findings.

In another study, McKenna and Zapas have demonstrated the dangers in assuming the incremental modulus response $\Delta G(t)$, obtained by superposing a small deformation on top of a larger deformation, is the same as the small-strain, viscoelastic modulus $G(t)$.[102] This procedure has been used by a number of researchers[103,104,105,106,107] as a means of probing the structure of polymers including the aging behavior. Using the Kaye-BKZ rheological constitutive equation along with experimental measurements, they showed that "(1) the incremental modulus at a given (aging) time t_e, after superposition of the large strain both decreases with increasing deformation and increases with increasing t_e, and (2) the apparent incremental relaxation spectrum shifts to shorter times and narrows relative to that of the spectrum representing the small strain relaxation response."

Watts and Perry have studied aging effects in polycarbonate using both mechanical and dielectric methods.[108] Samples which were "as moulded" and those which were annealed at 120°C for 3 hours differed by a factor of 4 in impact strength but exhibited almost identical dielectric β-relaxations. They found that the energy dissipated by local β-

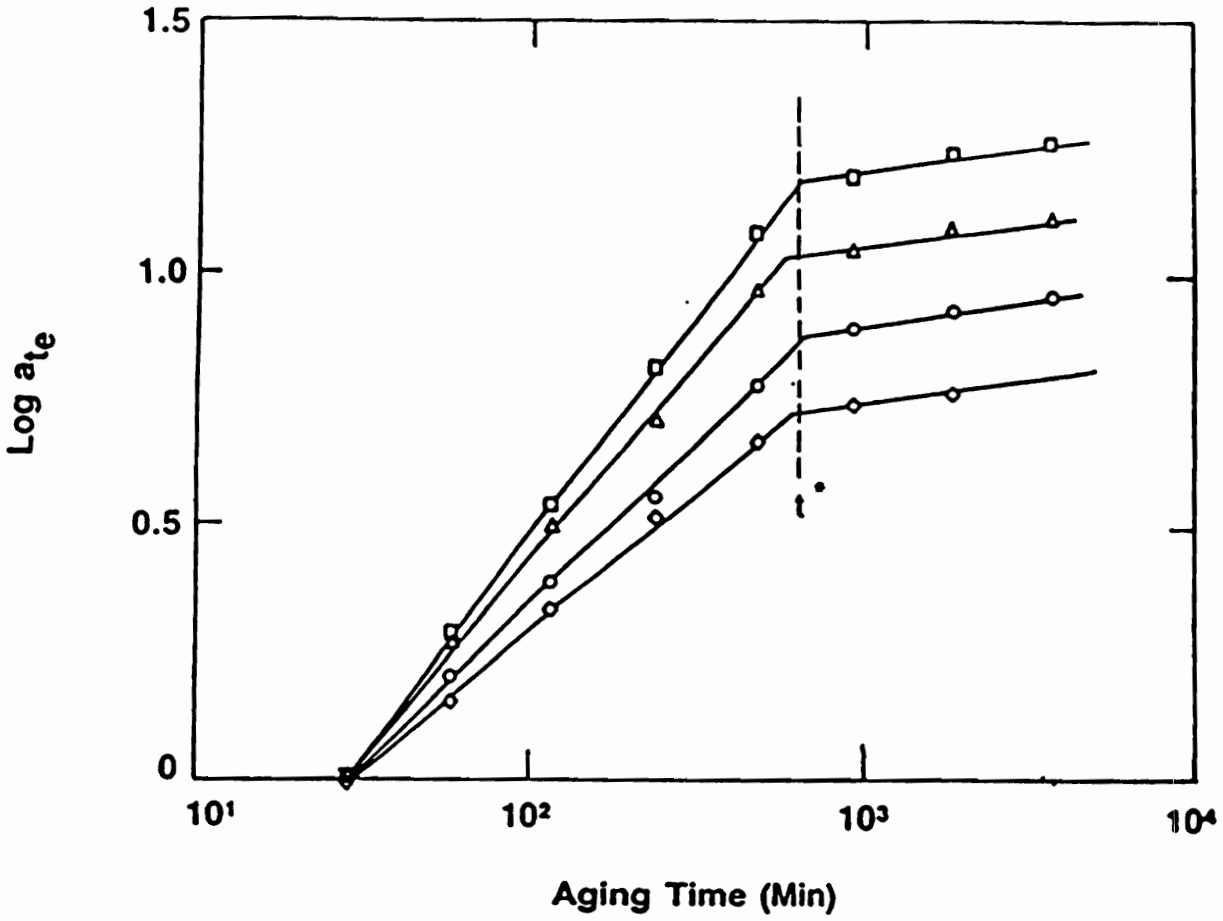

Figure 2.2-16. Mechanical shifting a_T as a function of aging time. Each curve represents a different stress level with squares representing 1 MPa, triangles representing 5 MPa, circles representing 10 MPa, and diamonds representing 15 MPa. Note that t^* is insensitive to the applied stress (from [98]).

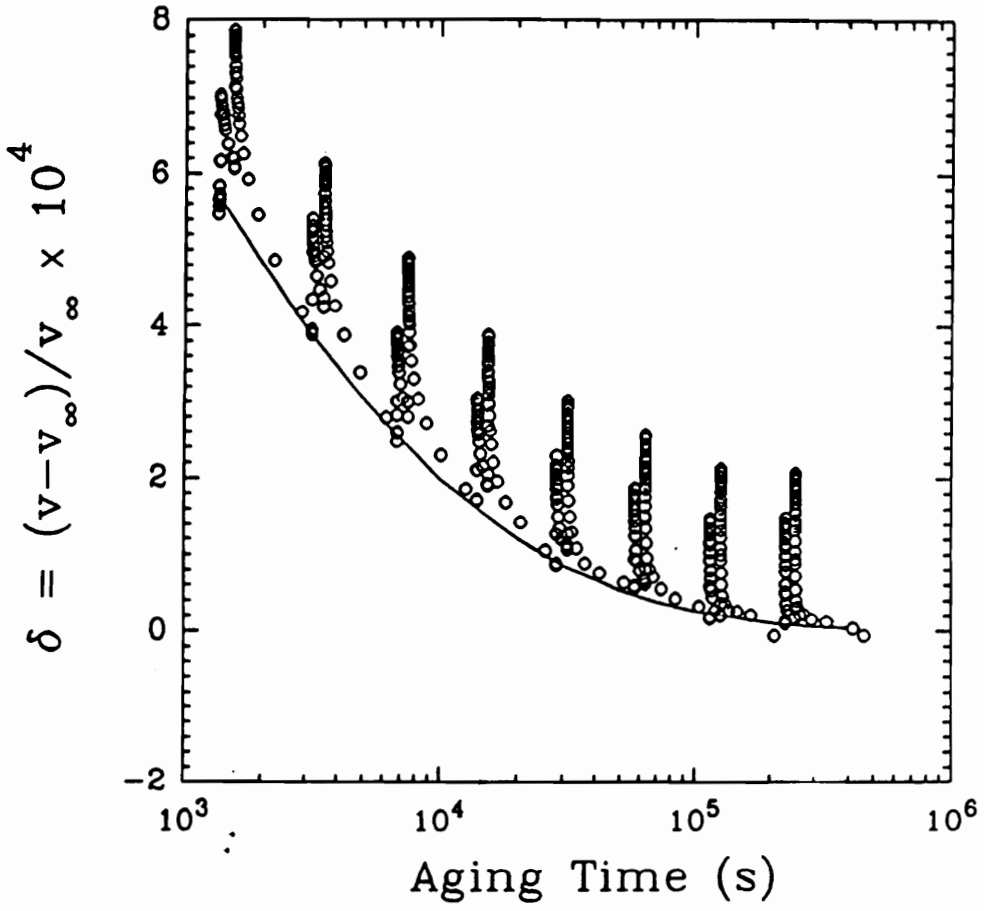

Figure 2.2-17. Volume relaxation curve for epoxy sample at Tg-8.9°C in torsional dilatometer. Sample is periodically loaded at 3% strain. The solid line represents the underformed baseline (from [98,100]).

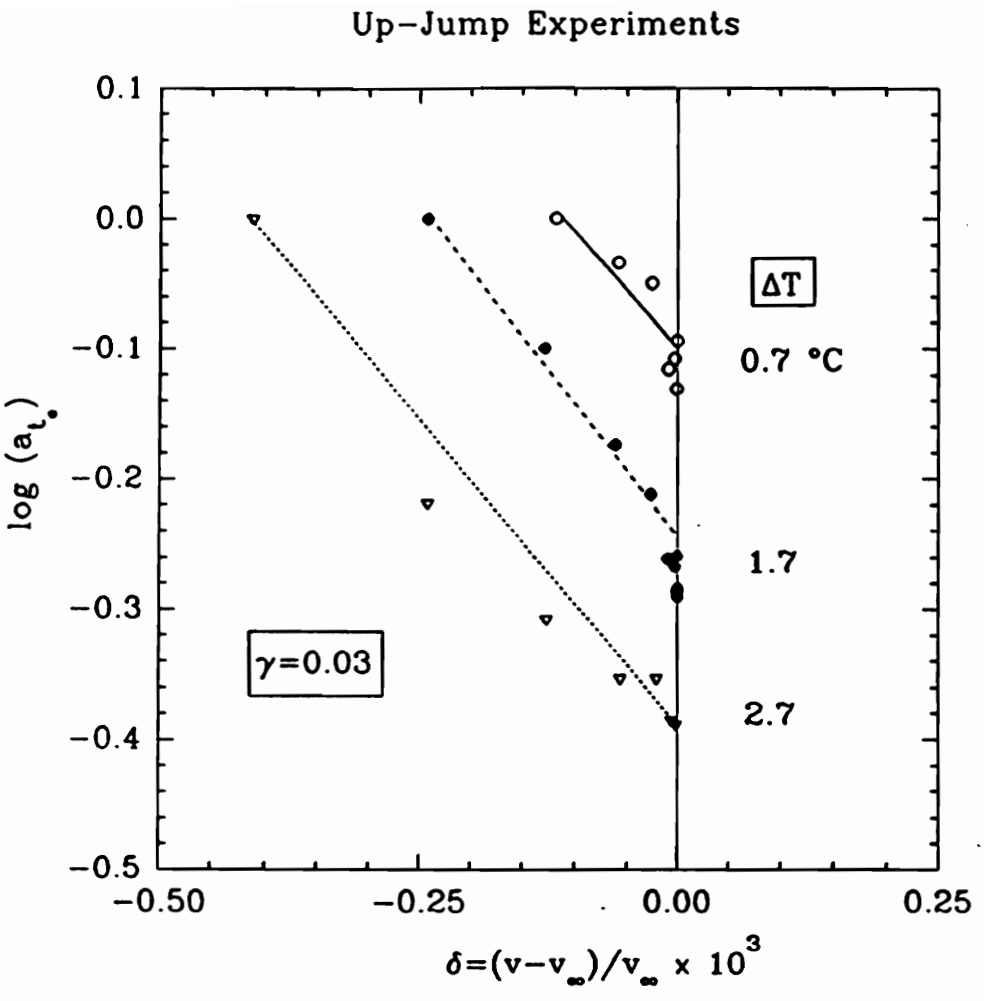

Figure 2.2-18. Results of an up-jump experiment comparing a_T with δ. Note that a_T is still changing at $\delta = 0$ (from [98]).

relaxations is a contributory factor to polycarbonate's toughness but not necessarily the sole factor. They also found that the β peak does not change significantly during aging even though a ductile/brittle transition occurs. From the dielectric data, they estimated that only 17% of the total chain units are mobile in the glassy state based on the number of dipole moments active.

Bubeck and coworkers studied the tensile and biaxial yield behavior of aged bis-A polycarbonate, various polyestercarbonates (T_g from 153°C to 190°C), and polysulfone (T_g = 190°C).[109] Samples were aged to various times up to 64 days at 120°C. The polyestercarbonates were found to have superior aging resistance based on the yield behavior. Their results, which included density and dynamic mechanical measurements, indicated that both free volume arguments and arguments based on molecular entanglements are inadequate for predicting resistance to embrittlement (the entanglement arguments assume that higher entanglement densities provide better resistance to brittle failure, not necessarily a reduction in the rate of physical aging). Aging time to brittle failure did not correlate with the measured density changes nor did it correlate with the T_g. Instead, the authors believe that molecular chain conformational effects, which are directly related to molecular structure, play an important role in determining physical aging resistance. For example, the addition of terephtalate linkages to the polyestercarbonate is believed to stiffen the chain slightly. Consequently, when the polymer vitrifies, this chain stiffening somehow preserves the more favorable chain conformations for deformation (i.e. those that allow for greater ductility).

2.2.4 Calorimetric Studies

Experimentally, changes in entropy and enthalpy are determined via the specific heat function.[74] Differential scanning calorimetry (DSC) represents one the easiest methods of accurately determining this function. The importance of calorimetric measurements stems from the fact that enthalpy relaxes in a similar manner to volume during physical aging. In fact, with the relation $H = U + PV$, the enthalpy will be directly proportional to the volume change--with the pressure as a proportionality constant--in the event that no internal energy changes occur with aging. DSC is a much easier method of measuring aging than dilatometry. One drawback is that DSC measurements require heating the sample through (or into the vicinity of) T_g in order to measure ΔH so, unlike dilatometry, continuous measurement of enthalpy relaxation is not possible.

A recent review of enthalpy relaxation in amorphous polymers is presented by Hodge.[110] He points out that the study of physical aging with DSC would be better named "enthalpy recovery" instead of the more commonly used "enthalpy relaxation" because it is the enthalpy recovered during heating which is recorded and analyzed. Bair[111] and Wunderlich[112] have provided detailed accounts on the use of DSC for measuring the glass transition and Tg related phenomena. A description of the physical aging measurement process is provided by Petrie.[113] During a DSC aging test, the sample is heated at a controlled rate through the glass transition. Any enthalpy that relaxed during the aging process will be regained at or near the glass transition and will show up as an endotherm as in Figure 2.2-19. The dashed line represents the freshly quenched sample whereas the solid line represents the aged sample. There are at least two different ways to determine the recovered enthalpy from the endotherm. The first method involves simply measuring the area under the endotherm as referenced to an unaged baseline. A second, more accurate method is to subtract the small "exotherm" which occurs at the onset of Tg from the larger endotherm. This exotherm, which represents an initial undershoot of the aged enthalpy function as compared with the unaged baseline, is usually significant only at longer effective aging times. It should be realized that the process of heating the sample

through T_g will in some way alter the state of aging and consequently, the results of the measurement. An example is shown in Figure 2.2-20 where a sample of Aroclor 5460 is aged for 195 minutes and then heated at different rates through the glass transition. Notice that the recovered endotherm is lower for the slower heating rates. Nonetheless, the increase in energy absorbed at the faster heating rates is equal, within experimental error, to the calculated values based on the difference in the observed glass transition temperatures.

The more common method for studying aging is to anneal the sample for different times and then measure the enthalpy change with DSC. Sample data for atactic polystyrene are shown in Figure 2.2-21. Except when close to equilibrium, the recovered enthalpy will usually fall along a straight line when plotted against the log of the aging time. This is the same behavior seen with the volume recovery. Often, the aging data is fit to the various kinetic theories such as the Narayanaswamy [77] or KAHR[116] (Kovacs, Aklonis, Hutchinson, Ramos) models using a fictive temperature approach described earlier. [114,115] Moynihan and coworkers combined the Narayanaswamy equation with the Kolrausch-Williams-Watts (KWW) equation

$$\phi(t) = \exp[-(t / \tau_o)^{\beta}] \qquad (2.2\text{-}20)$$

and then applied Boltzmann superposition principles to arrive at an accurate description of Cp for various heat histories. For the KWW equation, $\phi(t)$ is a stretched exponential decay function which accurately represents a wide range of relaxation processes in amorphous materials, the parameter τ_o is a characteristic relaxation time (determined by way of the Narayanaswamy equation), and β is a measure of non-exponentiality ranging from 0 to 1. See Hodge[110] or Kovacs and coworkers[116] for more details on this application.

As was hinted to earlier, it is expected that volume and enthalpic relaxation should behave similarly although not necessarily identically. O'Reilly[117] reviewed a number of studies in which comparisons of relaxation behavior between various test methods were

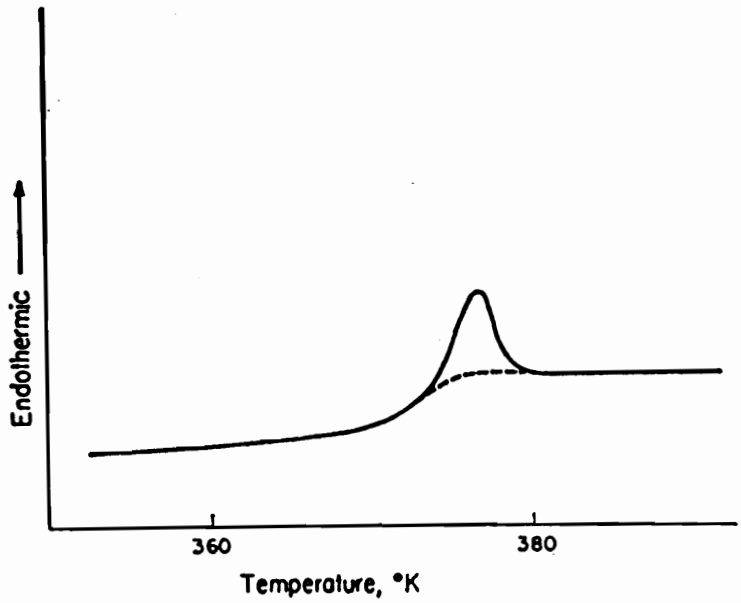

Figure 2.2-19. DSC scans of atactic PS at 5°C/min. Sample was quenched to 295 K from 400 K, annealed 3 hrs. at 365 K. The dashed line represents an unannealed sample (from [113]).

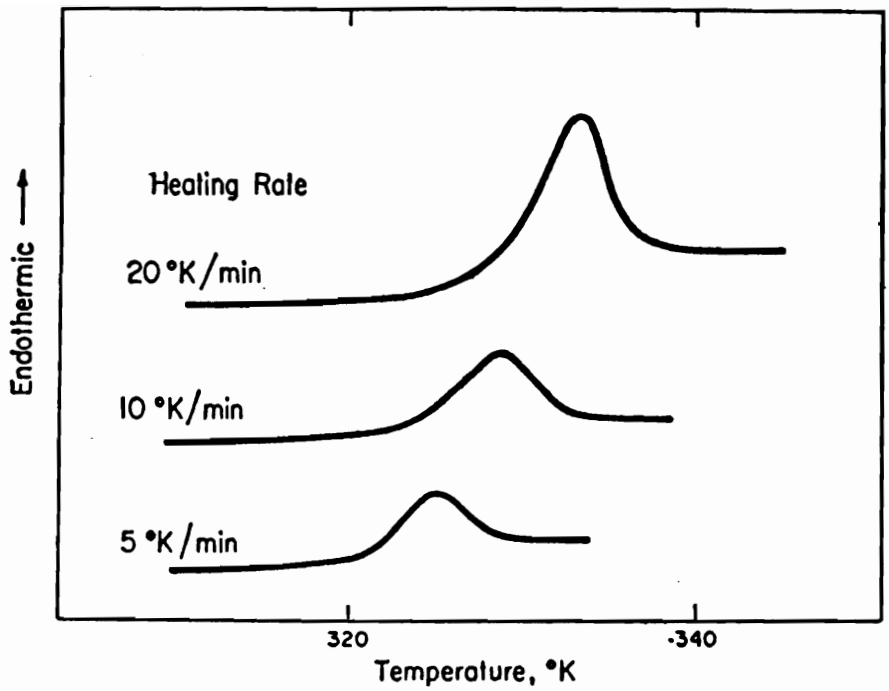

Figure 2.2-20. DSC scans of Aroclor 5460 annealed 195 min. at 306 K. (from [113]).

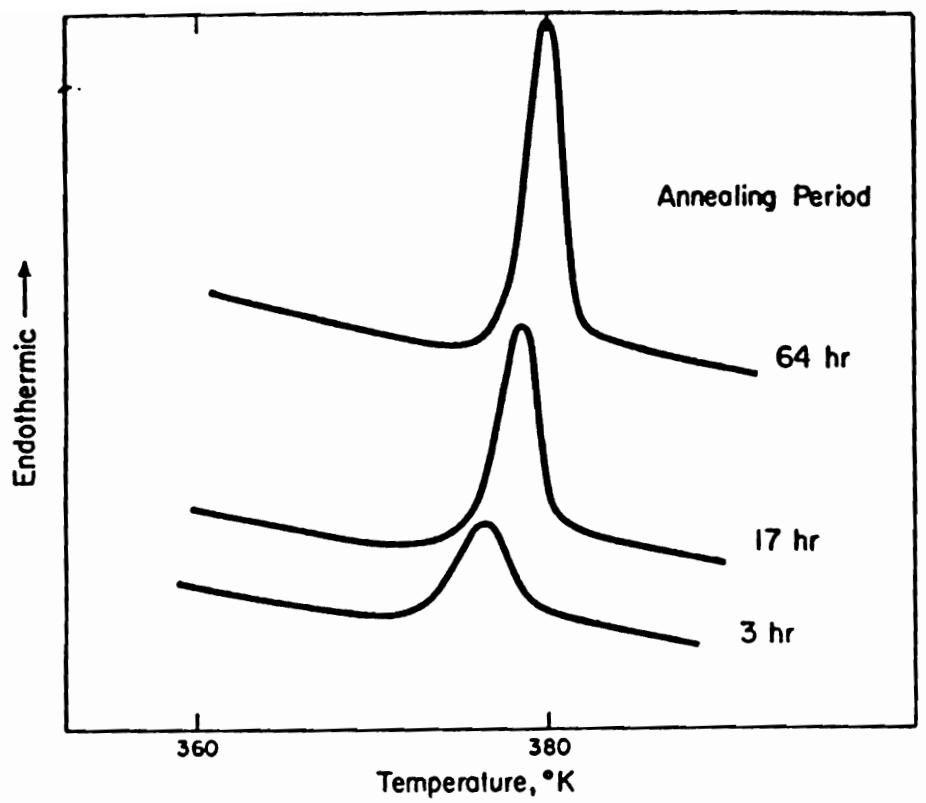

Figure 2.2-21. DSC scans of atactic PS annealed at 355 K for various annealing times. Heating rate was 5°C/min (from [113]).

made. Some of these are again described here. Chow and Prest[118] showed that the phenomenological models derived from volume and enthalpy relaxation are equivalent.[74] Adachi and Kotaka[119] found that volume and enthalpy relaxations were similar but not quite the same for both a broad and narrow MWD polystyrene. They determined that the change in enthalpy per unit change in volume (obtained by correlating enthalpy and volume relaxation data) was approximately 2.0 kJ/cc. If one instead calculates $(\partial H/\partial V)$ from thermodynamics ($= \Delta C_p/\Delta\alpha * V$) a much smaller value of 0.9 kJ/cc is obtained.[117] It is uncertain why this discrepancy exists but it appears that the enthalpy changes are larger than expected from specific heat measurements since the observed volume changes are consistent with other values.[117] Mijovic and Ho[120] showed that the relaxation times for enthalpy relaxation and viscoelastic relaxation were comparable. Mijovic and coworkers[74] warn, however, that viscoelastic measurements involve the application of a stress which will affect the relaxation process. Sasabe and Moynihan[121] analyzed poly(vinyl acetate) and found that the enthalpic and volumetric relaxations were longer than the dielectric and viscoelastic relaxations. This is demonstrated in Figure 2.2-22. O'Reilly and Sedita found that the temperature dependence of the dielectric and enthalpic relaxation times are the same for PS, PC and tetramethyl polycarbonate, along with the associated blends.[122]

Berens and Hodge[123] studied PVC treated with a variety of thermal, mechanical and vapor treatments. They found that the magnitude and not the position of the endothermic peaks was dependent on the sample treatment prior to aging. Peaks were enhanced by increased rates of quenching, mechanical stressing, and by prior exposure to a swelling vapor. However, the presence of a vapor during aging supressed the endotherms.

Robertson has expressed some concern with the use of DSC for measuring enthalpy relaxation based on predictions from a theoretical model in which he developed.[124] Possible problems that are predicted to occur include " (1) underestimation of the conformational heat capacity, (2) the incorrect comparison of specimens aged at different temperatures and (3) uncertain energy of the quenched state." These problems arise because of the distributions of free volume that occur. Robertson notes however, that

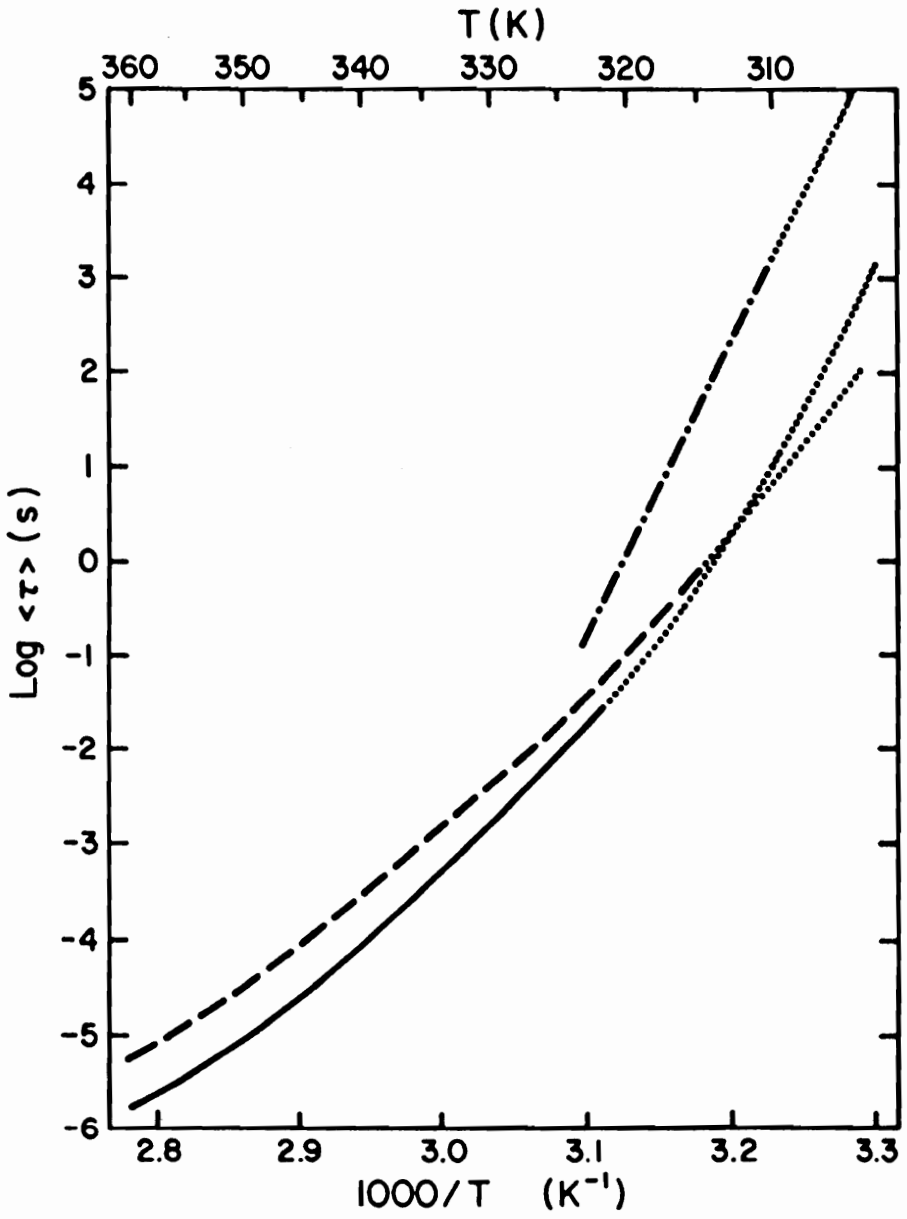

Figure 2.2-22 Arrhenius plot of mean relaxation times for poly(vinyl acetate) versus temperature for enthalpy (·-·-·-), dielectric (- - - -), and viscoelastic relaxation (——) (from O'Reilly [117] after Sasabe and Moynihan [121]).

the predictions are questionable because of the uncertainty present in several of the critical parameters.

2.2.5 Positron Annihilation Studies

Positron annihilation is a relatively new tool which can give quantitative information on the number and size of free volume holes in a polymer. Compared to other tools such as photochromic and fluorescence probes, positron annihilation has a much smaller effective probe size thereby providing greater measurement sensitivity coupled with a lower likelihood of hole distortion. X-ray scattering, while not causing any structural distortion, is not nearly as sensitive at resolving changes in the atomic scale voids.[125] Positrons are nothing more than the antiparticles of electrons. They can be formed from a radioisotope such as ^{22}Na which is coated onto the sample to be measured. Positrons that are injected into the sample penetrate anywhere from 10 to 10000 μm so they effectively reach the bulk of the sample before annihilating.[126]

Although there are different modes of annihilation, the most important for polymers is that of ortho-positronium (o-Ps) annihilation. Ortho-positronium is a hydrogen-like atom consisting of a proton and a positron and having a diameter of 1.06 Angstroms. It forms when an electron captures a positron during the slowing down of the injected positron. Like positrons, ortho-positronium preferentially resides in atomic size holes (i.e. free volume sites). The larger the hole, the longer the lifetime of the ortho-positronium prior to annihilation by a "pick-off" process with a neighboring electron. Herein lies the basis for the positron annihilation technique. By measuring the lifetimes of the o-Ps atoms, the hole size can be determined by direct correlation with known references.

Because the formation and annihilation of positrons is associated with the release of photons of differing energies (1.28 MeV and 511 keV respectively), lifetimes can be determined by using a pair of detectors--one tuned to detect the birth signal and one for the annihilation--along with the proper supporting electronics. Typical o-Ps lifetimes in a polymer are 1 to 2 nanoseconds so resolution of the system is very important. The number

of annihilation counts, or the intensity I_3, is proportional to the number of holes present in the sample. And, as stated before, the average lifetime of the o-Ps, denoted as τ_3, is related to the size of the holes. Combining the two gives a measure of the total free volume in the sample.

During positron annihilation lifetime spectroscopy (PALS), the annihilation spectra is curve fit as the sum of exponentials in order to obtain τ_3 and I_3.[125]

$$N(t) = \sum I_i \exp(-t / \tau_i) + B \qquad (2.2\text{-}21)$$

where B is a constant and N(t) is the total spectra. Generally the sum is only carried out with the first 3 terms. The first two are related to para-Ps and unbound positron annihilation respectively and are not important for the study of free volume. Note that with this procedure only an average value for τ_3 and I_3 is determined. To account for the distribution of lifetimes, Jean and coworkers extended (2.2-21) to include a continuous spectrum of τ's, [125]

$$N(t) = \int_0^\infty I(\tau) \exp(-t / \tau) d\tau + B \qquad (2.2\text{-}22)$$

An example of the application of this equation is shown in Figure 2.2-23 for polypropylene exposed to different levels of hydrostatic pressure. Clearly the pressure causes a decreasing average hole size, as expected, based on the changes in the lifetimes.

Before looking at some representative studies, it is first necessary to relate τ_3 to the mean hole radius. This is done via a simple quantum mechanical model which assumes a particle in a spherical box. By using zeolites with known hole sizes to fit the empirical parameters, one arrives at[127,126]

$$\tau_3 = \frac{1}{2}\left[1 - \frac{R}{R + 1.66} + \frac{1}{2\pi} \sin \frac{2\pi R}{R + 1.66}\right]^{-1} \qquad (2.2\text{-}23)$$

where τ_3 is in nanoseconds and R is the hole radius. Although this equation is based on a rather crude model, more detailed models based on finite potentials have shown that it is

still valid as long as the empirical parameters are properly curve-fitted.[128] Jean and Shi have extended this model further to account for elliptical instead of spherical holes.[129] The authors found that an elliptical hole should have a shorter o-Ps lifetime than a spherical hole of the same volume due to the enhanced probability of pick-off annihilation occurring along the more narrow, minor axis of the ellipse. This has practical implications since it is doubtful that free volume sites are perfectly round. In a previous paper, Jean and coworkers[130] had applied angular correlation positron annihilation (ACAR) to stretched PEEK samples--cold drawn to a stretch ratio of 2.6--and already shown that the holes had ellipsoidal geometries with an average aspect ratio of 2.6+/-0.2.

There have been a number of applications of PALS to physical aging and mechanical deformation. Generally it is found that I_3 decreases significantly while τ_3 changes negligibly with physical aging.[131,132,127] This implies that the average hole diameter does not change, only the number of holes decrease. Figure 2.2-24 shows this behavior for bis-A polycarbonate. It is possible that the lack of accounting for the distributed nature of the hole sizes may be the cause for the constant "mean" value of τ_3 seen during physical aging. Application of Eqn. (2.2-22) may help to better resolve this issue.

Jean and coworkers have applied Eqn (2.2-22) in order to determine the free volume distribution in polystyrene as a function of temperature.[133] Their results are reproduced in Figure 2.2-25. Note that the roll-off at low free volume is in the vicinity of a 1 to 2 angstrom hole, the limit of detection of the positron technique. A comparison of their data with the Cohen-Turnbull theory shows large deviations at higher volumes (> 100 cubic angstroms). In addition, a comparison of the PALS data with results from a photochromic probe show that the PALS is less sensitive to larger diameter holes. Using molecular dynamic simulations, Roe found that larger void cavities in glassy polyethylene were constantly expanding and contracting with a period as short as 5 to 10 ps.[134] The polyethylene is predicted to have a T_g between 175 and 225 K depending on molecular weight (i.e. number of segments in the model) and actual cooling rate. If this expansion and contraction of free volume is also occurring in the polystyrene glass, then it is possible

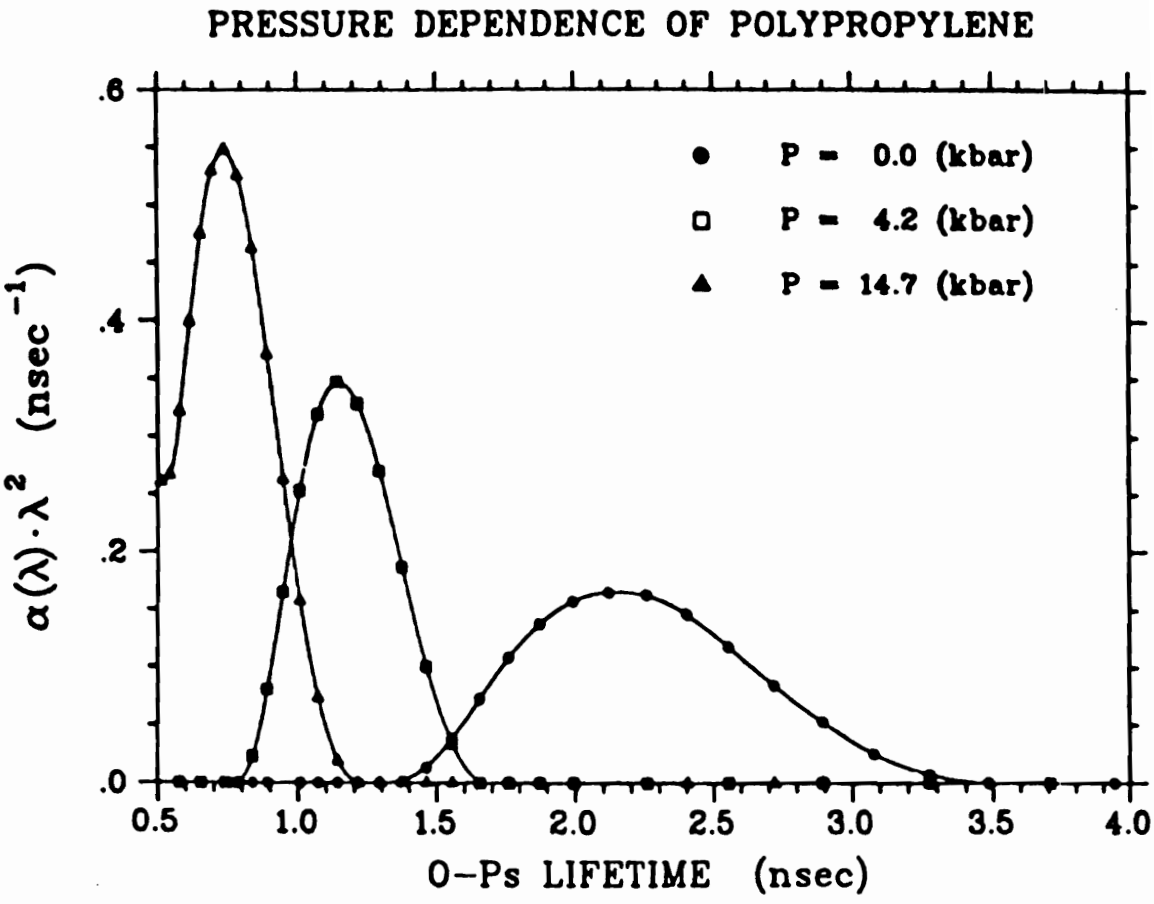

Figure 2.2-23. Effect of hydrostatic pressure on the o-Ps lifetime spectrum in polypropylene (from [125]).

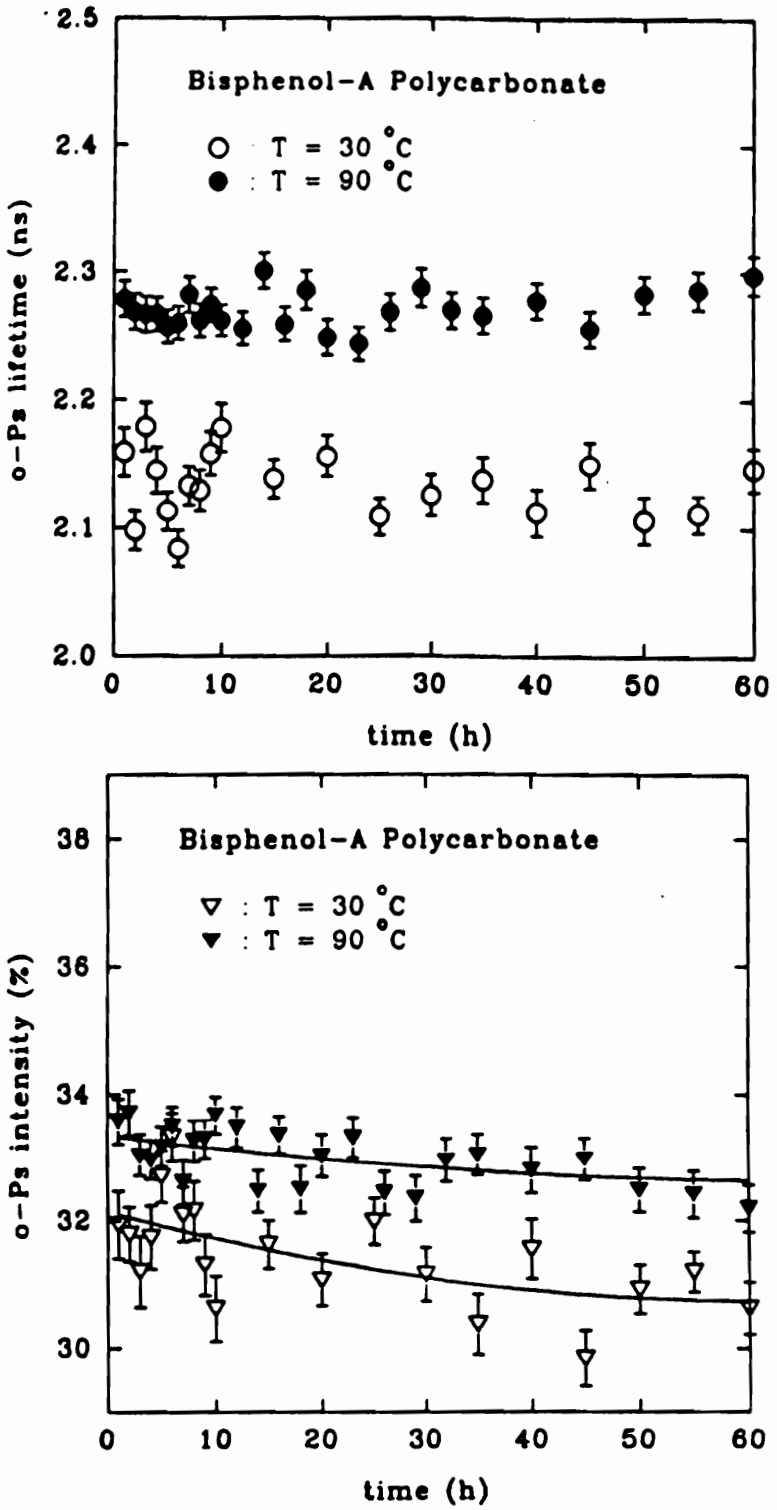

Figure 2.2-24. Physical aging of PC at 30 and 90°C. The top curve is τ_3 and the bottom is I_3 (from J. E. Kluin, et al., *Macromolecules 25,* 5089 (1992).

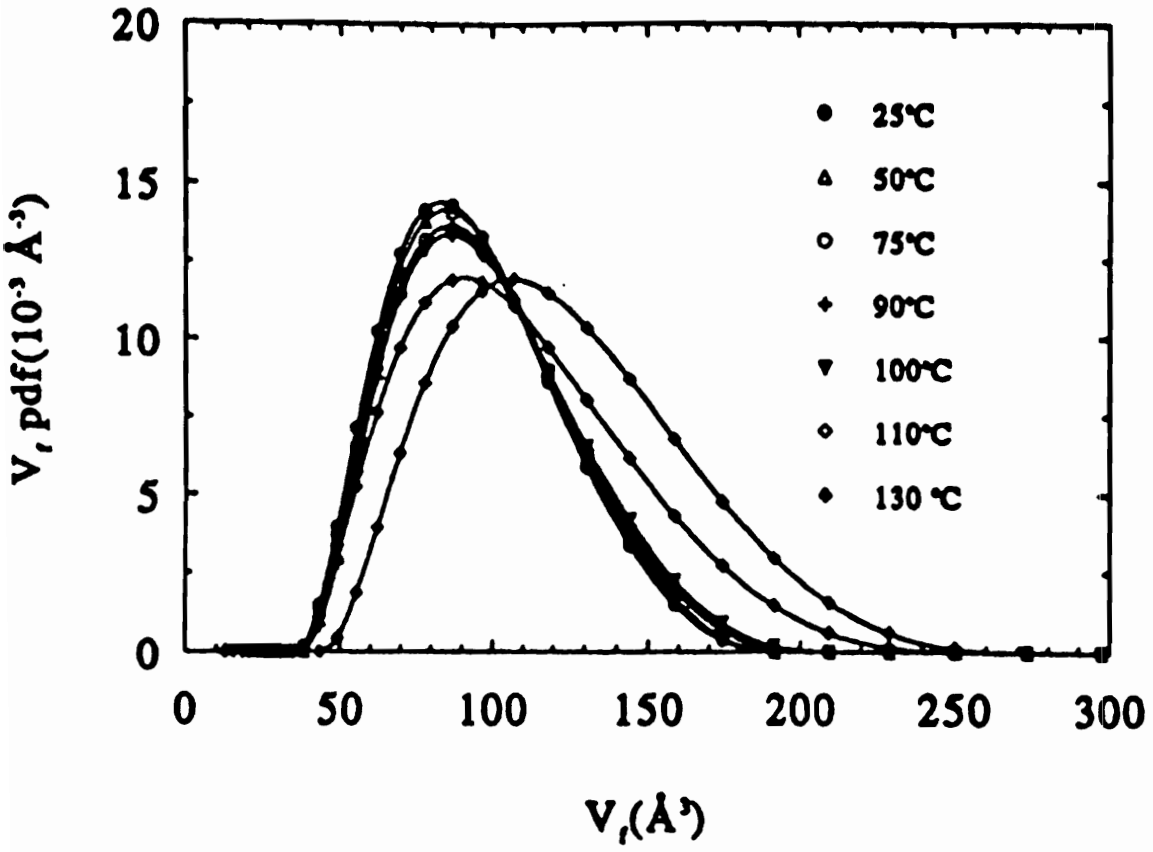

Figure 2.2-25. Free volume distribution in polystyrene at different temperatures from PALS data (from [133]).

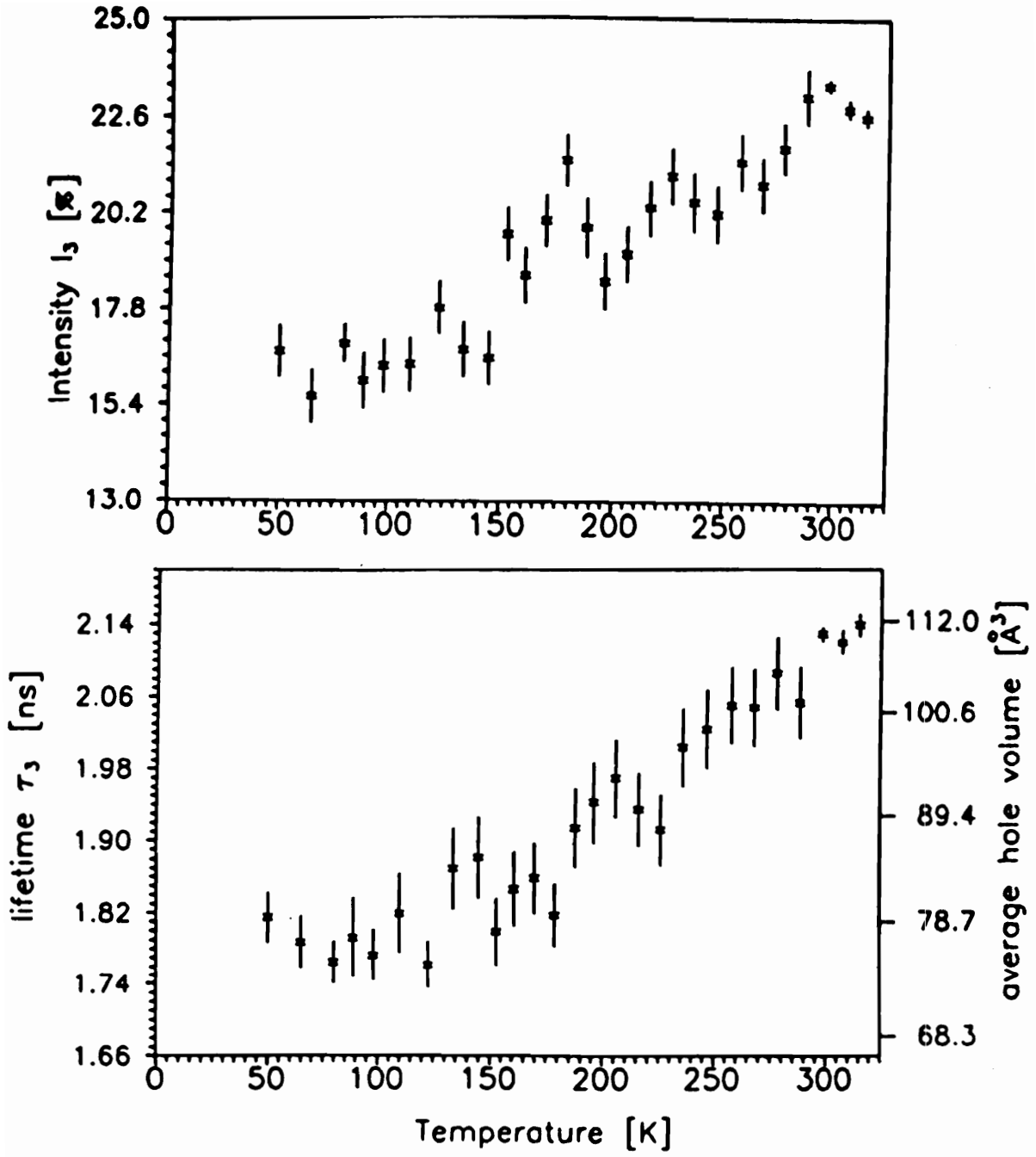

Figure 2.2-26. PALS data for polycarbonate as a function of temperature (from [135]).

that this fluctuation in the larger holes may be responsible for the lack of PALS sensitivity to the larger holes. Keep in mind that the o-Ps lifetime is 1 to 2 ns whereas the hole diameters are changing on a picosecond time scale. A comparison of the data with the theory of Simha and Somcynsky gives much better results.

Kristiak and coworkers used PALS to probe the free volume microstructure of polycarbonate at low temperatures.[135] Their data is shown in Figure 2.2-26 as a function of temperature. A transition in the free volume behavior was found to occur at approximately 130 K as seen in the change in slopes in Figure 2.2-26. They hypothesized that a partial flipping motion of the phenyl ring is responsible for this transition.

Ruan and coworkers studied the effects of static tensile deformation on the annihilation behavior of polycarbonate.[136] They found that the apparent free volume--based on τ_3 measurements--increased with tensile strain up to 4% at which point it leveled off (the intensity, or number of holes, remained constant however). This is in apparent contradiction to the density data for polycarbonate, described earlier, wherein the density actually increased with stretching. It is important to note, however, that the density data involved strains considerably higher than the 4% in the PALS work and it is uncertain what is happening to the density at smaller strains. In addition, the "leveling off" of the PALS free volume at 4% may be in some way related to high strain densification. The authors also studied the effects of physical aging on the strained samples. The samples were aged at room temperature while being maintained at 3% strain. After 200 hrs., the strain was released and aging allowed to continue. It was found that the fractional free volume actually dropped to a lower value than the original unstrained level after unloading.

Liu and coworkers[137] studied the effects of cyclic stress on the structural changes in aged polycarbonate. They found the lifetime τ_3 increased with cyclic stressing as long as crazing did not occur. The intensity, I_3, decreased with cycling. They attributed these changes to an increase in structural damage in the sample causing larger hole sizes, while

at the same time, the possiblility for hole coalescence which would explain the decrease in the intensity, I_3.

Even with these apparent successes, positron annihilation is still not without its share of controversy. Li and Boyce[138] believe that during extended PA testing, an electric field will build up in the polymer possibly affecting the lifetime measurements. It has been shown elsewhere that the presence of an external electric field will decrease the probability of o-Ps formation in several polymers.[139,140,141] Therefore the observed decrease in I_3 would be unrelated to structural relaxation. This has obviously been very controversial. However, by not running extended tests with any given sample, this problem can be avoided.

2.3 Orientation in Polymers

There are a number of excellent books and papers available which describe the characterization of orientation in polymers.[142,143,144,145] Only the techniques most appropriate for studying orientation in amorphous glasses will be reviewed. This includes the quantification of the orientation state by way of the Hermans' orientation function.

Orientation is an important fact of life for polymers. It is present to some degree in most end-use plastic products so its effects on aging should not be neglected. Many of the more common fabrication processes such as injection molding and extrusion (profile, sheet, etc.) introduce some level of orientation even when it is not necessarily desirable. Others such as thermoforming, injection and extrusion blow molding, calendering, and film blowing introduce a greater degree of orientation which is usually, but not always, beneficial to the final product. Lastly, there are other processes such as fiber spinning, film tentering, stretch blow molding, and double-bubble film blowing where high orientation is the goal. These processes generally involve crystalline or semi-crystalline polymers and the orientation process can act to induce or modify the crystal formation. It is important to realize that the crystal structure in polymers can and often does have a

different preferred orientation than the amorphous chains. This adds extra complications to the orientation analysis.

2.3.1 Hermans' Orientation Function

To aid in explaining the concept of orientation, the reader is referred to Figure 2.3-1. This shows a polymer chain with end to end chain distance R, oriented at an angle θ to the z axis. The coordinate system x-y-z represents a laboratory frame of reference which is fixed in space. Generally the directions are taken to coincide with the machine or primary stretch direction (MD), the transverse direction (TD) and the thickness or normal direction of a stretched sample. For uniaxial orientation, the Hermans' orientation function f, is defined as [142]

$$f = \frac{3 < \cos^2 \theta > -1}{2} \qquad (2.3\text{-}1)$$

where the angled brackets represent an average over all of the chains in the system. The orientation function f can vary between -0.5 and 1 with 1 representing perfect orientation along the z-axis ($\theta = 0°$), $f = 0$ representing a completely random unoriented state ($\theta = 54°$), and $f = -1/2$ representing perfect orientation at an angle $\theta = 90°$. Note that in dealing with multi-phase systems such as blends or in crystalline polymers, a separate function f_i, is required for each phase. This complicates the determination of the orientation since multiple analytical techniques are usually required to distinguish each phase. Application of one "average" orientation function to a multicomponent system is not generally recommended. A limitation of the orientation function is that it only conveys a second moment average of the orientation state in the polymer. A more accurate means of describing the state of orientation would be to define an orientation envelope or to include higher order moments. In general, however, mechanical properties and other signifcant quantities are often found to be adequately modeled by the second-moment average.[146] In addition, second moment averages are much easier to obtain experimentally.

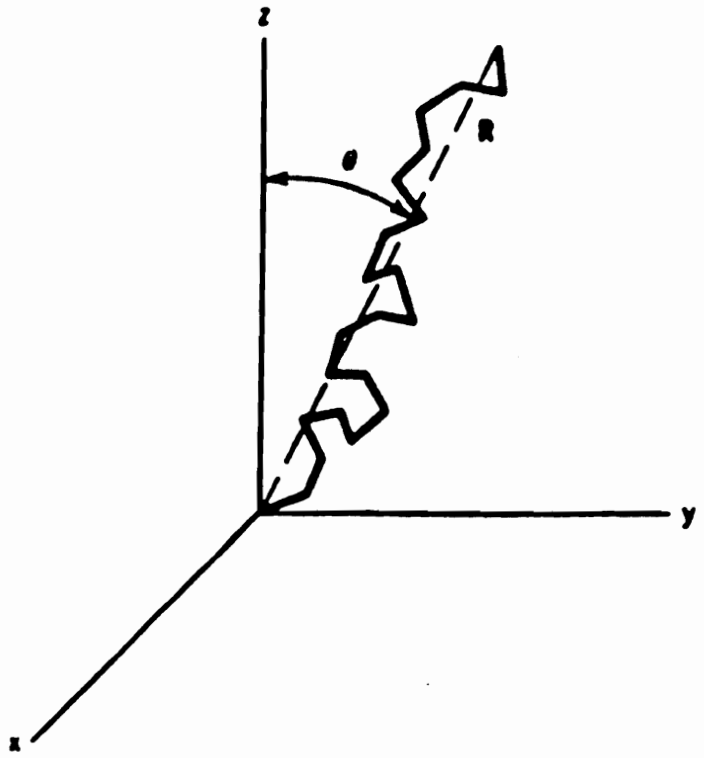

Figure 2.3-1. Orientation of polymer chain with respect to laboratory frame of reference (from [142]).

2.3.1 Methods for Determining Orientation

One of the more common methods for measuring orientation in amorphous polymers is via optical birefringence.[142] The birefringence is defined as the difference in refractive index *n*, between two orthogonal directions in the material. The refractive index is defined as the ratio of the speed of light in a vacuum to the speed of light in the material of interest. Because there are 3 mutually orthogonal directions, there will be three values of birefringence although only two are found to be independent.

$$\begin{aligned} \Delta_{xy} &= n_x - n_y \\ \Delta_{xz} &= n_x - n_z \\ \Delta_{yz} &= n_y - n_z = \Delta_{xz} - \Delta_{xy} \end{aligned} \qquad (2.3\text{-}2)$$

For uniaxially oriented systems (with the stretch direction along the z-axis), only one value for the birefringence is required since the refractive indices in the two perpendicular directions (x and y) are the same. With glassy amorphous systems, an additional type of birefringence known as distortional or glassy birefringence can occur. This birefringence is due to distortion of the bond angles and bond lengths in the system. It can arise from thermal residual stresses which occur due to a rapid quench, or from stressing a glassy polymer in general. Cold drawing would produce some glassy birefringence in addition to normal orientational birefringence. Glassy birefringence is often used by engineers in the area of photoelasticity, as a means to determine stress differences in a loaded component.[147]

Birefringence can be measured in a number of ways. One method is to measure the refractive indices directly as with an Abbe' refractometer. Another method is to place the sample, oriented appropriately, between crossed polarizers and analyze the intensity of transmitted light. This can be done with a photomultiplier or by using a compensator such as the commonly used Babinet compensator. The interested reader is referred to the references cited earlier for a complete description of these methods.

To relate the birefringence of an amorphous polymer to the Hermans' orientation function requires an additional parameter $\Delta°$, known as the intrinsic birefringence. This is the birefringence for a polymer assuming it is perfectly oriented ($f = 1$). This leads to the relation,

$$f = \frac{\Delta}{\Delta^o} \qquad (2.3\text{-}3)$$

Polycarbonate has an intrinsic birefringence of 0.236 as measured by Biangardi,[148] a value of 0.062 by Struik,[145] and a value of 0.106 by Pietralla.[149] In this study, the intrinsic birefringence was found to be 0.16. There are a number of ways to determine this parameter. The first involves calculation using bond polarizabilities and follows the procedures outlined by Denbigh.[150] This approach neglects internal field effects which are often significant.[144,151] The alternate and more accurate method is to determine $\Delta°$ by extrapolation of experimental measurements. This involves combining simultaneous birefringence measurements with another technique such as infrared dichroism, sonic velocity, or x-ray. First, the birefringence is measured for a series of samples having differing levels of orientation. Next the orientation function is determined for the same series with an alternate technique and the values plotted together. By extrapolating the existing data to the value $f = 1$, the value for $\Delta°$ is then determined.

Sonic velocity, or sonic modulus measurement as it is also called, involves measuring the speed of sound through the sample. Sound waves will, in general, travel faster down the chain axis than transverse to it. The implications to orientation measurement are obvious. By comparing the sonic velocity of an oriented sample to that of the unoriented sample, one can determine the orientation function by way of[152]

$$f = 1 - \frac{c_u^2}{c^2} \qquad (2.3\text{-}4)$$

where c_u is the unoriented sonic velocity and c is the oriented sonic velocity. Because of some simplifying assumptions made during the derivation, the above equation breaks

down for highly oriented systems or as f approaches 1. If desired, the sonic modulus of the sample can be determined by $E = \rho c^2$ where ρ is the sample density. As with birefringence measurements, determination of orientation functions for multiphase systems is more complicated and the reader is referred to the reviews described earlier for more details.

Other common methods for measuring orientation include x-ray and dichroism measurements.[142, 153] X-ray measurements are generally most useful for crystal orientation and see only limited use in purely amorphous systems. On the other hand, infrared (IR) dichroism measurements have the advantage of often being able to determine the orientation of both crystalline and amorphous phases simultaneously, as well as being able to easily study multiphase systems. IR dichroism involves measuring the absorption spectra for a sample using a polarized incident infrared source. Samples must be thin enough for accurate absorption measurements to be made. The various phases in the material will selectively absorb the radiation differently so their orientations can be determined independently of one another. Polymeric materials absorb in the IR range because of changes in the vibrational states of any induced dipoles. Depending on field symmetry, each vibrating dipole may contribute to one of the absorption peaks seen in the spectra. It is important to know the angular orientation α of the chromophore's transition moment with the chain backbone in order to determine the orientation function. For example, the "stretch" of a carbonyl group has a transition moment which is nearly perpendicular to the chain backbone (i.e. $\alpha \sim 90°$). This is one of the drawbacks of using dichroism since the chromophores contributing to a given absorption peak may not be known for a given polymer (however, even knowing the chromophore does not guarantee that α is known). To complicate matters, many of the absorption peaks may overlap making it difficult to find one which is acceptable for quantitative analysis.

The next step in dichroism measurements is to measure the absorption A ($A = \log(I_o/I)$ where I and I_o are the transmitted and incident intensities respectively) for the sample with the polarizer aligned parallel and then perpendicular to the machine direction.

Note that only one polarizer is needed unlike birefringence meaurements where two crossed polarizers are generally required. The dichroism D is defined as

$$D = A_{par} / A_{perp} \qquad (2.3\text{-}5)$$

and is related to the orientation function by

$$f = \left(\frac{D_o + 2}{D_o - 1}\right)\left(\frac{D - 1}{D + 2}\right) \qquad (2.3\text{-}6)$$

where D_o represents $2\cot^2 \alpha$. This term accounts for the orientation of the chromophore relative to the chain axis. The sensitivity of the dichroism technique depends on α. If α equals 54.7°, then the orientation function cannot be determined.

2.3.3 Shrinkage of Oriented Samples

Struik has presented a very thorough methodology for predicting shrinkage in polymer samples after orientation and parts of it will be reviewed here.[145] This is important for this work since shrinkage behavior is one of the main differences between samples which have been cold drawn and those which are hot-drawn. The process often involves non-isothermal creep behavior so an effective time, λ_{eff}, has been defined as

$$\lambda_{eff}(t) = \int_0^t a[T(\varsigma), T_r]\, d\varsigma \qquad (2.3\text{-}7)$$

where a is a shift factor depending on the instantaneous temperature and the reference temperature T_r. The parameter ζ is a dummy variable. As with the physical aging tests, the shift factor allows for the determination of a creep curve at some given temperature based only on a creep curve already known at some other reference temperature. It is assumed that temperature has no other effect than to change the rate of creep and therefore shift the reference curve horizontally along the time axis. In most cases, Boltzmann superposition applies although more general derivations were presented where this was not assumed. These usually provided the same results, however. For simplicity

of argument, it will be assumed that superposition holds. Accordingly, the orientation process is treated as a series of step loadings (i.e. stress control) in which the Boltzmann integral can be applied. By choosing a reference temperature and then shifting into the effective time domain (λ_{eff}), one can predict shrinkage behavior as a multi-stepped creep process.

The first prediction presented is the shrinkage which occurs after hot drawing. The sample is assumed to be stretched at some temperature T_o above T_g and at a stress σ_o. After stretching, the sample is quenched to a temperature T_1 in the glass. After a short waiting period, the stress is removed and the recovery measured. If the loading stress σ_o was small to begin with, then the shrinkage strain can be accurately predicted by

$$\varepsilon_{shr}(t) = \sigma_o F_{orient}(T,t) \approx \sigma_o F_{unor}(T,t) \qquad (2.3\text{-}8)$$

where F_{orient} and F_{unor} are the oriented and unoriented compliances. Note that small loading stresses imply small internal stresses in the glass and little difference between the compliance function before and after loading. This can be conceptualized through the spring and dashpot model in Figure 2.3-2. The dashpot viscosity is assumed to be almost infinite below T_g and about zero above T_g. It is further assumed, however, that the dashpot viscosity strongly decreases with increasing stress. As an example, when a polymer is stretched above its T_g, the dashpot will flow freely and only orientation in the rubbery spring will occur. However, upon quenching, the dashpot locks in place and the internal stress of the rubbery spring acts against it. For low internal stresses, little yielding of the glassy spring-dashpot combination occurs and (2.3-8) holds. However, for higher internal stresses (or higher σ_o), the dashpot will flow more readily and the shrinkage strain increases. The equality on the left hand side of (2.3-8) is still applicable but the approximation to the right is not. F_{orient} will now be significantly less than the unoriented compliance. Note that with high internal stresses, (2.3-8) only holds at temperatures well below T_g. For high internal stresses and temperatures approaching T_g, we have

$$\varepsilon_{shr}(t) > \sigma_o F_{orient}(T,t) \qquad (2.3\text{-}9)$$

since excessive yielding and flow is occurring in the dashpot.

The same analysis can be extended to cold drawn samples. By stretching in the glass, much higher internal stresses are entailed in order for flow and drawing to occur. The loading stress must exceed the yield stress in order for flow to occur. After drawing, the remaining internal stress is approximately equal to the yield stress of the sample at the stretch temperature. Therefore the sample is already in a nearly unstable state. Since the yield stress generally drops with increasing temperature--this corresponds to a slight decrease in the viscosity of the dashpot--any attempts to raise the temperature will mean that the internal stress becomes higher than the yield stress and shrinkage occurs. Restated, cold-drawn samples will generally show excessive shrinkage at temperatures just above the stretch temperature. This is further shown in Figure 2.3-3 for polycarbonate.

2.4 Review of Aging Studies on Oriented Polymers

There have been a limited number of studies on the physical aging behavior of oriented systems, most related to cold drawing. This section will review these studies along with other papers that examine orientation-molecular mobility relations in polymers. Emphasis will be on polycarbonate data whenever applicable.

One of the only melt drawn studies was performed by Struik.[154] Here tensile creep measurements were made on melt oriented (rigid) PVC drawn at 82°C. The Tg was not specified but the stretch temperature was listed as being above Tg (a typical Tg for rigid PVC is about 80 °C). Samples were drawn up to a maximum stretch ratio of 2.2X and then quenched to 20°C at which point aging commenced. Analysis of the shift rates from the creep tests at 20°C showed little change with increased stretching. This data, in addition to the compliance values, is reproduced in Figure 2.4-1, as a function of stretch ratio. Struik believes that, because the level of molecular reorientation is actually very small in most oriented polymers (i.e. very low orientation functions), the aging behavior

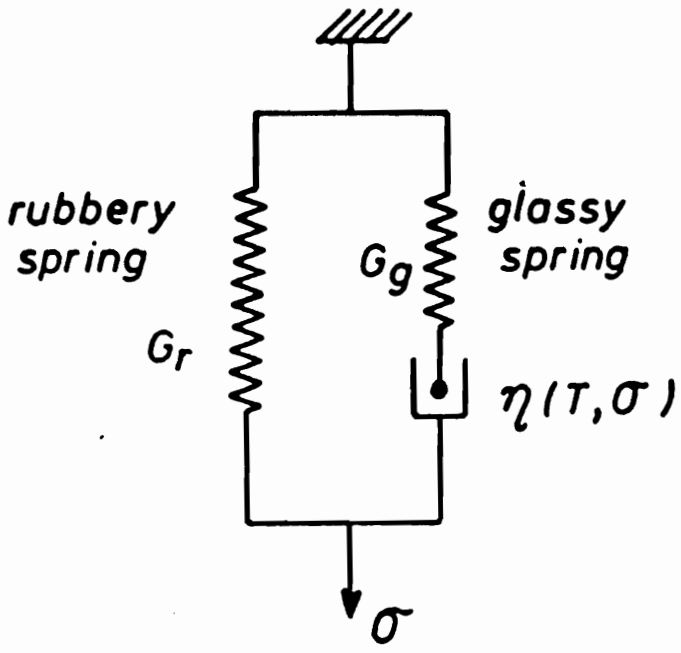

Figure 2.3-2. Mechanical analog for glassy state (from [145]).

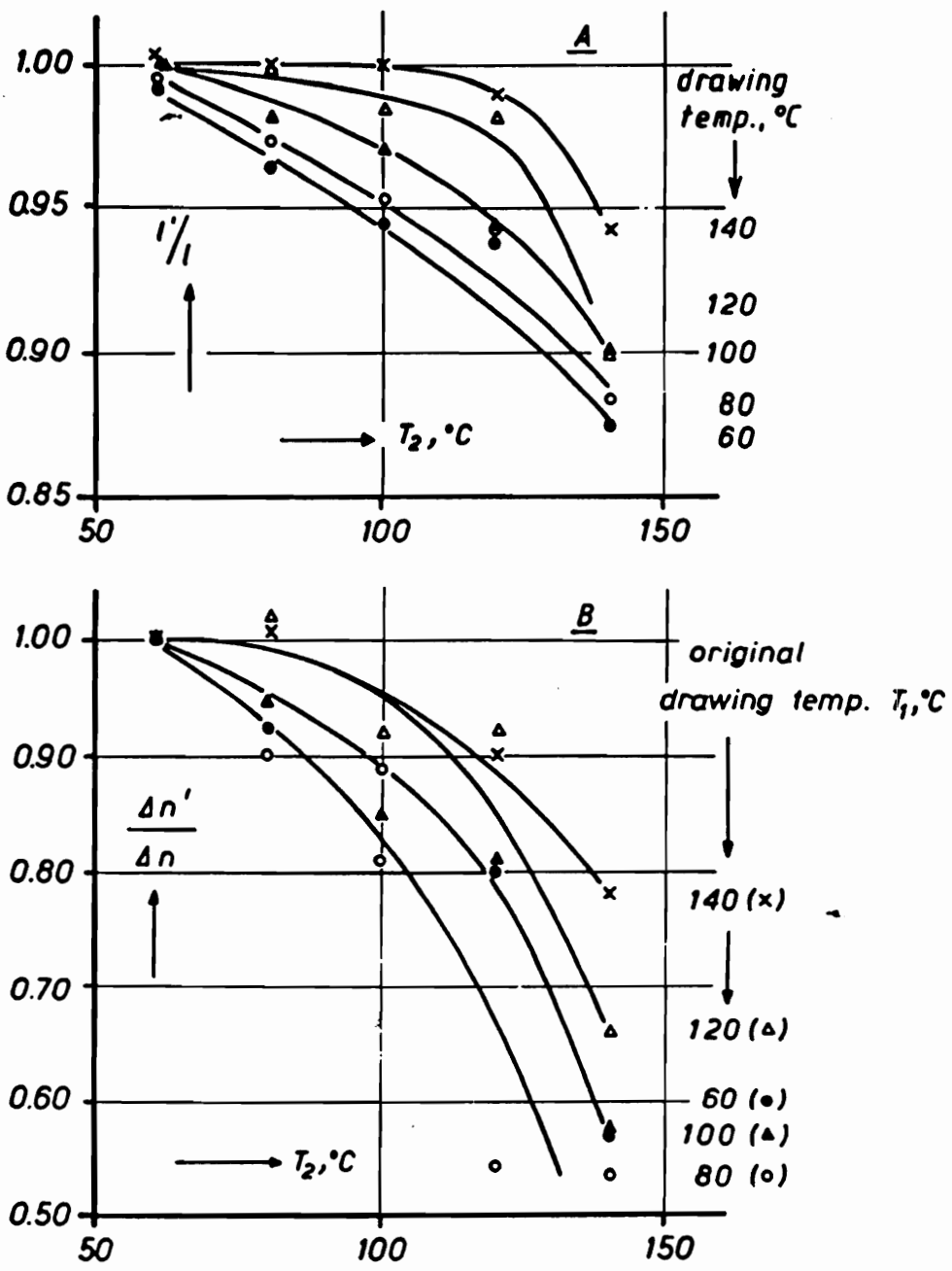

Figure 2.3-3. Fractional residual length l'/l and birefringence Δn'/Δn for samples of polycarbonate cold drawn at various temperatures T_1. Recovery at T_2 during 1/2 hour (from [145]).

should not be significantly affected. No data on the orientation functions or possible formation of crystallinity in the stretch samples was presented.

Pixa and coworkers[155] analyzed the effects of cold drawing polycarbonate at room temperature. Volume relaxation rates of the cold drawn samples were compared with isotropic samples using volume dilatometry. Stretch ratios were typically 1.7 for all samples tested. They found that volume relaxation rates were nearly 2.5 times higher for the cold drawn samples than for the isotropic samples at room temperature. Another important finding was that polycarbonate actually densified upon stretching. Nonetheless, even with the initial densification, the cold drawn samples still showed faster rates of volume relaxation. This has important implications for the concepts of free volume and molecular mobility. With the cold drawn samples, their lower specific volume would normally indicate a lower free volume and therefore a lower molecular mobility. A lower mobility, on its own accord, should then result in a slower volume relaxation rate. Since the relaxation rate was not slower, it is suspected that the free volume theory may be inadequate. Also, it may be possible that the distribution of the free volume, and not just the total amount, is the important factor.

That density increases in polycarbonate with stretching has also been observed by others for cold drawing[156,157,158,159] and by Ito and coworkers for hot drawing.[160] Density data plotted as a function of stretch ratio for the hot drawn samples is shown in Figure 2.4-2. It is important to understand the implications of this density increase. Normally, for a glassy continuum undergoing mechanical deformation, there will be a slight increase in volume. This is true as long as the Poisson's ratio is less than 0.5, the incompressible limit. Rubbery polymers approach this limit so hot drawing is expected to produce very little volume change (but still a slight increase). Glassy polymers typically have values in the neighborhood of 0.35 so cold drawing should produce significant dilatation.

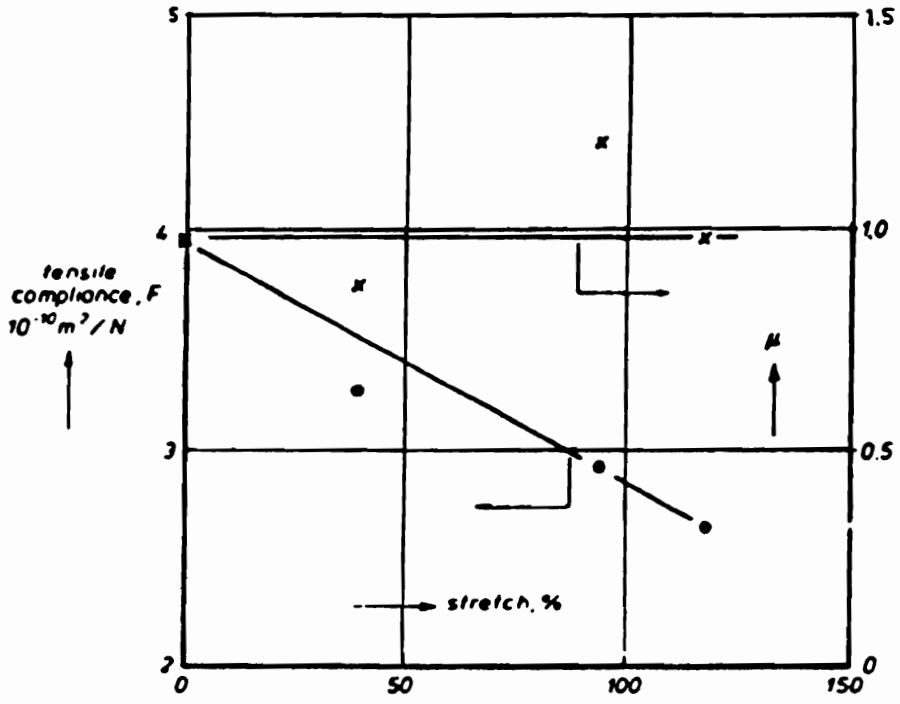

Figure 2.4-1. Shift factors and tensile compliance for rigid PVC versus the % stretch. Stretching performed above Tg (from [154]).

A comparison of the room temperature density data of Pixa and coworkers (cold drawn) with that of Ito and coworkers (hot drawn) shows a larger increase in density for the hot drawn samples with stretching. The cold drawn samples showed a density increase of 0.0017 to 0.0020 g/cc when drawn to a stretch ratio of 1.7. The hot drawn samples showed a density increase at the 1.7 draw ratio of 0.005 g/cc and a 0.009 g/cc increase at the 3.0 draw ratio. A "normal" 1.7X cold drawn sample showing no extraordinary densification would undergo a density *decrease* of 0.17 g/cc assuming a Poisson's ratio of 0.35! Keep in mind that a direct comparison is difficult since the stretch conditions were entirely different.

Bartos and coworkers[161] studied the physical aging behavior of cold drawn polycarbonate using dilatometry, X-ray, electron spin resonance (ESR) spectroscopy and some dynamic mechanical measurements. Samples were cold drawn up to 80% elongation at room temperature. They also experienced the same density increase for polycarbonate as described earlier. Volume relaxation rates were found to be about twice as high for the cold drawn samples as compared with the undrawn samples. In fact, it has been shown that between room temperature and 100°C, the rate of volume relaxation will be roughly twice that of isotropic polycarbonate.[162] This is in good agreement with the results of Pixa and coworkers[155] described earlier. Above 100°C, the volume relaxation rates were about the same. Using the absolute small angle X-ray intensity in the small angle regime, the particle density fluctuation (or volume fluctuation) was determined by way of

$$\frac{\delta\langle N^2\rangle}{\langle N\rangle} \sim \frac{I(s)}{I_o} \qquad (2.4\text{-}1)$$

where I_O is the primary beam intensity, $I(s)$ is the beam intensity at scattering vector s, and N is the particle density. It was found that the fluctuations increase due to drawing, even though the density is higher in the stretched sample (see Figure 2.4-3). These larger fluctuations correlate with the volume relaxation data, dissappearing above 100°C. This dissapearance also correlates with a secondary transition (denoted the α' transition) which

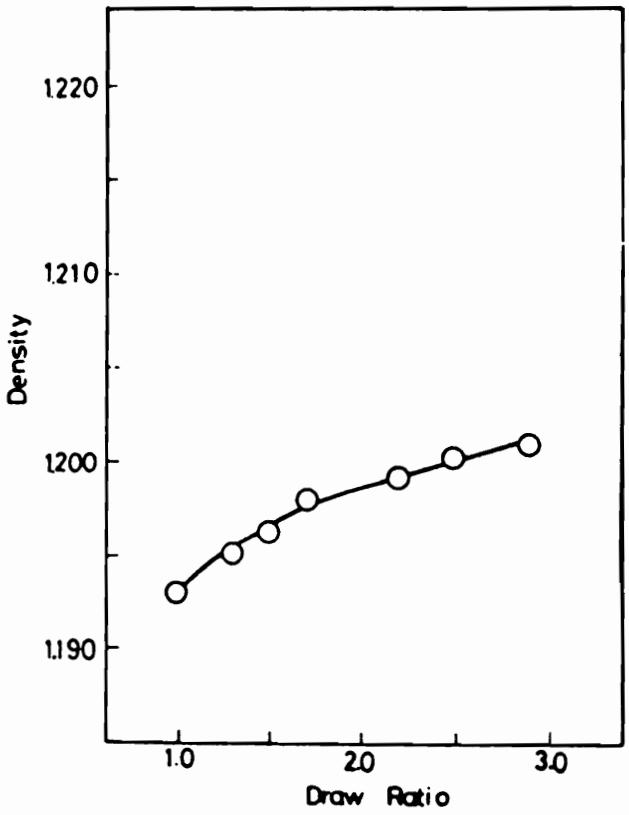

Figure 2.4-2. Density of hot drawn polycarbonate versus draw ratio (from [160]).

occurs in PC around 80 to 100°C. The higher mobility derived from this transition might be responsible for the narrowing of the free volume distribution and/or the relaxation of any internal stresses; either of which may be the cause of the enhanced volume relaxation rates. In contrast, ESR results did not agree with the X-ray data.[161] Instead, the ESR data indicate that the free hole space available is decreasing upon stretching. This may be partially explained by the larger probe size. The ESR probe is only sampling the larger free volume holes which may be behaving differently than the rest of the hole distribution. The authors theorize that a larger concentration of smaller holes forms upon stretching whereas the large hole concentration is decreasing slightly. Although the net free volume would increase, the ESR data would "see" a decrease due to its limited sampling capability. In addition, dynamic shear moduli were determined over a range of temperatures for the oriented samples before and after aging. This data is replotted in Figure 2.4-4. The important feature is the decrease in tanδ with increased aging between 0°C and 100°C. The high relaxation rates here are in agreement with the high volume relaxation rates discussed earlier.

Trznadel and coworkers[163,164] have followed shrinkage stresses in cold drawn polycarbonate and polyester as a function of aging time. These results were coupled with DSC, thermal expansion and birefringence measurements. For their first set of experiments, samples of PC were cold drawn at room temperature to a draw ratio of 1.9. The samples were then allowed to age at room temperature while changes in length, birefringence (Δn), and residual shrinkage stress (σ_r, the maximum stress obtained upon ramping the temperature of a constrained sample) were measured as a function of aging time. The data is shown in Figure 2.4-5. This data has been normalized with respect to the unaged values. In the figure, s refers to the residual strain and is defined as

$$s = \frac{\lambda - 1}{\lambda_m - 1} \tag{2.4-2}$$

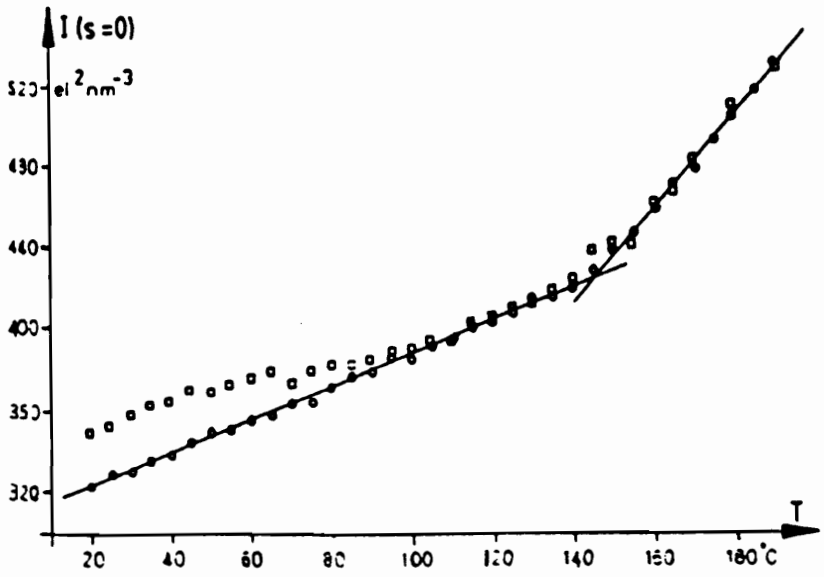

Figure 2.4-3. X-ray scattering intensity at s=0 representing thermal density fluctuations. Circles indicate isotropic PC and squares represent cold drawn PC (from [161].

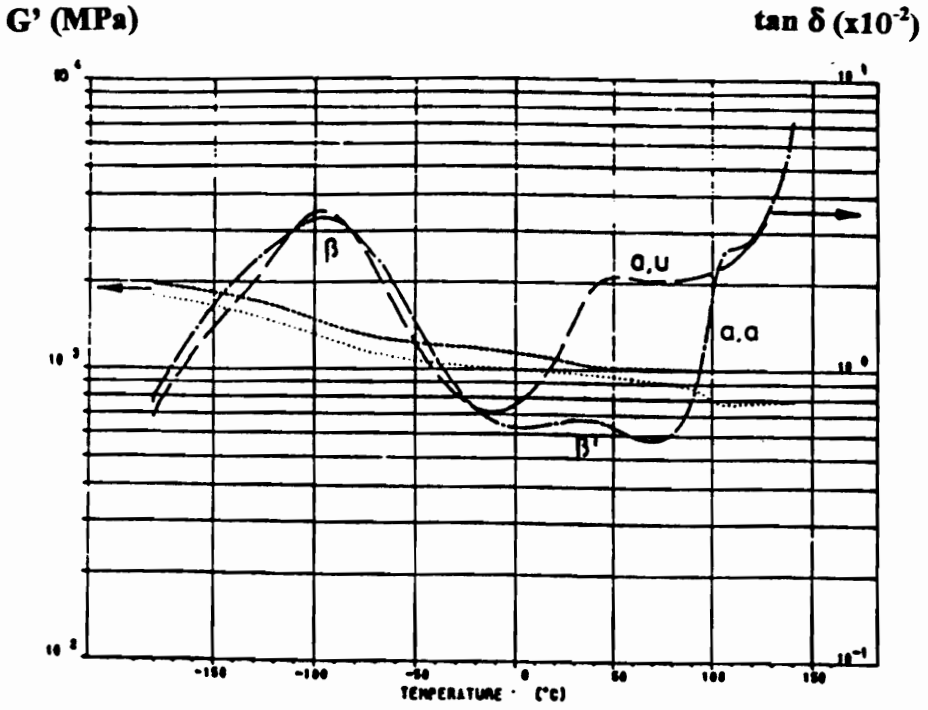

Figure 2.4-4. Dynamic shear data for cold-drawn polycarbonate. "a,u" represents anisotropic and unaged whereas "a,a" represents anisotropic and aged at 60°C for 12 days (from [161]).

where λ is the instantaneous stretch ratio and λ_m is the initial unaged stretch ratio. It is clear that the rate of birefringence loss is slightly larger than the change in length, whereas, the loss in residual shrinkage stress increases at an even faster rate than birefringence. LeGrand, studying the effects of residual stresses in polycarbonate bars at room temperature, also found the high residual stress relaxation with no significant dimensional changes.[165] These findings indicate that the cold drawn chains are able to relax by intermolecular slipping without necessarily affecting the overall dimensions of the sample. These results are important since they indicate significant chain mobility even in the glassy state. Both authors conclude that much of what is occuring with the cold drawn samples during physical aging can be attributed to the relaxation of internal stresses.

In another experiment, Trznadel and coworkers[164] followed the previously described shrinkage measurements with DSC measurements at the same heating rate. Samples were again aged at room temperature for different times and in both the cold-drawn and isotropic states. DSC measurements were performed on each sample both with the length constrained and allowing for free shrinkage of the sample ends. A sub-Tg endotherm occurred in the cold-drawn samples which grew in magnitude and moved toward higher temperatures with increased aging. A plot of the endotherms for the unconstrained, cold-drawn polycarbonate as a function of room temperature aging time is shown in Figure 2.4-6. This intermediate endotherm disappeared upon aging in the isotropic samples. It has been previously suggested that the intermediate endotherms which occur initially in isotropic samples are due to non-relaxed stresses in the sample which quickly disappear with annealing.[166] A comparison with the shrinkage force measurements showed that the onset of the DSC endotherm correlated well with the temperature of stress appearance. Additionally, the temperature at which the shrinkage force is a maximum correlates with the peak of the DSC endotherm. The authors attributed this endotherm to a combination of entropy and energy effects which occur during shrinkage. Consequently, the onset and magnitude of this shrinkage are determined by the residual stresses present in the sample

which are gradually disappearing with increased aging. Thermal shrinkage measurements have also been used by Kato and Kambe[167] to study cold drawn polycarbonate.

Generalized creep studies have been performed by Lundberg and Jansson[168] on hot drawn polycarbonate samples. Samples were first aged at 120°C for 24 hours in order to minimize any further changes brought about by physical aging. Linear and nonlinear compliance values were determined for the longitudinal and transverse directions as well as for volume straining. All values were found to decrease to some degree with stretch ratio. In particular, it was found that the 100 second isochronous volume compliance decreased linearly with increasing stretch ratio. In other words, stress dilatation decreases with increased orientation which makes sense, considering the density is already higher for the oriented samples.

Combinations of stress relaxation and dynamic tests on polycarbonate film were used by Haidar and Smith[169] to study physical aging in polycarbonate film. Film samples were first aged for 1 month at 120°C. Next they were subjected to a static elongation of 2.6% at varying temperatures and a small sinusoidal strain was superimposed periodically. The static elongation effectively rejuventated the sample. Storage moduli were determined from the superimposed sinusoid as a function of aging time. The aging rate, μ, was found to be independent of the sinusoid frequency. However, the aging rate was found to increase linearly with increasing static elongation to a value higher than would normally be found with conventional isotropic samples.

Relaxations in uniaxially cold-drawn polycarbonate were studied by Yianakopolous and coworkers[170] using Thermally Stimulated Depolarization and Polarization Current (TSDC, TSPC). Samples were stretched to a draw ratio of between 1.6 and 2.1 at temperatures from room temperature up to 120°C (and with varying drawing rates). No spontaneous polarization resulting from the preferential orientation of dipoles was found to occur in the cold drawn samples. Cold drawing of a PC thermoelectret, however, was found to reduce most of the sample's charge. This normally only can occur by heating the

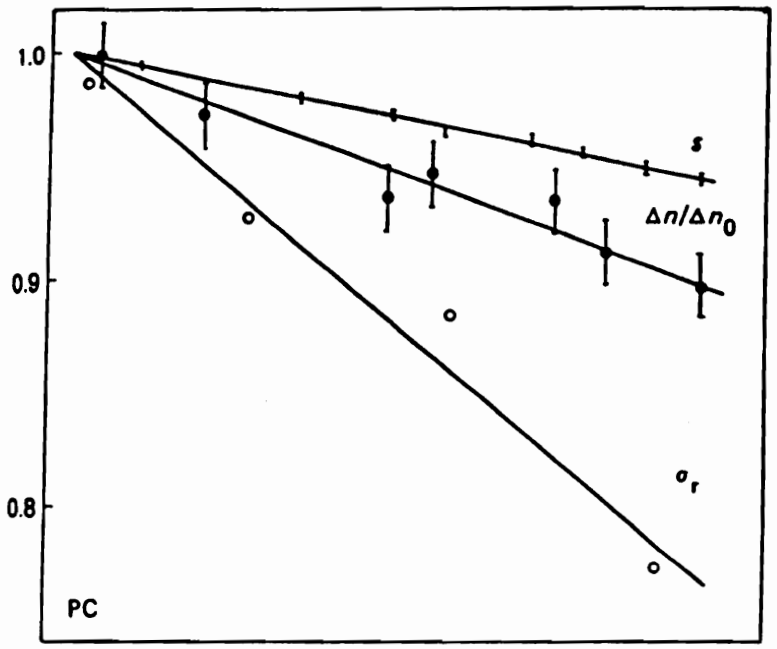

Figure 2.4-5. Dimensional relaxation, s, relative birefringence $\Delta n/\Delta n_o$, and relative value σ_r of maximum shrinkage stress plotted vs.aging time (at room temperature) for oriented PC (from [163]).

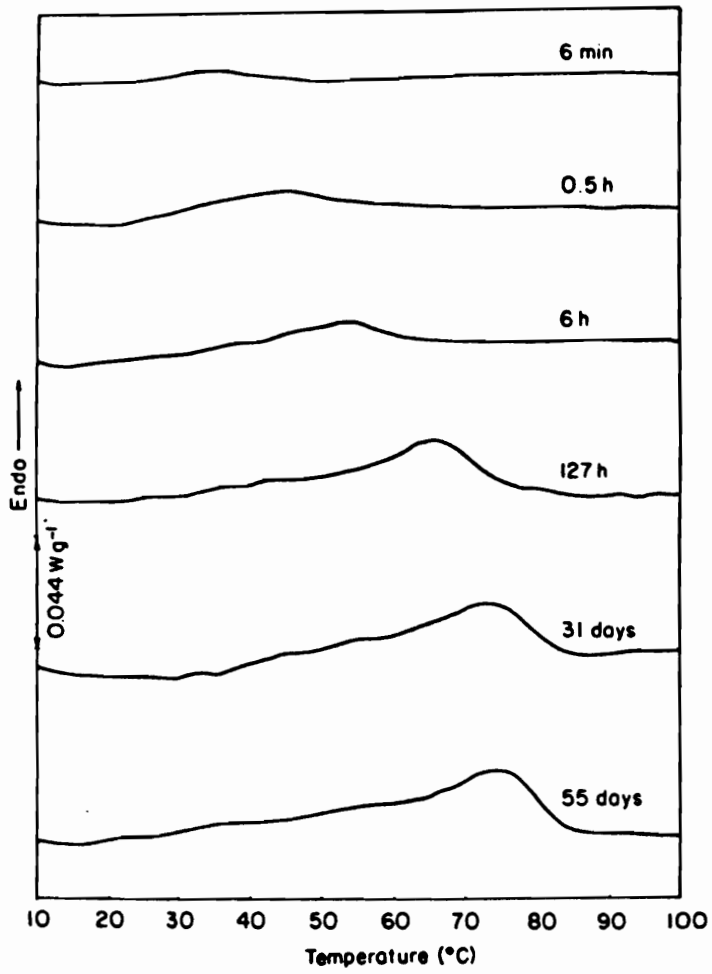

Figure 2.4-6. Expanded view of sub-Tg endotherms in cold-drawn PC as a function of aging time (from [164]).

sample above T_g. It is therefore speculated that this "deformation activated discharge" is the result of enhanced molecular mobility in the cold drawn samples. TSPC and TSDC experiments also detected an intermediate transition in the oriented samples at around 60 to 80°C which was not seen in the isotropic samples. The authors attribute this transition to field-induced orientation of a number of repeat units brought about by the increased free volume and molecular mobility accompanying the drawing process.

Lunn and Yannas performed a comprehensive study of the orientation of polycarbonate (hot and cold drawing) using infrared spectroscopy.[171] There were a number of important findings relating to the molecular mobility of oriented polycarbonate. Their study involved dichroism measurements at 1364 and 2971 cm^{-1} corresponding to the in-phase symmetric bending and asymmetric stretching of the two methyl groups respectively. First, it was found that the dimensional stability of the drawn polycarbonate increased with increasing stretch temperature. Samples cold drawn at a given temperature would begin to lose orientation with aging time above a certain threshold temperature. This threshold temperature increased with increasing stretch temperature. Samples hot drawn at T_g+5°C did not reach this threshold until about 120°C. This in some ways contradicts conventional wisdom. It is normally assumed that a glassy polymer possesses insufficient mobility for a significant change in orientation to occur (i.e. a true "frozen" state occurs). This applies anywhere below T_g. Lunn's data shows, however, that there is significant mobility at even 30°C below T_g for loss of orientation to occur. The authors' work also showed the presence of cooperative motions between chain segments and no change in interchain bonding with orientation. It was found, however, that the 2971 cm^{-1} absorption peak was lower in frequency for the samples with parallel polarization than for those with perpendicular polarization. These frequency shifts were independent of stretch temperature. Since the parallel polarization corresponds with the chains aligned with the machine direction, it is believed that the slight shift in frequency was associated with the better packing order of these oriented chains. The perpendicular polarization would constitute those chains lying perpendicular to the stretch direction thereby having a lower

packing density and less vibrational hindrance. These findings also appear to correlate with the increasing density phenomenon described earlier.

In summary, the process of cold drawing is found to have a significant effect on the mobility and physical aging rate of polycarbonate and other polymers. This is believed to be due to the partial relaxation of residual stresses although further investigation is warranted. In contrast, no significant studies were present on the effects of hot drawing except for Struik's work with PVC.[154] Struik's data did not show an increase in aging rate although there was significant scatter in the data. Struik's data are in agreement with the residual stress theory since the hot drawn samples should have minimal residual stresses. Nonetheless, more work is needed to fully characterize the aging behavior, particularly the volume relaxation, before any comparisons can be made.

2.6 References

1 G. B. McKenna, *Comprehensive Polymer Science, Vol 2. Polymer Properties*, C. Booth and C. Price, Eds., Pergamon, Oxford, 1990.

2 M. R. Tant and G. L. Wilkes, *Polym. Engr. Sci. 21*, 874 (1981).

3 M. R. Tant, M. S. Thesis, Virginia Polytechnic Institute and State University, Blacksburg, Virginia, 1979.

4 J. J. Aklonis and W. J. MacKnight, *Introduction to Polymer Viscoelasticity*, John Wiley and Sons, New York 1983.

5 I. M. Ward, *Mechanical Properties of Solid Polymers*, Wiley-Interscience, New York 1971.

6 J. D. Ferry, *Viscoelastic Properties of Polymers*, Wiley and Sons, New York, 1971.

7 N. G. McCrum, B. E. Read, and G. Williams, *Anelastic and Dielectric Effects in Polymeric Solids*, Dover, New York, 1967.

8 R. S. Porter and J. F. Johnson, Eds., *Analytical Calorimetry*, Plenum, New York, 1969.

9 B. Wunderlich, *Thermal Analysis*, Academic Press, Boston, 1990.

10 P. Ehrenfest, *Proc. K. Ned. Akad. Wet. 36*, 153 (1933).

11 R. A. Swalin, *Thermodynamics of Solids*, 2nd Edn., Wiley, New York, 1972.

12 P. G. Shewmon, *Transformations in Metals*, McGraw-Hill, New York, 1969.

13 G. Rehage and W. Borchard in *The Physics of Glassy Polymers*, R. N. Hayword, Ed., Wiley, New York, 54, 1973.

14 W. Kauzmann, *Chem Rev. 43*, 219 (1948).

15 J. H. Gibbs, *J. Chem. Phys. 25*, 185 (1956).

16 J. H. Gibbs and E. A. DiMarzio, *J. Chem. Phys. 28*, 373 (1958).

17 E. A. DiMarzio and J. H. Gibbs, *J. Chem. Phys. 28*, 807 (1958).

18 P. J. Flory, *Principles of Polymer Chemistry*, Cornell University Press, Ithaca, NY, 1953.

19 M. L. Huggins, *Ann. N. Y. Acad. Sci. 43*, 1 (1942).

20 J. M. G. Cowie and P. M. Toporowski, *Eur. Polym. J. 4*, 621 (1968).

21 J. A. Faucher, *J. Polym. Sci. Pt. B, 3*, 143 (1965).

22 R. B. Beevers and E. F. T. White, *Trans. Faraday Soc. 56*, 744 (1960).

23 K. Uebrreiter and G. Kanig, J. *Chem. Phys. 18*, 399 (1950).

24 E. A. DiMarzio, *J. Res. Natl. Bur. Stand., Sect. A 68A*, 611 (1964).

25 E. A. DiMarzio and J. H. Gibbs, *J. Polym. Sci. 40*, 121 (1959).

26 J. M. Gordon, G. B. Rouse, J. H. Gibbs and W. M. Risen, Jr., *J. Chem. Phys. 66*, 4971 (1977).

27 T. S. Chow, *Ferroelectrics 30*, 139 (1980).

28 E. A. DiMarzio and F. Dowell, *J. Appl. Phys. 50*, 6061 (1979).

29 E. A. DiMarzio, *J. Res. Natl. Bur. Stand., Sect. A, 68A*, 611 (1964).

30 G. Gee, P. N. Hartley, J. B. M. Herbert, and H. A. Lanceley, *Polymer 1*, 365 (1960).

31 R. S. Witte and R. L. Anthony, *J. Appl. Phys. 22*, 689 (1969).

32 P. Mason, *Trans. Faraday Soc. 55*, 1461 (1969).

[33] W. V. Johnston and M. Shen, *J. Polym. Sci., Part A-2 7*, 1983 (1969).

[34] G Adams and J. H. Gibbs, *J. Chem. Phys. 43*, 139 (1965).

[35] S. Matsuoka, *Relaxation Phenomena in Polymers*, Hanser, New York, 1992.

[36] H. Vogel, *Phys. Z. 22*, 645 (1921).

[37] G. S. Fulcher, *J. Am. Ceram. Soc. 8*, 339 (1925).

[38] G. Tammann and W. Hesse, *Z. Anorg. Allg. Chem. 156*, 245 (1926).

[39] R. N. Haward, *The Physics of Glassy Polymers*, John Wiley and Sons, New York, 26, 1973.

[40] A. Bondi, *J. Phys. Chem. 58,* 929 (1954).

[41] M. H. Cohen and D. Turnbull, *J. Chem. Phys. 31*, 1164 (1959).

[42] D. Turnbull and M. H. Cohen, *J. Chem. Phys. 34*, 120 (1961).

[43] R. Simha and T. Somcynsky, Macromolecules 2, 342 (1969).

[44] T. Somcynsky and R. Simha, *J. Appl. Phys. 42*, 4545 (1971).

[45] J. A. Faucher, J. *Polym. Sci.* , *Pt. B, 3*, 143 (1965).

[46] G. Pezzin, F. Zillio-Grandi and P. Sammartin, *Eur. Polym. J. 6*, 1053 (1970).

[47] S. Loshaek, *J. Polym. Sci. 15*, 391 (1955).

[48] T. G. Fox, and S. Loshaek, *J. Polym. Sci. 15*, 371 (1955).

[49] M. Gordon and J. S. Taylor, *J. Appl. Chem.* 2, 493 (1952).

[50] G. Williams, *Trans. Faraday Soc., 60*, 1556 (1964).

[51] L. C. E. Struik, *Physical Aging in Amorphous Polymers and Other Materials*, Elsevier, New York, 1978.

[52] L. C. E. Struik, *Internal Stress, Dimensional Instabilities and Molecular Orientations in Plastics*, John Wiley and Sons, New York, 77, 1990.

[53] L. C. E. Struik, *Physical Aging in Amorphous Polymers and Other Materials*, Elsevier, New York, 1978.

[54] T. A. Litovitz and P. Macedo, *Proceedings International Conference on Physics of Non-Crystalline Solids*, J. A. Prins, Ed., North Holland, Amsterdam, 1965.

[55] R. N. Hayward, *J. Macromol. Sci. C4*, 191 (1970).

[56] F. Bueche, *J. Chem. Phys. 36*, 2940 (1962).

[57] R. Wimberger-Friedl and J. G. de Bruin, *Macromolecules 29,* 4992 (1996).

[58] S. Matsuoka, H. E. Bair, S. S. Bearder, H. E. Kern, and J. T. Ryan, *Polym. Eng. Sci. 18*, 1073 (1978).

[59] S. Matsuoka and H. E. Bair, *J. Appl. Phys. 48*, 4058 (1977).

[60] N. Bekkedahl, *J. Res. Natl. Bureau Stds 42*, 145 (1949).

[61] P. Zoller, "Dilatometry" in *Encyclopedia of Polymer Science and Engineering*, Vol. 5, John Wiley and Sons, New York, 1983.

[62] O. S. Tyagi and D. D. Deshpande, *J. Appl. Poly. Sci. 37*, 2041 (1989).

[63] J. E. McKinney and M. Goldstein, *J. Res. Natl. Bur. Stand., Sect. A, 68A*, 273 (1964).

[64] H.-J. Oels and G. Rehage, *Macromolecules 10*, 1036 (1977).

[65] C. A. Angell and W. Sichina, *Ann. N. Y. Acad. Sci. 279*, 53 (1976).

[66] A. Quach and R. Simha, *J. Appl. Phys. 42*, 4592 (1971).

[67] A. J. Kovacs, *J. Polym. Sci. 30*, 131 (1958).

[68] L. C. E. Struik, *Internal Stress, Dimensional Instabilities and Molecular Orientations in Plastics*, John Wiley and Sons, New York, 7, 1990.

[69] R. Greiner and F. R. Schwarzl, *Rheo Acta 23*, 378 (1984).

[70] A. J. Kovacs, *Fortschr. Hochpolym.-Forsch. 3*, 394 (1963).

[71] A. J. Kovacs, *J. Polym. Sci. 30*, 131 (1958).

[72] A. J. Kovacs, *Adv. Polym. Sci. 3*, 394 (1963).

[73] D. Ng and J. J. Aklonis, in *Relaxations in Complex Systems*, Eds. K. L. Ngai and G. B. Wright, U.S. Government Printing Office, Washington D.C., 1985.

[74] J. Mijovic, L. Nicolais, A. D'Amore and J. M. Kenny, *Poly Eng. Sci. 34*, 381 (1994).

[75] A. Q. Tool and C. G.Eichlin, *J. Am. Ceram. Soc. 14*, 276 (1931).

[76] A. Q. Tool, *J. Am. Ceram. Soc. 29*, 240 (1946).

[77] R. Gardon and O. S. Narayanaswamy, *J. Am Ceram. Soc. 53*, 380 (1970).

[78] O. S. Narayanaswamy, *J. Am. Ceram. Soc. 54*, 491 (1971).

[79] I. M. Hodge, *J. Non-Crystalline Solids 131-133*, 435 (1991).

[80] P. B. Macedo and T. A. Litovitz, *J. Chem. Phys. 62*, 245 (1965).

[81] O. V. Mazurin, P. Kluyer, and S. V. Stolyar, *Glastech Ber. 56*, 1148 (1983).

[82] F. S. Howell, P.A. Bose, P. B. Macedo, and C. T. Moynihan, *J. Chem. Phys. 78*, 639 (1958).

[83] D. J. Plazek and J. H. Magill, *J. Chem. Phys. 45*, 3038 (1966).

[84] G. W. Scherer, *J. Am. Ceram. Soc. 67*, 504 (1986).

[85] S. Matsuoka, *J. Rheol. 30*, 869 (1986).

[86] I. M. Hodge, *Macromolecules 20*, 2897 (1987).

[87] W. M. Prest Jr., J. M. O'Reilly, F. J. Roberts, and R. A. Mosher, *Polym. Eng. Sci. 21,* 1181 (1981).

[88] G. Scherer, *Relaxation in Glass and Composites*, Wiley, New York, 1986.

[89] S. Matsuoka, *J. Rheol. 30*, 869 (1986).

[90] M. Goldstein, *J. Chem. Phys. 64*, 4767 (1976).

[91] B. E. Read, *J. Rheol. 36*, 1719 (1992).

[92] B. E. Read, *J. Non-Crystalline Solids 131-133*, 408 (1991).

[93] B. E. Read, P. E. Tomlins, and G. D. Dean, *Polymer 31*, 1204 (1990).

[94] S. S. Sternstein and T. C. Ho, *J. Appl. Phys. 43*, 4370 (1972).

[95] S. S. Sternstein, *Polym. Prepr. 17*, 136 (1976).

[96] F. A. Myers and S. S. Sternstein, *Proceedings VIIth International Congress on Rheology*, C. Klason and J. Kubat Eds., Goteborg, 260, 1976.

[97] L. C. E. Struik, *Polymer 21*, 962 (1980).

[98] G. B. McKenna, *J. NonCrystalline Solids*, in press.

[99] C. G'Sell and G. B. McKenna, *Polymer 33*, 2103 (1992).

[100] M. M. Santore, R. S. Duran, and G. B. McKenna, *Polymer 32*, 2377 (1991).

[101] A. Lee and G. B. McKenna, *Polymer 31*, 423 (1990).

[102] G. B. McKenna and L. J. Zapas, *Poly. Engr. Sci. 26*, 725 (1986).

[103] K. L. Ngai and A. F. Yee,"Nonlinear Behavior of Glassy Polymers," in *Relaxations in Complex Systems*, K. L. Ngai and G. B. Wright, Eds., U.S. Government Printing Office, 1985.

[104] T. L. Smith and T. Ricco, Paper DT7, Division of High Polymer Physics, 1984 Meeting of the American Physical Society, Detroit, (1984).

[105] H. J. Kolman, K. Ard, and C. L. Beatty, *ACS Org. Coatings Plastics Chem. 45*, 732 (1981).

[106] A. F. Yee and M. T. Takemori, *J. Polym. Sci. Polym. Phys. Ed. 20*, 205 (1982).

[107] B. Escaig, *Polym. Eng. Sci. 24*, 737 (1984).

[108] D. C. Watts and E. P. Perry, *Polymer 19*, 248 (1978).

[109] R. A. Bubeck, S. E. Bales, and H.-D. Lee, *Poly Eng. Sci. 24*, 1142 (1984).

[110] I. M. Hodge, *J. Non-Crystalline Solids 169*, 211 (1994).

[111] H. E. Bair, "Glass Transition Measurements by DSC," *in Assignment of the Glass Transition*, ASTM STP 1249, R. J. Seyler, Ed., Philadelphia 50-74, 1994.

[112] B. Wunderlich, *Thermal Analysis*, Academic Press, Boston, 1990.

[113] S. E. B. Petrie, *J. Poly Sci. A-2 10*, 1255 (1972).

[114] I. M. Hodge and A. R. Berens, *Macromolecules 15*, 762 (1982).

[115] I. M. Hodge and G. S. Huvard, *Macromolecules 16*, 371 (1983).

[116] A. J. Kovacs, J.J. Aklonis, J. M. Hutchinson, and A. R. Ramos, *J. Poly. Sci., Poly. Physics Ed. 17*, 1097 (1979).

[117] J. M. O'Reilly, *CRC Critical Reviews in Solid State and Materials Science 13*, 259 (1987).

[118] T. S. Chow and W. M. Prest Jr., *J. Appl. Phys. 53*, 6578 (1982).

[119] K. Adachi and T. Kotaka, *Polym. J. 14*, 959 (1982).

[120] J. Mijovic and T. Ho, *Polymer 34*, 3865 (1993).

[121] H. Sasabe and C. T. Moynihan, *J. Polym. Sci. Phys. Ed. 16*, 1447 (1978).

[122] J. M. O'Reilly and J. S. Sedita, *J. Non-Crystalline Solids 131-133*, 1140 (1991).

[123] A. R. Berens and I. M. Hodge, *Macromolecules 15*, 756 (1982).

[124] R. E. Robertson, *J. Appl. Phys. 49*, 5048 (1978).

[125] Y. C. Jean and Q. Deng, *J. Polym. Sci. B30*, 1359 (1992).

[126] P. Hautojarvi and A. Vehanen, in *Positrons in Solids*, P. Hautojarvi Ed., Springer-Verlag, Berlin, 1979.

[127] J. E. Kluin, et al., *Macromolecules 26*, 1853 (1993).

[128] H. Nakanish, S. J. Wang and Y. C. Jean, *in Positron Annihilation Studies of Fluids*, S. C. Sharma, Ed., World Science, Singapore 292 (1988).

[129] Y. C. Jean and H. Shi, *J. of Non-Crystalline Solids 00.* 4032 (1994).

[130] Y. C. Jean, H. Nakanishi, L. Y. Hao, and T. C. Sandreczki, *Physical Review B 42*, 9705 (1990).

[131] A. J. Hill, P. J. Jones, J. H. Lind, and G. W. Pearsall, *J. Polym. Sci. A26*, 1541 (1988).

[132] A. J. Hill, J. K. Heater, and C. M. Agrawal, *J. Polym. Sci. B28*, 387 (1990).

[133] J. Liu, Q. Deng, and Y. C. Jean, *Macromolecules 26*, 7149 (1993).

[134] R.-J. Roe, in *Advances in Polymer Science, Vol. 116. Atomistic Modeling of Physical Properties*, L. Monnerie and U. W. Suter, Eds., Springer-Verlag, Berlin, Vol 116, 1994.

[135] J. Kristiak, J. Bartos, K. Kristiakova, O. Sausa, and P. Bandzuch, *Physical Review B 49*, 6601 (1994).

[136] M. Y. Ruan, et al., *Macromolecules 25*, 2407 (1992).

[137] L. B. Liu, D. Gidley and A. F. Yee, *J. Polym. Sci. B30*, 231 (1992).

[138] X. S. Li and M. C. Boyce, *J. Poly. Sci. B31*, 869 (1993).

[139] W. Brandt and H. Feibus, *Phys. Rev. 174*, 454 (1968).

[140] W. Brandt and J. Fans, *Phys. Rev. B2*, 1425 (1970).

[141] O. E. Mogensen, *Appl. Phys. 6*, 315 (1975).

142 G. L. Wilkes, "Rheooptical Properties," in *Encyclopedia of Polymer Science and Engineering, Vol 14*, John Wiley and Sons, New York, 542, 1983.

143 "Structure and Properties of Oriented Polymers," I. M. Ward, Ed., John Wiley and Sons, 1975.

144 R. S. Stein, *Rubber Chemistry and Technology 49*, 459 (1976).

145 L. C. E. Struik, *Internal Stresses, Dimensional Instabilities and Molecular Orientations in Plastics*, John Wiley and Sons, New York, 1990.

146 R. Samuels, *Structured Polymer Properties*, John Wiley and Sons, New York, (1974).

147 H. T. Jessup and F. C. Harris, *Photoelasticity: Principles and Methods,* Dover, New York, 1960.

148 H. J. Binagardi, *Bestimmung der Orientierung und molekularen Ordnung in Polymeren, Kunststoff Forschung 1*, H. Kaufer, Ed., Tecn Un. Berlin, 1980.

149 M. Pietralla, H. r. Schubach, H. R. Dettenmaier, and B. Heise, *Prog. Colloid Polymer Sci. 71*, 125 (1985).

150 K. G. Denbigh, *Trans Faraday Soc.36*, 936 (1940).

151 R. L. Lowell and R. S. Stein, *J. Chem. Phys. 47*, 2985 (1967).

152 R. S. Stein and G. L. Wilkes, "Physico-Chemical Approaches to the Measurement of Anisotropy," in *Structure and Properties of Oriented Polymers,* I. M. Ward, Ed. John Wiley and Sons, New York, 57, 1975.

153 B. E. Read, "Ultra-Violet, Visible and Infra-Red Dichroism," in *Structure and Properties of Oriented Polymers,* I. M. Ward, Ed. John Wiley and Sons, New York, 150, 1975.

154 L. C. E. Struik, *Physical Aging in Amorphous Polymers and Other Materials*, Elsevier, New York, 1978.

155 R. Pixa, *et. al.*, *Polymer Bulletin 16,* 381-387 (1986).

156 K. H. Hellwege, J. Hennig and W. Knappe, *Kolloid-Z.uZ.f. Polymere 186*, 29 (1962).

157 T. E. Brady and G. S. Y. Yeh, *J. Appl. Phys. 42,* 4622 (1971).

158 D. G. LeGrand, *J. Appl. Polymer Sci. 16*, 1367 (1972).

159 W. A. Spitzig and O. Richmond, *Polymer Eng. Sci. 19*, 1129 (1979).

160 E. Ito, K. Sawamura, and S. Saito, *Colloid and Polymer Sci. 253*, 480-484 (1975).

161 J. Bartos, J. Muller and J. H. Wendorff, *Polymer31,* 1678 (1990).

162 J. Muller, *J. Thesis*, Deutsches Kunststoff-Institut, Darmstadt, (1989).

163 M. Trznadel and M. Kryszewski, *Polymer 29*, 418-425 (1988).

164 M. Trznadel, T. Pakula, and M. Kryszewski, *Polymer 29*, 619-625 (1988).

165 D. G. LeGrand, *Proceedings of the XI International Congress on Rheology*, Brussels, Belgium (1992).

166 D. C. Watts and E. P. Perry, *Macromolecules 19*, 248 (1978).

167 T. Kato and H. Kambe, *J. Appl. Poly. Sci. 22,* 1767-1774 (1978).

168 L. Lundberg and J. F. Jansson, *Polymer 35*, 2084-2089 (1994).

169 B. Haidar and T. L. Smith, *Polymer 31*, 1904-1908 (1990).

170 G. Yianakopoulos, J. Vanderschueren, and J. Niezette, *IEEE Transactions on Electrical Insulation 24*, 429-438 (1989).

171 A. C. Lunn and I. V. Yannas, *J. Poly. Sci., Polymer Physics Ed., 10*, 2189-2208 (1972).

3.0 DILATOMETRIC AND MECHANICAL CREEP BEHAVIOR OF HOT DRAWN ATACTIC POLYSTYRENE AND BISPHENOL-A POLYCARBONATE

3.1 Introduction

Physical aging is a well documented and practically important phenomenon which occurs in glassy materials. This is apparent from the number of reviews addressing this topic in the literature.[1,2,3,4,5] In the case of amorphous polymers, quenching the sample from above T_g into the glassy state introduces a non-equilibrium structure where physical properties change with time. The most common changes are a densification of the polymer and a gradual decrease in ductility. The reader should not confuse this with chemical aging where chemical/compositional changes such as UV degradation, crosslinking, and hydrolysis may occur. Instead, physical aging is completely reversible and simply heating the material above T_g erases any of the aging-induced property changes.

The fact that most amorphous polymers are processed above T_g and then quenched into the glass makes physical aging an important concern for any designer. Couple this with the fact that most processing methods introduce at least some degree of orientation,[6] intentional or not, and one of the motivations for this study becomes clear. If orientation is indeed found to enhance, or even alter, the aging behavior of an amorphous glass, then the design criteria will need to be modified accordingly. Unfortunately, there is very little data available in the literature pertaining to aging in oriented systems so the designer must rely on guidelines developed for isotropic systems.

Ideally for this type of study, one is interested in the effects of molecular orientation in purely amorphous systems. A few studies in the literature have been performed on hot drawn systems[7,8] (i.e. stretched above T_g) however interpretation of the results is

complicated by the possible formation of strain-induced crystallinity. Since strain-induced crystallinity varies with degree of orientation and the crystalline regions essentially do not physically age, it becomes very difficult to deconvolute the effects of amorphous orientation from the overall changes in physical aging behavior.

A number of studies also exist with regard to aging behavior in cold-drawn systems (the polymer is stretched below T_g).[9, 10] Here, crystallinity is generally less of a problem than are the high internal stresses which develop from stretching a glass. As with the crystallinity, these glassy internal stresses have a significant influence on the aging behavior making interpretation of the data very difficult. A more detailed discussion of theses various studies along with the differences between cold and hot drawing is provided in a later section.

For this study, samples of bisphenol-A polycarbonate (PC) and atactic polystyrene (PS) have been hot-drawn to various stretch ratios, quenched to room temperature to freeze in the orientation, and then held isothermally at temperatures below T_g while relaxation behavior was measured. These systems do not undergo measurable strain-induced crystallization so the problems discussed above are avoided. Volume relaxation was monitored using dilatometry, and mechanical relaxation using creep measurements. Supplemental tests including the determination of isothermal linear shrinkage with time and the density at room temperature were also performed to help in the characterization of the oriented state. While both dilatometry and mechanical creep are applied routinely to the study of isotropic polymers, they each pose their own special problems when applied to oriented systems. These problems primarily arise from the sub-Tg shrinkage which occurs during annealing and will be discussed in more detail in the experimental section.

3.1.1 Aging Rate Determination

Dilatometry and creep provide slightly different methods for measuring the "rate" of physical aging. For volumetric measurements the volume relaxation rate β is defined as

$$\beta = -\frac{1}{V(t)}\frac{dV(t)}{d\log(t)} \qquad (3.1\text{-}1)$$

where V(t) is the volume at time *t*. β has a value between 10^{-4} and 10^{-3} for most polymers in their "normal" aging temperature range. "Normal" means the temperature range between T_g and the first main-chain secondary transition. This usually defines the range where molecular motion in the glass is still significant. Alternatively, one can measure the rate of linear relaxation α_l which is analogous to Equation (3.1-1) except V(t) is replaced by the length L(t). For isotropic systems β equals $3\alpha_l$. For anisotropic systems, however, α_l will vary in each material direction. For uniaxial orientation, β will equal $\alpha_{md}+2\alpha_{td}$ because of symmetry. The subscripts MD and TD refer to the machine (stretch) and transverse directions respectively.

For creep measurements, the mechanical shift rate is defined as

$$\mu_h = -\frac{d\log(a_h)}{d\log(t_e)} \qquad (3.1\text{-}2)$$

where a_h is the horizontal shift factor required to properly superimpose the creep curve at aging time t_e with the reference curve. The subscript *h* refers to horizontal shifting as there is also a vertical shifting counterpart which will be discussed in more detail later. The value for μ_h is usually very close to one over the "normal" aging temperature range which is between T_g and the secondary transition temperature corresponding to chain backbone motions.[1] Outside this temperature range, μ_h approaches (but is not necessarily) zero.

While μ_h and β are defined similarly, they do not follow the same trend with changes in aging temperature. Struik has defined a parameter *S*, denoted the volume sensitivity where[1]

$$S = 2.303\frac{\mu_h}{\beta} \qquad (3.1\text{-}3)$$

The volume sensitivities for a wide range of isotropic polymers were shown to increase significantly with decreasing T. Struik has also shown how S can be related to the molecular mobility M,

$$S = \left[\frac{\partial \ln M}{\partial (ffv)} \right]_T \qquad (3.1\text{-}4)$$

where ffv is the fractional free volume. The strong increase in S with decreasing temperature indicates that a polymer can still undergo significant changes in mechanical mobility (i.e. ductility) at low temperatures, even though specific volume is changing only very little with time. This is not in line with predictions of the free volume models such as the WLF equation, however. For the free volume theory, S should be a constant function of temperature.

3.1.2 Hermans' Orientation Function

In this study, it is the degree of orientation, rather than the aging temperature which is of most interest. Therefore, to characterize the orientation state of the uniaxial system, one can apply the Hermans' orientation function f, which can be determined from birefringence measurements[11]

$$f = \frac{\Delta}{\Delta^o} = \frac{3 < \cos^2 \theta > -1}{2} \qquad (3.1\text{-}5)$$

Here Δ is the birefringence ($\Delta = n_{md} - n_{td}$ where n is the refractive index and the subscripts MD and TD refer to the machine and transverse direction respectively), Δ^o is the intrinsic birefringence (i.e. the birefringence for a perfectly oriented chain), and θ is the angle between the stretch direction (MD) and the chain axis. The angle brackets denote an average over all of the chains. The orientation function will assume the value of zero for an unoriented system, one for perfect orientation along the stretch direction, and -1/2 for perfect orientation along the TD. These cases correspond to average values for θ of 54.7°, 0°, and 90° respectively. It is emphasized that this equation only applies to single-

phase systems and therefore will not be applicable for semi-crystalline polymers. Fortunately, as stated earlier, neither polycarbonate nor atactic polystyrene exhibit any strain-induced crystallization upon hot drawing.

3.2 Review on Previous Studies of Aging in Oriented Systems

3.2.1 Cold versus Hot Drawing

There have been a limited number of studies on the physical aging behavior of oriented systems, most related to cold drawing (i.e. stretching below T_g). Both cold and hot drawing introduce entropic stresses due to alignment of the polymer chains. However, cold drawn samples are at a much higher internal stress state due to the addition of "glassy" stresses caused by distortion of the van der Waals bonds. These distortional stresses are responsible for a number of behavioral changes in the polymer. For example, cold drawn samples generally show considerable shrinkage (>10% recovery) at temperatures well below T_g.[12] Hot drawn samples, on the other hand, do not show significant shrinkage except at temperatures near (and above) T_g. Struik[12] discusses the shrinkage behavior of amorphous polymers and provides a simple model for the differences in shrinkage between cold and hot drawn polymers. The interested reader should refer to this source for more information.

The process of cold drawing is also "less incompressible" than hot drawing. This means that more free volume is introduced into the polymer upon cold stretching. This is a result of the fact that the Poisson's ratio for a glass is typically about 1/3 as compared to ca. 1/2 (the incompressible limit) for rubbers. Since mobility is related to free volume (see Equation (4)), it is expected that cold drawn samples will exhibit different aging behavior than hot drawn samples.

3.2.2 Aging Studies on Hot-Drawn Samples

One of the only hot-drawn studies was performed by Struik.[7] Here tensile creep measurements were made on melt oriented (rigid) PVC drawn at 82°C. The Tg was not specified but the stretch temperature was listed as being above Tg (a typical Tg for rigid PVC is about 80 °C). Samples were drawn up to a maximum stretch ratio of 2.2X and then quenched to 20°C at which point aging commenced. Analysis of the shift rates from the creep tests at 20°C showed little change with increased stretching although there was considerable scatter in the data. Struik suggested that, because the level of molecular reorientation is actually very small in most oriented amorphous polymers (i.e. very low f), the aging behavior should not be significantly affected. No data on the orientation functions or possible formation of strain-indueed crystallinity in the stretched samples was presented. Nonetheless, rigid PVC is known to possess some crystallinity.

Mukherjee and Jabarin[8] measured enthalpy relaxation and mechanical properties as a function of orientation in biaxially and constrained uniaxially stretched PET (T_g=80°C, stretch temperature = 100°C). They found a correlation between the ductile-brittle transition and the enthalpy of relaxation. In addition, it was suggested that molecular orientation significantly reduces the enthalpy of relaxation. As discussed earlier, however, results must be interpreted with caution since significant levels of strain-induced crystallization occurred (based on their density measurements). This effectively reduces the amount of amorphous region undergoing physical aging as was also shown by Tant and Wilkes.[13]

3.2.3 Aging Studies on Cold Drawn Polymers

Pixa and coworkers[9] have analyzed the effects of cold drawing polycarbonate at room temperature. Volume relaxation rates for cold drawn samples having a stretch ratio of 1.7 were 2.5 times higher than the isotropic controls. Bartos and coworkers[10] found the

oriented value of β to be twice as high under similar testing conditions. In fact, it has been shown that between room temperature and 100°C, the rate of volume relaxation is roughly twice that of isotropic polycarbonate.[14] Above 100°C, the volume relaxation rates do not vary much with orientation.

Another important finding by Pixa and coworkers was that polycarbonate actually densified upon stretching.[9] This has also been observed for polycarbonate by others for cold drawing[15,16,17,18] and by Ito and coworkers for hot drawing.[19] The densification is less in the cold drawn samples due to the Poisson effect. Nonetheless, even with the initial densification, the cold drawn samples still showed faster rates of volume relaxation.

Using the absolute small angle X-ray intensity in the small angle regime, Bartos found that the density fluctuations increase due to drawing, even though the density is higher in the stretched sample.[10] These larger fluctuations correlate with the volume relaxation data, dissappearing above 100°C. These large fluctuations are indicative of a broader free volume distribution in the cold drawn samples. This could explain the higher volume relaxation rates exhibited by the cold drawn samples.

Trznadel and coworkers[20,21] have followed shrinkage stresses in cold drawn polycarbonate and polyester as a function of aging time. They found that the rate of birefringence loss (normalized to the unaged birefringence) is slightly larger than the change in normalized length, whereas, the loss in residual shrinkage stress increases at an even faster rate than birefringence. Studying the effects of residual stresses in polycarbonate bars at room temperature, LeGrand also found high residual stress relaxation with no significant dimensional changes.[22]

Lunn and Yannas performed a comprehensive study of the orientation of polycarbonate (hot and cold drawing) using infrared spectroscopy.[23] They found that the dimensional stability of the drawn polycarbonate increased with increasing stretch temperature. Samples hot drawn at Tg+5°C did not reach this threshold until about 120°C. Their work also showed the presence of cooperative motions between chain

segments and no change in interchain bonding with orientation. They did find, however, that bonding strength perpendicular to the stretch direction increased with orientation (based on frequency shifting of the absorption peaks) which may be a result of shorter interatomic distances and better chain packing.

Even with all of the findings discussed in the previous studies, it is still uncertain how molecular orientation affects physical aging. It is clear, however, that internal glassy stresses significantly enhance aging. This, by itself, is important to a designer since residual stresses often exist in commercial plastic products. Nevertheless, the focus of this study is segmental/chain orientation. The only way to sufficiently isolate molecular orientation is to hot draw polymers that do not crystallize. This is why atactic PS and PC were chosen for this study. The experimental details for stretching these polymers will now be discussed.

3.3 Experimental

3.3.1 Film Stretching

Samples of Makrolon 2608 bisphenol-A polycarbonate were stretched uniaxially at 160°C using a T. M. Long film stretcher. The film samples, prior to stretching, had a nominal T_g of 150°C as determined from DSC measurements using a 20°C/minute heating rate. The number average molecular weight, M_n, was 16,500 g/mol and was obtained from solution viscosity measurements (THF at 23°C). The M_n was determined from the viscosity average molecular weight M_v by assuming a polydispersity of 2 and applying correction factors.[24] The PC samples, with initial gauge lengths of 10 cm, were stretched with a crosshead speed of 12.7 cm/s to elongation ratios of 1.25X, 1.5X, 2X and 2.5X. Assuming an intrinsic birefringence of 0.16 for PC (based on sonic modulus measurements[25]) the maximum f obtained was ca. 0.19 at 2.5X.

Samples of Dow 685D atactic polystyrene having a Tg of 103°C (from DSC at 20°C/min) were stretched at 120°C. These samples had an M_n of 174,000 g/mol and an M_w of 297,000 g/mol from GPC. The polystyrene was stretched at a rate of 17.8 cm/s to a final stretch ratio of 2X and 4X. It was found to have a maximum orientation function of 0.11 at 4X assuming an intrinsic birefringence of -0.16 [26]. These low values for f in PC and PS are typical of amorphous polymers in general. In fact there have been few if any references to f values in amorphous polymers being greater than 0.2. To achieve higher functions during hot stretching usually requires the formation of strain-induced crystallinity which then helps to lock the amorphous orientation in place.

After stretching, samples were quenched below T_g with a blast of cold air in order to freeze in orientation. Because of fluctuations in the stretching environment, the orientation function for a given stretch ratio will vary slightly from sample to sample. Orientation was therefore determined for each sample by way of birefringence measurements using an Abbe refractometer (Na D-line, 589.3 nm). For a given sample, the point-to-point variability in orientation function was +/- 0.01. Variability in the average value of f for different samples of a given stretch ratio was +/- 0.03 at the highest stretch ratios.

3.3.2 Density Measurement

Density data were obtained using a gradient column made with salt solutions of either potassium bromide or sodium bromide and water. Setup of the column followed standard procedure with a minimum of 5 glass beads of differing densities being used to calibrate the column. The temperature was maintained at approximately 23°C +/- 0.1°C. A minimum of 1 hour was allowed for the samples to reach their equilbrium position after placement in the column although typically, they were allowed to equilibrate overnight. Typically 3 to 4 samples were tested for each orientation.

3.3.3 Shrinkage Measurement

One of the motivations for performing isothermal shrinkage measurements was to determine over what temperature range creep measurements could be performed. Excessive shrinkage makes it very difficult to obtain accurate creep curves since the shrinkage component of strain has to be removed. Another motivation is that shrinkage is a good indicator of the molecular mobility in oriented systems. Shrinkage measurements were performed on 2.5X samples of PC ($f = 0.16$) and 4X samples of PS ($f = 0.11$) using a Seiko TMA 100 in the tensile mode. Samples of the film approximately 4 mm wide, 0.2 mm thick, and 25 mm long were mounted in the test fixture after it was preheated to the annealing temperature. After mounting the sample, it took approximately 2 to 3 minutes to reach temperature equilibrium. Measurements were started when the temperature was within one degree of the annealing temperature. A small preload of 7 grams was applied to maintain sample alignment in the test fixture. After accounting for the weight of the mounting clamps (~ 3 grams), the resulting tensile stress exerted on the sample was nominally 50 kPa or less which produces a negligible strain in the glassy state. All tests were run isothermally out to 10 hours. Shrinkage temperatures ranged from 70°C to 132°C for PC and 50°C to 90°C for PS. Emphasis was placed on this temperature regime since lower temperatures resulted in almost immeasureable shrinkage rates. Higher annealing temperatures resulted in an α–transition (T_g) dominated shrinkage which exceeded the accurate measurement limits of the TMA. Simultaneous measurement of birefringence with annealing was also performed but the loss in orientation was almost negligible except at the highest annealing temperatures. Because the changes in birefringence did not significantly exceed the scatter range of the measurement, the results are not reported.

3.3.4 Dilatometry

3.3.4.1 Construction of the Dilatometer

A dilatometer has been constructed based on recommendations provided by Dr. Greg McKenna of the National Institute of Standards and Technology (NIST). Unlike more conventional volume dilatometers, this system combines a linear variable differential transformer (LVDT), commonly used in linear dilatometry, with a larger-bore capillary section which results in high accuracy and ease of sample preparation (see Figure 3.3-1). The capillary bore used in this dilatometer is 4.16 mm in diameter unlike the 0.5 to 2 mm range used in conventional dilatometers. Because of this larger diameter, there is less variation in the diameter along the length and the development of a calibration curve is no longer as critical. The potential problem of contaminants plugging the bore is also alleviated. The bore is connected to the main reservoir which has an inner diameter of 22 mm and is where the sample is held. The sample consisting of approximately 3 to 5 grams of the polymer film cut into rectangular strips (~ 1 cm wide by 4 cm long), was inserted into the bottom along with a glass plug prior to the sealing of the glass. The plug acts to displace extra volume thereby requiring less mercury as well as preventing heat damage when the glass is sealed.

To detect the height of the capillary, a small aluminum float is placed on top of the mercury meniscus to which a connecting rod is attached. The other end of the connecting rod is attached to the LVDT core. Counterweighting is applied so that the net weight on the float is 1 gram. Excessive weight would cause the float to submerge. The LVDT is a Trans-Tek 230-0216 with a full scale linear range of +/- 0.5 inches and a maximum nonlinearity error of 0.25% full scale. Signal conditioning is performed using a Trans-Tek Model 1003 transducer indicator. Upon recalibration, it was found that the LVDT had even greater precision over a specific, narrow displacement range. This narrow range was sufficient in length for the isothermal annealing runs and provided a reduction in total error

in the measurement. For non-isothermal temperature ramps, the whole length of the LVDT is required in order to measure the larger column displacements.

The oil bath used in the experiments was a Haake Type B with an N4 controller. Its controlling accuracy is rated at +/- 0.01°C. Measurement of the actual bath temperature with time showed a very small amplitude oscillation (amplitude ~ 0.02°C) with a period of approximately 30 seconds superimposed on the set temperature. The standard deviation and standard error (i.e. the standard deviation divided by the square root of the number of samples tested--a measure of the variability of the mean) were 0.027°C and 0.0009°C respectively. The relatively high standard deviation was due mostly to this oscillation. Its effect was minimized by averaging the LVDT signal over a few periods of this oscillation bringing the effective temperature error (standard deviation) just under 0.01°C. No long term drift in the bath tempeature was detected.

The dilatometers were placed under vacuum for 12 to 24 hours after being sealed in order to remove any trapped moisture or gases. Next, the evacuated dilatometer was filled with triple distilled mercury via a three way stopcock mounted to the top of the capillary. After filling, the system was maintained under vacuum for approximately two days in order to remove trapped air. Normal procedures in the literature for isotropic samples allow for degassing the samples continuously at elevated temperatures in order to obtain the most efficient gas removal. This is often supplemented by alternately dipping the sample in hot and cold water. Higher temperatures cause the gas bubbles in the mercury to expand making it easier for them to coalesce and float to the top. At the completion of degassing, the isotropic sample could be heated to a temperature above Tg and any physical aging erased prior to the actual dilatometric measurements. With the oriented samples used in this study, however, care had to be taken not to allow the sample to reach elevated temperatures since there is no way to "pre-erase" the aging prior to

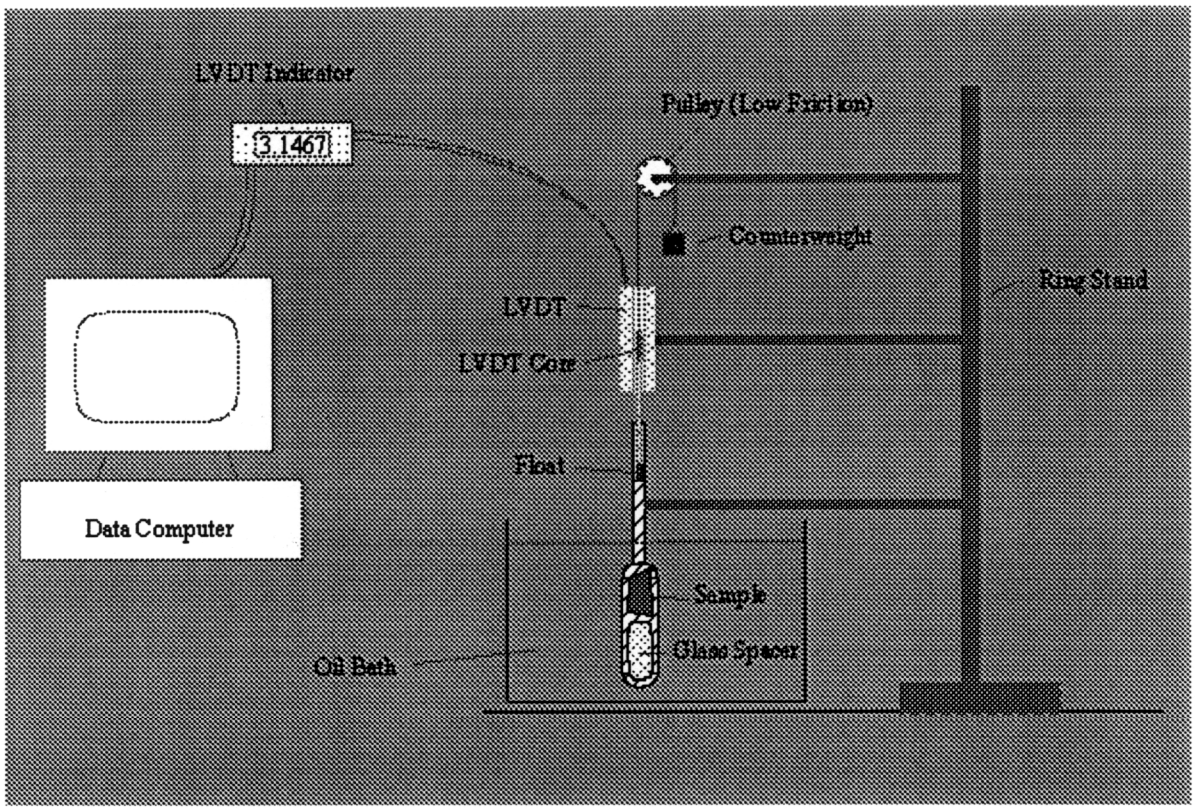

Figure 3.3-1. Schematic of dilatometer

dilatometric measurement. In essence, each dilatometer constructed for an oriented sample was good for only one measurement!

After completion of the degassing procedure, the sample was maintained at atmospheric pressure for 24 hours prior to testing. It was found by accident that the mercury/gas bubbles in the dilatometer exhibited a slight but measurable volume relaxation after removal of the vacuum which subsided after about 5 to 10 hours. This mercury "relaxation" was large enough to significantly alter the measured relaxation rates of the polymer systems. It is uncertain why this relaxation occurs but it is believed that trapped air, which has coalesced under vacuum, diffuses back into the mercury after the vacuum is removed thereby causing the overall volume to decrease. Keep in mind that surface tension plays a role in the effective pressure of any gas molecules in a liquid. Smaller bubbles will feel a higher pressure (and a higher density) whereas larger bubbles will feel less surface tension induced pressure and will therefore have a lower density. As the gas diffuses back into the mercury, the bubbles will be smaller and even more dense resulting in a net relaxation of the volume of the system. This phenomenon should definitely be investigated further since in many ways it mimics the free volume relaxation which occurs in glassy systems (even though it is occurring in the liquid state).

3.3.4.2 Dilatometry Error Analysis

Because of the high sensitivities involved, a large number of factors have to be accounted for in correcting the dilatometric data. These error sources can be roughly divided into three categories: measurement error, thermal fluctuation error, and error due to trapped air. Each will now be discussed in more detail along with equations for estimating the uncertainty.

The fundamental principle of dilatometry is the amplification of very small sample volume changes to a detectable level by way of a small diameter capillary tube. The smaller the capillary, the greater the amplification. Unfortunately, smaller capillary tubes can also have more variability in the diameter which leads to one source of measurement

error. Normally, the capillary diameter is "calibrated" by drawing mercury through the tube to various heights and then weighing. From this, a profile of the capillary diameter with distance is determined and used to correct subsequent experiments. This procedure was also performed on the large bore (4.16 mm diameter) Trubore^{tm} tubing used in this work and no detectable fluctuations in diameter could be measured. The tubing tolerances (diameter) are rated at +/- 0.001 cm by the manufacturer although calibration measurements showed slightly tighter tolerances for the tubing tested.

The next source of measurement error occurs in the actual meaurement of the capillary height, which, in this study, is accomplished via the LVDT. With the reduced displacement range discussed earlier, the LVDT used in this work had a maximum uncertainty of 0.00069 cm. Even smaller errors can be obtained by going to a shorter LVDT stroke length. However, a longer stroke length is easier to mount and also allows for non-isothermal measurements. There is also a source of error due to the thermal stability/drift of the LVDT which must be included when high bath temperatures and non-isothermal studies are performed. Fortunately, in the case of the isothermal measurements performed in this work, it can be neglected.

Starting with the volume change V for a given mercury column height L and diameter D,

$$V = \pi \frac{D^2}{4} L \tag{3.3-1}$$

one arrives at the measurement volume error dV_m by

$$dV_m = \pi \left[\left(\frac{D^2}{4} dL \right)^2 + \left(\frac{DL}{2} dD \right)^2 \right]^{1/2} \tag{3.3-2}$$

where dL and dD are the LVDT error and capillary diameter error respectively. For the current study, an uncertainty value dV_m of approximately 0.000094 cm^3 at the 99% confidence limit (3σ) was obtained. Note that this value changes slightly with the total volume change since dV_m is a function of L. This error is also equivalent to the limit of

detection (LOD where LOD = 3σ) whereas the limit of quantitization (LOQ where LOQ= 10σ) is 3.01 x 10^{-4} cm^3.

Temperature variations have already been discussed previously. Slight changes in the temperature cause variations in the capillary height brought about by thermal expansion of the mercury, sample, and glass. Long term temperature stability is essential for isothermal measurements and temperature control of 0.015°C or better is recommended.[27] Short term variations are not a major problem since the thermal mass of the dilatometer/sample system is high and the thermal relaxation times can be quite long (a few hundred seconds for the dilatometers constructed in this work). For non-isothermal measurements, the user must subtract out the (large) contribution of capillary expansion/contraction brought about by thermal expansion of the mercury and glass.

For isothermal measurements, the volume error due to temperature fluctuations dV_T is defined as

$$dV_T = \left[\left(\alpha_{Hg} - \alpha_g \right) V_{Hg} + \alpha_{samp} V_{samp} \right] dT \qquad \text{(3.3-3)}$$

where α_{Hg} is the thermal expansion for mercury (1.8 x 10^{-4} $°C^{-1}$), α_g is the thermal expansion of glass (10^{-5} $°C^{-1}$), α_{samp} is the thermal expansion of the polymer at the aging temperature (2.9 x 10^{-4} $°C^{-1}$ for glassy PC, 1.5 x 10^{-4} $°C^{-1}$ for glassy PS), V_{hg} is the volume of mercury, V_{samp} is the sample volume, and dT is the fluctuation in temperature (~ 0.01 °C for this work). Note that the values of α used in Equation (3.3-3) are volumetric thermal expansion coefficients and should not be confused with the linear relaxation rate α_l defined earlier. For a 3 gram polymer sample, the temperature related error is approximately 4 x 10^{-5} cubic centimeters at the 99% limit. In the case of nonisothermal measurements, the various thermal expansion coefficients must be applied to subtract the volume change component of the mercury expansion during heating or cooling.

Error due to trapped air is not as important for isothermal studies as it is for non-isothermal tests. The effect of the trapped air is to alter the net thermal expansion of the

system during heating or cooling. For isothermal experiments, the only problem that could occur is if small bubbles of trapped air coalesce and/or somehow break free, thereby escaping out the top. This would obviously reduce the volume of the system slightly and result in error. There is also the problem with the gas bubble/mercury relaxation occurring after removal of the vacuum, as described earlier. Although it is uncertain whether the latter is actually due to the trapped gas, its effects can be virtually eliminated by waiting a sufficient length of time prior to testing.

Determination of the trapped air requires measuring the change in the height of the mercury column after removal of the degassing vacuum. The associated volume change is related to the volume expansion/contraction of the gas bubbles brought about by the pressure change, in addition to the compressibility induced volume changes of the mercury and polymer. An ideal gas law is normally assumed for the calculation and all of the gas is, on average, assumed to be centrally located in the middle of the dilatometer (~ 100 mm below the top of the mercury column). Therefore, with no vacuum applied, the pressure on the bubble is 760 + 100 mm of Hg whereas with the vaccuum, the pressure is only approximately 100 mm Hg. The resulting volumes based on the ideal gas law are

$$\frac{V_{vac}}{V_{atm}} = \frac{P_{atm}}{P_{vac}} \approx \frac{860}{100} \qquad (3.3\text{-}4)$$

Since the experimental volume change V_{vac}-V_{atm} has been measured, one can use Equation (3.3-4) and solve for V_{atm}. This value for V_{atm} has typically been 0.008 to 0.010 cm^3 which is slightly higher than the 0.0021 cm^3 obtained by Bekkedahl using a nearly equivalent amount of mercury.[28] This might be due to the fact that the sample in this work was composed of multiple film strips as opposed to one solid piece of polymer. This would provide more "interstitial" sites between strips for air to be trapped. Regardless, the amount of air present is not large enough to alter the non-isothermal test results.

Neglecting the effect of trapped air, since it is small, the total error (3σ) in volume measurement becomes

$$dV = \left(dV_T^{\,2} + dV_m^{\,2} \right)^{1/2} \tag{3.3-5}$$

which, for this work, is approximately 1×10^{-4} cm^3. This can be converted into an uncertainty in density measurement since

$$\rho = \frac{m_{samp}}{V_{samp}} \tag{3.3-6}$$

which leads to

$$d\rho = \left[-\frac{m_{samp}}{V_{samp}^{\,2}} dV \right] = -\frac{\rho}{V_{samp}} dV \tag{3.3-7}$$

For a 3 gram sample, $d\rho$ is 5×10^{-5} g/cc at the 99% confidence limit. Even greater accuracy can be obtained by going to a larger sample mass as was done with some of the isotropic samples. Since the oriented samples only existed in film form, it was felt that packing too much into the dilatometer would introduce excessive trapped air and result in even more error (which would also be very difficult to quantify). Therefore, a compromise was reached in which some accuracy was sacrificed in exchange for good wetting of the film.

There are other sources of error which are difficult to quantify but also should be mentioned. With the application of the LVDT, care must be taken to minimize vibration, properly align the transducer, minimize extraneous magnetic fields (this includes making sure that all connnecting rods and mounting fixtures are non-magnetic) and watching for thermal drafts which can slightly change the sensitivity of the LVDT, not to mention the overall temperature of the upper section of the dilatometer. Vibrations probably caused the biggest error here since it was almost impossible to completely isolate the system from nearby pedestrian traffic, laboratory hood vibrations, etc.

3.3.4.3 Dilatometric Tests

Samples of PC with varying orientation functions were aged isothermally at 90°C and 120°C for approximately 300,000 seconds (5 days). Samples of PS were aged at 60°C. The temperatures of 60°C for PS and 90°C for PC were determined after first analyzing the shrinkage data. They were a compromise between faster volume relaxation/aging rates and minimal shrinkage. One does not want the added effect of shrinkage convoluted into the aging data when performing creep measurements (and it was desirable to use the same aging temperatures for both the creep and dilatometric measurements). Supplemental dilatometric measurements were performed for PC at 120°C precisely to see how the added effect of shrinkage might affect the volume relaxation data. Consequently, because of the high shrinkage, no creep measurments were performed at this higher temperature.

Each dilatometer is good for only one measurement so it is important to maximize the useful data gained from it. For that reason, some of the PC samples, after being aged at 90°C, were then heated to 120°C where they were allowed to relax further. If sufficient aging time is allowed after this "T-jump", the relaxation rate obtained should eventually be the same as if the polymer had been aged wholly at 120°C.[1] This provides an additional data point at 120°C and a useful check of the reproducibilty of the data. It may also provide an indication as to whether shrinkage is affecting the volume relaxation process. Naturally, these points will be distinguished from the normal 120°C measurements.

Time zero is defined when the dilatometer was first inserted into the oil bath. Approximately 5 to 10 minutes was required for the sample, mercury, and glassware to attain thermal equilibrium. All data was normalized to the volume at 16 minutes (~1000 seconds) at which time thermal equilibrium was guaranteed. Note that only relative volume changes were measured for both polymers.

3.3.4.4 Linear Dilatometric Tests

Because of the anisotropy in the uniaxially oriented samples, it is expected that there will be a directional dependence to the volume relaxation rate. Unfortunately, volume dilatometry only gives the total change in volume and says nothing about directional dependence. To circumvent this problem, a 50 mm sample of 1.5X PC was annealed at 90°C for 6 days in a manner similar to the shrinkage measurements described earlier. This intermediate orientation was chosen since it would result in less shrinkage. The longer times were required in order for shrinkage to subside and true, aging related length/volume changes to predominate. Linear relaxation rates were determined for samples tested in both the MD and TD directions. From this, the relative relaxation rates (α_{md} and α_{td}) in the different material directions could be compared to gain an understanding of the anisotropy of the relaxation process. In addition, a value for β could also be obtained from this technique ($\beta=\alpha_{md}+2\alpha_{td}$) although the error is significantly greater as compared with volume dilatometry. Because of the high error involved and the testing time required, only a few samples were tested in this manner. Nevertheless, all showed qualitatively the same behavior.

3.3.5 Tensile Creep Measurements

Tensile creep measurements were performed using a Seiko TMA 100 outfitted with a tensile testing fixture. This fixture was modified from the original to allow for longer sample lengths. Rectangular tensile coupons were cut from the stretched film samples having a nominal width of 2 mm and a length of 50 mm. The long direction of the tensile samples was parallel to the MD. Sample thickness varied with stretch ratio but was typically around 0.2 mm. Creep loading schedules followed the standard procedure outlined by Struik.[1] Loads were applied at 1 hr., 2 hrs., 4 hrs., 8 hrs. and 16 hrs. The loading time for each test was one-tenth of the aging time in order to keep the measurement time short compared with the changing aging condition. Creep strains were

generally 0.1 to 0.2% or less. The loading rate for the TMA was 150 g/min (0.025 N/s). This resulted in a loading time of approximately 20 to 30 seconds--considerably longer than dead load testers. Consequently, the first minute of creep data was discarded.

Both horizontal and vertical shifting were employed to form a master curve at a reference time of 4 hours. In addition to the horizontal shift rate μ_h defined in Equation (3.1-2), a vertical shift rate can be defined

$$\mu_v = -\frac{d \log a_v}{d \log t_e} \tag{3.3-8}$$

where a_v is the vertical shift factor. Vertical shifting accounts for a decrease in the instantaneous compliance D_o brought about by the aging process.

Creep aging studies were performed at 60°C for PS and 90°C for PC since shrinkage was reasonably small at these temperatures. Corrections for this shrinkage was still required, however, and the procedure is depicted in Figure 3.3-2. The baseline, which is decreasing with time due to shrinkage, was linearly extrapolated into the creep region. The creep data was then corrected by subtracting the extrapolated baseline. This, in effect, rotates the baseline to the horizontal. The fact that shrinkage is highest at short annealing times is the main reason aging times less than 1 hour were not utilized.

The TMA is a relatively "soft" instrument from a compliance standpoint. Left uncorrected, this softness can lead to considerable error in the sample absolute compliance. Compliance corrections were applied electronically by the TMA after first performing a "calibration" run with a 5 mm steel sample (this steel sample approximates a nearly infinite stiffness spring so that the measured deformation is due almost solely to the instrument). Even with this correction however, the error in absolute compliance is still expected to be significant. Fortunately, for creep-aging studies, what is of more importance is the relative changes in compliance with creep and aging time (which the instrument can provide accurately). Therefore it is emphasized that the "absolute" compliance values shown are only approximate.

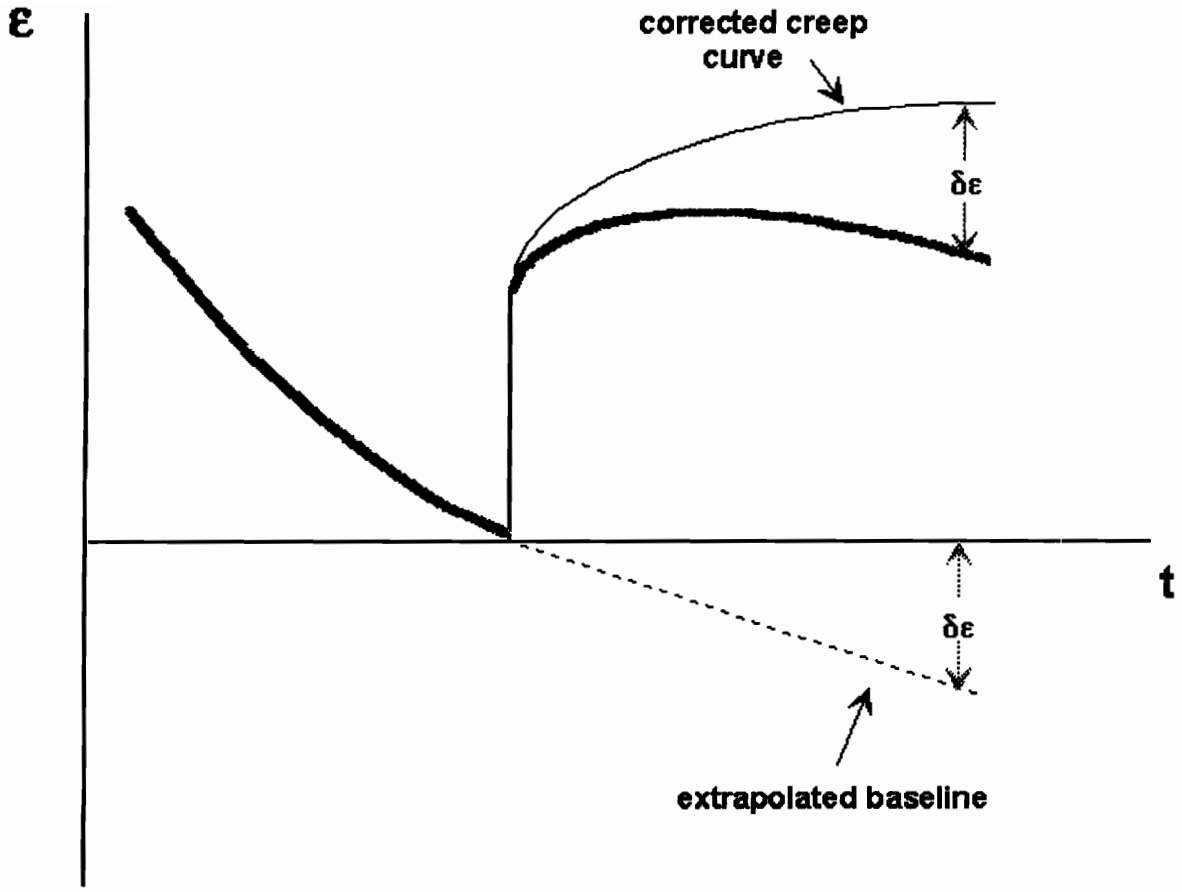

Figure 3.3-2. Methodology for shrinkage correction of creep curves.

Another source of compliance error results from variations in sample geometry. Point-to-point sample thickness varied by approximately 5% which correspondingly altered the cross-sectional area. In addition, some of the samples exhibited slight curvature which arose from surfaces stresses formed during the quenching process. This curvature produces artificially high values for the compliance since any sample bend acts as a "soft" spring. Remember that any attempt to relieve these stresses (and straighten the sample) by annealing at high temperature will alter the aging/orientation state of the sample! This curvature also varied with stretch ratio due to differences in thickness which, in turn, altered the residual stress formation during quenching. Curvature was much higher in the PC samples as compared to the PS samples.

Tests were also performed on samples cut parallel to the TD direction in an attempt to measure differences in relaxation behavior. The PS samples showed excessive micro-cracking during the creep testing so the tests were discontinued. The PC samples did not crack but were instead plagued with a high degree of sample curvature due to "bowing" of the stretched film. This curvature was so high as to affect the horizontal shifting behavior resulting in artifically high values for μ_h. A few samples having minimal curvature were tested and this data has been utilized along with the MD data.

3.4 Results

3.4.1 Density Measurements

Room temperature density data for the stretched polycarbonate samples are shown in Figure 3.4-1 and for polystyrene in Figure 3.4-2. The density ρ, is found to increase in approximately a linear manner with increasing f except at the lowest orientation functions for PC where it decreases slightly. As discussed earlier, this density increase with orientation for polycarbonate has also been reported in the literature.[29,30,31] The initial

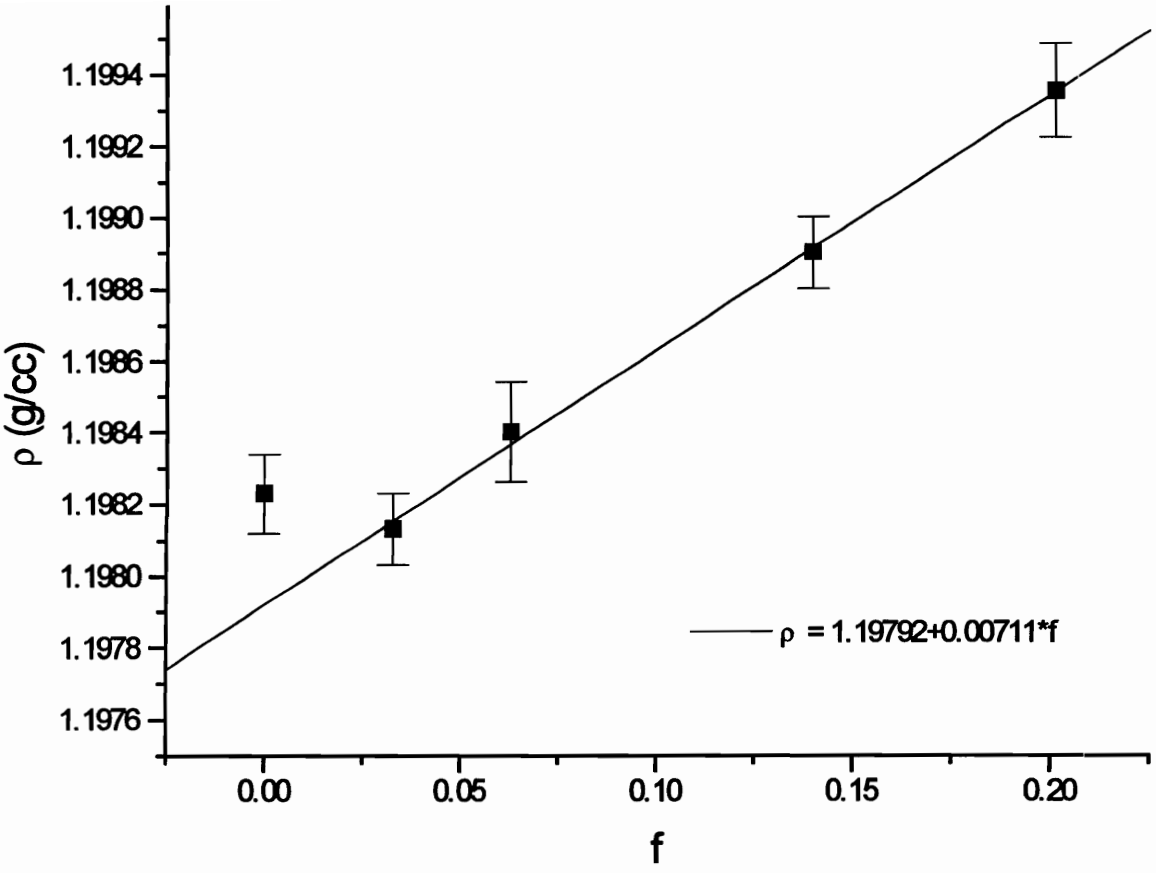

Figure 3.4-1. Room temperature density for PC versus *f*. Line fit only through high *f* data to illustrate linearly increasing trend.

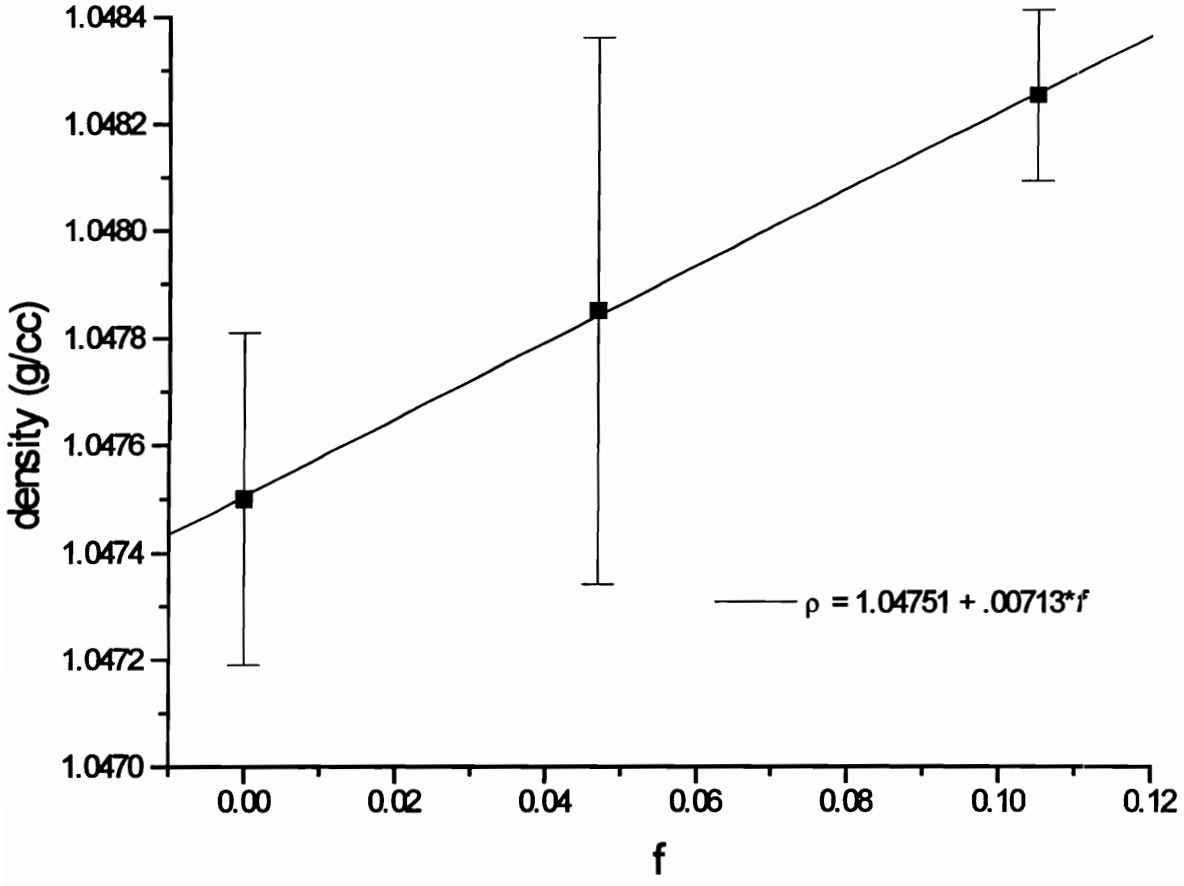

Figure 3.4-2. Room temperature density data for PS (same scale as for PC).

down turn in PC density is believed to be the result of the expected Poisson-type dilatation as predicted from continuum mechanics. The increase in density at high f, however, is *not* predicted by continuum mechanics and is possibly the result of better chain packing and the squeezing out of free volume with increased orientation. This decrease in free volume with stretching should imply a reduction in molecular mobility, however, later data will show that mobility may actually be enhanced. This could represent a serious breakdown of the free volume theory.

The density data presented here for PC differ slightly from the literature values. Ito and Hatakeyama's[31] density data for hot drawn PC vary from an isotropic density of 1.1920 g/cc to a value of 1.1945 g/cc at $f = 0.17$. While the absolute magnitudes of their densities are lower than those reported here, the relative changes in density with f are about the same. A key difference, however, is that their data do not show the initial decrease in density as shown in Figure 3.4-1. Phillips and coworkers[30] obtained a density of 1.1920 g/cc for isotropic PC and a value of 1.1990 g/cc at f=0.17. While the latter is in good agreement with the data in Figure 3.4-1, their unoriented density is much lower.

It is uncertain why the densities reported here are slightly higher as compared to the literature. Some of the current measurements on unoriented samples have resulted in densities as low as 1.1970 g/cc. However, these low readings were most likely due to voids in the film or air bubbles which have attached to the sample. The density gradient column will generally err toward lower densities for this very reason. It is possible that differences in measurement technique may be partially responsible for the density difference since both Ito and Phillips used flotation/immersion techniques. Still another factor may be time dependent aging/densification of the samples. Measurements were generally made a few days after stretching due to the logistics of moving the samples from the film stretcher to the density column. This would result in a slightly higher density than for samples measured immediately after stretching.

The large scatter in the PS data is partially the result of brittle microcracking which occurred in the samples when punched out of the film stock. PC is much more ductile and

did not exhibit this microcracking. While no measurements were made on low-f PS samples, it is suspected that it too will show the initial down turn in density. Nonetheless, it is the densification that is the most interesting since it defies conventional wisdom. This densification implies that free volume distribution and shape are probably undergoing significant change. How this affects mobility and physical aging behavior still remains to be answered.

3.4.2 Shrinkage Results

The shrinkage data as a function of annealing temperature are shown in Figures 3.4-3 and 3.4-4 for PC and PS respectively. The data is plotted as $L(t)/L_o$ where L_o is the initial stretched sample length. Shrinkage is a measure of molecular mobility in the oriented sample. Interestingly, the shrinkage is quite significant well below the T_g of the material. *Keep in mind, however, that total shrinkage is only of the order of 1% recovery.* The onset of measureable shrinkage occurs in the vicinity of 50°C for PS and 70 to 80°C for PC. These temperatures also correspond to secondary transitions for both polymers. The transition at 50°C for PS is denoted the β transition (not to be confused with the volume relaxation rate β_v) and is thought by Illers and Jenckel[32] to be a result of motion in regions where phenyl groups have less steric hindrance. In contrast, Takayanagi[33] suggests the origin is due to localized twisting of the main chain. The transition at 70 to 80°C for PC is denoted the α' transition. While the exact motion is unknown, Illers and Breuer believe it is due to non-equilibrium stresses which are frozen into the sample since it dissappears rapidly with annealing.[34] Regardless, it still represents a molecular motion of some form.

Above 70°C for PS and 100°C for PC, the shrinkage becomes so large as to make creep measurements nearly impossible. The shrinkage occuring during annealing will

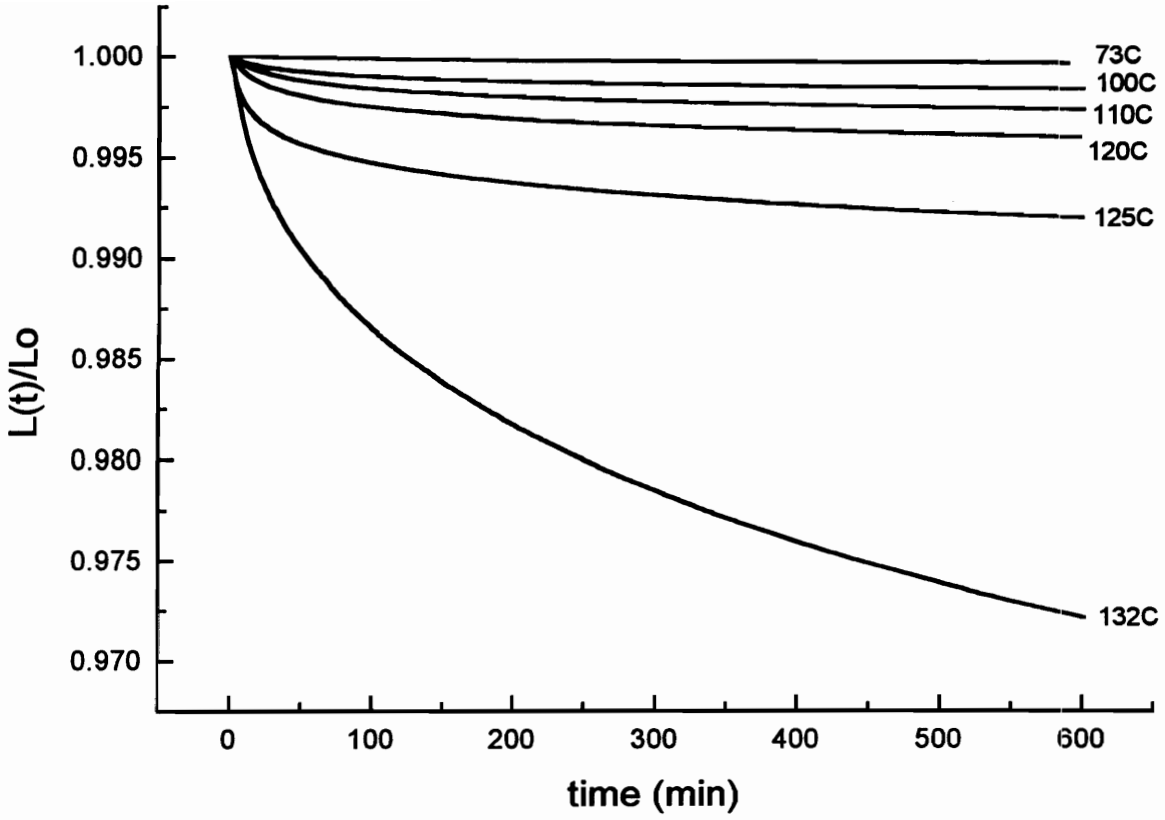

Figure 3.4-3. Isothermal shrinkage curves for 2.5X PC (f=0.16).

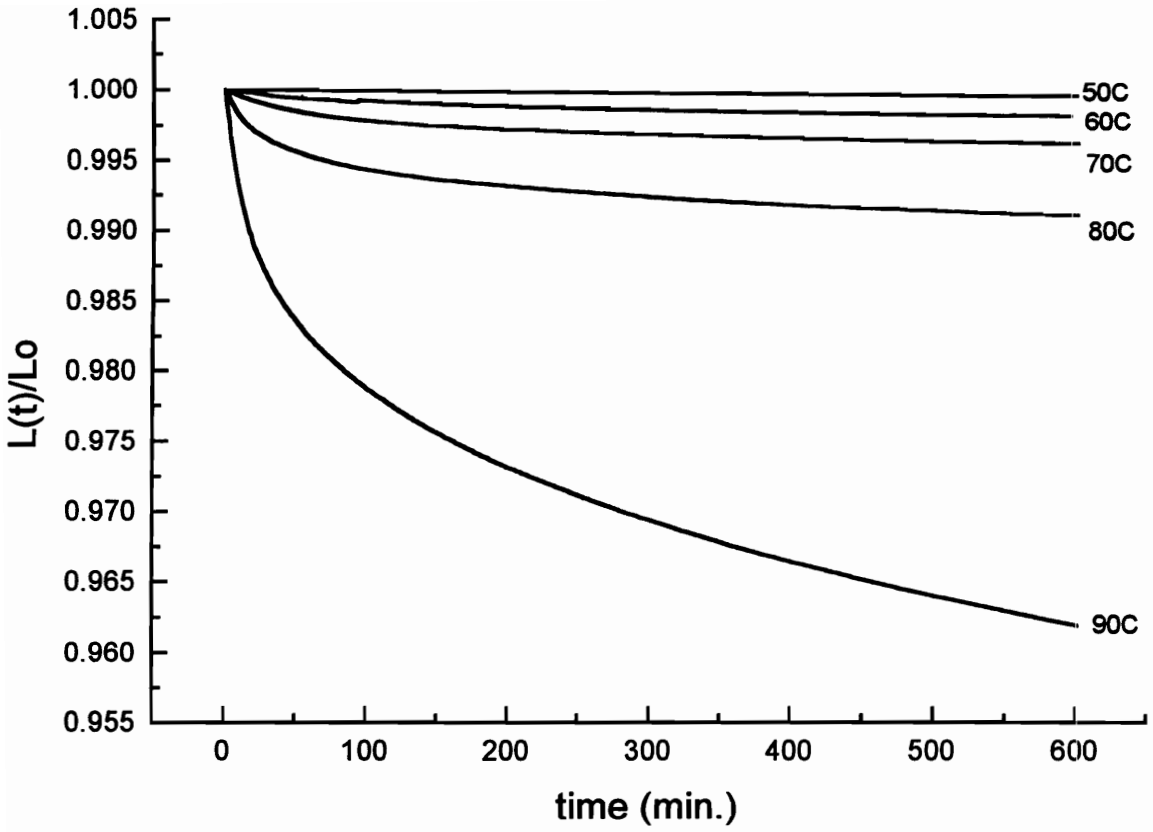

Figure 3.4-4. Isothermal shrinkage curves for 4X PS (f=0.10).

overwhelm the measurement of any creep strain occuring in the sample. It is likely that the main chain motion of the glass transition is becoming more significant in this higher range of temperatures.

As an addendum to the sub-T_g shrinkage measurements, some of the samples were immersed in an oil bath at 160°C (120°C for PS) for one minute to determine the total recoverable shrinkage. In the vast majority of the samples tested, shrinkage recovery was greater than 99%. Assuming affine deformation, this indicates that the molecular stretch ratio was equal to that of the actual macroscopic stretch ratio. Therefore negligiblerelaxation of orientation occurred between stretching and quenching into the glass. This is still a long way from perfect orientation however (hence the low values of *f*). One can predict the theoretical maximum stretch ratio λ_{max} for complete chain extension ($f = 1$) from[35]

$$\lambda_{max} = \frac{R_{max}}{\langle R^2 \rangle_o^{1/2}} = \left[\frac{q^2}{C_\infty M_o} \right]^{1/2} M^{1/2} \qquad (3.4\text{-}1)$$

where R_{max} is the extended chain end-to-end distance (equal to qL_oM/M_o where L_o is the segment length), $\langle R^2 \rangle$ is the mean square end-to-end distance for the unperturbed chain, M is the molecular weight, M_o is the molecular weight for a given segment link and C_∞ is the characteristic ratio. The parameter q is a correction factor to account for the reduction in end-to-end length due to the fixed valence angle (q=0.83 for C-C backbones). For PS Equation (14) simplifies to

$$\lambda_{max} = 0.0364 M^{1/2} \qquad (3.4\text{-}2)$$

assuming an M_o of 52 g/mol (half of the repeat unit molecular weight) and a C_∞ of 10.[36] Utilizing the M_n of 174,000 g/mol from the GPC data, one arrives at a theoretical maximum extension ratio of 15 for PS (much less than the 4X ratio used here).

For polycarbonate one can follow a slightly different procedure using data from Williams and Flory.[37] They determined a value of $\langle R^2 \rangle / M = 0.85$ A^2/g-mole wt. for a

virtual bond length of 7 Angstroms. This virtual bond is approximately half of the repeat unit. For an M_n of 16,500 g/mol (see Experimental) one arrives at an $\langle R^2 \rangle$ of 140 nm^2. The virtual bonds are joined at 112° which also results in a $q = 0.83$, so R_{max} is calculated to be approximately 75 nm (applying an $M_o = 129$ g/mol). Combining the results produces a λ_{max} of 6.3 for PC. The theoretical maximum stretch ratios for both polymers are a factor of 2 to 4 higher than the experimental stretch ratios. This should help to elucidate why the orientation functions for oriented amorphous polymers are so small. Attempts to stretch either PS or PC to these higher theoretical stretch ratios will generally result in film tearing and breakage long before the theoretical limit is reached. The stretch temperature could be increased to minimize this tearing, however higher molecular mobility will cause the orientation to partially relax out during stretching.

3.4.3 Dilatometric Results

Sample volume relaxation curves for PS at 60°C are illustrated in Figure 3.4-5. Each curve represents a different value of orientation function *f*. Similar curves for PC at 90 °C and 120°C are shown in Figures 3.4-6 and 3.4-7 respectively. Typical curves for the PC T-jump experiments, where the sample was first annealed for 300,000 seconds at 90°C and then heated to 120°C for further aging, are depicted in Figure 3.4-8. Time zero for this T-jump experiment was taken when the bath first reached 120°C (heatup time was approximately 5 minutes). The data in Figure 3.4-8 only illustrates the 120°C annealing portion of the experiment.

The data in the above figures is plotted as $\Delta V/V_o$ where V_o is the initial volume at the start of the experiment and ΔV is simply $V(t)-V_o$. When plotted in this form on a log time scale, the slope of the curve becomes equal to the volume relaxation rate β defined as

$$\beta = -\frac{1}{V(t)}\frac{dV(t)}{d\log(t_e)} \cong -\frac{1}{V_o}\frac{dV(t)}{d\log(t_e)} = -\frac{d(\Delta V / V_o)}{d\log(t_e)} \qquad (3.4\text{-}3)$$

The approximation results from the fact that V(t)>>dV(t). The steeper the slope of the volume relaxation curves, the higher the rate of volume relaxation. Inspection of Figures 3.4-5 through 8 show that the relaxation rate is approximately constant for long annealing times. Only for the PS samples at very short annealing times, and for the T-jump experiment in Figure 3.4-8 does one see time dependent changes in β. Therefore the volume relaxation rates were obtained from the data at t_e of ca. 100,000 seconds. These values for β plotted as a function of f are shown in Figure 3.4-9 for PS and Figure 3.4-10 for PC. Of obvious significance is the fact that the oriented samples as a whole tend to relax at a faster rate than the unoriented samples. This will be discussed in more detail later. First it is important to compare the isotropic values for β with the literature data in Figure 2.2-5 as a check of the accuracy of the dilatometer. The (isotropic) literature value for PS at 60°C is approximately 7×10^{-4} and for PC at 90°C is 5.5×10^{-4}.[38] At 120°C the literature value is 7.5×10^{-4}.[38] These values are in excellent agreement with the experimental data in Figures 3.4-9 and 10 thus confirm the dilatometer's accuracy.

As a final volumetric measurement, a biaxially oriented sample of polycarbonate stretched 1.5X by 1.5X (simultaneous stretch using same conditions as for the uniaxial samples) was dilatometrically tested at 120°C. The motivation was to see if there was a significant difference between uniaxial and biaxial stretching. The resulting value for β was 13.5×10^{-4} which is slightly higher than the 1.5X and 2.5X uniaxial samples, although the difference is not statistically significant.

3.4.3.1 Linear Dilatometry

The linear relaxation curves for the 1.5X PC sample aged at 90°C are shown in Figure 3.4-11 along with an isotropic control. The MD and TD curves represent different samples cut from the same film stock, and in approximately the same location. Values for α_l were obtained at times greater than 1000 minutes since thermal shrinkage was greatly reduced at this point resulting in less curvature. What is of great importance is the fact

that the volume relaxation occurs almost solely along the MD or stretch direction. In fact, the transverse direction actually expands slightly. This indicates that thermal shrinkage may play a role in the enhanced volume relaxation rates of the oriented samples. It is almost as if the oriented chains are being "reeled in" during annealing while simultaneously being packed into an ever tighter structure. However, since changes in f and sample length were small, it is likely that this reorientation is only occurring on a local scale and is not due to long range reptation.[39]

It is also noted that the calculated values for β were slightly lower than those obtained from volume dilatometry. This is believed to be due to a combination of poorer temperature control and the sample creep arising from the tensile stress. This creep would counteract some of the volume relaxation occurring during aging resulting in an artificially low value for β. Nonetheless, this relative change in β between the isotropic and oriented samples is approximately the same for both the linear and volume dilatometric measurements.

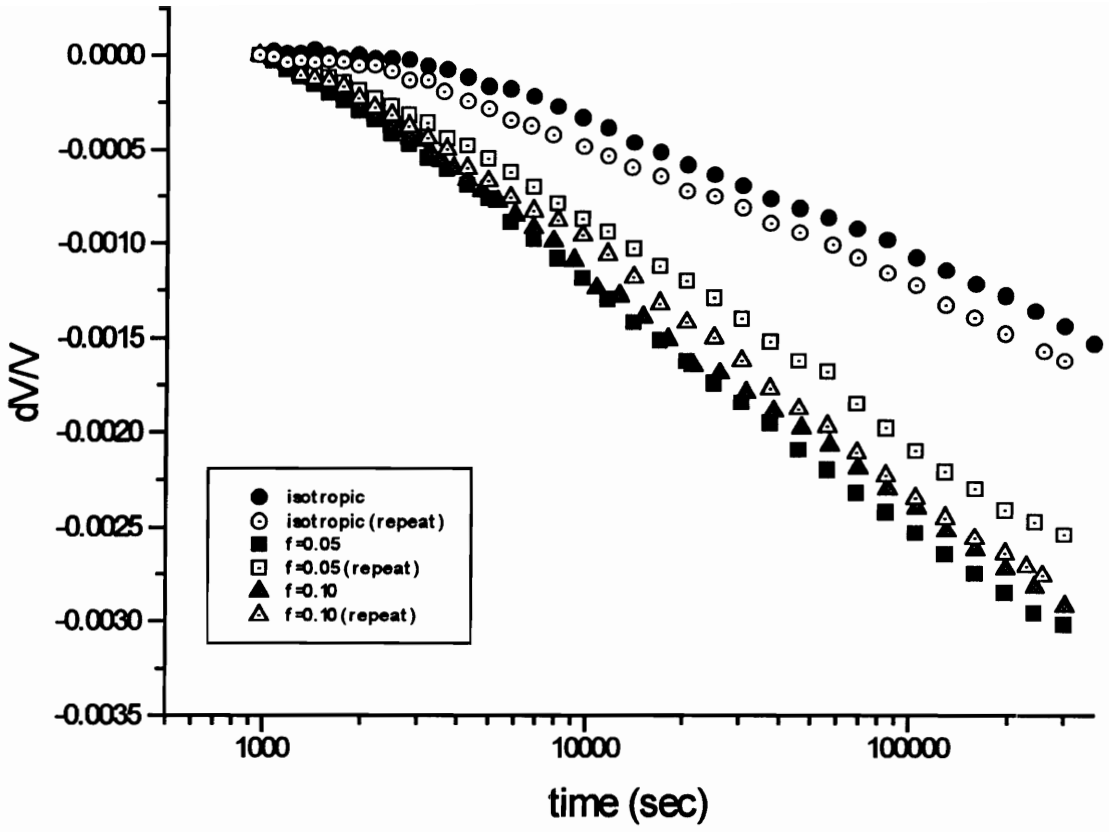

Figure 3.4-5. Volume relaxation data for PS at 60C

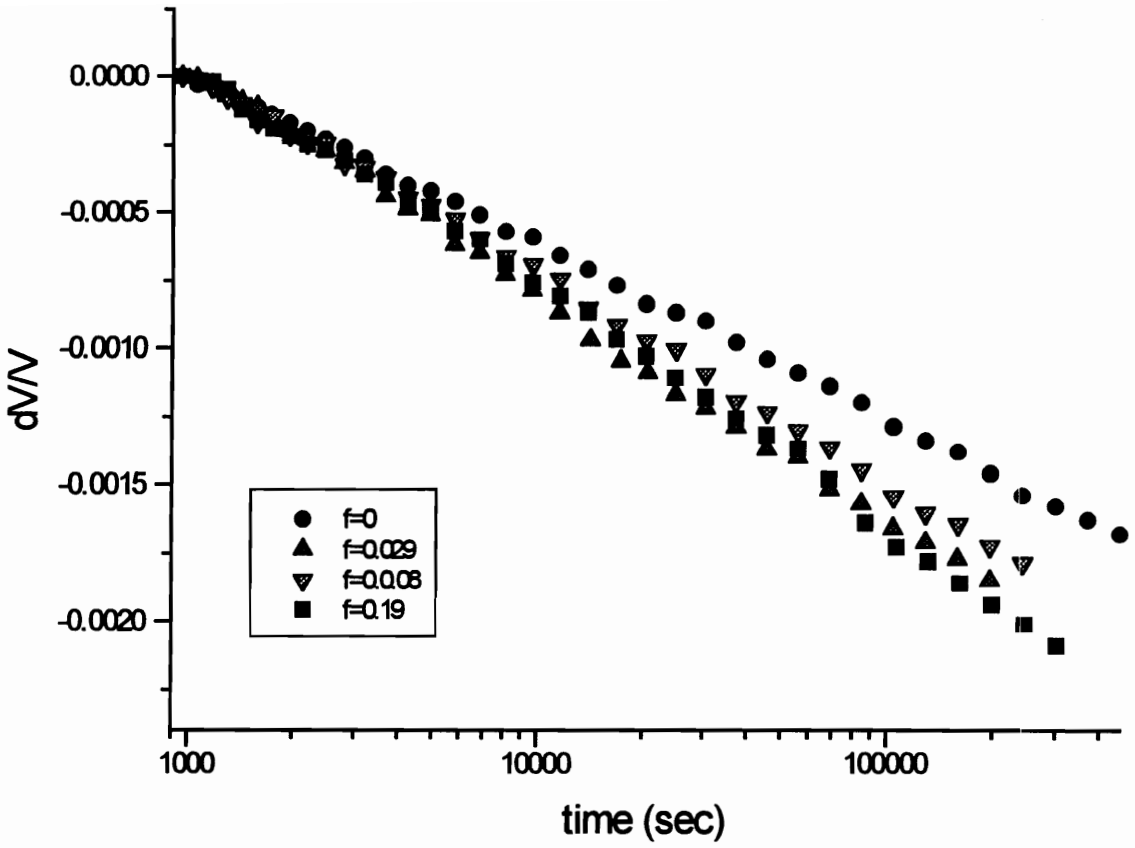

Figure 3.4-6. Isothermal volume relaxation of PC at 90C. Data scatter similiar to PS data in Fig. 3.4-5.

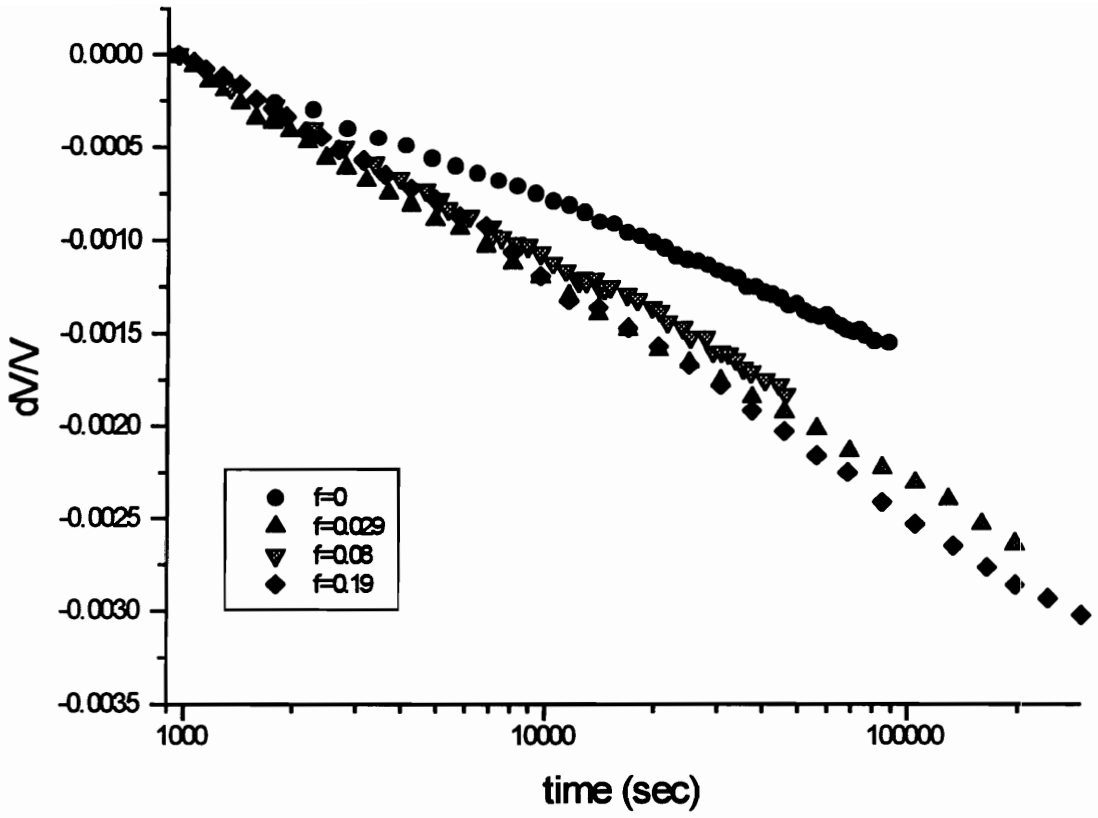

Figure 3.4-7. PC volume relaxation data at 120C.

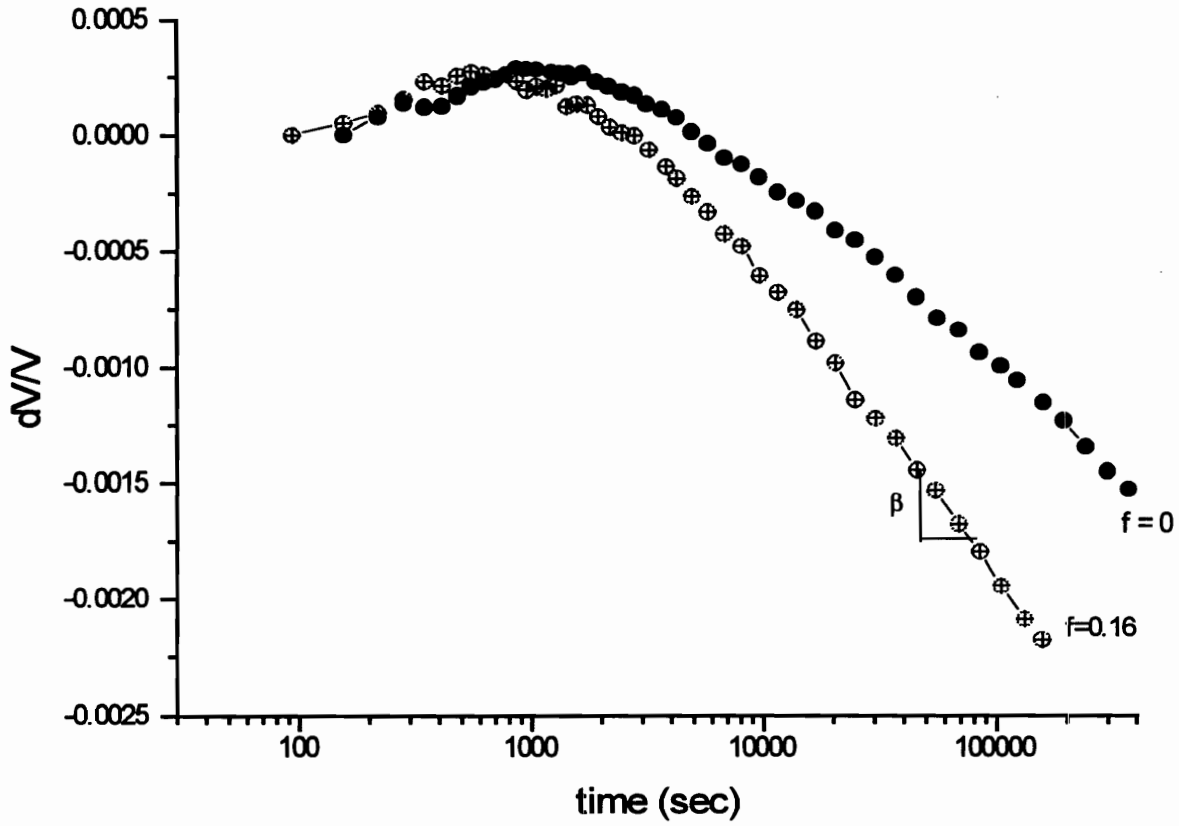

Figure 3.4-8. Temperature jump for PC to 120C after 5 days annealing at 90C.

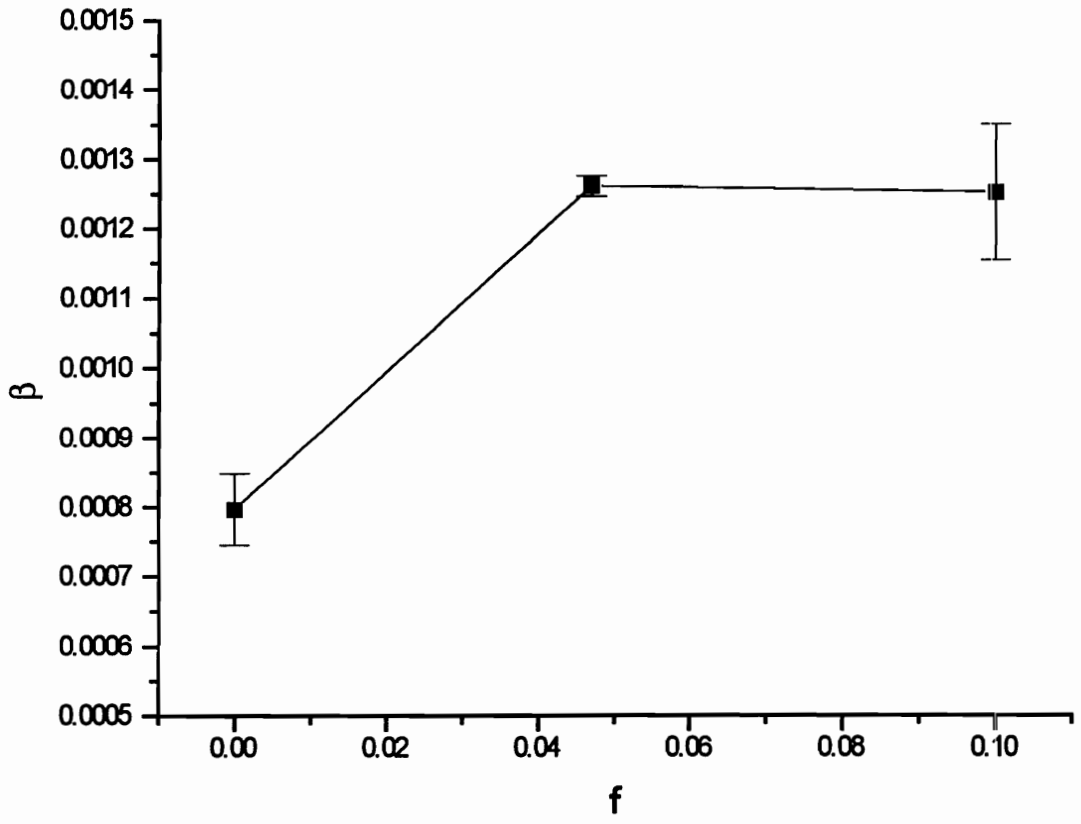

Figure 3.4-9. Volume relaxation rates for PS at 60C.

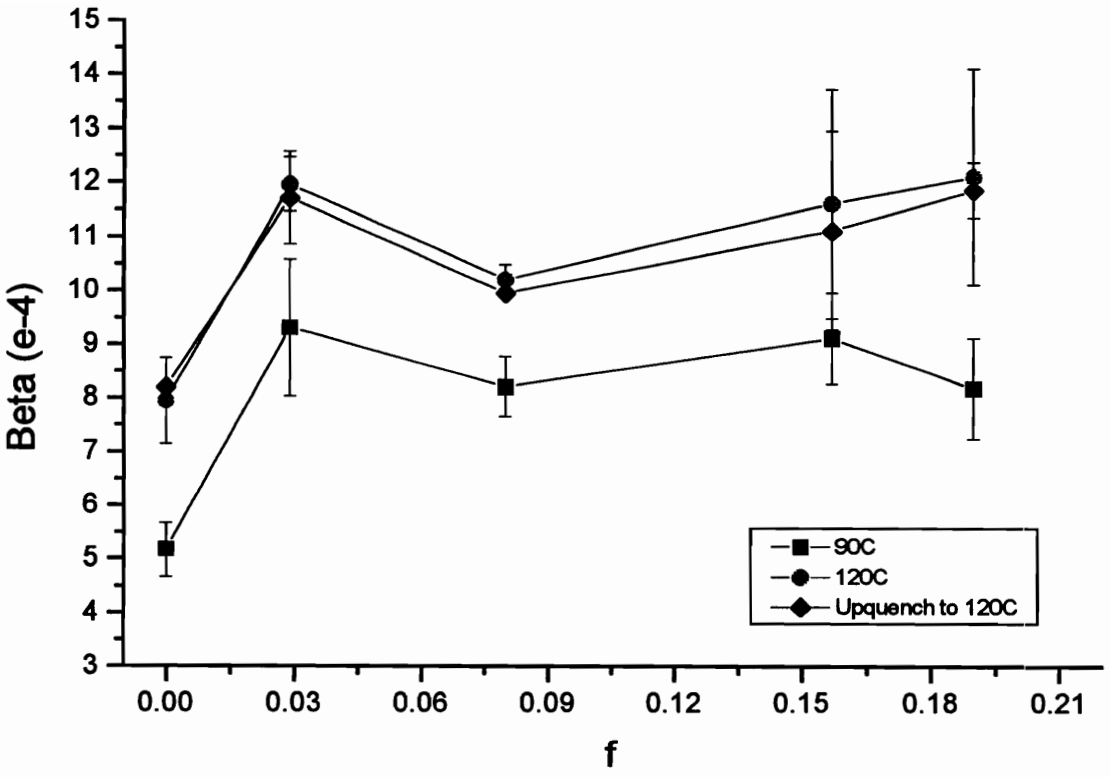

Figure 3.4-10. Volume relaxation rates for PC at various temperatures.

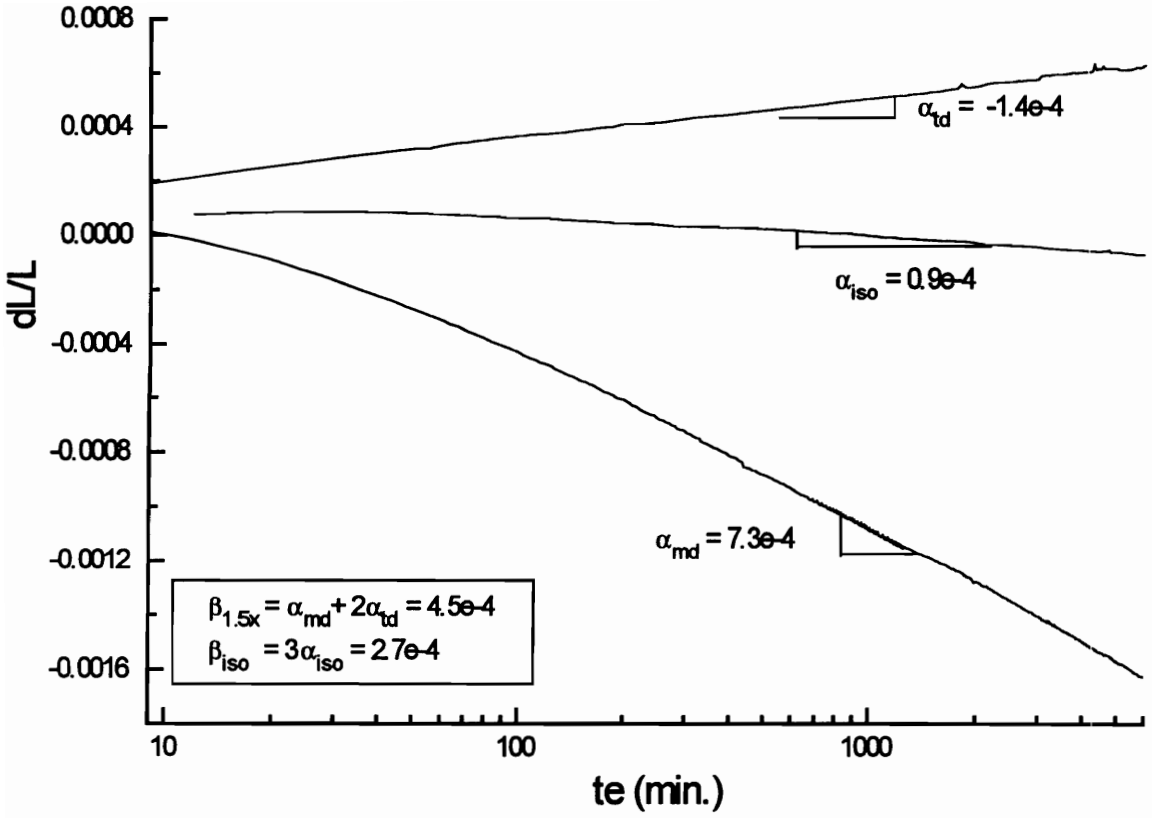

Figure 3.4-11. Linear relaxation rates for a 1.5X PC sample in the MD and TD directions. Isotropic control also tested for comparison. Test temperature was 90C.

3.4.4 Results from Tensile Creep Testing

For illustrative purposes, the entire time-aging time superposition process will be shown for a single PS sample. Following this, compliance curves for each polymer at varying values of f will be displayed along with the resulting shift factors. In order to compare the effects of orientation on the shape of the creep compliance curve, only the data at the 4 hr. reference time (which is essentially the same as the master curve) will be plotted together and the retardation behavior compared and contrasted.

3.4.4.1 Formation of a Master Curve

A sample set of creep curves for an oriented polystyrene sample (f=0.105) is shown in Figure 3.4-12. Both horizontal and vertical shifting were employed to obtain the master curve in Figure 3.4-13. The refererence time for the shifting was 4 hours. Notice that there were some "imperfections" in the overlap which are probably a result of noise in the initial creep curves, error during shrinkage correction (particularly due to the assumption of a linear form for the slope correction), and error incurred during the horizontal and vertical shifting. That this is attributable to "noise" and shifting error is particularly true since the overlap error occurred randomly for different samples and different orientation functions. For cases where the overlap error is large and *cannot* be attributed to shifting error, then one must be careful in the interpretation since thermorheological simplicity no longer applies. Fortunately, this latter scenario was not a problem in this study.

The horizontal and vertical shift factors for the master curve in Figure 3.4-13 are plotted as a function of aging time in Figures 3.4-14 and 3.4-15 respectively. From these plots the mechanical shift rates μ_v and μ_h can be determined from the slopes of the curves. Compliance curves for PS at 1X and 2X, and for PC at 1X, 1.25X, 1.5X and 2.5 X are shown in Figures 3.4-16 through 21 respectively. All required some vertical shifting in order to form the master curves (not shown).

3.4.4.2 Shift Rate Data for PC and PS

The resulting horizontal shift factors as a function of aging time are shown in Figures 3.4-22 and 23 for PS and PC respectively. The slopes represent the horizontal shift factors which are seen to decrease slightly with increasing orientation. The horizontal shift factors μ_h, for PS are plotted in Figure 3.4-24 as a function of *f*. Similar values for the PC samples are shown in Figure 3.4-25. The vertical shifting rates for PC did not change significantly with *f* and had a value of 0.010 +/- 0.004. For PS, the values were more erratic with some of the curves requiring no vertical shifting and some with shift rates up to 0.02. It is uncertain why this variability exists. The horizontal shift factors are more important since they indicate how the retardation time spectra change with aging time. The data in Figure 3.4-24 and 25 imply that the aging rates from a mechanical standpoint decrease upon orienting the sample. This is in contradiction to the volume relaxation data discussed earlier.

3.4.4.3 Comparison of Compliance Curves

Compliance curves for PS and PC at t_e equal to 4 hours and varying values of *f* are compiled in Figures 3.4-26 and 3.4-27 respectively. Each of these curves—for a given value of *f*—is the average of 2 to 3 separate runs. There is a stark difference in retardation behavior for the PS with the oriented samples having a much shorter average retardation time (i.e. more rapid upward curvature) than the unoriented sample. For the PC, this difference is not nearly as pronounced although the trend is the same

The drop in overall compliance for the PS samples is also much greater with increasing *f*. For PC the change in compliance does not become significant until high *f*. It is uncertain whether the trend is real or the result of the compliance errors described in the experimental section. It does, in some ways, mimic the trend in density data where the density initially decreases then increases with *f*. Regardless, the PC compliance appears to

be much less sensitive to orientation effects than PS even though PC is more oriented (based on changes in f).

The compliance curves in Figures 3.4-26 and 3.4-27 were fit to Struik's creep equation[1]

$$D(t) = D_o \exp(t / \tau)^{\gamma} \qquad (3.4\text{-}4)$$

which is a modified form of the KWW or stretched exponential equation. Here D_o is the instantaneous compliance, τ is the retardation time, and γ is a "stretching" exponent so named because of the way it alters the effective retardation spectrum. All of the curves (not just the average curves shown in Figures 3.4-26 and 27) were first fit to this equation while allowing D_o, τ, and γ to vary. Because of the equation's inherent non-linearity, the goodness-of-fit is less sensitive to slight changes in γ; however, these slight changes bring about larger changes in τ. To minimize this variability, the curves were refit allowing only D_o and τ to vary while fixing γ at the average value. The resulting data are shown in Figures 3.4-28 and 29. Interestingly the retardation times decrease substantially with f although the change is less pronounced for PC. Values of γ for PS increase slightly with orientation whereas in PC they do not follow a well defined trend. These changes in γ could be significant or just an artifact of the curve-fitting process. The TD data for PC are found to follow approximately the same trend as the MD data. There are some slight differences in the values relative to the MD data, nevertheless there are insufficient data points to make a detailed comparison.

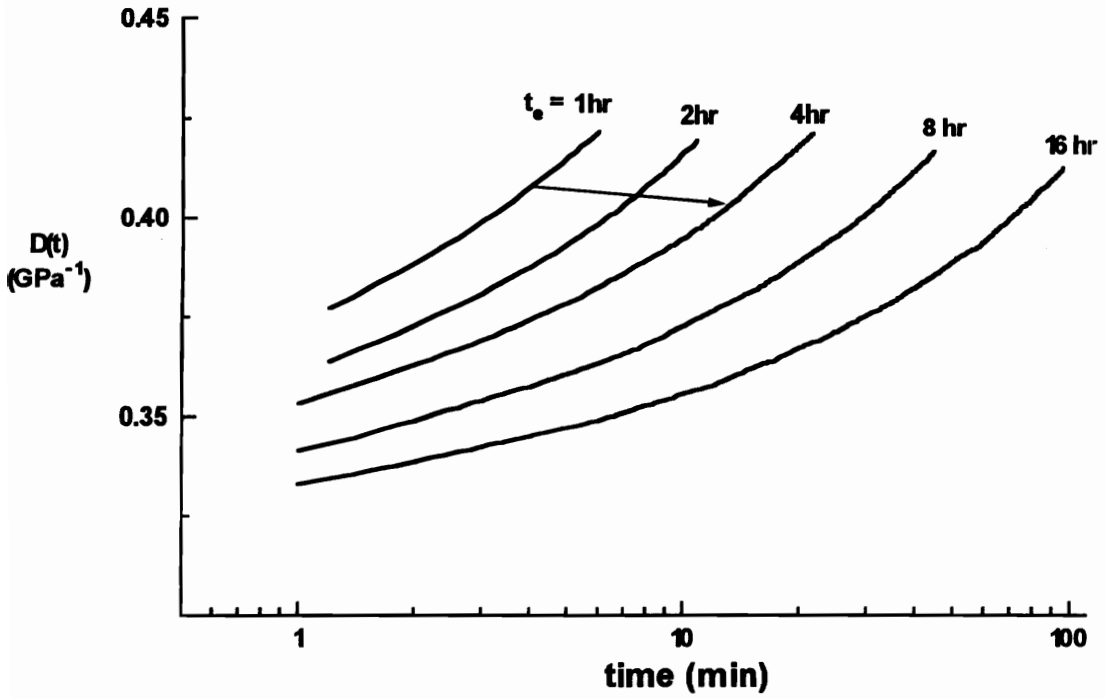

Figure 3.4-12. Corrected creep curves for oriented PS (f=0.10) at 60C.

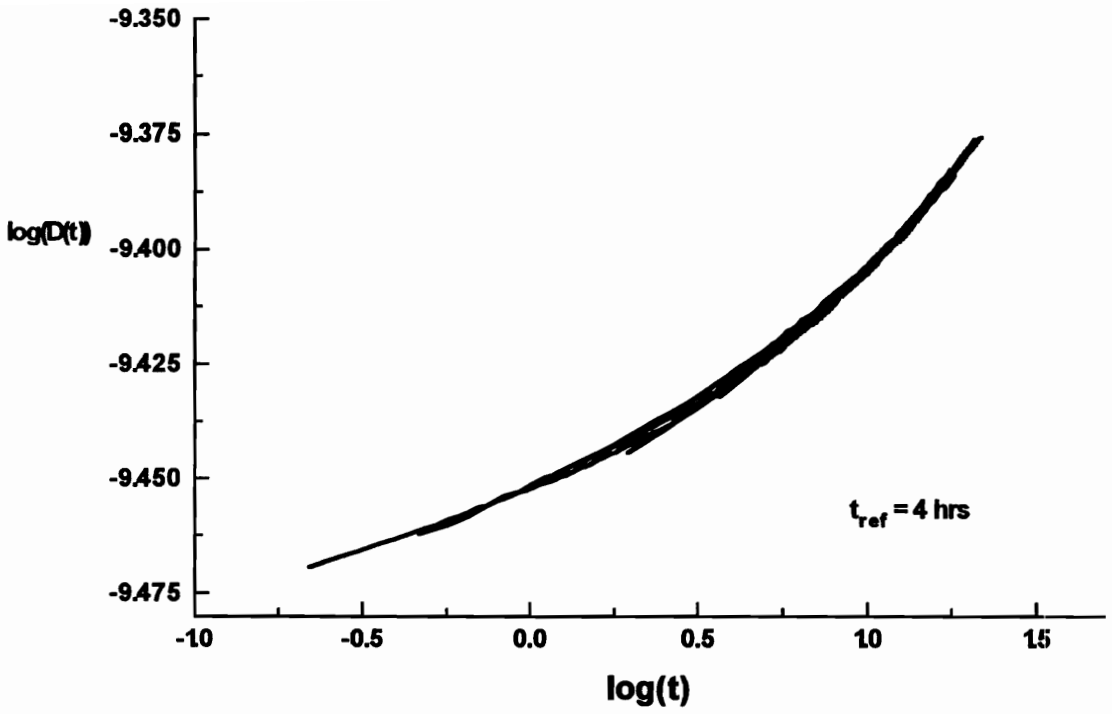

Figure 3.4-13. Master curve at a reference time of 4 hrs. for oriented PS at 60C.

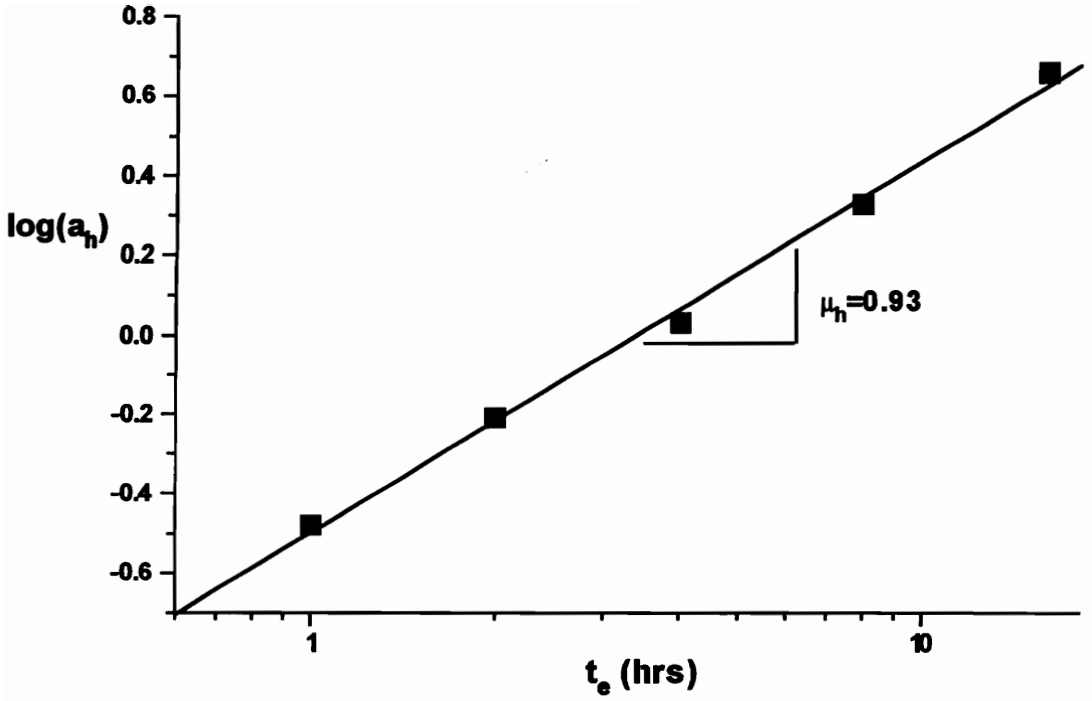

Figure 3.4-14. Horizontal shift rates for oriented PS at 60C.

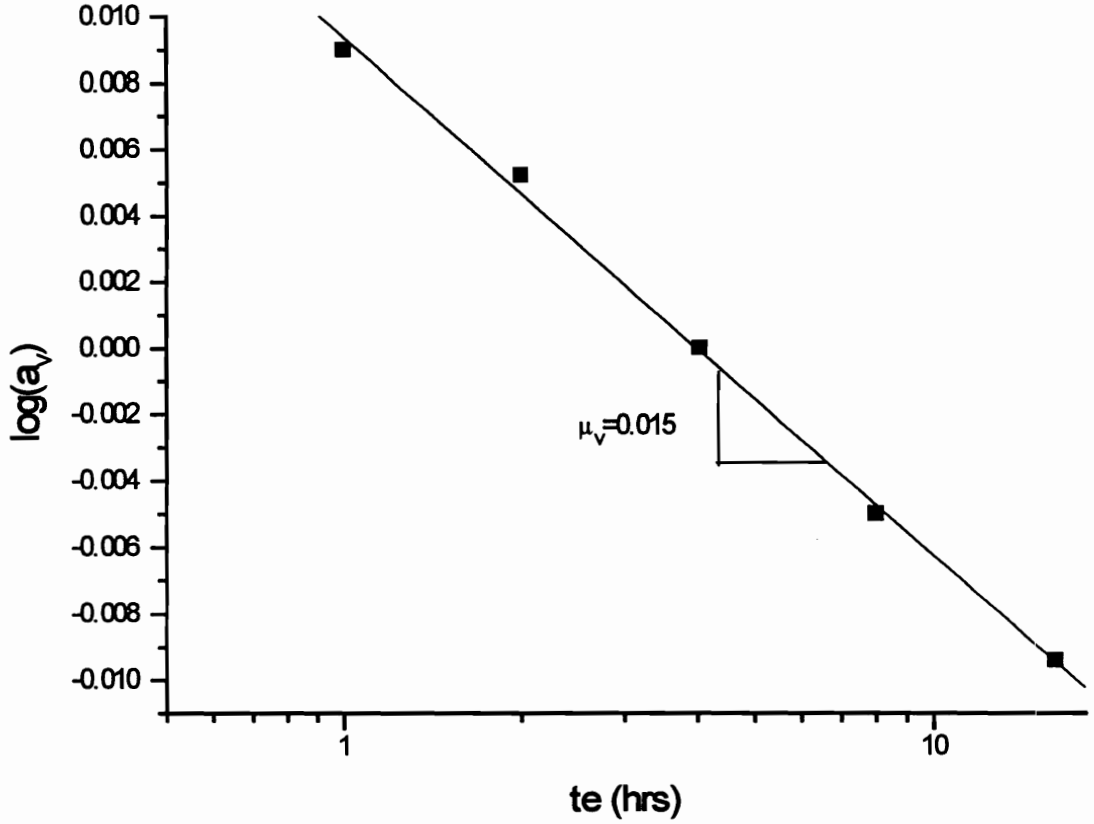

Figure 3.4-15. Vertical shift rate plot for oriented PS at 60C.

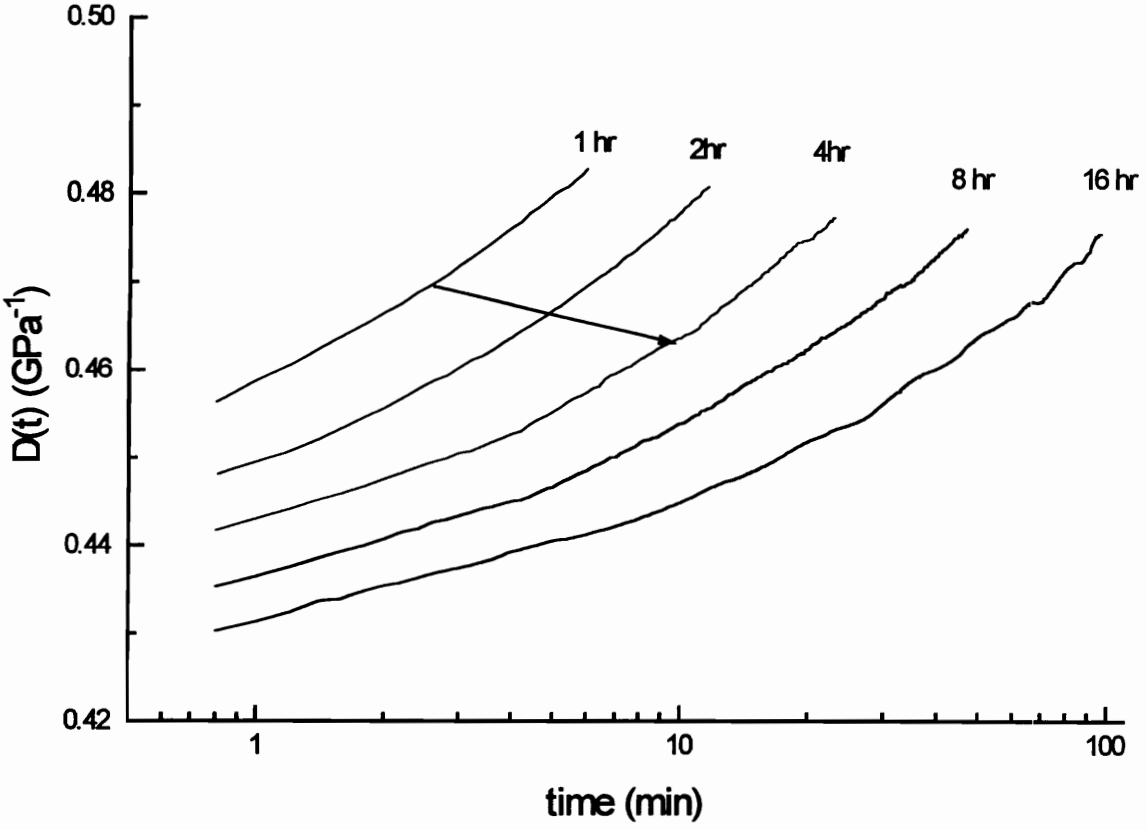

Figure 3.4-16. Creep curves for isotropic PS at 60C.

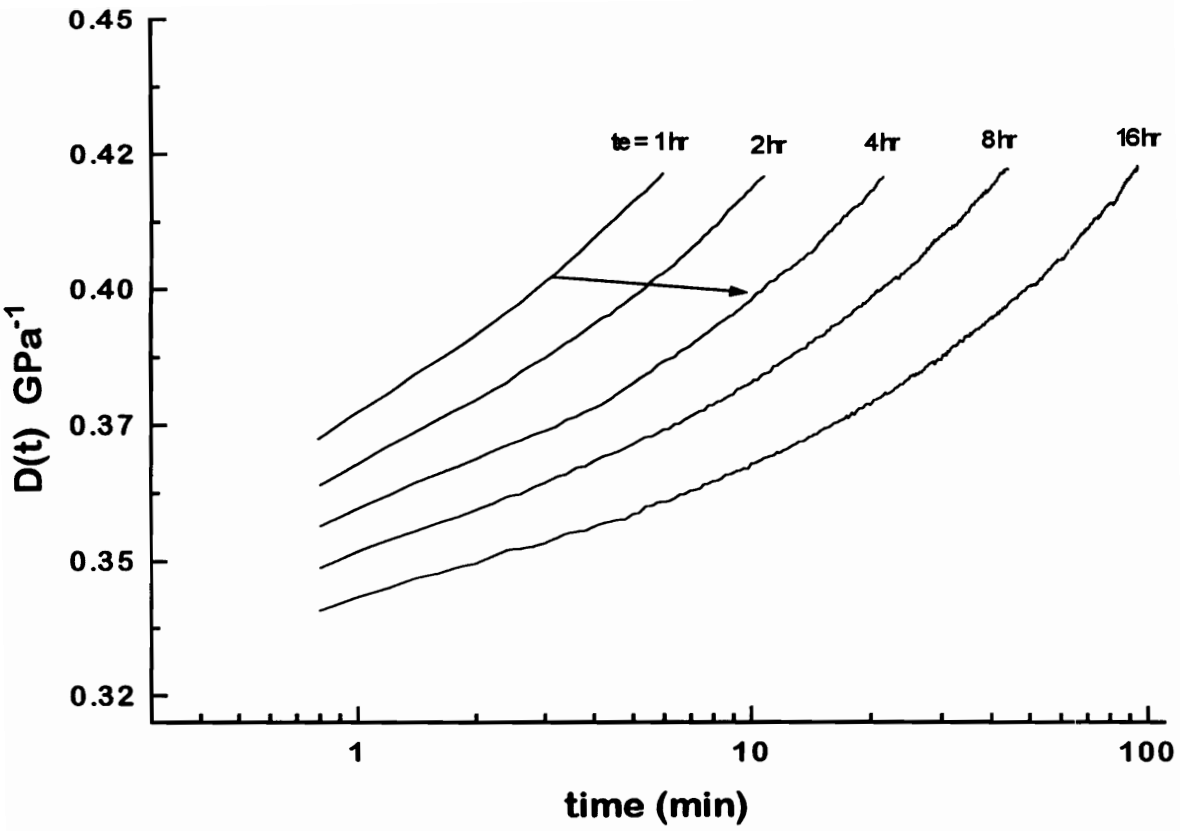

Figure 3.4-17. Creep curves for 2X PS at 60C (f = 0.05).

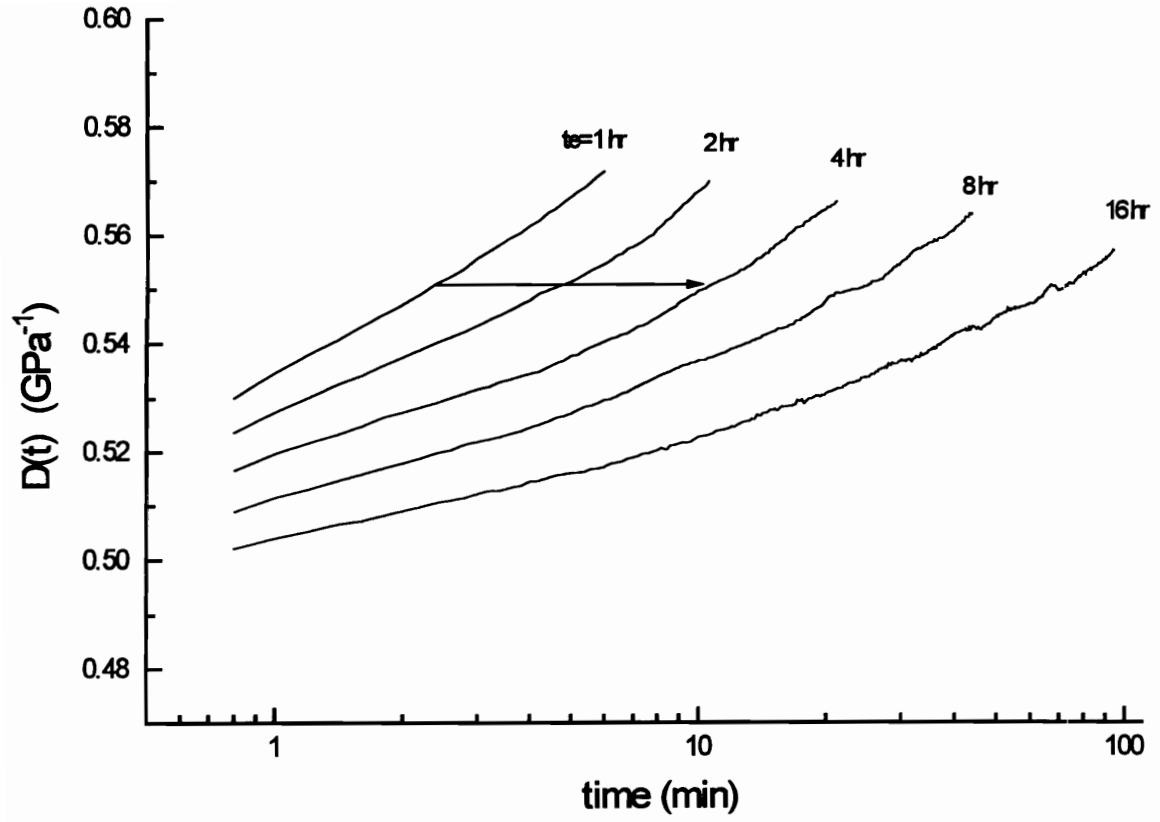

Figure 3.4-18. Creep curves for isotropic PC at 90C (f = 0.10).

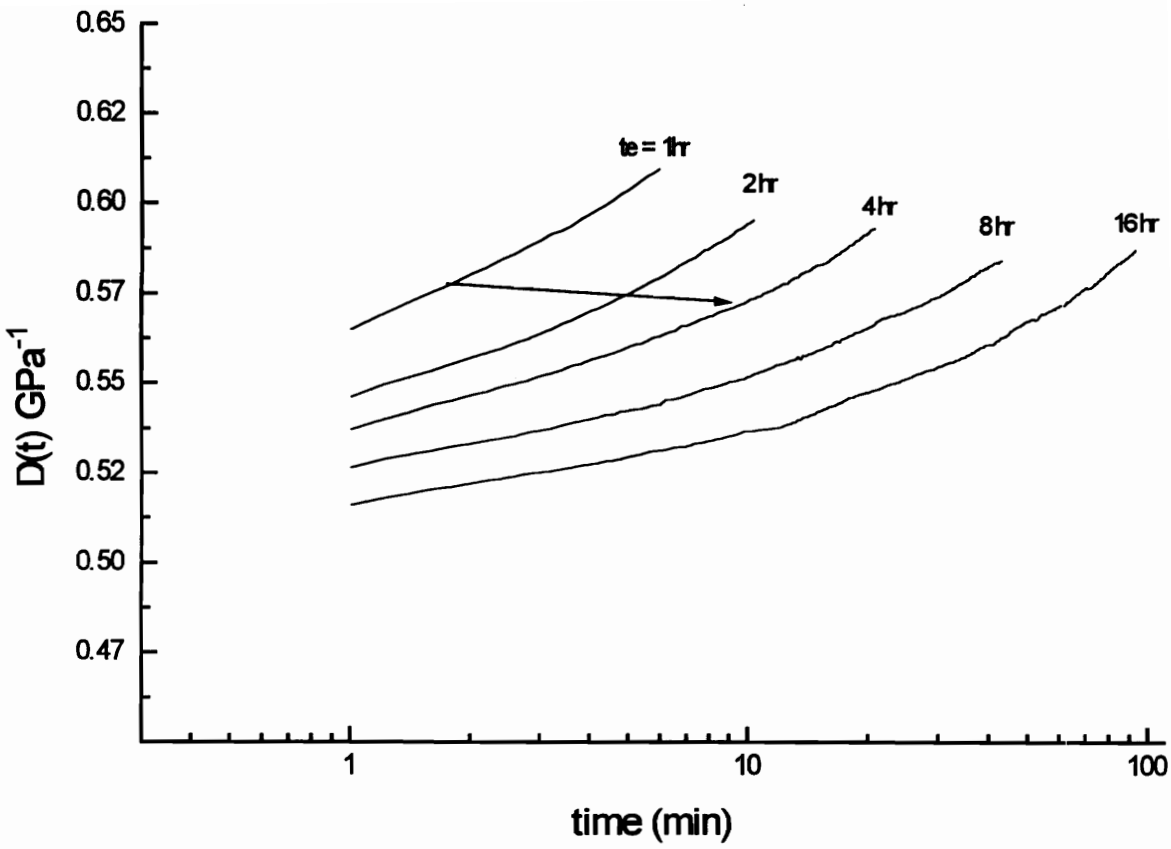

Figure 3.4-19. Creep for 1.25X PC at 90C (f=0.025).

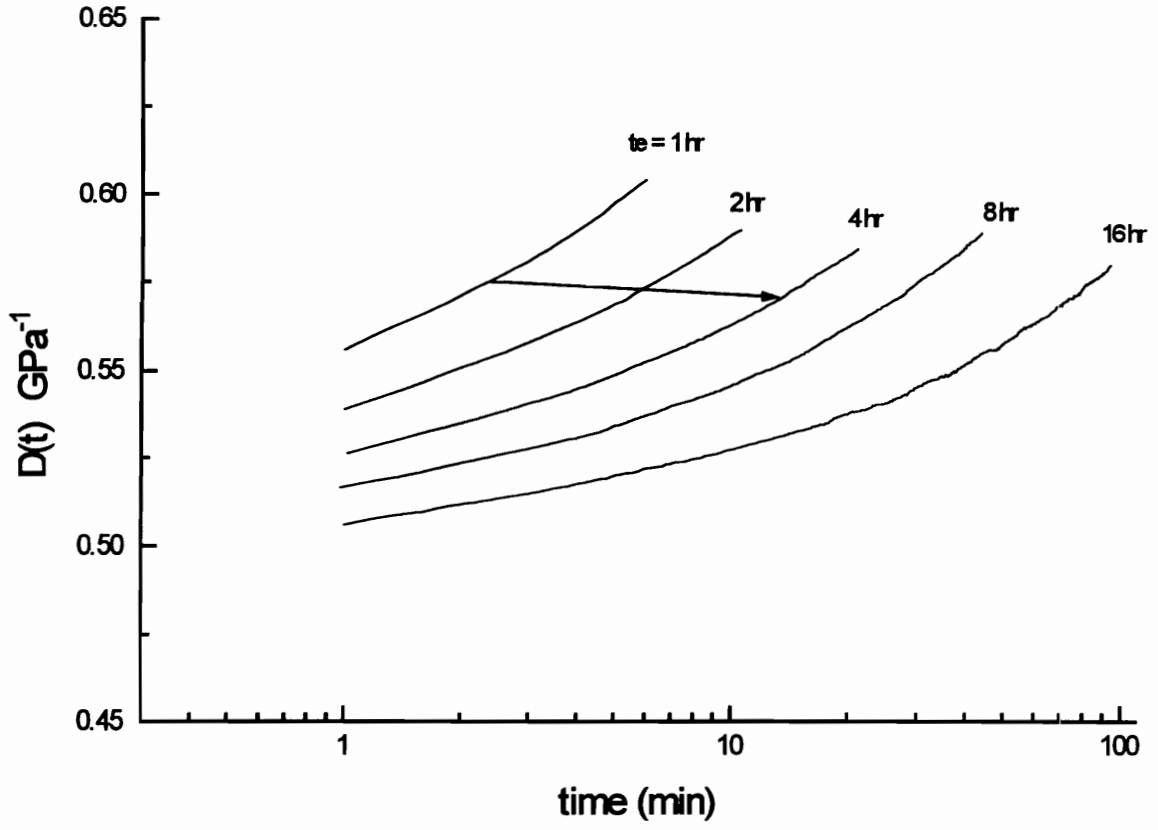

Figure 3.4-20. Creep curves for 1.5X PC at 90C (f = 0.085).

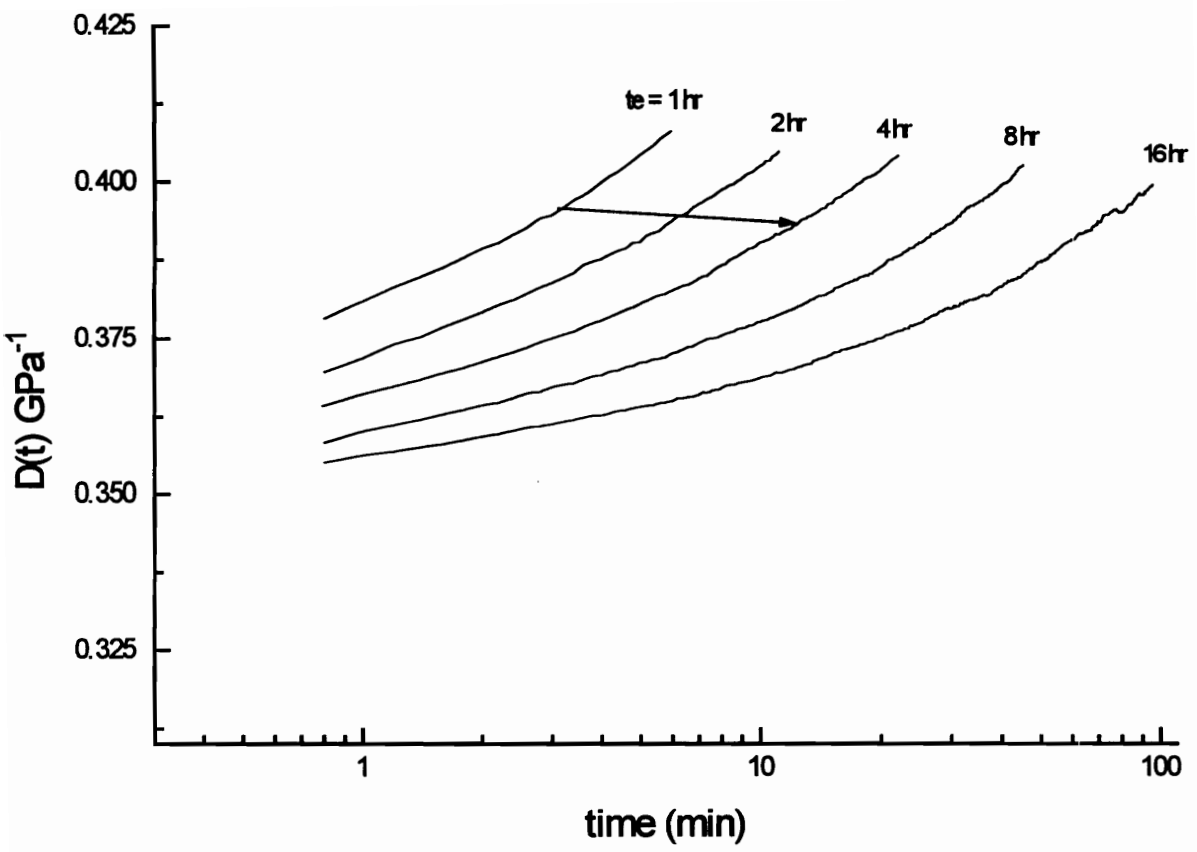

Figure 3.4-21. Creep curves for 2.5X PC at 90C (f=0.14).

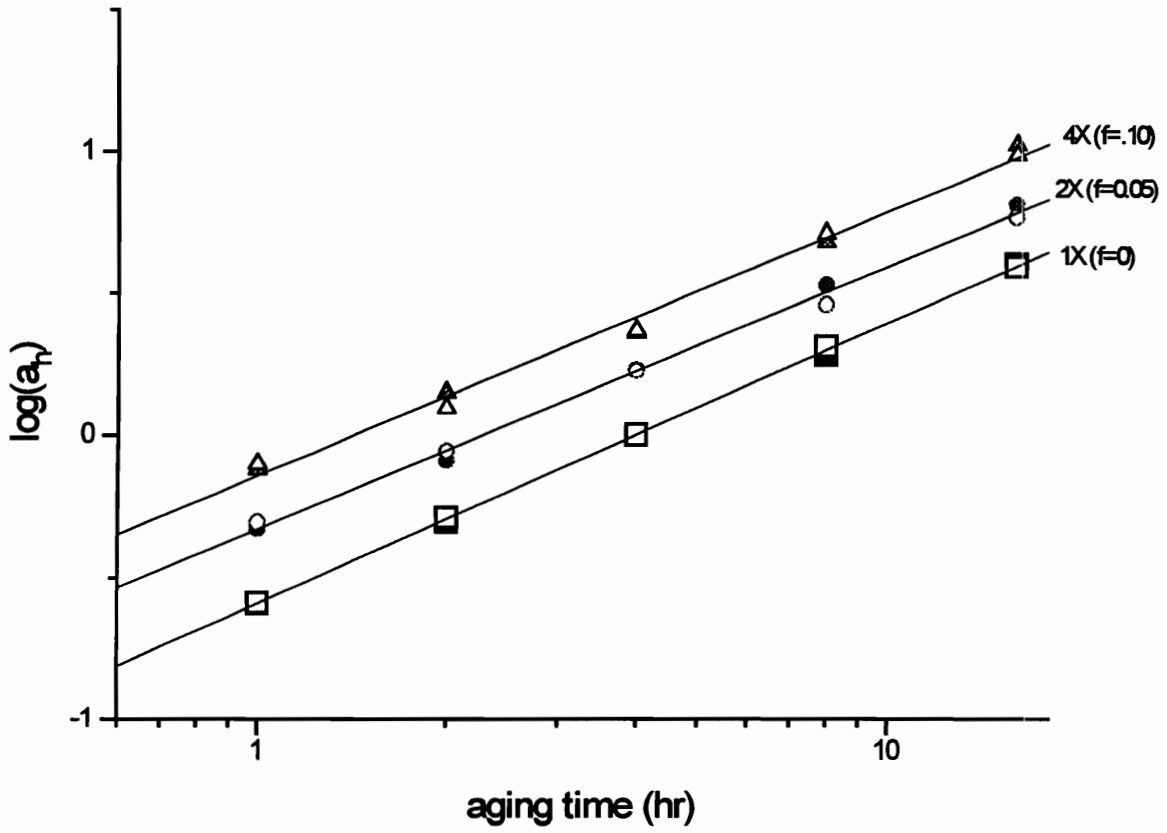

Figure 3.4-22. Horizontal shift factor plot at different orientations for PS. The vertical scale corresponds with the 1X sample only. The other curves were vertically offset for clarity.

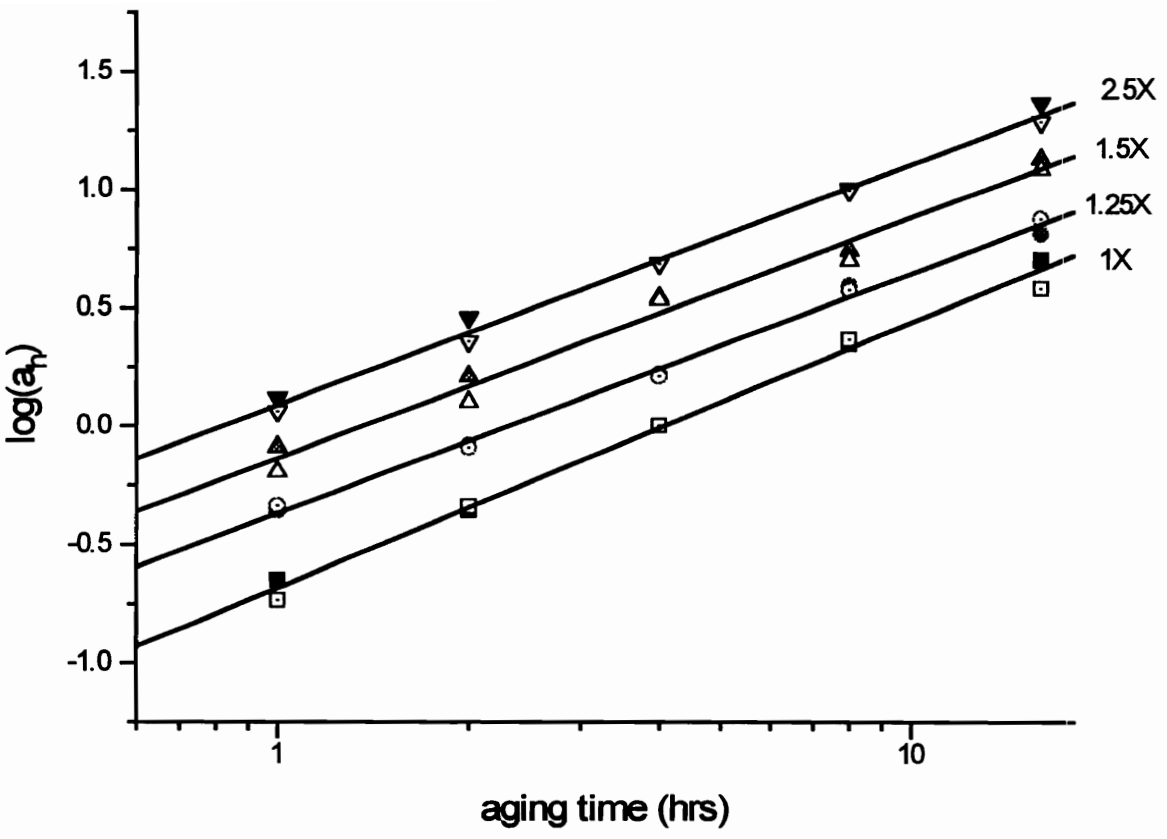

Figure 3.4-23. Horizontal shift factors at different orientations for PC. The vertical scale corresponds with the 1X sample only. The other curves were vertically offset for clarity.

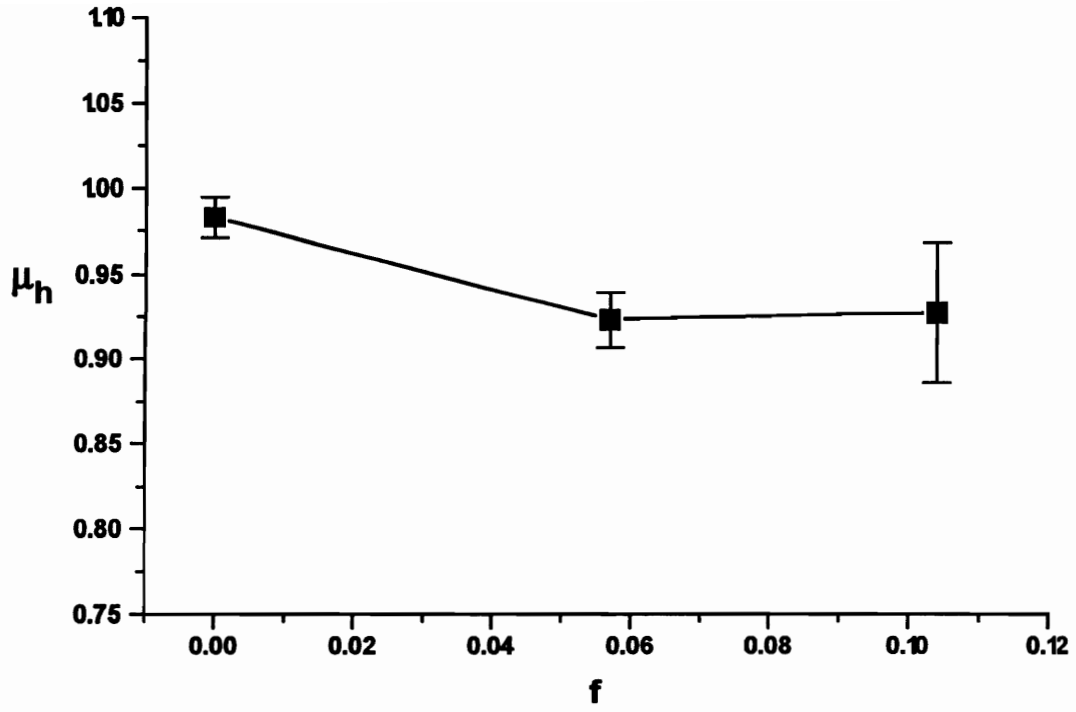

Figure 3.4-24. Horizontal shift factors for PS at 60C versus *f*.

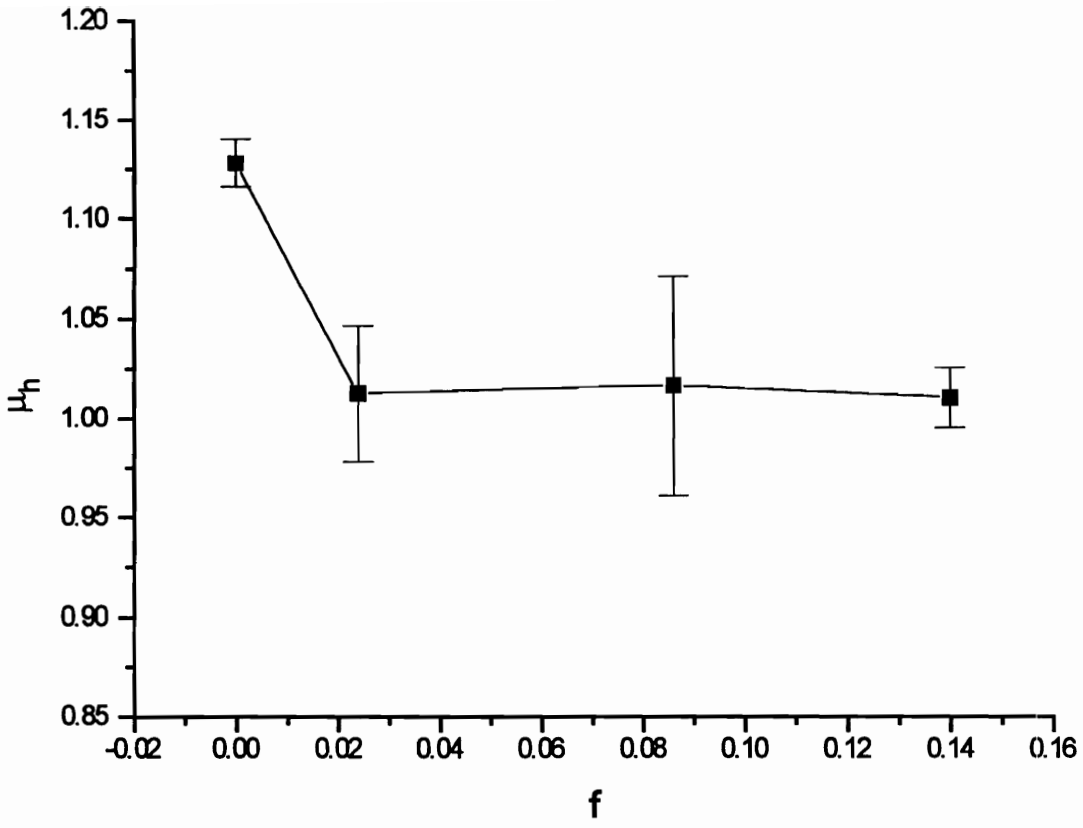

Figure 3.4-25. Horizontal shift rate for PC at 90C versus *f*.

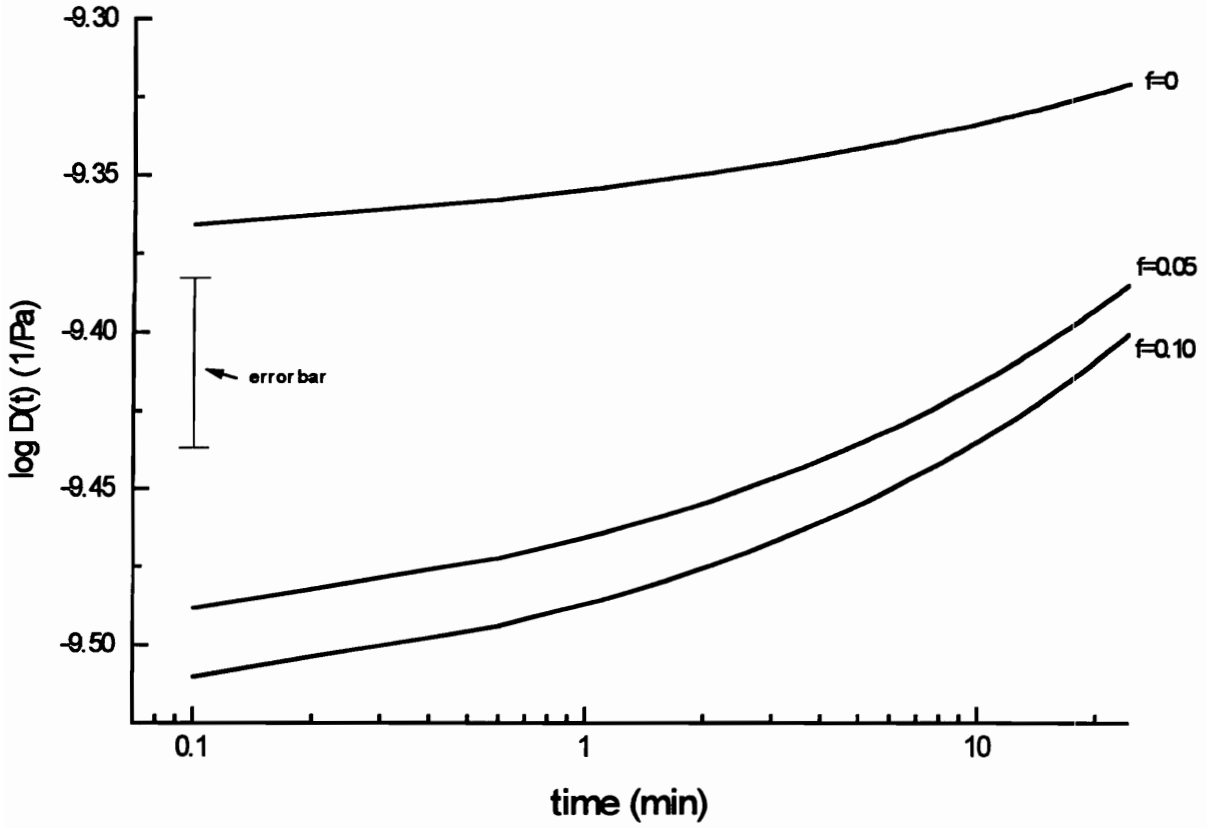

Figure 3.4-26. Polystyrene compliance curves after 4 hrs at 60C

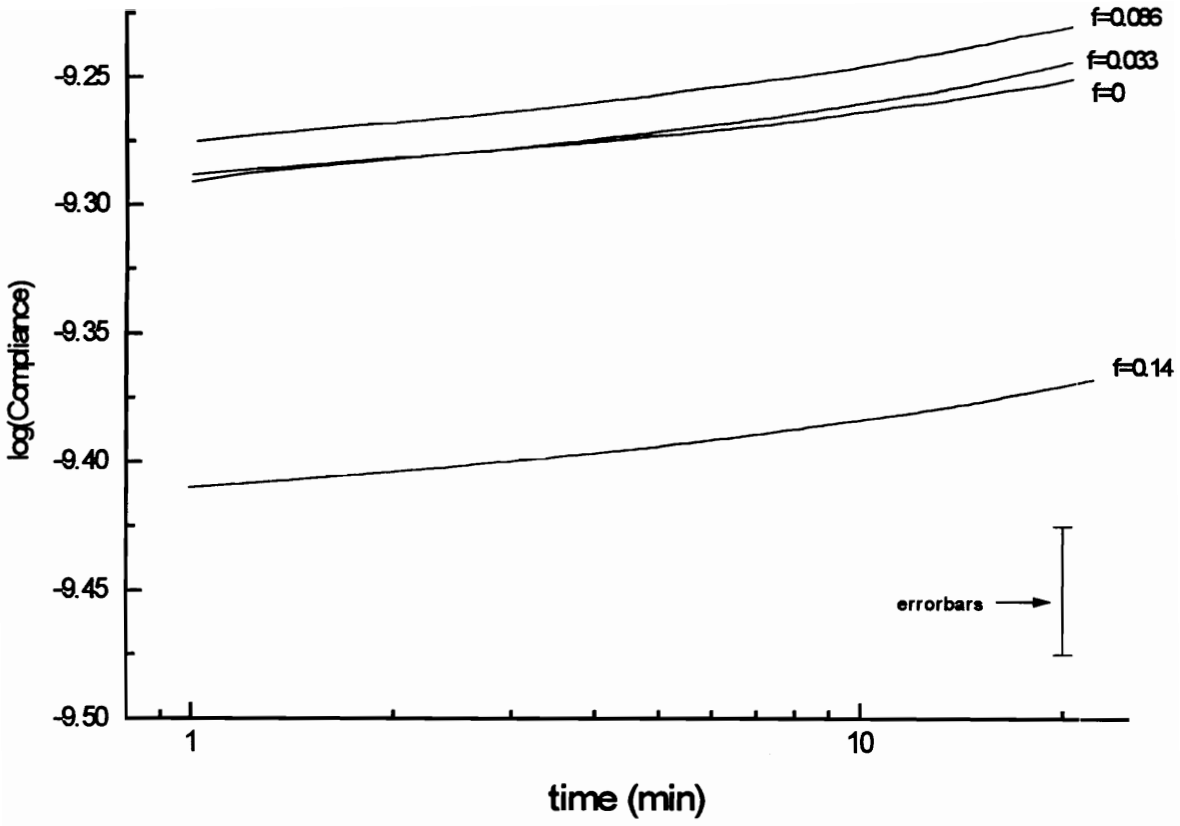

Figure 3.4-27. Polycarbonate creep compliance curves after 4 hrs. at 90C.

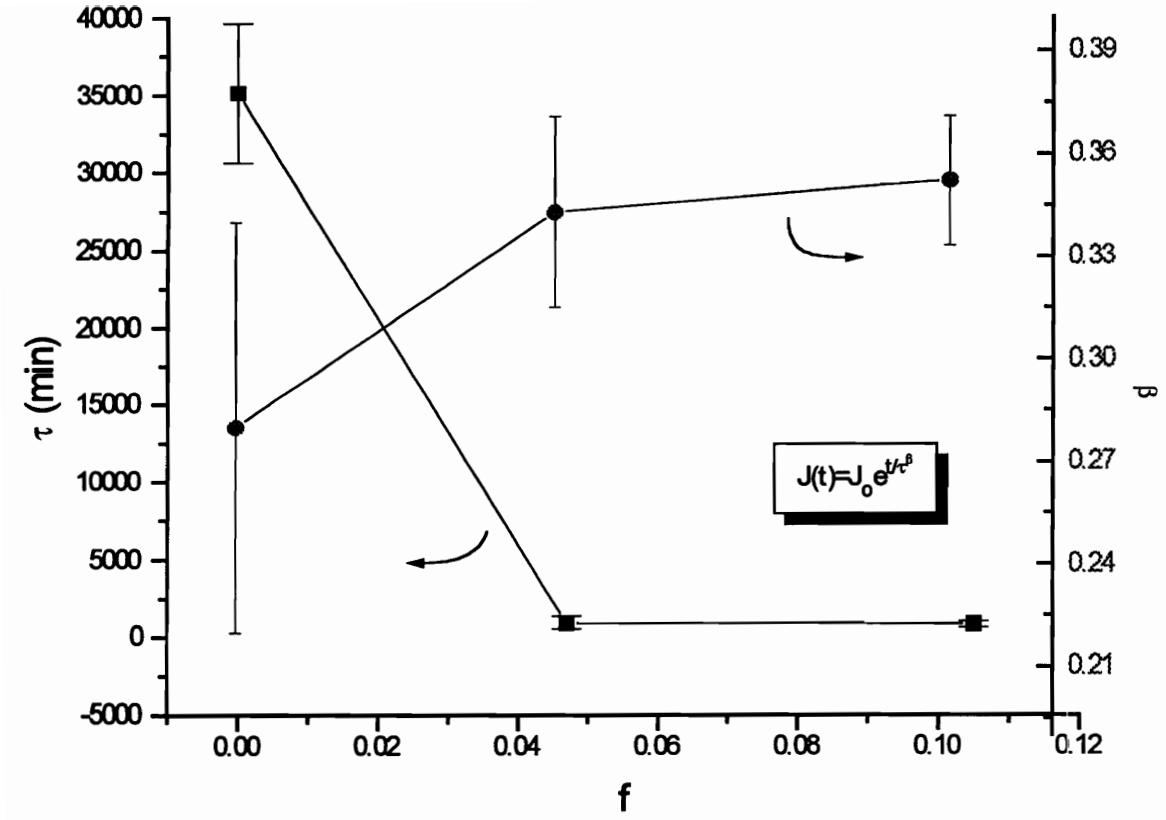

Figure 3.4-28. Fitted creep parameters for PS to Struik's creep equation.

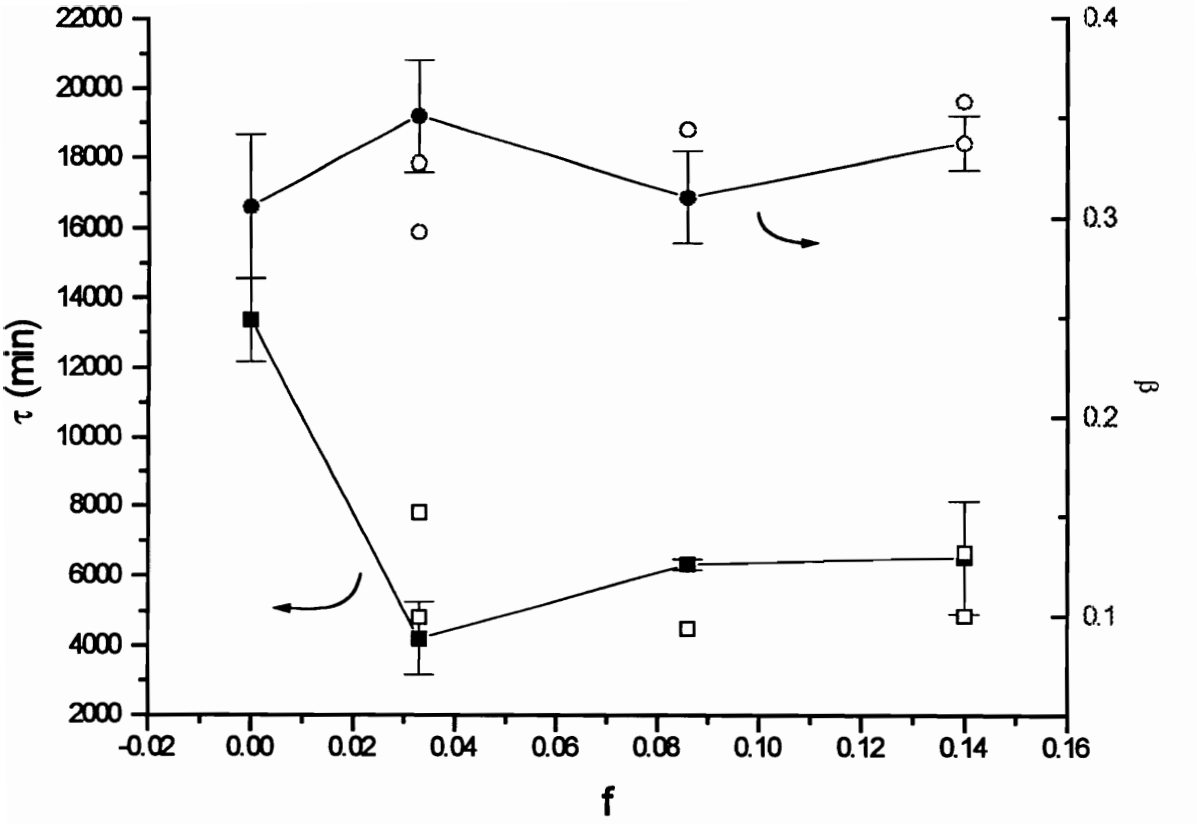

Figure 3.4-29. Data fit to Struik's creep equation for PC. TD data denoted by hollow symbols.

3.5 Discussion

The increase in density at high f (Figure 3.4-1 and 2) implies that the free volume decreases with stretching. Likewise, at low f one notes a slight increase in free volume (for PC). It is speculated that this transitional behavior is due to competing effects. At low stretch ratios, the deformation follows conventional continuum mechanics and, initially, expansion occurs due to the Poisson effect. As extension is increased however, the chains begin to pack better and the resulting densification begins to dominate. If better chain packing did not occur with stretching, then the density would be expected to decrease monotonically.

If one assumes that the free volume theory is applicable, then the mobility and physical aging rate are expected to decrease with orientation (at high f) due to the increasing density. Inspection of the dilatometric data, however, proves otherwise. Consequently, the free volume theory seems to be of little use in predicting the changes occurring in oriented samples.

It is interesting that the dilatometric data show an increase in volume relaxation rate with orientation (55% increase for PS, 40 to 60% increase for PC depending on temperature) and that almost all of this contraction occurs in the stretch direction. It is peculiar, however, that once oriented, the value for β changes very little with further stretching. This is true even for the biaxially oriented sample. It is as if the process of orientation itself, and not the degree of orientation, is responsible for the higher relaxation rates. *It is again important for the reader to realize that the oriented samples are undergoing higher rates of volume relaxation even though they have less free volume initially.* This indicates that there is another mechanism at work (besides free volume) which is promoting the process. This is similar to recent findings showing that the addition of antiplasticizers--which decreased the free volume--did not significantly affect the aging rate.[40] Of course it is also possible that the distribution of free volume hole

sizes and shapes, and not just the total free volume, is responsible for the unusual relaxation behavior. In fact, Bartos an coworkers observed a broadening of the free volume distribution in cold drawn PC via SAXS measurements.[10]

Another interesting dilatometric trend exists in the case of PS and relates to the presence of an "induction time" in Figure 3.4-5. The lag time before significant volume relaxation is longer in the unoriented sample (ca. 4000 seconds as opposed to 1000 seconds for the oriented sample) indicating that stretching somehow accelerates the initiation of the relaxation process. In effect, orientation causes a decrease in the net relaxation time of the system. Although this lag time is not visible in the polycarbonate data, it may have occurred at much shorter times before thermal equilibrium was established.

Contrary to the dilatometric results, the mechanical creep data show a decrease in physical aging rate with increasing f based on the horizontal shift behavior alone. The shift rate μ_h undergoes a slight drop upon stretching and then changes little with further increases in f. While opposite in direction, this is similar to the trend seen with the volume relaxation data. It is possible that the discrepancy is due to the difference in time scales for the two processes. The creep measurements involve effective relaxation/retardation times of one minute or greater. Volume relaxation,on the other hand, is more likely a function of the faster segmental motions (with the possible exception of the induction times which were of the order of minutes) which are orders of magnitude faster.

It is uncertain why the creep data is in disagreement with Struik's data for rigid PVC.[7] One possibility is the formation of strain-induced crystallinity in the PVC. Another is the fact that the scatter in Struik's data is higher than shown here. This is not surprising considering the corrections required to account for shrinkage. A large number of tests were performed in the present study in order to reduce the error bars sufficiently for accurate comparison.

This decrease in horizontal shift rate indicates that the retardation spectrum for an isotropic sample shifts to longer times at a faster rate than for an oriented sample. This implies that an isotropic sample should lose ductility more quickly than an oriented sample, everything else being equal. Nevertheless, it says nothing about how the orientation alters the initial spectrum. To gain this information, one must look at the retardation times in Figures 3.4-28 and 29. Here it is seen that orientation causes a significant drop in the retardation time and, as with the μ_h and volume relaxation data, the values do not change significantly upon further stretching. So, in addition to the oriented relaxation spectra showing a lower shift rate, they also start with a much shorter retardation time.

The shorter retardation time of the oriented samples may be interrelated with the faster volume relaxation rates although, as stated previously, it is possible that the two processes operate on different effective time scales. Why these relaxation/retardation times are shorter in the oriented samples remains to be answered. It is possible that the the mobility differences are a result of changes in the rotational isomeric state induced by orientation. Abe and Flory[41] have shown through rotational isomeric state (RIS) calculations that the number of trans segments in a network of polyethylene chains will increase (at the expense of gauche (+/-)) upon stretching. The same arguments should apply to PS and PC with the number of trans segments increasing at the expense of cis segments in the case of PC. One might also theorize an additional (discrete) quantity of free volume or "hole" associated with a cis or gauche "kink" in the chain. As stretching proceeds and the number of these "kinks" is diminished, then the associated "holes" would dissappear resulting in a net drop in total free volume. While this is only conjecture, it may help to explain the densification which occurs with elongation.

Unfortunately, this rotational isomerization does not explain the constancy of β with changes in f for oriented samples. If the rotational isomerization were indeed responsible for the increase in β, then it would seem that the volume relaxation rate should continue to

increase with further stretching. Since this is not the case, it is necessary look for another explanation. One possibility is that stretching actually raises the polymer chains to an activated energy state (which might be independent of f over the range studied). But what produces this activated state? It might be a result of internal stresses brought about by stretching; the internal stresses due either to distortion of the van der Waal's bonds (glassy distortional stresses), or entropic stresses brought about by orientation. The former should be small in magnitude since the material was hot-drawn. For the cold drawn studies cited in the literature review, however, the distortional stresses would be large and are most likely the cause for the accelerated volume relaxation rates seen there. The presence of entropic stresses in the glassy state is still controversial. The whole concept behind rubber elasticity and entropic stresses hinges on the idea that the chains are rapidly rearranging and deviations from the most probable position cause the stress. If a chain is then frozen in place, as with a glass, there is no basis for the force to exist. Struik[12] argues that glassy polymers do exhibit entropic stresses because motion is never completely frozen. That is, the thermal motions of the glassy segments are still enough to produce the entropic stresses. This is also supported by the shrinkage data in Figures 3.4-3 and 4 and the fact that almost all of the volume relaxation occurs in the stretch direction (see data insert in Figure 3.4-11). It is doubtful that this shrinkage was caused by glassy distortional stresses since these should have relaxed out considerably prior to the hot drawn sample being quenched into the glass.

It is also possible that the activated energy state is a result of the net change in the intermolecular force fields (as for example with the Lennard-Jones potential) brought about by the molecular rearrangement and flow. The density is changing with f so interatomic distances must also be changing even if only slightly. In addition, the changes in interatomic distance are not the same in the MD and TD with the TD distances being slightly smaller on average. Therefore the average intermolecular force (or spring constant) is expected to vary in the two directions as well. This is in agreement with Lunn and Yannas' IR study of PC where the nominal 2971 cm^{-1} absorption peak shifted to a

greater extent for parallel versus perpendicular polarization in oriented samples. This is most likely due to a difference in vibrational spring constants in the two perpendicular directions. The anisotropy in spring constant might provide for preferential, if not faster, relaxation in one direction relative to another (although on a macroscopic scale we do not see this anisotropy with the TD 4 hr. compliance data).

The previous argument could also be restated in terms of a modification of the free volume theory. The effect of orientation will be to change the free volume distribution with regard to the size, number, and shape of the holes. One might expect a transition from isotropic to ellipsoidal free volume sites with stretching. In fact, this has already been observed by Jean and coworkers using positron annihilation and 2-D angular correlation (2D-ACAR) measurements on similarly stretched polycarbonate samples.[42] Obviously the relaxation kinetics are going to vary with hole size and shape and also with regard to location relative to the oriented segments. This is expected to lead to an anisotropy in relaxation behavior as well.

Assuming that an activated state is responsible, how does it produce the changes in volumetric and mechanical behavior? If we consider bond rotation and molecular rearrangement, in general, to involve an activation energy barrier, then the effect of the activated energy state will be to lower that barrier. In the case of volume relaxation, lower barriers will result in more rapid segmental rearrangement so denser chain packing is more easily facilitated. This increase in the rate of segmental rearrangement might also be the cause for the reduced creep retardation times (Figures 3.4-28 and 29). The decrease in μ_h is more difficult to explain assuming the decrease is significant. It is tentatively hypothesized that the activated state of the oriented chains somehow offsets the shifting of the retardation spectra to longer times. In other words, the relaxation mechanism for the oriented polymer chains is less affected by the changes brought about by aging (i.e. decreased free volume, increased cooperative motions, etc.). This insensitivity to aging of the oriented samples is apparent in the volume sensitivity data shown in Figure 3.5-1. For both PS and PC, S drops significantly for the oriented

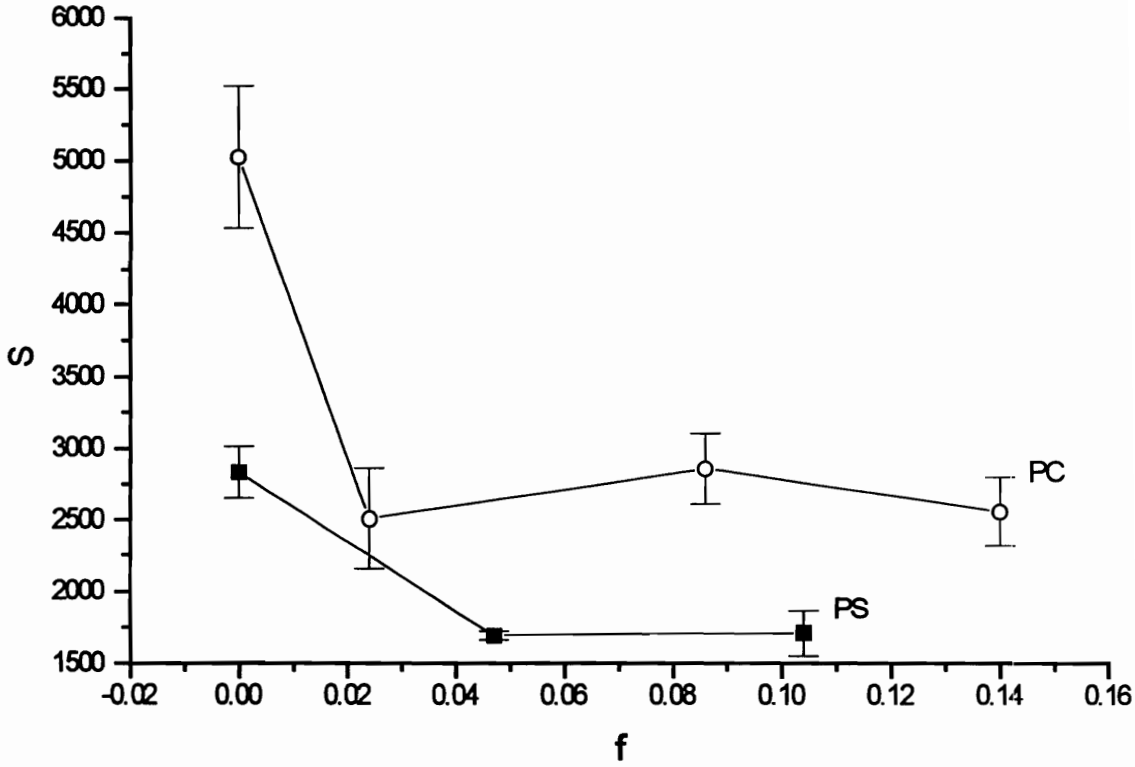

Figure 3.5-1. Volume sensitivity versus *f* for PC and PS.

samples. Referring back to Equation (3.1-4), the change in mobility for a given change in free volume is lower in the oriented samples. It may be that only a portion of the retardation spectrum is affected but the net effect is still an apparent reduction in the shifting rate.

3.6 Summary

It has been shown that orientation has an effect on physical aging although the magnitude of this effect varies with the measurement method. Dilatometric data show an increase in aging rate in oriented samples with length contraction occurring only along the stretch direction. This is in agreement with previous dilatometric studies of cold drawn PC although the latter show a larger aging rate enhancement upon stretching.[9,10]

Creep/mechanical shift rates, on the other hand, show a slight decrease with drawing. In both cases, however, it is not the degree of orientation which matters, only the fact that the polymer has been stretched. Further analysis of the creep compliance data shows that the effective retardation time decreases significantly with stretching. This implies that the chain segments are able to reorganize more quickly in the oriented samples which may explain the faster volume relaxation rates. The volume sensitivity, S, also decreases with f so the stretched samples are less sensitive to free volume relaxation than their unoriented counterpart.

It is speculated that the unusual orientation-aging behavior observed in this study is a result of strain-induced rotational isomerization and/or the formation of an activated state. Stretching causes a shift in the distribution of bond rotation angles which might subsequently alter the volume/mechanical relaxation behavior. It also may explain the densification which occurs with stretching. The mechanism for the formation of the activated energy state is uncertain although a few possibilities have been suggested. These include internal stresses, anisotropy in the net intermolecular force field, and free volume redistribution. More work is needed to better determine which, if any, of these

mechanisms is best at describing the unusual aging phenomena. The next two chapters will try to answer this question by a combination of thermodynamic, positron annihilation and diffusion measurements. Because this is a new area for physical aging research, even more work is needed, particularly on other materials, to determine what trends are similar to those observed here. Finally it is hoped that other researchers will take advantage of the perturbing effects that orientation has on structure as a means for better understanding the physics of the glassy state.

3.7 References

1 L. C. E. Struik, Physical Aging in Amorphous Polymers and Other Materials, Elsevier, New York, 1978.

2 M. R. Tant and G. L. Wilkes, *Polym. Engr. Sci. 21,* 874 (1981).

3 G. B. McKenna, *Comprehensive Polymer Sci, Vol. 2. Polymer Properties,* C. Booth and C. Price, Eds., Pergamon, Oxford, 1990.

4 I. M. Hodge, *J. Non-Crystalline Solids 169,* 211 (1994).

5 J. M. Hutchinson, *Prog. Polym. Sci. 20,* 703 (1995).

6 L. S. Thomas and K. J. Cleereman, *SPE Journal 28,* 61 (1972).

7 L. C. E. Struik, *Physical Aging in Amorphous Polymers and Other Materials*, Elsevier, New York, 1978.

8 S. Mukherjee and S. A. Jabarin, *Polym. Engr. Sci. 35,* 1145 (1995).

9 R. Pixa, *et. al.*, *Polymer Bulletin 16,* 381-387 (1986).

10 J. Bartos, J. Muller and J. H. Wendorff, *Polymer31,* 1678 (1990).

11 G. L. Wilkes, "Rheooptical Properties," in *Encyclopedia of Polymer Science and Engineering, Vol 14.*, John Wiley and Sons, New York, 542, 1983.

12 L. C. E. Struik, *Intenal Stresses, Dimensional Instabilities and Molecular Orientations in Plastics,* John Wiley and Sons, New York, 1990.

13 M. R. Tant and G. L. Wilkes, *J. Appl. Polym. Sci. 26,* 2813 (1981).

14 J. Muller, *J. Thesis*, Deutsches Kunststoff-Institut, Darmstadt, (1989).

[15] K. H. Hellwege, J. Hennig and W. Knappe, *Kolloid-Z.uZ.f. Polymere 186*, 29 (1962).

[16] T. E. Brady and G. S. Y. Yeh, *J. Appl. Phys. 42*, 4622 (1971).

[17] D. G. LeGrand, *J. Appl. Polymer Sci. 16*, 1367 (1972).

[18] W. A. Spitzig and O. Richmond, *Polymer Eng. Sci. 19*, 1129 (1979).

[19] E. Ito, K. Sawamura, and S. Saito, *Colloid and Polymer Sci. 253*, 480-484 (1975).

[20] M. Trznadel and M. Kryszewski, *Polymer 29*, 418-425 (1988).

[21] M. Trznadel, T. Pakula, and M. Kryszewski, *Polymer 29*, 619-625 (1988).

[22] D. G. LeGrand, *Proceedings of the XI International Congress on Rheology*, Brussels, Belgium (1992).

[23] A. C. Lunn and I. V. Yannas, *J. Poly. Sci., Polymer Physics Ed., 10*, 2189-2208 (1972).

[24] *Polymer Handbook*, J. Brandrup and E. H. Immagut, Eds., John Wiley and Sons, New York, 1975.

[25] R. S. Stein and G. L. Wilkes, "Physico-Chemical Approaches to the Measurement of Anisotropy," in *Structure and Properties of Oriented Polymers*, I. M. Ward, Ed., John Wiley and Sons, New York, 150, 1975).

[26] R. S. Stein, *J. Appl. Phys. 32*, 1280 (1961).

[27] G. McKenna, personal communication, June, 1994.

[28] N. Bekkedahl, *J. Research Natl. Bureau Standards 42*, 145 (1949).

[29] E. Ito, K. Sawamura, and S. Saito, *Colloid and Polymer Sci. 253*, 480 (1975).

[30] D. W. Phillips, A. M. North and R. A. Pethrick, *J. Appl. Polym. Sci. 21*, 1859 (1977).

[31] E. Ito and T. Hatakeyama, *J. Poly. Sci., Polym. Phys. Ed. 13*, 2313 (1975).

[32] K. H. Illers and E. Jenckel, *J. Poly. Sci. 41, 528 (1959).*

[33] M. Takayanagi, *Mem. Fac. Eng. Kyushu Univ. 23*, 1 (1963).

[34] K. H. Illers and H. Breuer, *J. Colloid Sci. 18*, 1 (1963).

[35] P. J. Flory, *Statistical Mechanics of Chain Molecules*, Interscience, New York, 1969.

[36] D.Y. Yoon, P. R. Sundarajan, and P. J. Flory, *Macromolecules 8*, 776 (1975).

[37] A. D. Williams and P. J. Flory, *J. Polym. Sci. A-2, 6,* 1945 (1968).

[38] R. Greiner and F. R. Schwarzl, *Rheo Acta 23,* 378 (1984).

[39] L. Lundberg, B. Stenberg, and J.-F. Jansson, *Macromolecules 29,* 6256 (1996).

[40] *Macromolecules 29,* 4992 (1996).

[41] Y. Abe and P. J. Flory, *J. Chem. Phys. 52,* 2814 (1970).

[42] Y. C. Jean, Y. Rhee, Y. Lou, M. D. Shelby, G. L. Wilkes, *J. Appl. Polym. Sci. B34, 2975 (1996).*

4.0 THERMODYNAMIC CHARACTERIZATION OF THE ORIENTED STATE OF BISPHENOL-A POLYCARBONATE

4.1 Introduction

Physical aging is a process in which many of the structural and physical properties of a glassy polymer change with time.[1,2,3,4] These changes occur because the glass is not at equilibrium. Unlike the rubbery state where molecular mobility is high and the polymer is at equilibrium, the glassy state chains are much less mobile and require a longer time to achieve their optimum packing configuration. It is this long, gradual relaxation toward steady state which manifests itself as the physical aging process.

The actual rate of the aging process depends on the proximity of the annealing temperature to the glass transition temperature (T_g) along with various chemical/structural factors. Furthermore, the results from the previous chapter have shown that molecular orientation also has an influence, with oriented samples of bis-A polycarbonate and atactic polystyrene having *ca.* 50% higher volume relaxation rates as compared with the isotropic controls. In addition, creep measurements for both polymers showed a lower effective retardation time for the oriented samples which is in agreement with the dilatometric data. These findings are significant in the sense that most commercially produced plastic products have at least some degree of orientation present. This orientation may be intentional in the case of film blowing, tentering and blow molding, or incidental in the case of residual stresses in extruded or injection molded products. Regardless, the discovery that orientation enhances aging rates may require some rethinking of the plastics design process.

The objective of the current study is to better understand why (and how) orientation influences physical aging. This will not only help with the design process, but will also further the knowledge base on physical aging in a general sense. To accomplish this task,

a series of oriented, unaged bisphenol-A polycarbonate film samples have been tested by measuring density, static and dynamic mechanical properties, and thermal properties in an attempt to characterize how structure and mobility change with orientation. A few tests have also been performed on physically aged samples but only for qualitative, comparative purposes. Physical aging rates are directly related to molecular mobility so knowledge of one should allow for a prediction of the other and vice-versa. A comparison with the volume relaxation data from the previous chapter should provide a useful check of this hypothesis.

4.1.1 Sample Stretching and the Herman's Orientation Function

Samples of bisphenol-A polycarbonate have been uniaxially hot drawn (i.e. stretched above T_g) to various stretch ratios using a T. M. Long film stretcher. The orientation state was quantified by means of the Herman's orientation function f, which can be determined from birefringence measurements for amorphous systems by[5]

$$f \equiv \frac{3 < \cos^2 \theta > -1}{2} \approx \frac{\Delta}{\Delta^o} \qquad (4.1\text{-}1)$$

Here Δ is the birefringence (i.e. n_{md}-n_{td} where n is the refractive index and the subscripts MD and TD refer to the machine and transverse directions respectively) , Δ^o is the intrinsic birefringence (i.e. the birefringence for a perfectly oriented chain), and θ is the angle between the stretch direction and the chain axis. The brackets denote an average over all of the chains. The orientation function will assume a value of zero for an unoriented system, a value of one for perfect chain alignment in the stretch direction, and a value of -1/2 in the case of perfect alignment perpendicular to the stretch direction. These cases correspond to average values for θ of 54.7°, 0°, and 90° respectively. For polycarbonate, and most amorphous polymers, the maximum obtainable f is only of the order of 0.2 to 0.3 as opposed to some crystalline polymers which can reach values of 0.5 or higher. This difference arises because the stretch temperatures needed to allow sufficient mobility for

full chain alignment, also allow the chains to rapidly relax back to the unoriented state. Crystalline regions--particularly strain-induced crystallization--are not significantly affected by the high stretch temperatures. Not only do they serve as anchor points for the other amorphous chains (much like crosslinks) which helps to reduce chain relaxation, but they can also realign in the stress field thereby enhancing the overall chain orientation.

A value of 0.16 +/- 0.02 for Δ° has been obtained by combining sonic modulus[6] and birefringence measurements. Literature listings of Δ° for polycarbonate vary widely including a value of 0.236 as measured by Biangardi,[7] a value of 0.106 by Pietralla,[8] and a value of 0.062 by Struik.[9] Struik's value is unusual in that it was determined by extrapolation of compliance and thermal expansion data as opposed to correlation with more standard methods such as sonic modulus or dichroism. It is uncertain why this wide disparity in literature values exists. Some of the difference can be attributed to the test error and poor resolution of dichroism, sonic modulus, and compliance/thermal expansion extrapolation (as compared with birefringence). It is, however, doubtful that this test error would account for all of the scatter in the Δ° values.

Finally, it is emphasized that Eqn. (4.1-1) only applies accurately to systems that are hot drawn and not those which are cold-drawn (i.e. stretched below T_g). Cold drawing, in addition to producing some alignment of the polymer chains, also causes significant distortion of the intermolecular van der Waals bonds.[9] This promotes distortional or glassy birefringence which contributes to the total birefringence and must be subtracted out (not an easy task) if a true measure of molecular orientation is to be obtained. For all aspects of this aging study, only hot-drawn samples were tested.

4.1.2 Relaxation Mechanisms in Polycarbonate

There are two main transitions of importance in polycarbonate besides the α or glass transition at 150°C. Understanding how these transitions respond to orientation should provide insight into how orientation might affect physical aging behavior. The lowest

transition, at approximately -100°C, is denoted the β-transition. Watts and Perry[10] performed a dielectric study of this transition and how it varies with annealing. They found that unaged samples had an impact strength four times higher than annealed samples even though there was little change in the β relaxation. It was further determined from the dielectric data and application of Onsager's equation[11] that the ratio of groups activated respectively by the β and α processes is 0.21:1. This corresponds to approximately 17% of the total chain units being mobile in the glassy state. They (along with other researchers[12,13]) were able to resolve the β transition into two separate transitions, β_1 (−80°C at 0.01 Hz) and β_2 (-120°C at 0.01 Hz) having activation energies of 45 kJ/mol and 10-30 kJ/mol respectively. The higher transition, β_1, has been associated with the movement of strongly dipolar carbonate groups which are restricted by the phenyl groups.[10, 12, 13] Aoki and Brittain believe the β_2 transition to be due to motion of the phenyl groups in cooperation with the carbonyl groups.[13] Davenport and Manuel disagree, believing instead that the β_2 motion is that of two methyl and two phenyl groups moving in unison. Their results were based on NMR second moment measurements.[14] Lee and coworkers[15] have recently proposed a "bundle" model where the low temperature relaxation (β_2) arises from intrabundle motions and β_1 arises from interbundle motion. The "bundle" in their model refers to a local region of aligned chains which can undergo a range of cooperative type motions. Clearly, the mechanism behind the β transition(s) is still controversial and more studies are needed.

The shoulder which occurs at ca. 70 to 90°C is referred to as the α' transition. It is denoted with a prime because it is not generally considered a true equilibrium transition. Illers and Breuer[16] believe that this transition is due to non-equilibrium stresses which are frozen into the sample although the exact mechanism of this relaxation has not been identified.

4.2 Experimental

4.2.1 Sample Preparation

Extrusion cast samples of Makrolon 2608 bisphenol-A polycarbonate film (Tg= 150°C from DSC at 20°C/min. heating rate, M_n=16,500 g/mol from solution viscosity in THF assuming polydispersity of 2 and applying correction factors[17]) were stretched uniaxially at 160°C using a T. M. Long film stretcher. The crosshead speed was 12.7 cm/s and the initial gauge length was 10 cm resulting in an initial strain rate of 125%/sec. Samples were typically drawn to stretch ratios of 1.25X, 1.5X, 2X and 2.5X. After stretching, samples were quenched below T_g with a blast of cold air in order to minimize any relaxation. Orientation was determined via birefringence measurements using an Abbe refractometer (Na D-line, 589.3 nm). Because samples were stretched at different times and fluctuations exist in the stretching environment, a given stretch ratio will not always produce exactly the same orientation function f in a sample. For a given stretched sample, the point-to-point variability in f was approximately +/- 0.01. The average sample-to-sample variability was +/- 0.03.

4.2.2 Shrinkage Recovery

Shrinkage recovery measurements were performed on some of the unaged samples by dipping a 5 cm strip of the film in a hot oil bath at 160°C for one minute and then measuring the new length. The "molecular" stretch ratio can be defined as

$$\lambda_{mol} = \frac{L_o}{L_s} \tag{4.2-1}$$

where L_o is the initial unshrunk sample length (typically 5 cm) and L_s is the length after shrinkage. In the vast majority of samples tested, shrinkage recovery was greater than 99% indicating that the molecular stretch ratio λ_{mol} was the same as the "machine" stretch

ratio Λ. This implies that little if any relaxation of the chains occurred during the stretching process. Of course, this assumption of significant molecular extension (and zero relaxation) probably only applies accurately to the longer chains. For the shorter chains it is doubtful that sufficient entanglements existed to allow for chain stretching in the first place.

4.2.3 Tensile Testing

Tensile data were obtained using an Instron with a crosshead speed of 51.4 mm/minute. The test procedure conforms in part to ASTM D882 however sample size had to be decreased due to the limited useful area of the stretched film stock. Samples were cut in rectangular strip form with a gauge length of 51.4 mm and a width of 12.7 mm. The initial strain rate was 100%/minute.

4.2.4 Density

Density data were obtained using a gradient column made with salt solutions of either potassium bromide or sodium bromide and water. The column was maintained at approximately 23°C. A minimum of 1 hour was allowed for the samples to reach their equilbrium position after placement in the column.

4.2.5 Dynamic Mechanical Measurements

Dynamic mechanical spectra were acquired using a Seiko DMS 210 in tensile mode. Samples were ramped at 1°C/minute from -160°C to 170°C and scanned at discrete frequencies from 0.01 to 20 Hz. Multiple runs were performed for each sample type and the curves averaged.

4.2.6 DSC

DSC characterization was performed with a Perkin-Elmer DSC 7 ramped at either 10°C or 20°C per minute. The instrument was calibrated to indium and zinc standards and a sapphire reference was applied to each run. Because of the effect of shrinkage on the DSC signal, samples were run with and without lid crimping. The uncrimped samples actually consisted of one piece of film, trimmed in size so that shrinkage would not cause it to curl up along the edges of the sample pan. A lid was placed on the film to act as a weight in order to enhance thermal contact. These samples were generally run at 20°C / min. since their typical mass was only approximately 3 mg. For the crimped samples, 2 pieces of film were cut from the sample using a hole punch. Total sample mass was of the order of 10 mg so the ramp rate was reduced to 10°C/min. Crimping was performed with a standard Perkin-Elmer pan crimper. Because the resulting shrinkage at T_g has an effect on the accuracy of the signal, multiple runs were performed and the results averaged.

4.3 Results

The relationship between orientation function *f*, and sample stretch ratio Λ, is illustrated in Figure 4.3-1. The error bars are a result of the variability in oven temperature, quench rate, and sample thickness. This variability is precisely the reason that *f*, as opposed to Λ, is used as a measure of "orientation."

4.3.1 Density Measurements

Room temperature density data are plotted in Figure 4.3-2 as a function of *f*. The density ρ, is found to increase in approximately a linear manner with increasing *f* except at the lowest orientation functions where it decreases slightly. This density increase for polycarbonate has also been reported in the literature.[18,19,20] For example, Ito and Hatakeyama's[20] density data vary from an isotropic density of 1.1920 g/cc to a value of 1.1945 g/cc at $f = 0.17$. While the absolute magnitudes of their densities are lower than

those reported here, the relative changes in density with f are about the same. A key difference, however, is that their data do not show the initial decrease in density as shown in Figure 4.3-2. Phillips and coworkers[19] obtained a density of 1.1920 g/cc at f=0 and a value of 1.1990 g/cc at f=0.17. While the latter is in good agreement with the data in Figure 4.3-2, their unoriented density is much lower.

It is uncertain why the densities reported here are slightly higher as compared to the literature. Some of the current measurements on unoriented samples have resulted in densities as low as 1.1970 g/cc. However, these low readings were most likely due to voids in the film or air bubbles which have attached to the sample. The density gradient column will generally err toward lower densities for this very reason. It is possible that differences in measurement technique may be partially responsible for the density difference since both Ito and Phillips used flotation/immersion techniques. Still another factor may be time dependent aging/densification of the samples. Measurements were generally made a few days after stretching due to the logistics of moving the samples from the film stretcher to the density column. This would result in a slightly higher density than for samples measured immediately after stretching.

4.3.2 DSC Results

DSC heat capacity traces for the unaged samples are shown in Figure 4.3-3. The enthalpy endotherm at T_g is, in general, found to increase with increasing f. The α" secondary transition is also detectable manifesting itself as a slight change in slope of the heat capacity curves at approximately 80°C.

To gain meaning from the T_g endotherm, one must first understand what happens thermodynamically in the DSC. A stretched ideal rubber--ideal meaning a rubber whose entire stiffness is derived from entropic changes and not internal energy changes-- will not show any heat effects when it is allowed to *retract freely without the performance of work.*[21] This also applies to an (ideal) oriented polymer sample heated through T_g in a

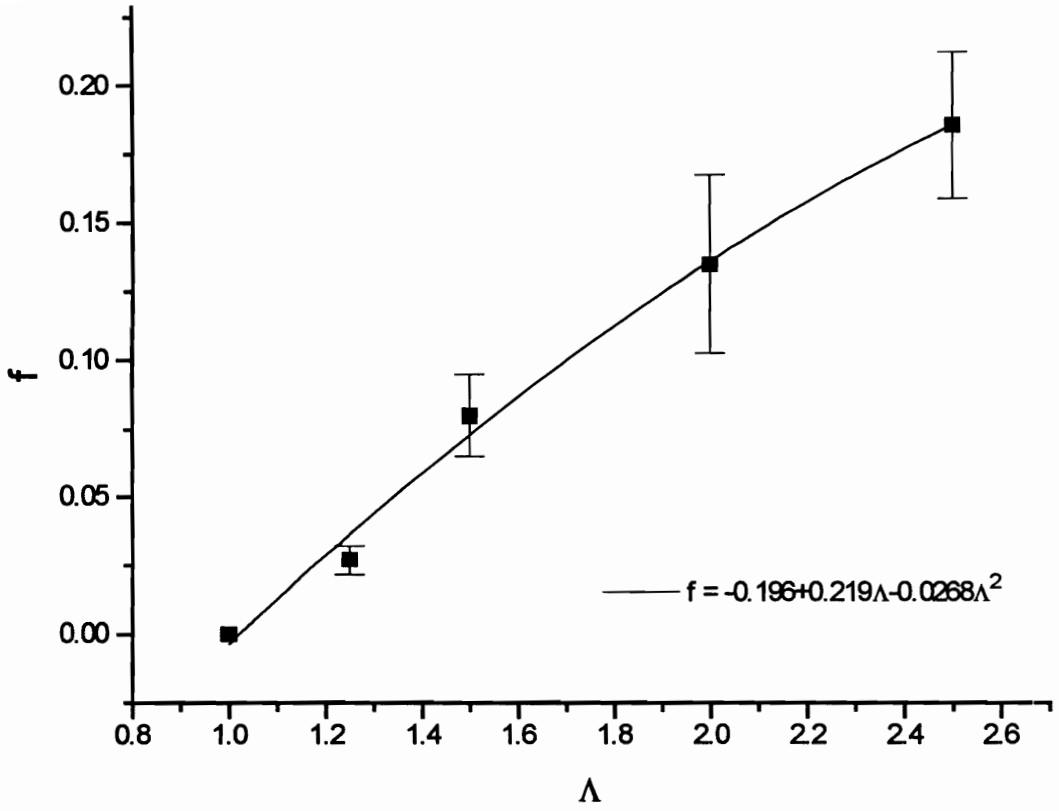

Figure 4.3-1. Orientation function for PC stretched uniaxially at 160°C versus stretch ratio.

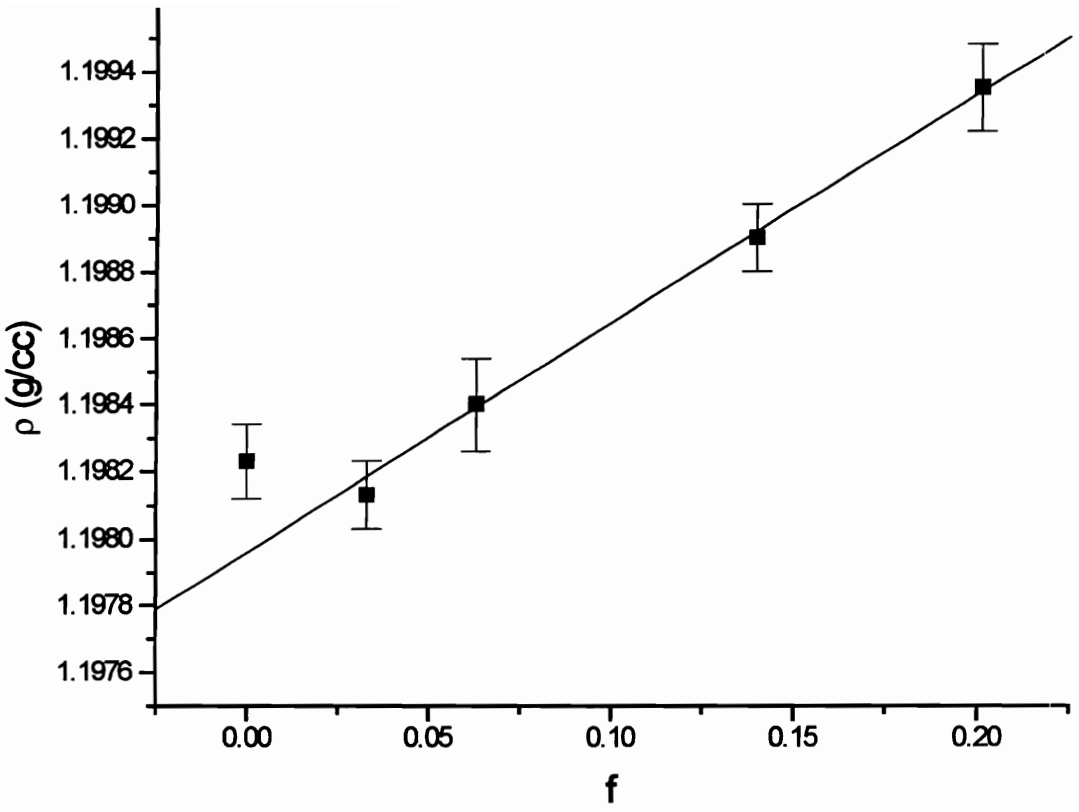

Figure 4.3-2. PC density at room temperature versus *f*. (Line is fit through high *f* points only in order to illustrate trend).

DSC if it is allowed to shrink freely. The DSC will still record a step change in C_p, which is common to all glass transitions, but no endotherms or exotherms. This can be clarified upon inspection of the first law:

$$\Delta U = Q - W = TdS_{rev} - (PdV - FdL) \qquad (4.3\text{-}1)$$

The heat flow term Q is obtained from the reversible component of the change in entropy. If the sample is allowed to shrink freely, the force *F* will equal zero and the expansion term *PdV*, will be very small which leads to W≈0. Therefore the heat flow Q will equal the change in internal energy (zero for an ideal rubber). The entropy still increases with retraction but it is irreversible and does not contribute to the heat flow. For systems that derive their stiffness from internal energy changes (i.e. most crystalline materials, steel, aluminum, etc.), Q will be high during free retraction. For these materials, DSC and other calorimetric methods might be useful for determining the "work of orientation." The interested reader should refer to the excellent review by Godovsky on deformation calorimetry.[22]

Most elastomers and oriented polymers systems are not ideal and derive a small fraction of their stiffness from internal energy changes. It is this small component of internal energy which is measured when DSC tests are performed with free shrinkage. Keep in mind that constrained relaxation will involve slightly different thermodynamics. In particular, any friction that occurs during shrinkage or deformation of the DSC pans should be taken into account in the thermal analysis since it contributes a work term to the heat balance. Attempts to run samples in crimped pans showed that the crimping did not prevent shrinkage although it may have contributed a small frictional work component to the heat flow. Nevertheless, comparison of the crimped and uncrimped results showed no significant differences which implies that the frictional effect was most likely very small.

To determine the enthalpy recovered at T_g, the heat capacity for the unoriented control was first subtracted from the oriented curve. This also provides a measure of the heat capacity change at different temperatures for a given value of *f*. A sample of this

subtracted curve is shown in Figure 4.3-4 for an oriented sample with $f = 0.17$. The difference in C_p between the oriented and unoriented states (i.e. $\Delta C_{pf}(f,T) = C_p(f,T) - C_p(0,T)$) varies considerably with temperature. In general, ΔC_{pf} is negative except in the vicinity of 75°C which also coincides with the α' transition for polycarbonate. ΔC_{pf} for other values of f also showed the same trends.

Of primary interest is the enthalpy difference between the oriented samples and the unoriented control at or near room temperature. This enthalpy difference is denoted as $\Delta H(f)$ and is defined as

$$\begin{aligned} \Delta H(f) &= H_g(f) - H_g(0) \\ &= [H_g(f) - H_r(f)] - [H_g(0) - H_r(0)] \\ &= -\int_g^r \Delta C_{pf}(f,T)\,dT \end{aligned} \qquad (4.3\text{-}2)$$

where "g" refers to the room temperature glassy value and "r" refers to the rubbery value at a temperature at least 10 to 20°C higher than T_g. Because shrinkage occurs above T_g, there will be no difference between the oriented and unoriented samples assuming shrinkage has reached completion. Consequently, $H_r(f)$ and $H_r(0)$ are equal. This allows for the substitution in the second line of Eqn. (4.3-2) above. Hence, the enthalpy difference $\Delta H(f)$ can be obtained by integrating $\Delta C_{pf}(f,T)$ in Figure 4.3-4 from room temperature to a temperature sufficiently above T_g, and then taking the negative of the integrated sum. Qualitatively this implies that larger endotherms at T_g yield more negative values of $\Delta H(f)$. In keeping with more traditional measures of enthalpy relaxation in physical aging studies, a new parameter, the recovered enthalpy $\Delta H_{rec}(f)$, is defined as

$$\Delta H_{rec}(f) = \int_g^r \Delta C_{pf}(f,T)\,dT = -\Delta H(f) \qquad (4.3\text{-}3)$$

which is simply the negative of $\Delta H(f)$.

To minimize error due to curve/baseline mismatch, integration was only performed between 100°C and 180°C. The $\Delta C_{pf}(f,T)$ data below this range, (i.e. from 30°C to 100°C) contributes only a negligible amount to the total area so the error in limiting the integration range is small. The data is plotted in Figure 4.3-5 along with a mechanical yield energy function which will be defined and commented on later. Unexpectedly, there is a slight decrease in $\Delta H_{rec}(f)$ at low orientations but then an increase with further stretching. This means that low f samples are actually at a slightly higher enthalpy than the unoriented samples. The opposite holds true at high f. Although this increase in recovered enthalpy is the same as seen with physical aging studies, keep in mind that all of the oriented samples here are unaged.

4.3.2.1 Tg vs. Orientation Function

Data for the T_g and ΔC_p are plotted as a function of orientation in Figure 4.3-6. Here ΔC_p is the difference in heat capacity between the liquid and glassy states at T_g (i.e. $\Delta C_p = C_{pl}-C_{pg}$) and should not be confused with $\Delta C_{pf}(f,T)$ described earlier. These ΔC_p values were obtained by linearly extrapolating the glassy and rubbery C_p curves to the isotropic T_g (determined from the inflection point) and then subtracting. The fact that C_{pl} is the same for all values of f indicates that C_{pg} (at T_g) must be decreasing with orientation. Wunderlich[23] discusses how skeletal and group vibrations in polymers contribute to the heat capacity. A decrease in C_{pg} most likely indicates that group/segmental vibrations are being restricted by either the chain alignment and/or the decreased free volume.

The T_g's shown in Figure 4.3-6 are actually "onset" values instead of the more traditional inflection point values, primarily because the enhanced endotherms at high f make it more difficult to determine an inflection point. The T_g is found to increase slightly with increasing f and appears to level off at higher orientations. This, as with the ΔC_p data, indicates a more restricted motion in the oriented samples. Data of Ito and

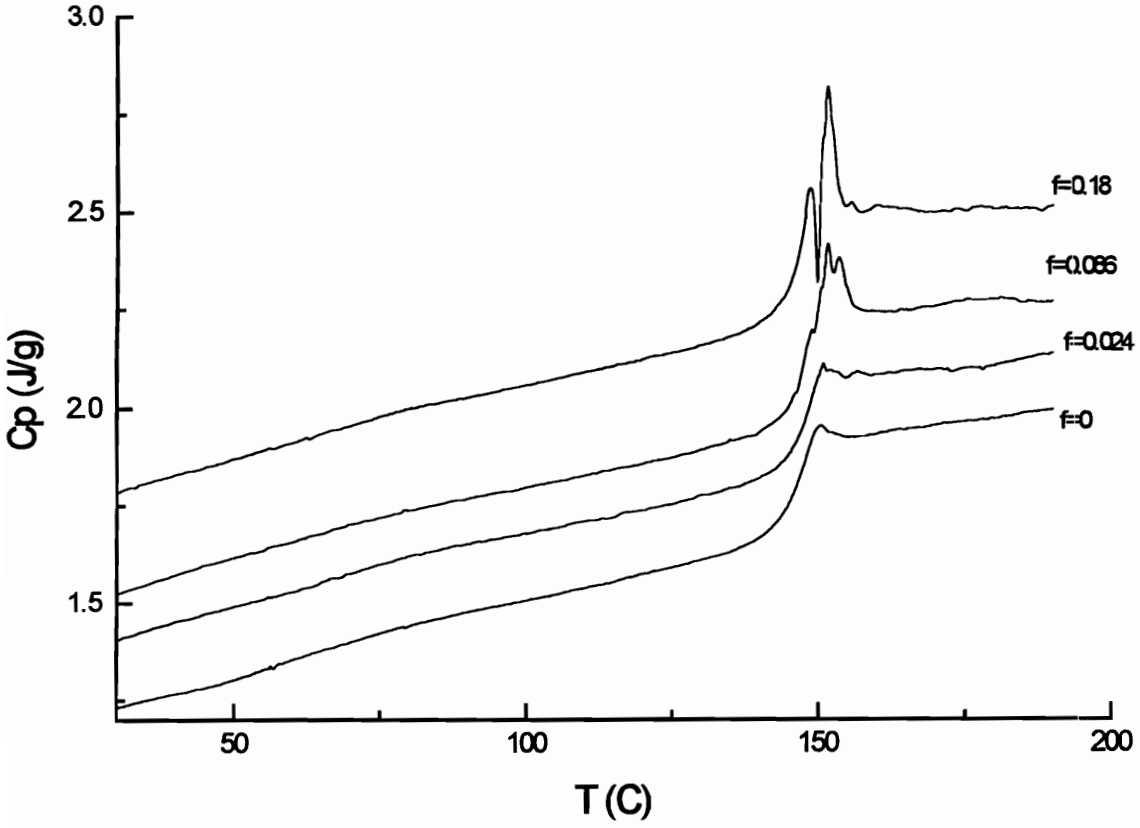

Figure 4.3-3. Heat capacity traces for PC.

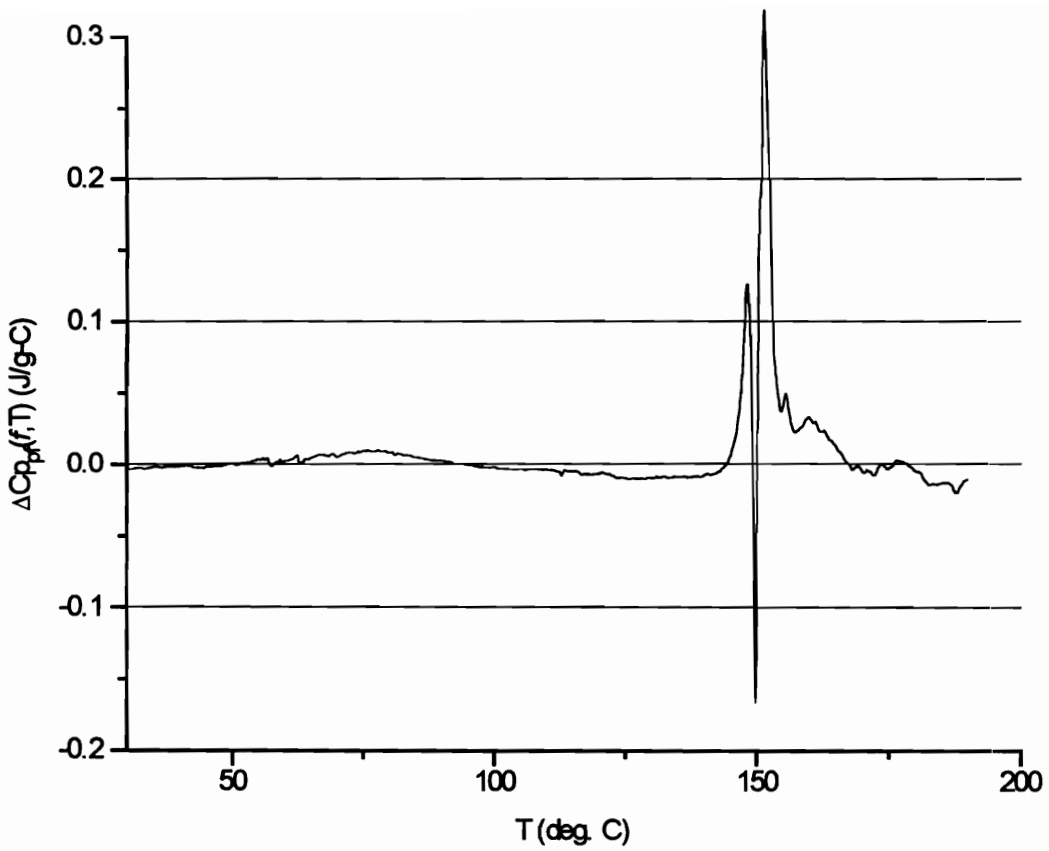

Figure 4.3-4. Heat capacity difference between an oriented (f=0.17) and an unoriented sample.

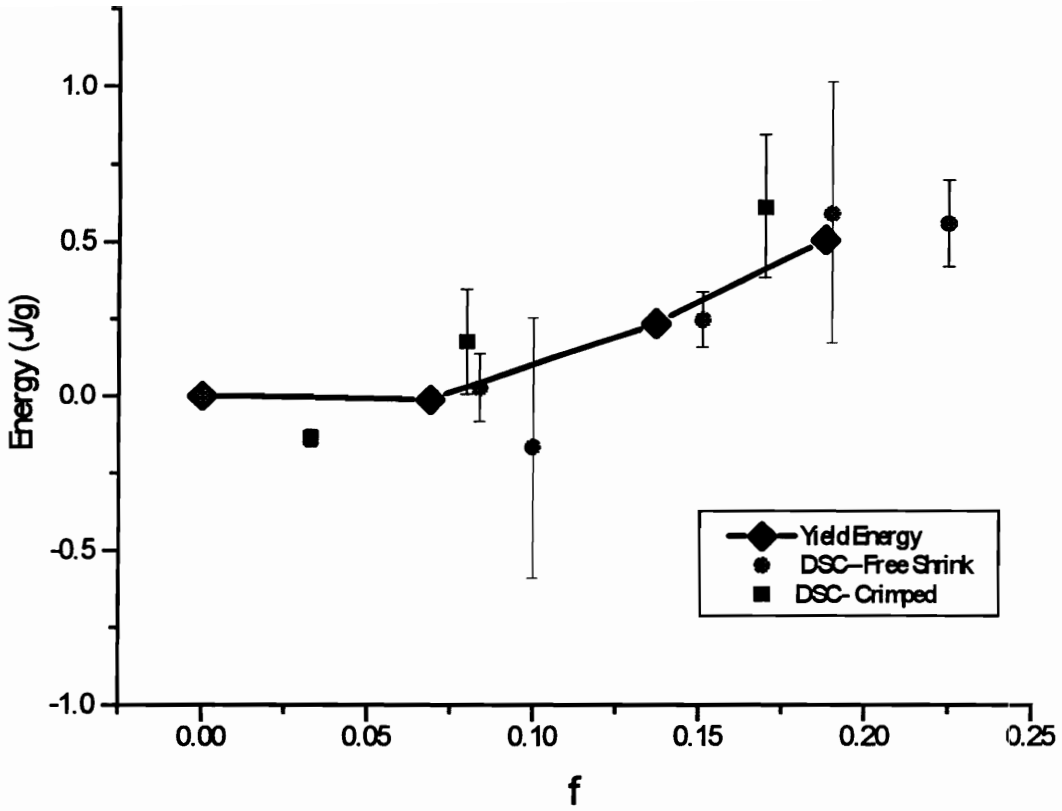

Figure 4.3-5. Comparison of mechanical yield energy and DSC recovered enthalpy vs. *f*.

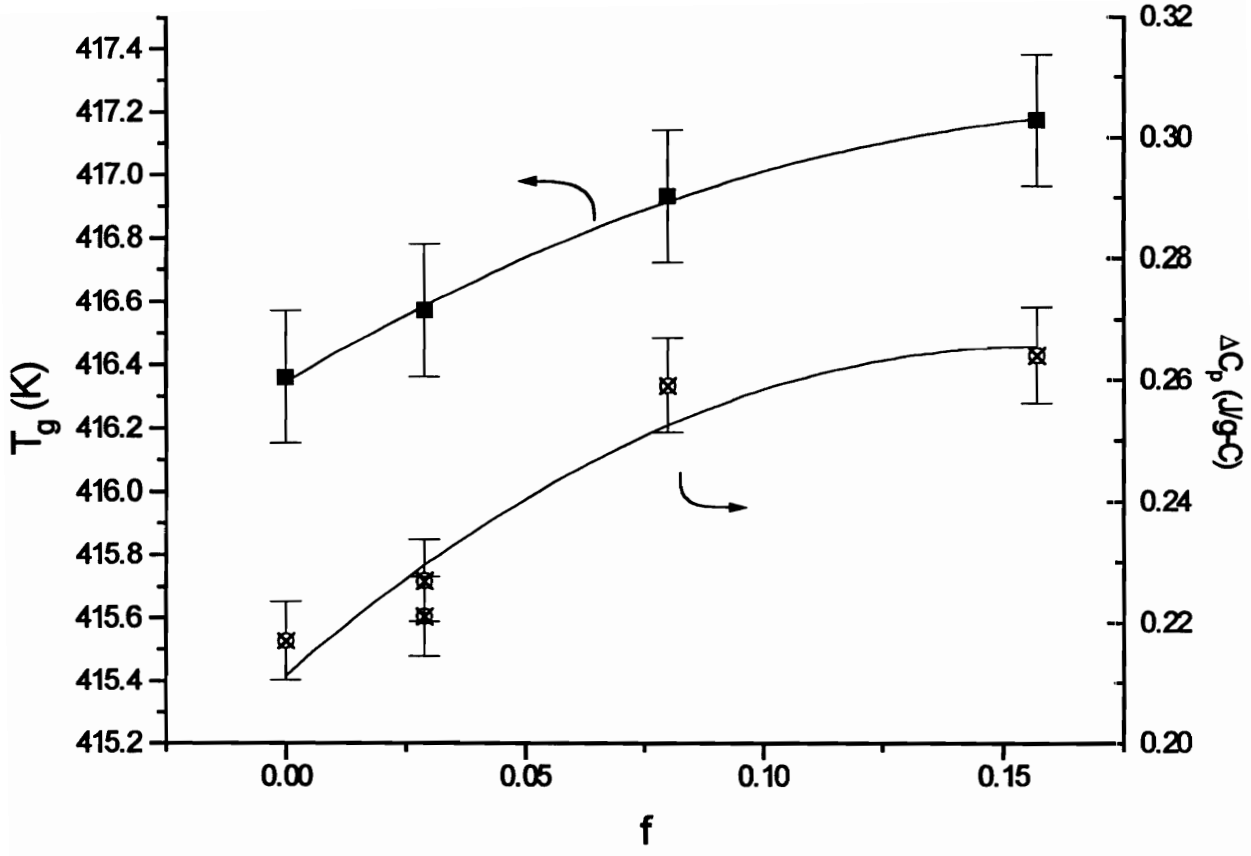

Figure 4.3-6. Tg and ΔC_p versus f for unaged PC.

Hatakeyama[20], in contrast to this work, show a maximum in T_g at an f of approximately 0.16. Interestingly, the relative change in T_g for a given change in f was much higher in their study for reasons which are unknown.

4.3.2.2 DSC Curves for Aged Samples

DSC traces for 1.5X PC (f=0.080) samples aged at 120°C are shown in Figures 4.3-8. Unoriented controls are also shown for comparison. Attempts to quantify the recovered enthalpy proved unsuccessful due to the scatter in the data so only qualitative findings will be discussed. The standard aging endotherm, which increases with aging time, is also observed for the oriented sample, however, there is a doublet in the oriented samples which is not present in the isotropic control. This doublet is also visible in the unaged 2.5X (f=0.18) sample in Figure 4.3-3 and for similarly aged 2X samples (not shown). It is possible that this doublet is the result of shrinkage in the DSC pan during heatup, with temporary separation of the sample from thermal contact with the pan causing a drop in C_p followed by a sharp increase once contact is regained. Notwithstanding, the fact that multiple measurements have shown the doublet to be consistently reproducible with respect to both the peak size and location indicates that it is probably *not* shrinkage causing the double endotherms, but some sort of bimodal relaxation time distribution instead. This follows because the sample-pan separation (from shrinkage) is expected to occur on a somewhat random and inconsistent basis. Therefore, the double endotherms would also have to be random and erratic in nature if shrinkage is the cause, and this is not observed experimentally.

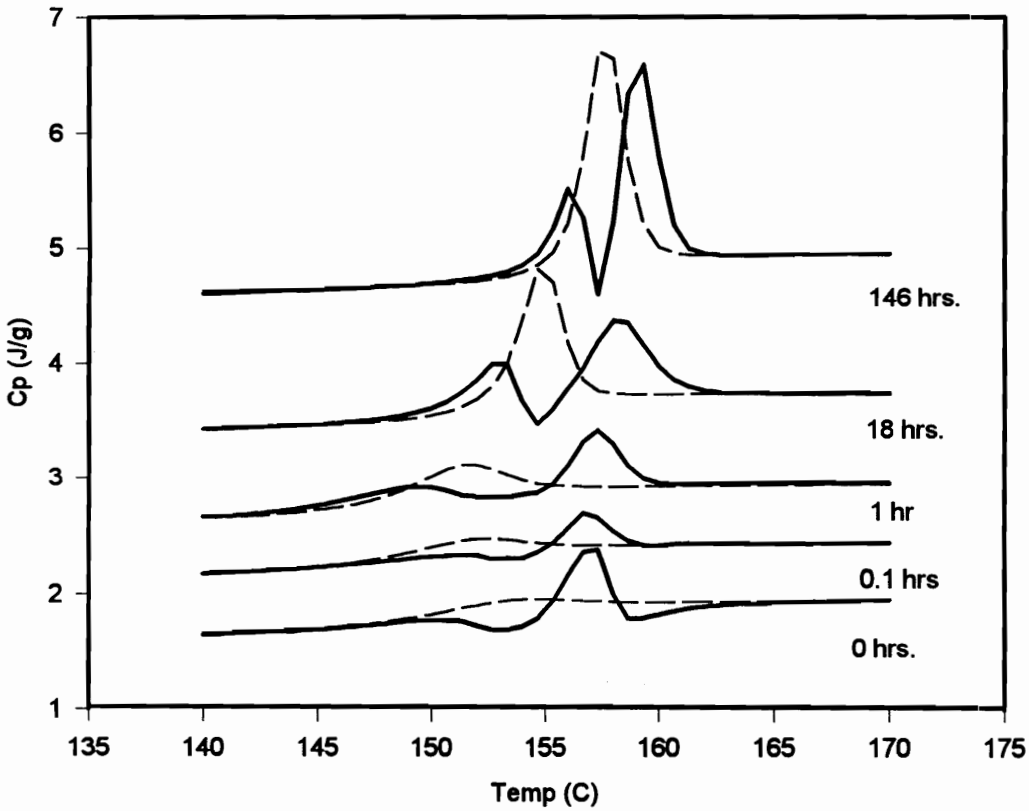

Figure 4.3-7. DSC traces for 1.5X PC ($f = 0.08$) aged at 120C (dotted line is isotropic control).

4.3.3 Tensile Properties

Sample tensile curves are shown in Figure 4.3-8 for both a 2.5X and 1X sample. In Figure 4.3-9, the yield stress in the machine and transverse directions are plotted versus the orientation function. The yield stress is taken as the maximum in the nominal stress-strain curve before flow occurs. Similar results for the modulus are shown in Figure 4.3-10. Surprisingly, the modulus in the TD direction is found to increase initially at low f and then decrease with further orientation--a trend similar but in the opposite direction to that of the density. It is uncertain whether this is significant or just a coincidence.

Based on ideas presented by Matsuoka,[24] one can apply the concept of the von Mises or energy-of-distortion theory to the combined data. This theory states that yielding will occur whenever a critical level of shear energy is reached. While for multi-axial stress states, determination of the shear energy can be fairly complicated, in the case of pure tension the critical shear energy is the same as the strain-energy at yield. This strain energy at yield can be determined graphically from the stress-strain plot or approximated as $\sigma^2/2E$.[24] Note that the approximation will generally underestimate the strain energy slightly. This strain energy at yield for a given orientation function f, is denoted $\varepsilon^*(f)$. Results for the machine and transverse directions are plotted in Figure 4.3-11. What is of more interest, however, is the difference in yield energy between the oriented and unoriented states. This strain energy difference $[\varepsilon^*(f) - \varepsilon^*(0)]$ is plotted versus the orientation function for the MD data along with the recovered enthalpy in the earlier displayed Figure 4.3-5. Note that the strain energy has been converted from a unit volume to a unit mass basis by dividing by the density. This strain energy difference is presumably connected with the additional energy input needed to overcome structural ordering and induce flow. This likely entails changes in rotational isomeric states, breakup of cooperative domains, creation of free volume, and a general increase in van der Waal bond distances. Of even greater interest is the fact that this quantity follows the same trend as

the enthalpy recovery and density data in addition to being of the same magnitude as the former. More discussion of this observation will be provided later.

4.3.4 Dynamic Mechanical Testing

In Figure 4.3-12, the dynamic loss modulus (E") in the machine direction at 1 Hz. for unaged polycarbonate is plotted as a function of temperature and *f*. A similar plot involving tan δ for the same samples is shown in Figure 4.3-13. All curves shown are the average of two or three measurements. Loss modulus is generally preferred over tan δ since it is more directly related to the relaxation spectrum, although the latter has the advantage of being dimensionless. For comparative purposes, E" and tan δ plots are also provided for PC aged 100 hrs. at 90°C (and loaded in the MD) in Figures 4.3-14 and 15. Comparison of the unaged and aged samples shows some interesting, but unusual trends.

Inspection of Figure 4.3-12 shows that E" is larger for the unaged oriented samples as compared with the unoriented samples. Nonetheless, there is no significant difference in the peaks at 1 Hz. for the various oriented samples. Likewise, the loss modulus of the unaged, oriented samples is also higher at the α' transition. In Figure 4.3-13, the tan δ values for the β peak are all approximately the same with the exception that the low and intermediate orientations seem to have a slightly narrower peak width. There is also some difference in the α' transition but this may well be attributed to measurement error.

The aged samples show a slight increase in the loss modulus at the β transition whereas the α' transition almost disappears. The tan δ data also shows a significant difference between the aged and unaged samples in the α' transition region. It is clear that the α' shoulder is very sensitive to physical aging whereas the β peak only changes slightly although the latter is easier to quantify accurately.

Loss moduli for unaged PC samples loaded in the TD are plotted versus temperature in Figure 4.3-16. A comparison with Figure 4.3-12 indicates that the β relaxation for the

1.25X sample ($f = 0.033$) has approximately the same relaxation strength (as determined from the area under the curve) in both the MD and TD directions. The higher f samples, however, have a lower relaxation strength in the TD as compared with the MD. This probably follows from the anisotropy of the sample and the difference in chain packing in the machine and transverse directions.

Determination of the activation energy for the β transition follows standard procedure where the peak frequency was plotted versus 1/T at tan δ_{max}. These Arrhenius plots are shown in Figure 4.3-17 for the unaged (MD) samples and for different orientation functions. The activation energy follows from

$$\ln\left(\frac{f_p}{f_{p\,ref}}\right) = \frac{-E_a}{R}\left(\frac{1}{T} - \frac{1}{T_{ref}}\right) \qquad (4.3\text{-}4)$$

where T_{ref} is a reference temperature, R is the gas constant and f_p is the peak frequency. The activation energies obtained for both the aged and unaged MD samples--obtained from the slope of the Arrhenius plot--are plotted as a function of f in Figure 4.3-18. Attempts to determine the activation energy at α' proved too inaccurate for comparative purposes. Nonetheless, for the β transition, the activation energy increased with orientation eventually leveling off at the higher values of f. Aging seemed to have only a negligible effect on the activation energy. A comparison of the unaged β-transition activation energies for the MD and TD loadings is shown in Figure 4.3-19. The TD samples show a smaller increase in the activation barrier as compared with the MD samples, except for the 1.25X sample. The implications of these results will be discussed in the next section.

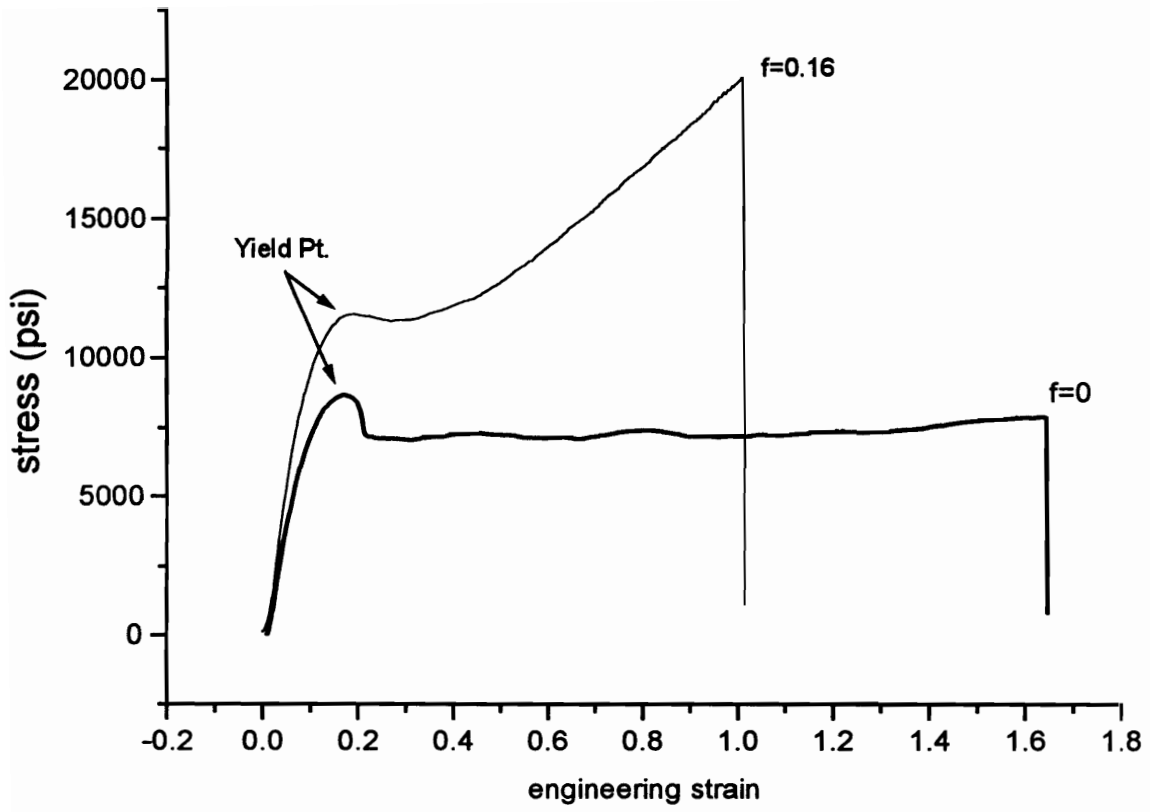

Figure 4.3-8. Sample MD tensile curves for PC.

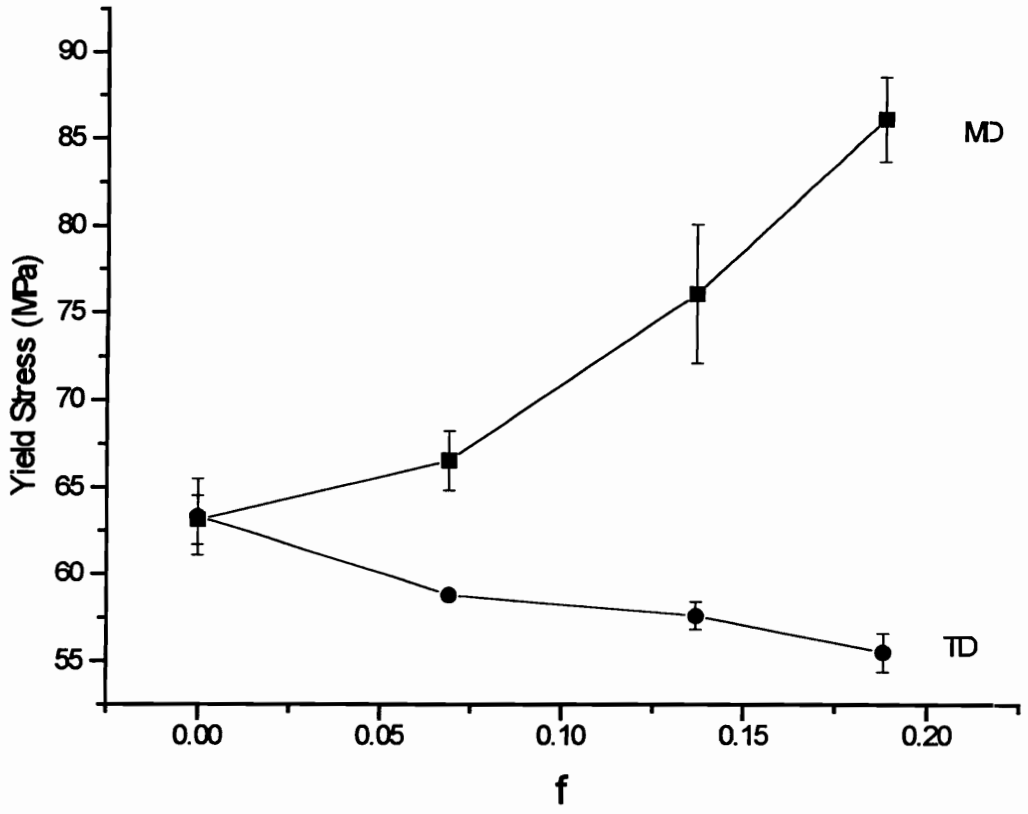

Figure 4.3-9. Yield stress data for PC.

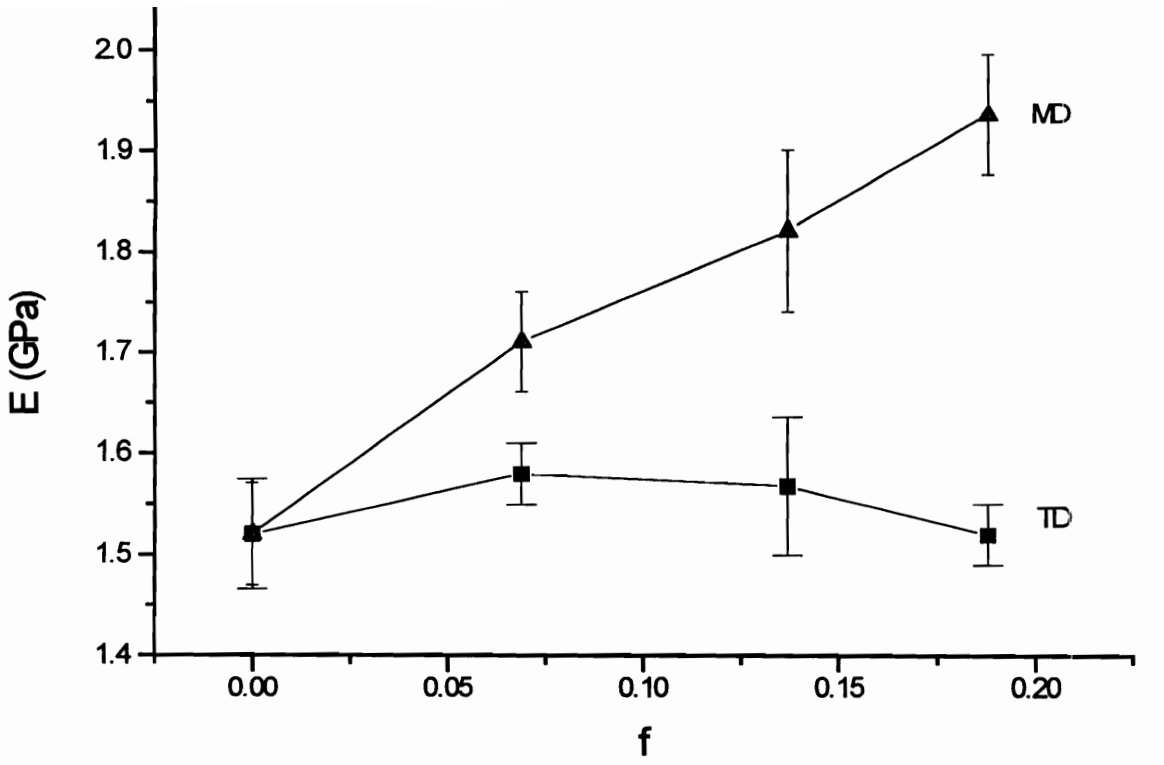

Figure 4.3-10. Modulus data for PC versus *f*.

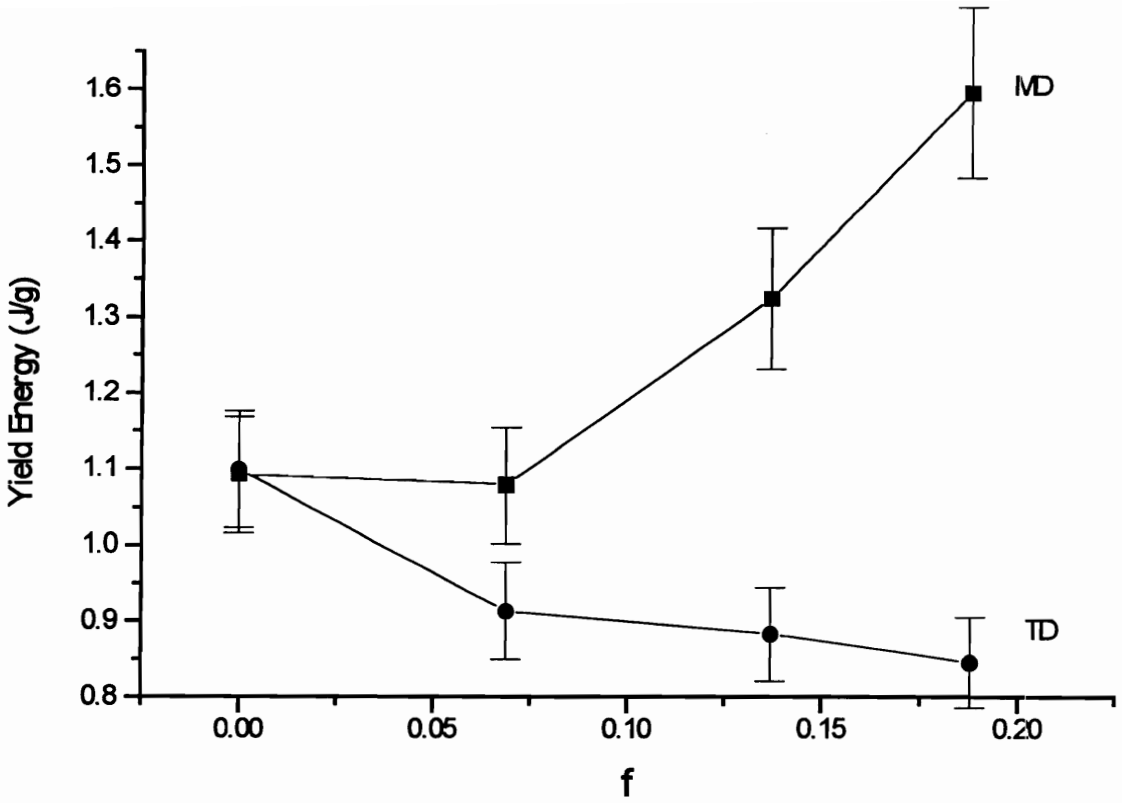

Figure 4.3-11. Energy-to-yield versus *f* for PC.

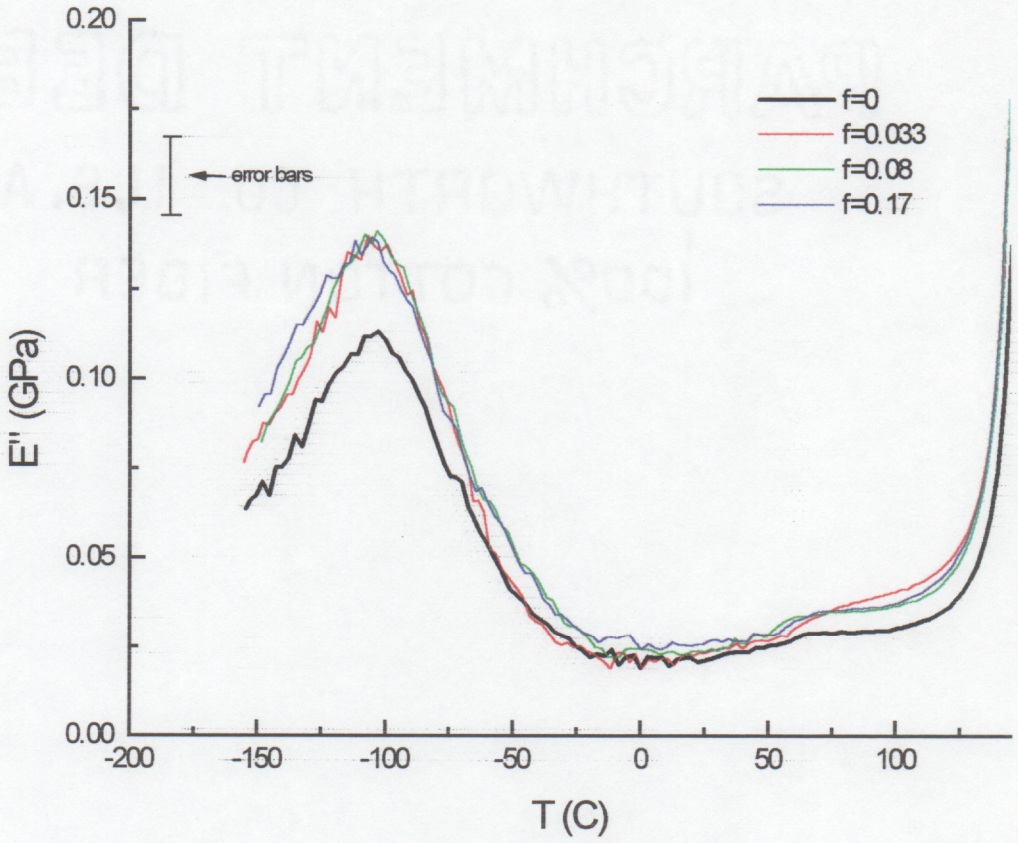

Figure 4.3-12. Loss modulus plots at 1 Hz. for unaged PC (MD).

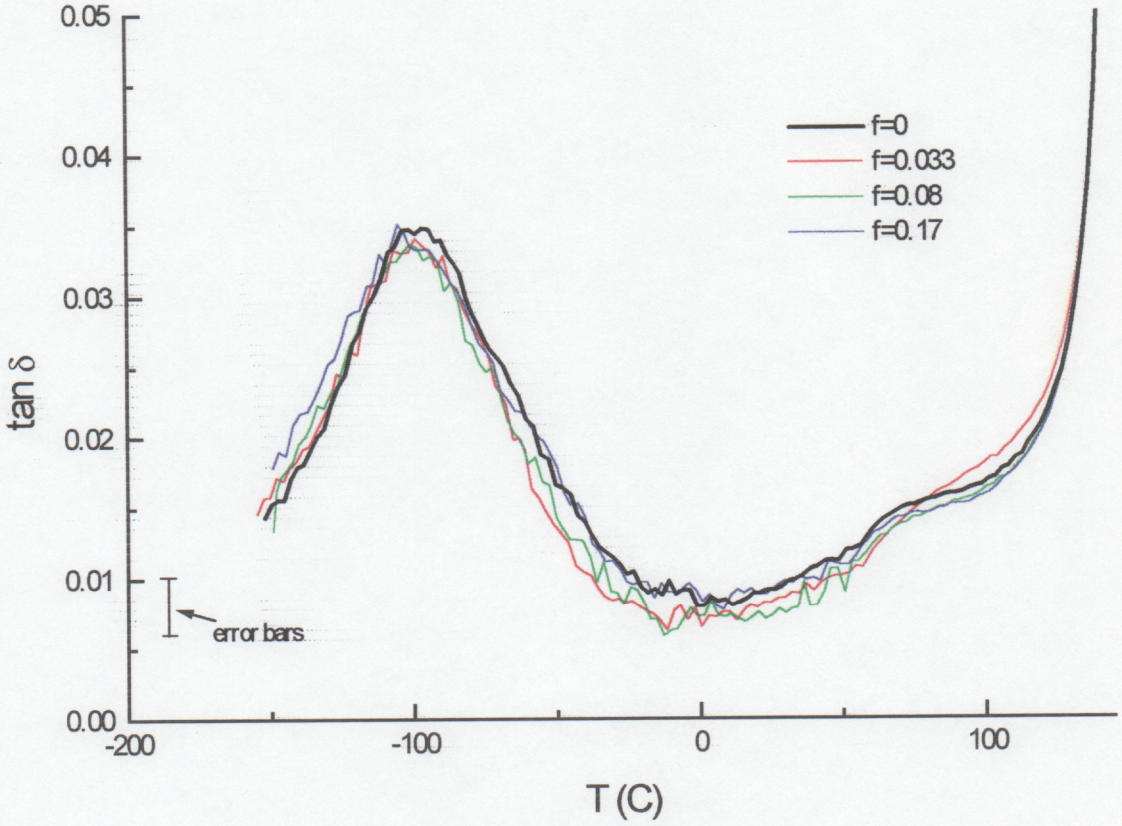

Figure 4.3-13. Tan delta data for unaged PC (MD).

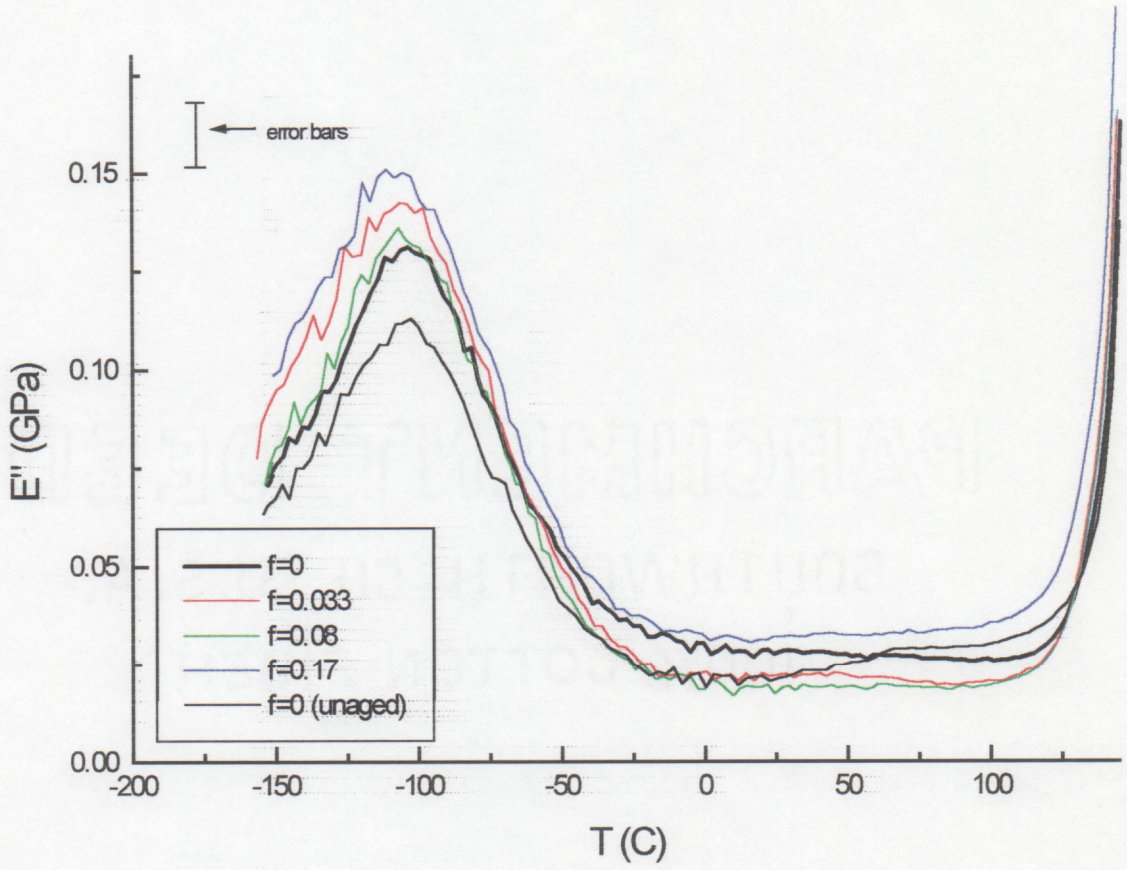

Figure 4.3-14. E" data for samples aged 100 hr. at 90C (MD).

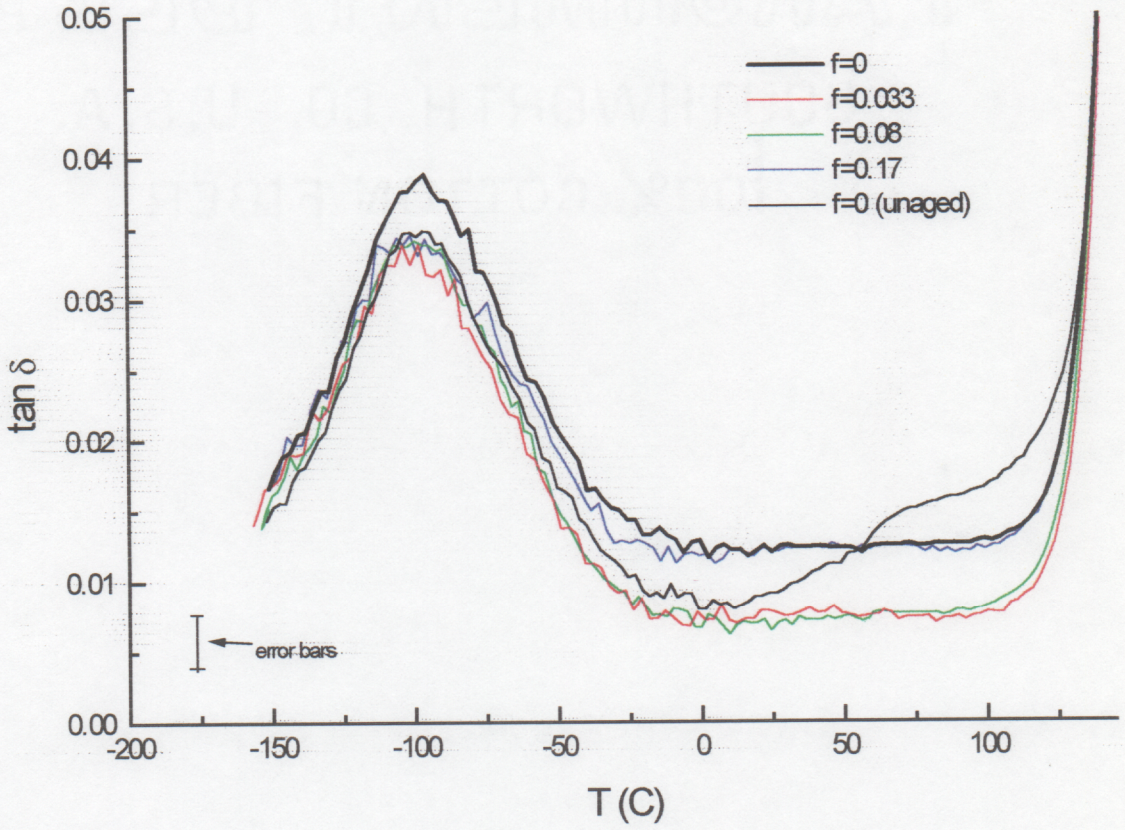

Figure 4.3-15. Tan delta data for sample aged 100 hrs. at 90C (MD).

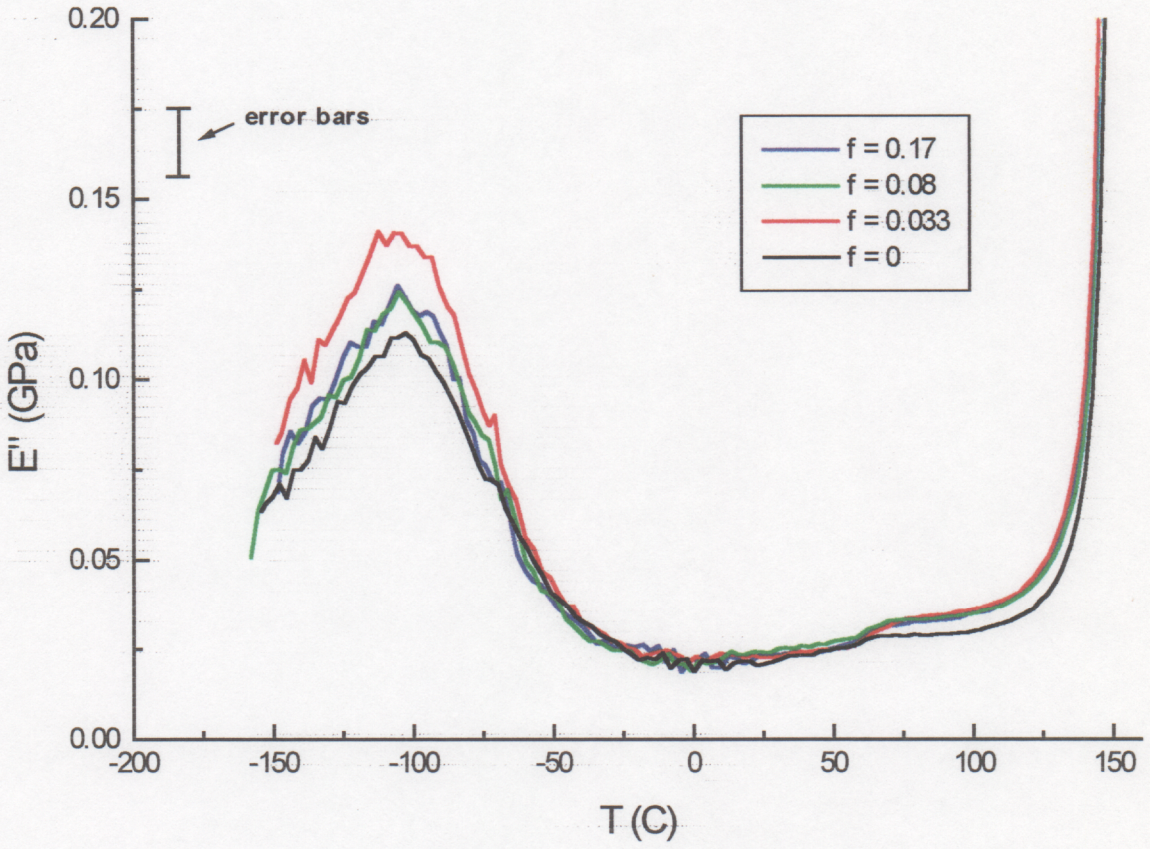

Figure 4.3-16. Loss modulus data for unaged PC loaded in the TD direction.

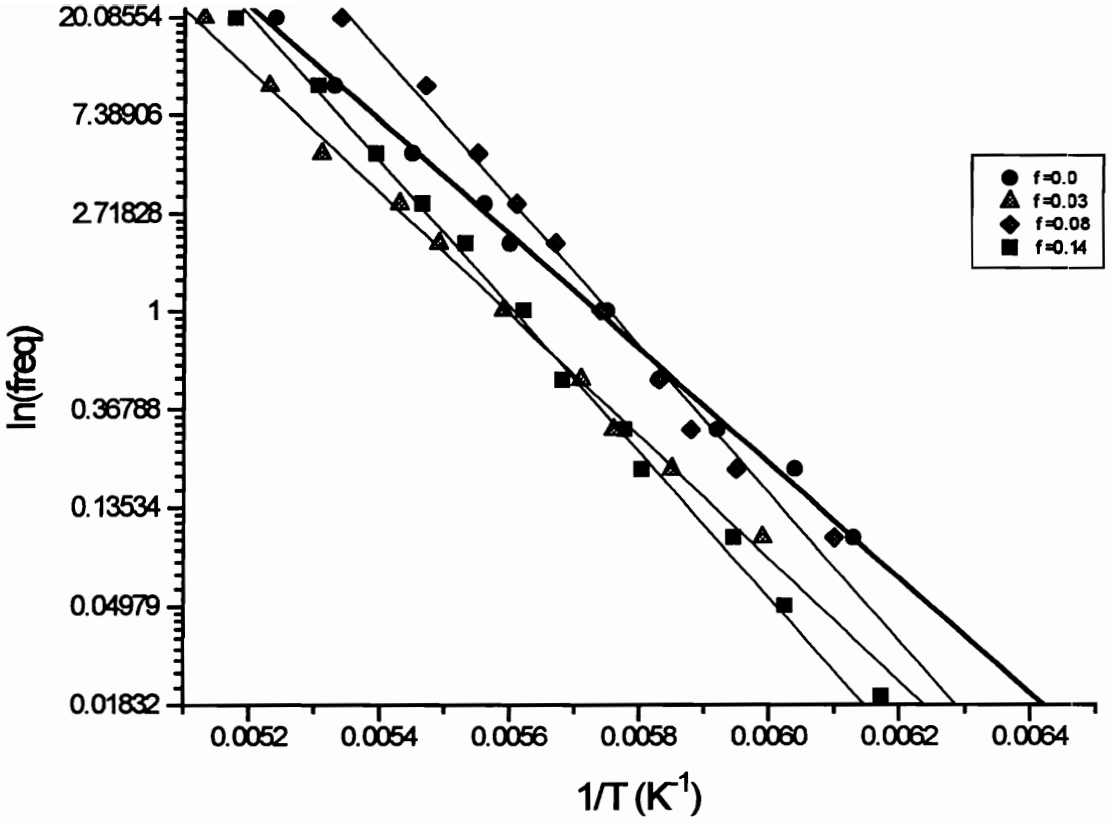

Figure 4.3-17. Activation energy plots for the Beta peak in unaged PC (MD).

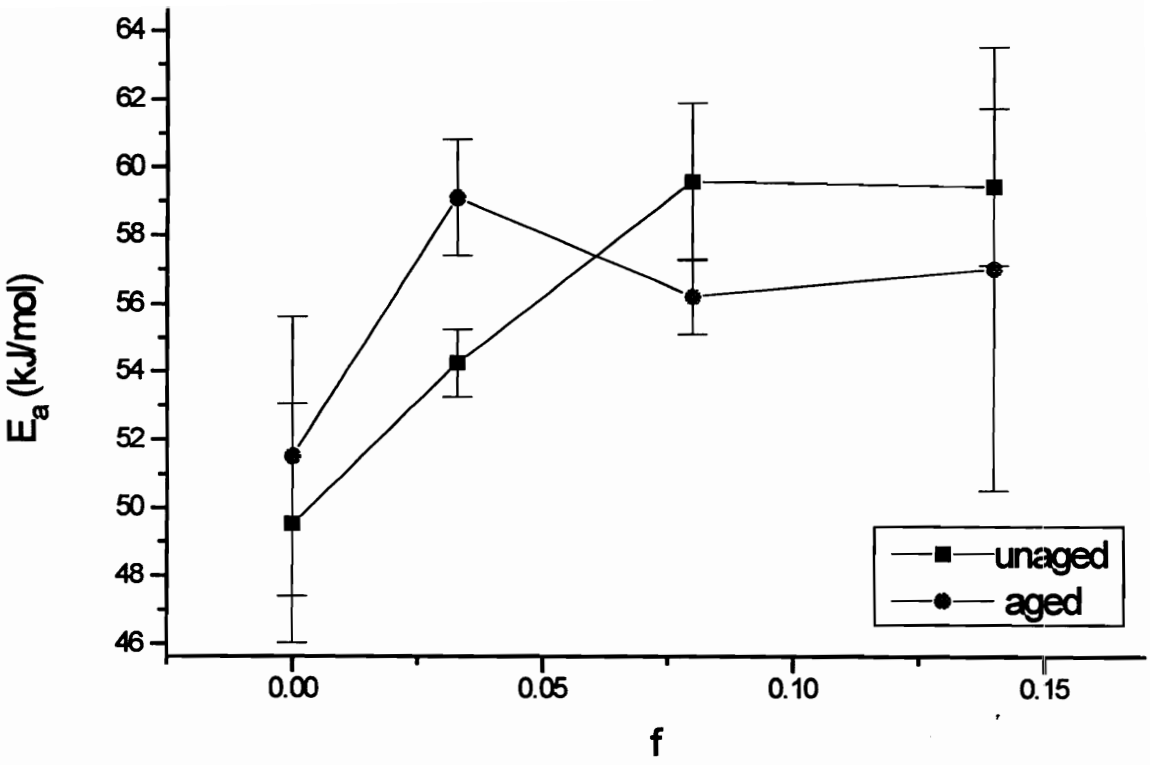

Figure 4.3-18. Activation energies as a function of *f* (MD loading).

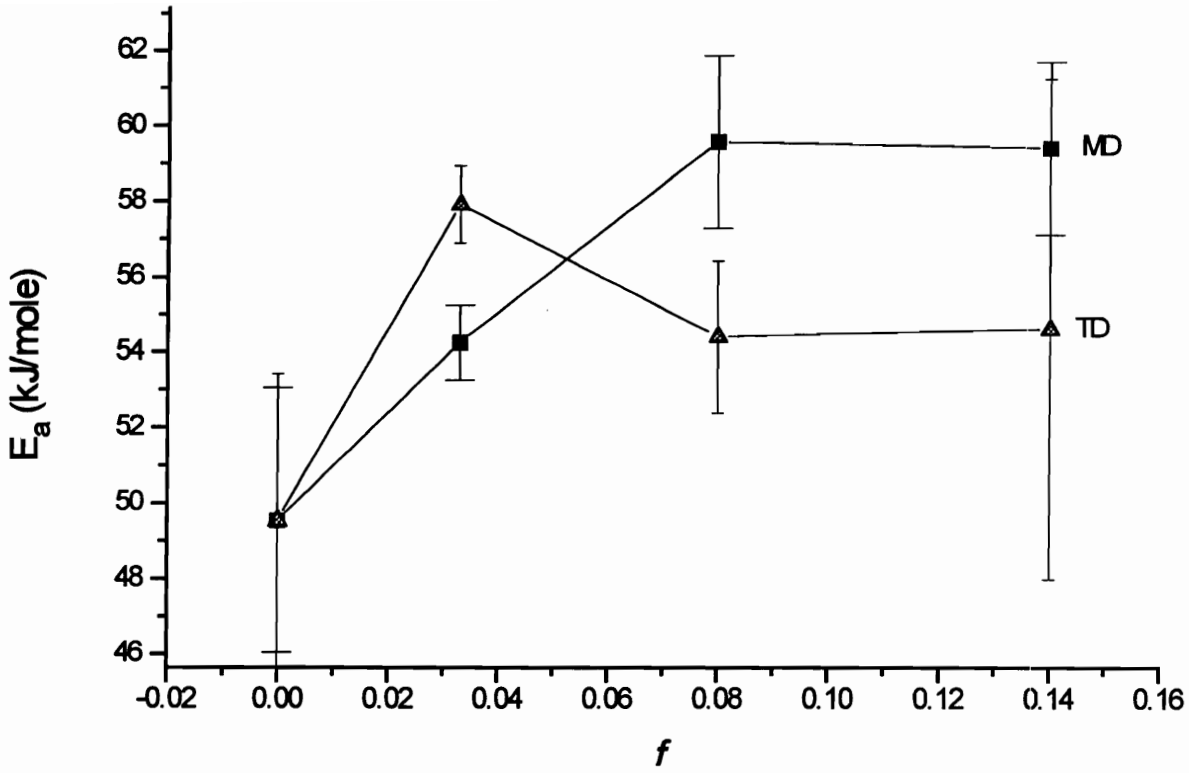

Figure 4.3-19. Comparison of unaged activation energies in the MD and TD directions.

4.4 Discussion

While hot-drawing produces significant molecular alignment, it is a misconception that most of the chains become aligned essentially parallel to the stretch direction. For example, knowing that the highest orientation function achieved was *ca.* 0.17 ($\Delta = 0.027$), and applying Equation (4.3-1), the average angle θ is calculated to be only 48°. Consequently, molecular alignment is a long way from perfect! If instead we use Struik's value[9] of 0.062 for the intrinsic birefringence, we obtain an f of 0.44 resulting in an average θ of 38°. This indicates somewhat better chain alignment but it is still far from having all of the chains parallel.

Nevertheless, the molecular rearrangement which does occur causes some significant changes in the polymer. Of particular interest are the changes in ρ, T_g, and E_a since each can provide useful information about the polymer configuration/structure. The first provides a direct measure of chain packing and free volume whereas the activation energy provides direct information about relaxation rates. The changes in T_g (along with other thermal properties) are useful in that they can be related to the structure through a variety of models. Naturally, a judicious choice of model is required in order to gain any useful information. In the next few sections, these structural aspects will be discussed in more detail along with the implications of the other experimental results.

4.4.1 Free Volume and Chain Packing

Referring to Figure 4.3-2, the density increase at high f indicates that the reorienting chains are packing better and "squeezing out" free volume. It is emphasized that this density increase at larger f is unexpected based on first principles. Stretching a polymer above T_g is generally considered a nearly incompressible process (i.e. Poisson's ratio ≈ 1/2) meaning no change in volume with stretching. If anything, the polymer density would be expected to decrease with stretching—a characteristic which is seen at low f. Strain-

induced crystallization might explain the densification, however, wide angle x-ray scattering (WAXS) has shown no crystallinity in these samples. There is also no evidence of it (i.e. strain-induced crystallization) occurring in the literature. In addition, the measured density increase is very small when compared to density increases induced by crystallization which are usually of the order of 0.01 g/cc or higher.

It is speculated that initially, the polymer dilates with stretching as with any "standard" material under strain. This is due to Poisson effect discussed above and would explain the initial drop in ρ at low f. However, a competing effect occurs as the chains become more aligned; they begin to pack better and reduce the free volume. The latter begins to dominate at high f, hence the upturn in Figure 4.3-2. If the chains were not able to pack better then the density would continue to drop with further stretching. Obviously the "ultimate" example of orientation enhanced packing would be strain-induced crystallization.

A comprehensive study of oriented polycarbonate using IR spectroscopy was performed by Lunn and Yannas which provides support for this concept of better packing in oriented polycarbonate.[25] Their study involved dichroism measurements at 1364 and 2971 cm^{-1} corresponding to the in-phase symmetric bending and asymmetric stretching of the two methyl groups respectively. They found that chain segments which lie parallel to the stretch direction had stronger intermolecular bonding as determined by frequency shifts in the incident polarized radiation. Consequently, chain segments lying perpendicular to the stretch direction exhibited weaker intermolecular bonding. This implies that chains which are oriented in the stretch direction have shorter interatomic distances, whereas chains oriented perpendicular to the stretch direction have longer interatomic distances. At first glance it might seem that the two effects cancel and that no net change in volume would occur. Remember, however, that by the definition of f, more of the chain segments are preferentially oriented in the stretch direction. The net effect is a decrease in the average interatomic spacing of the system and an increase in density.

4.4.2 The Effects of Stretching on T_g

It is apparent from Figure 4.3-6 that stretching has a small but significant influence on the T_g. Nevertheless, it remains to determine exactly what is causing this change. A number of models exist which relate various structural parameters (i.e. configurational entropy, hole energy, free volume, etc.) to the T_g. A good fit of the oriented data to one of these models would provide insight into the important changes taking place during stretching. With this goal in mind, a comparison of the T_g data to some of these models will now be discussed.

The simplest theory is the free volume theory which predicts an increase in T_g with decreasing free volume due to reduced mobility. It agrees qualitatively with the density and T_g data at high f but breaks down near the low f density minimum. For it to be in complete agreement, the glass transition temperature would have to go through a minimum at low f. This discrepancy implies that some other structural parameter must also be important to T_g.

From a configurational entropy standpoint, the increase in T_g with stretch ratio is also predicted by a modified form of the Gibbs-DiMarzio equation[26]

$$\frac{T_g(\lambda)}{T_g(\lambda = 1)} = \exp\left[\frac{G}{2\Delta C_p T_o}(\lambda^2 + 2\lambda - 3)\right] \qquad (4.4\text{-}1)$$

where λ is the uniaxial stretch ratio, G is the shear modulus at test temperature T_o, and ΔC_p is the heat capacity difference between the liquid and glassy states. While the above equation, which is derived from rubber elasticity, is strictly only applicable for a network, the entanglements in the polycarbonate can be treated as psuedo-crosslinks. Similarly, the parameter λ actually refers to the molecular stretch ratio although this can be equated with the sample stretch ratio Λ since shrinkage recovery was approximately 100% (see Equation (4.3-2)). The Gibbs DiMarzio equation predicts a thermodynamic glass transition temperature existing where the conformational entropy is zero. Since an

oriented chain has an inherently lower entropy, the effective glass transition is raised. The equation predicts a straight line for a plot of $\ln(T_g(\lambda)/T_g(1))$ versus $\lambda^2+2\lambda-3$ having a slope of $G/2\Delta C_p T_o$. The T_g data are plotted in this form in Figure 4.4-1. Although the data do not lie in a straight line, a fit of the data at low stretch ratios yields a value for $G/2\Delta C_p T_o$ equal to 0.0031 which is in good agreement with the data of DiMarzio for various rubbers.[26] If one assumes a T_o of 160°C, G of 10^6 Pa, and ΔC_p of 0.217 J/g-°C (from the DSC data), this yields a value of 0.0045 which is also in good agreement with the experimental data at small λ. This reasonably good correlation would indicate that configurational entropy is important. Nonetheless, the breakdown at high-*f* may indicate that configurational entropy alone is insufficient for predicting T_g behavior. It is also possible that the relationship used to calculate the entropy, which is based on rubber elasticity, is not accurate at high *f*. Nonetheless, the good agreement with configurational entropy at low *f* coupled with the good agreement observed with free volume at high *f* may indicate that both parameters are important.

A theory that combines the energy of free volume formation (designated the "hole energy" or E_h, by Kanig[27]) with an associated entropy change S_{cg}, has been outlined by Matsuoka.[24] If the volume at T_g is increased from the occupied volume V_o, to the total volume V_g, by addition of the free volume amount ΔV_g, then the total increase in hole enthalpy E_h is approximated as,

$$E_h = T_g S_{cg} = \frac{\Delta V_g}{V_g}\left[\frac{\Delta C_p}{\Delta \alpha}\right]_{T_g} \qquad (4.4\text{-}2)$$

where $\Delta\alpha$ is the difference in volume expansion coefficient between the liquid and glass (i.e. $\Delta\alpha = \alpha_l - \alpha_g$) and the function $\Delta V_g/V_g$ is simply the free volume fraction (*ffv*). The hole energy can also be thought of as the cohesive energy per mole. Empirical studies by Kanig,[27] Matsuoka,[24] and Bunn[28] have shown a correlation between various forms of

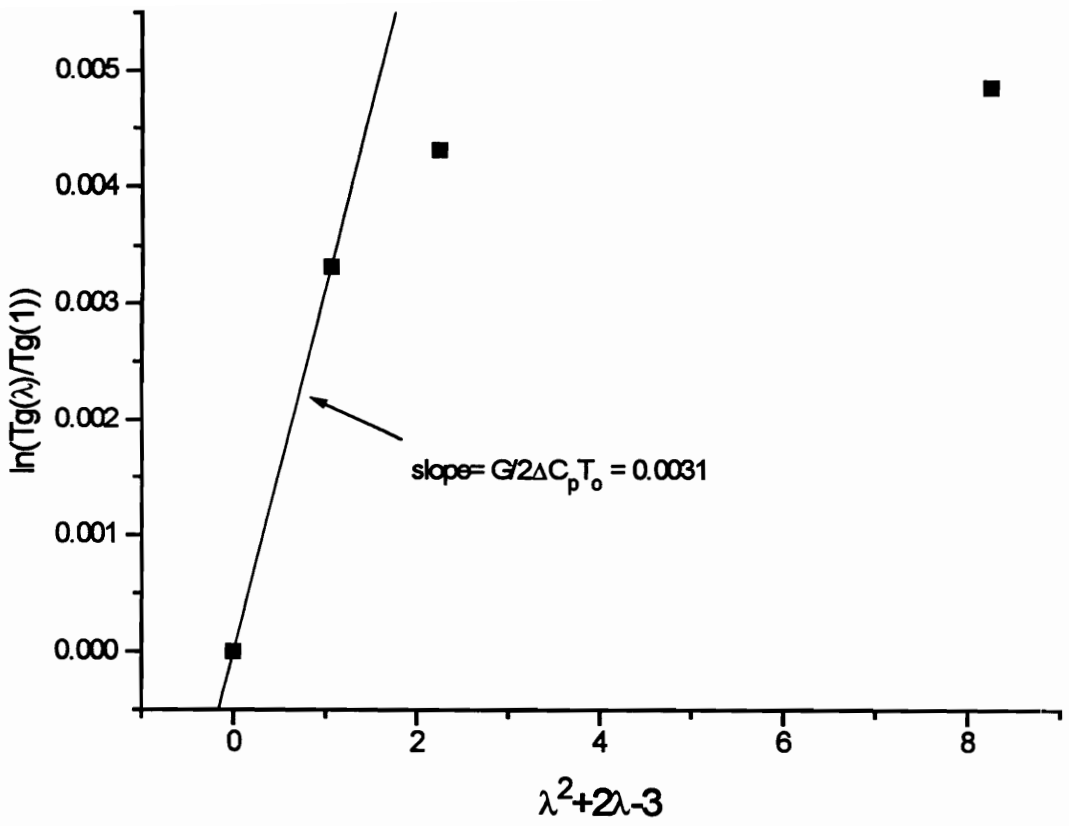

Figure 4.4-1. Gibbs-DiMarzio plot of Tg changes with stretch ratio.

the hole energy and both the glass transition temperature and conformer molecular weight *M*—a conformer being defined as the smallest segmental unit of rotation in a polymer. As an example, the hole energy per mole of conformers is shown to be proportional to ln(M). Likewise, the hole energy on a per gram basis is instead proportional to ln(M)/M. Matsuoka has derived the following equation relating T_g to ln(M)[24],

$$(T^* - T_o) \ln M = C_3 \tag{4.4-3}$$

where C_3 is a constant approximately equal to 1750 for most polymers (C_3 = 1788 for isotropic polycarbonate), T* is the temperature above which cooperative motions cease to exist (assumed to be 500°C), and $T_o = T_g - 50°C$. This relationship holds for a wide range of polymers. With some rearranging, the following relationship between lnM and T_g is obtained,

$$\ln M = \frac{1750}{550 - T_g} \tag{4.4-4}$$

For PC, the corresponding value for M is 85 g/mol of conformers which is approximately 1/3 the molecular weight of the polycarbonate repeat unit (254 g/mol).[24] This implies that three conformers exist per repeat unit and M is an average over these three units. These conformers might represent, for example, the two phenylene rotations and the carbonyl unit. As an additional example, for most vinyl polymers, M is approximately 1/2 of the repeat unit molecular weight indicating two conformers per repeat unit, one for each backbone carbon atom.

To test this model for the unaged oriented system, values of ln(M) were first determined as a function of *f* using Equation (4.4-4) and the T_g data in Figure 4.3-6. The results are shown in Figure 4.4-2. Next the hole energy was calculated using Equation (4.4-2). Values for $\Delta\alpha$ did not change significantly with orientation and a single value of 4.4×10^{-4} °C^{-1} (+/- 10^{-5}) (based on dilatometric testing) was assumed for all values of *f*. The fractional free volume (*ffv*) was obtained from the density data as a function of *f* after

assuming that the unoriented *ffv* was 0.025--the so called WLF free volume. This resulted in a calculated value for V_o of 0.9307 cc/g assuming an unoriented density of 1.1982 g/cc. This occupied volume does not change with *f* so values for *ffv* at other orientations can be calculated from the density data by

$$ffv = 1 - \rho V_o \tag{4.4-5}$$

Values of E_h calculated from Equation (4.4-2) are displayed in Figure 4.4-3 on a "per gram" basis. A check of the consistency of the theory was made by plotting E_h versus lnM in Figure 4.4-4 after first converting E_h to a "per mole of conformers" basis by multiplying by *M* (calculated from Equation (4.4-4)). The fact that the data fall reasonably close to a straight line indicates that the proposed proportionality between E_h and lnM is in reaonably good agreement with the data and that the theory appears to be applicable to oriented systems.

With the consistency seemingly verified, a more meaningful interpretation of the other results can be put forth. Inspection of Figure 4.4-3 shows that E_h increases with *f*, eventually reaching a plateau. This is true even though the free volume is decreasing. The entropy of hole formation S_{cg} —determined from Equation (4.4-2) and plotted versus *f* in Figure 4.4-5—is also found to increase with *f*. The increase in E_h indicates that the total cohesive energy between segments is increasing which, consequently, means enhanced interchain attraction and, effectively, a slight increase in the conformer size M. This increase in M implies that chain movements/rotations may become more restricted as there are now fewer conformers available per unit mass. Larger conformers and more restricted movement, in turn, lead to the increase in T_g. All of these results indicate a reduction in localized segmental mobility for the chain. In contrast, in Chapter 3.0, it was shown that physical aging rates were higher for the oriented samples as compared with the isotropic controls (although the rate did not depend on the *degree* of orientation). This implies that orientation somehow enhances mobility which is in contradiction to these results. It turns

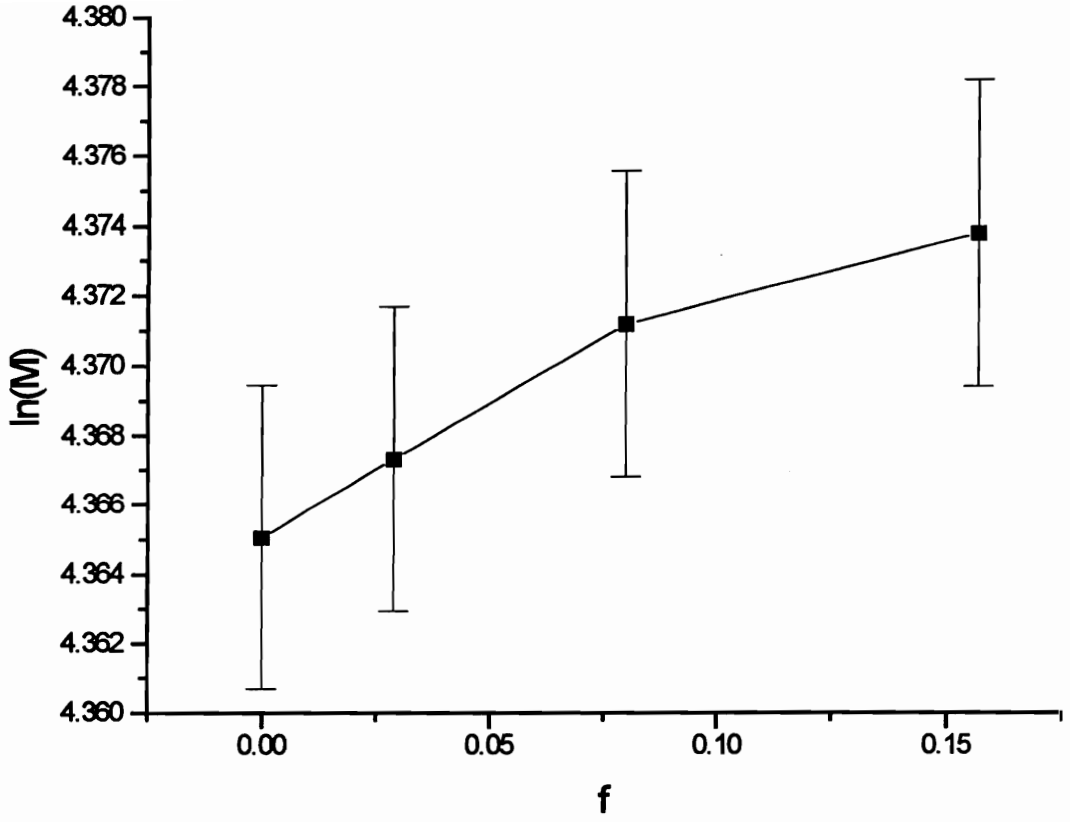

Figure 4.4-2. Conformer MW versus *f*.

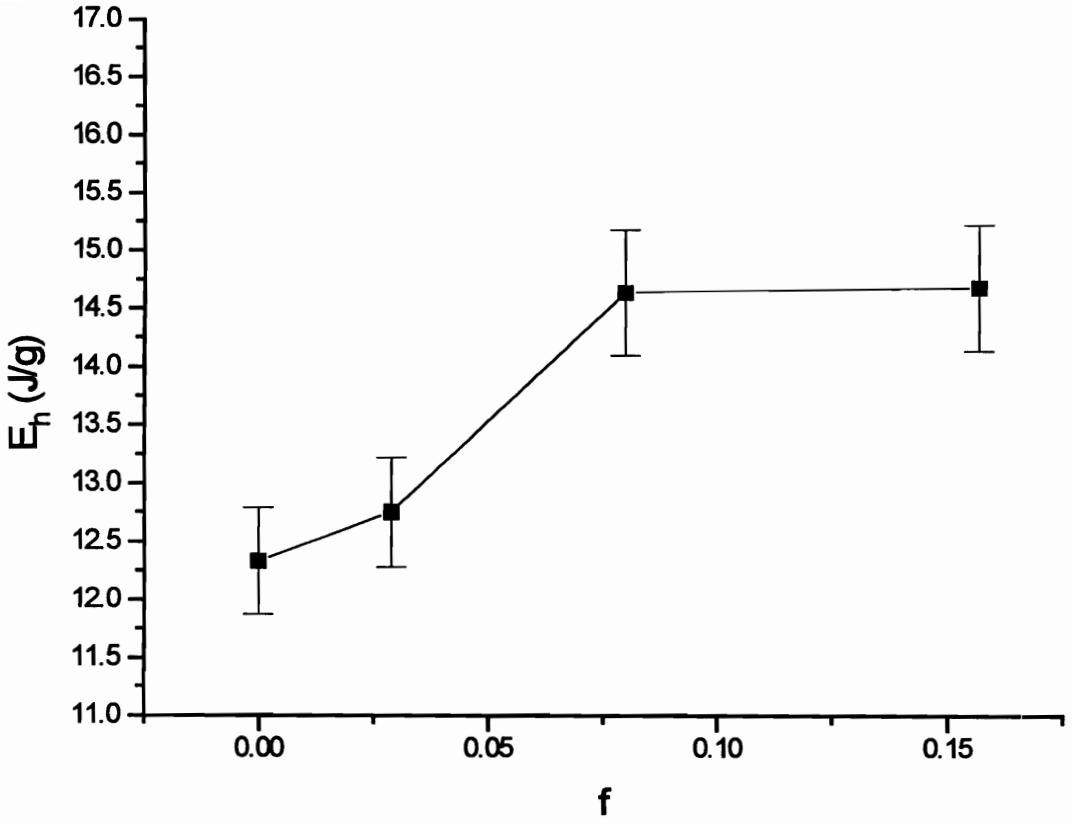

Figure 4.4-3. Hole energy (per gram basis) versus *f*.

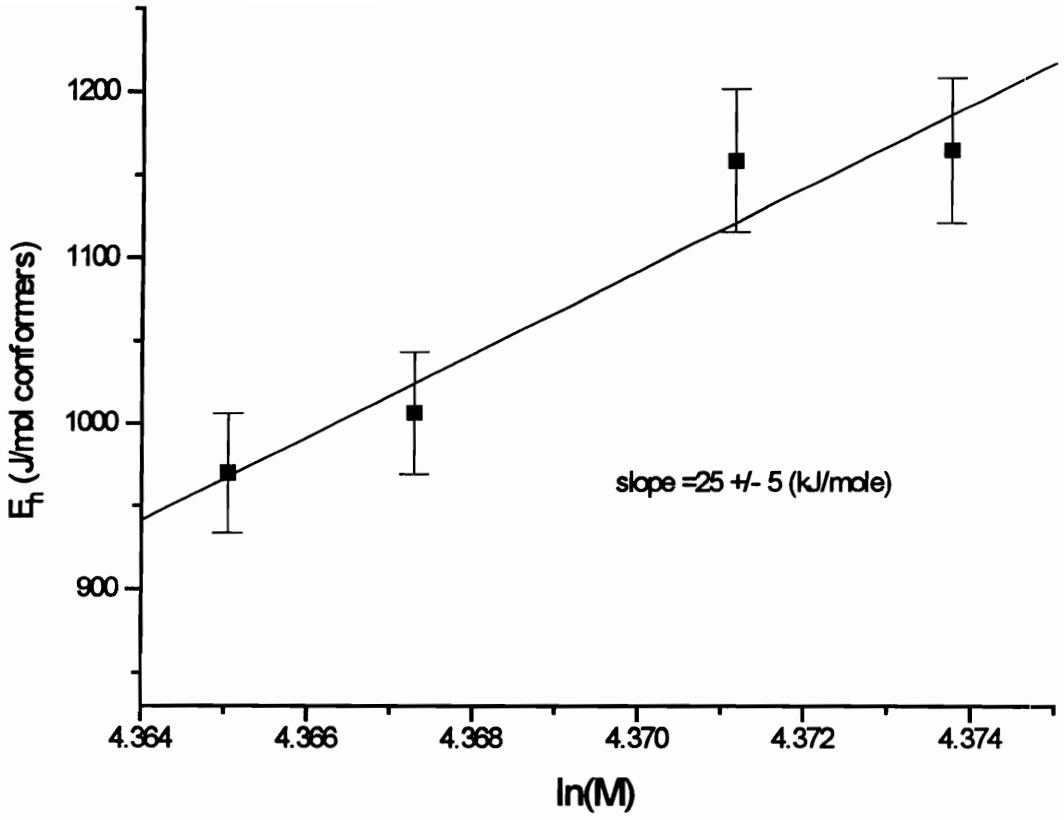

Figure 4.4-4. Hole energy for PC versus calculated ln(M).

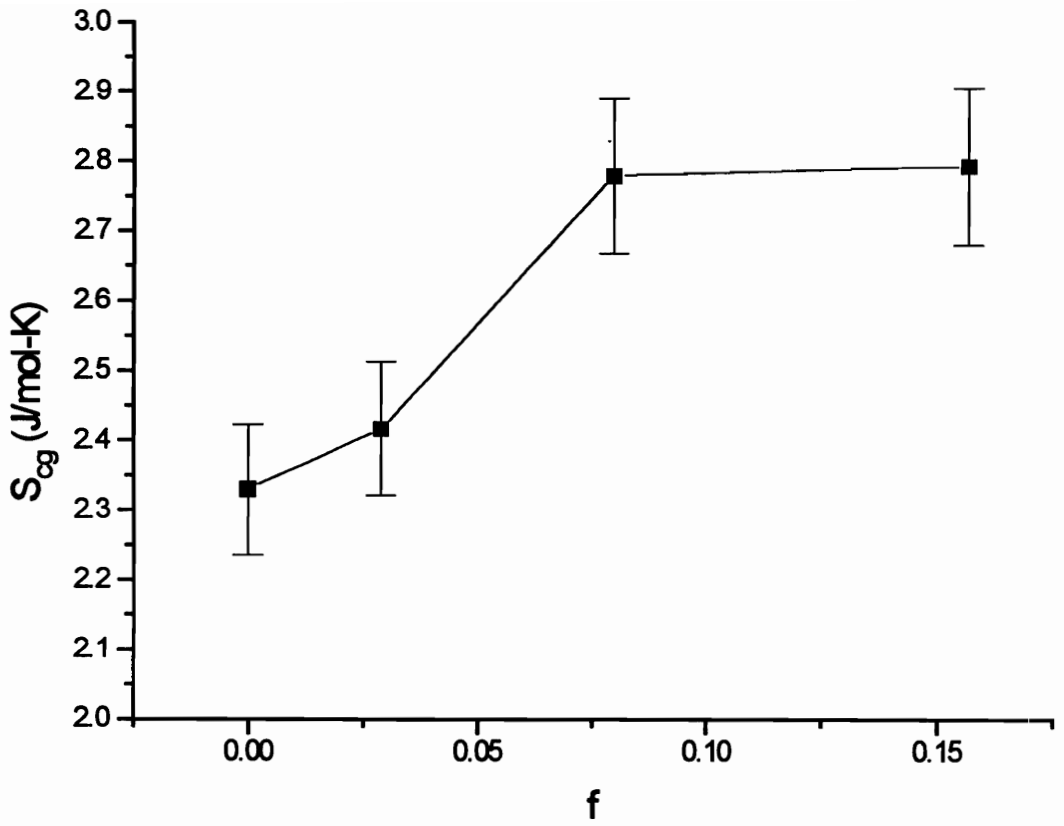

Figure 4.4-5. Hole formation entropy vs. f for PC as calculated from hole energy.

out that this paradox can be resolved with the dynamic mechanical data and this will be discussed in detail in a later section.

Another interesting concept arises when one parametrically compares the volume sensitivity (S) data in Chapter 3.0 (Figure 3.5-1) with the conformer molecular weight data (Figure 4.4-2). The sensitivity decreases with orientation as M increases. It is conjectured that this near inverse relationship is not a coincidence but is instead a direct cause and effect relation. The reasoning is as follows. The volume sensitivity is defined as the change in mobility for a given change in free volume. For a large conformer to be able to rearrange/rotate, it must have a sizeable quantity of free volume present locally. A smaller conformer can rearrange with even less free volume. If one considers mobility to be (crudely) defined as the number of segments/conformers that can rearrange/rotate in a given time, then, for a given change in free volume, a greater number of the smaller conformers will be able to move compared to the larger conformers. This implies a greater sensitivity in the small M samples. Obviously, this is still just a theory and further study is needed for verification.

4.4.3 Internal Energy

Inspection of Figure 4.3-5 seems to indicate that the recovered enthalpy and the density may be correlated. This is verified in Figure 4.4-6 where ΔH_{rec} is plotted parametrically as a function of ρ. This clearly shows a linear correlation between density and the recovered enthalpy. In other words, the system enthalpy decreases linearly with decreasing fractional free volume.

It should be emphasized that the changes taking place in ΔH are primarily due to changes in the internal energy ΔU, which is related to ΔH at constant pressure by

$$\Delta U = \Delta H - P\Delta V \qquad (4.4\text{-}6)$$

where ΔV is the volume change and P is the pressure (1 atm). For the volume changes occurring during stretching--as determined from the density data--$P\Delta V$ is on the order of 10^{-4} to 10^{-5} J/g which is only a tiny fraction of ΔH. Therefore one can make the approximation

$$\Delta U \cong \Delta H \tag{4.4-7}$$

which implies that the effect of density change on the work of expansion (i.e. the $P\Delta V$ term) is negligible.

Assuming that no chemical changes are taking place, the internal energy (or enthalpy) changes occurring in the polymer can be grouped into two principle components: those primarily due to changes in the intermolecular potential energy ΔU_{pot} (which includes changes in the hole energy E_h), and those brought about by changes in the rotational isomeric state ΔU_{rot}. For the former, increased density with f results in an increase in hole energy but a drop in intermolecular potential energy due to a decrease in average bond distance. For the latter, Abe and Flory[29] have shown through rotational isomeric state (RIS) calculations that the number of trans segments in a network of polyethylene chains will increase (at the expense of gauche (+/-)) upon stretching. In polyethylene, the trans configuration is at a lower energy than gauche (+/-) so stretching would lower ΔU_{rot}. In the case of polycarbonate, Williams and Flory[30] estimate the cis state in polycarbonate to be 1.3 kcal/mole higher than the trans state so the same argument would apply. As the polycarbonate is stretched, some of the cis conformations would change to trans resulting in a decrease in internal energy.

It is paradoxical that the hole energy E_h is increasing with f even though the system enthalpy is decreasing. The issue is further complicated by the fact that the change in E_h with stretching is 2 to 3 times larger than ΔH. One hypothetical way to compare these

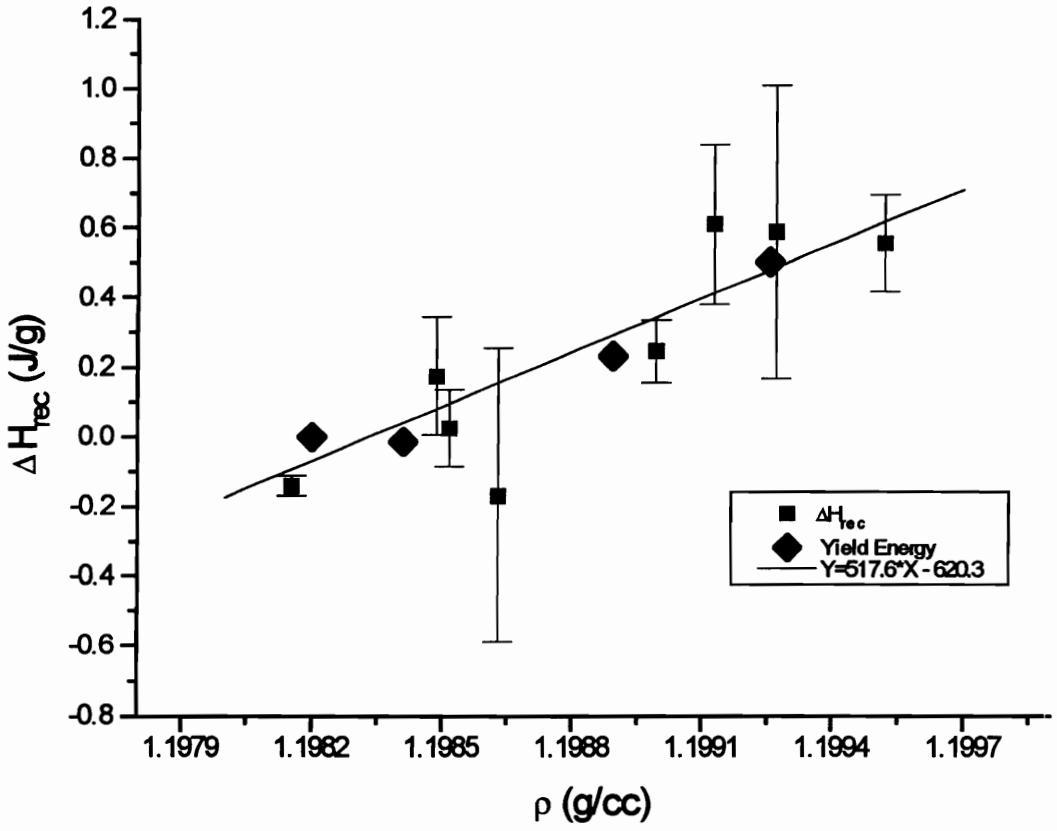

Figure 4.4-6. Correlation between density and recovered enthalpy (and yield energy).

values of E_h and ΔH is to envision the theoretical ground state at T_o as a function of orientation. This ground state consists of the polymer at maximum packing and with no free volume (i.e. the volume will equal V_o). Since the ground states will differ with orientation (both in the distribution of bond distances and rotational potential energies), the ground state internal energy H_o will also vary with *f*. This can be related to the measured ΔH by

$$\Delta H = \Delta H_o + \Delta E_h \tag{4.4-8}$$

where ΔH_o is the difference in ground state energy between the oriented and unoriented samples and ΔE_h is the difference in hole energy. The former is composed of contributions from both intermolecular potentials and changes in rotational conformational energy (i.e. $\Delta H_o \approx \Delta U_{pot} + \Delta U_{rot}$). As shown earlier, it is more difficult to add holes into the oriented samples (because of the greater interchain attraction) so ΔE_h increases with *f*. If indeed, these values of E_h are accurate, then a large negative change in ΔH_o with stretching is required in order to compensate. This, however, is not unreasonable since the greater interchain attraction of the oriented samples also translates to a lower ΔU_{pot}.

At first glance, however, the component ΔU_{pot} might not be expected to change since V_o is assumed constant and therefore, the average bond distance must also remain constant. Despite this fact, the distribution of bond distances is expected to vary. This is important since the Lennard-Jones type potential energy well is a nonlinear function of bond distance. Therefore pair potentials will also vary with the net result being a non-zero value for ΔU_{pot}. It is also possible that the closest atomic neighbors in an oriented sample might differ slightly from the isotropic case resulting in different attraction potentials; this would also affect ΔU_{pot}.

Another potential scenario is that changes in the rotational isomeric state energy ΔU_{rot} are the dominant cause of the decrease in ΔH (or increase in ΔH_{rec}). In the ground state,

the oriented chains will be at a much lower energy since there are fewer cis "kinks" present. A second reason--which does not require the concept of a ground state--is that changes in isomeric state can also lead to changes in volume. For example, one might assume a certain volume which is associated with a cis "kink" in the chain. When these "kinks" are removed leaving an all trans chain (planar zig-zag), it is much easier for it and other chains to pack more closely. If it is assumed that some average δV occurs for each bond rotation--along with the corresponding change in conformational energy--then this leads to a one-to-one relationship between density and enthalpy change as depicted experimentally in Figure 4.4-6.

One test of this hypothesis, would be to pick different polymers that vary in energy between rotational states, and see if there is a correlation between the slope in the enthalpy-density plot and this rotational energy difference. A parameter equivalent to this energy difference between rotational states, termed the flex energy ε, is used in the Gibbs-DiMarzio equation. In fact, Simha and Boyer have shown that the ratio ε/kT_g possesses the "universal" value of 2.26 for all polymers.[31,32] Applying this to the oriented data, ε must increase with f since T_g increases. This is in line with the earlier data showing an increase in M. Both imply a stiffening of the chain with increased orientation.

4.4.3.1 Internal Energy-Volume Relations from Rubber Elasticity

In terms of hot-drawing polycarbonate, one can also apply thermodynamic relations from rubbery elasticity. This is brought about primarily as a check of the consistency of the results and also to determine where the contributions to the enthalpy change are originating. In particular, one would like to determine how much of the change in enthalpy/internal energy is due solely to volume change and how much is due to conformational changes at constant volume. While polycarbonate is not a crosslinked network, the entanglements act like virtual crosslinks. It will therefore be *assumed* that the thermodynamic changes which occur during stretching above T_g are frozen into the

sample during the quench into the glassy state. In other words, the energy changes which occur during cooling are approximately the same for both the oriented and unoriented samples so they can be neglected. Under constant pressure stretching (as performed with the polycarbonate in this study) the force F is determined from the entropy S and internal energy U by[33,34]

$$F = \left(\frac{\partial H}{\partial L}\right)_{P,T} - T\left(\frac{\partial S}{\partial L}\right)_{P,T} \cong \left(\frac{\partial U}{\partial L}\right)_{P,T} - T\left(\frac{\partial S}{\partial L}\right)_{P,T} \qquad (4.4\text{-}9)$$

where the approximation follows from Equation (4.4-7). Following a procedure similar (but slightly different) to that outlined by Aklonis and MacKnight,[34] the internal energy can be expanded by application of the chain rule resulting in

$$dU = \left(\frac{\partial U}{\partial V}\right)_{L,T} dV + \left(\frac{\partial U}{\partial L}\right)_{V,T} dL \qquad (4.4\text{-}10)$$

where the term $(\partial U/\partial L)_{V,T}$ is often referred to as f_e, the internal energy component of force at constant volume. This parameter, along with the other partial derivative, $(\partial U/\partial V)_{L,T}$, describes the partitioning of ΔU between length and volume changes. Rearranging (4.4-10) yields,

$$\left(\frac{\partial U}{\partial V}\right)_{P,T} = \left(\frac{\partial U}{\partial V}\right)_{L,T} + \left(\frac{\partial U}{\partial L}\right)_{V,T}\left(\frac{\partial L}{\partial V}\right)_{P,T} \qquad (4.4\text{-}11)$$

where the first term on the right hand side can be rewritten in terms of the compressibility κ, and the volumetric thermal expansion coefficient α,

$$\left(\frac{\partial U}{\partial V}\right)_{L,T} = \alpha T / \kappa - P \qquad (4.4\text{-}12)$$

For a unit mass, (4.4-11) and (4.4-12) can be rewritten in terms of the density as

$$\left(\frac{\partial U}{\partial \rho}\right)_{P,T} = -\frac{1}{\rho^2}\left(\frac{T\alpha}{\kappa} - P\right) + \left(\frac{\partial U}{\partial L}\right)_{V,T}\left(\frac{\partial L}{\partial \rho}\right)_{P,T} \qquad (4.4\text{-}13)$$

The left hand side, which represents the net change in U for a given change in density, can be approximated as the negative of the slope of the data in Figure 4.4-6. This equals

-517.6 J-cc/g^2 (+/- 96 J-cc/g). The parameter $(\partial L/\partial \rho)_{P,T}$ can be determined from the data in Figures 4.3-1 and 2 although this is unnecessary. Assuming a temperature T of 160°C, a rubbery thermal expansion coefficient α of 6.3 x 10^{-4} °C $^{-1}$ obtained from dilatometry, and a compressibility κ of 0.4 x 10^{-9} Pa^{-1} (approximated from Van Krevelin's empirical method[35]), the internal energy change with density at constant L (i.e. the first term on the RHS) can be calculated. It has a value of 507 J-cc/g (the error is estimated at +/-100 J-cc/g based on the uncertainty in κ) which is very close to the value of 517.6 J-cc/g for the LHS. Inserting these values into Equation (4.4-13) indicates that $(\partial U/\partial L)_{V,T}$, and consequently f_e, must therefore be small (or zero).

This result indicates that the internal energy changes come primarily from the changes in volume and not from any isochoric conformational changes which might also be occurring. While this has only been verified in this study for PC, Treloar[33] has also reached similar conclusions for other systems and attributes the change in U to a change in interatomic distances. While at first glance, this might seem to rule out changes in rotational isomeric state as a source for the internal energy change, keep in mind that it may still be possible for a volume change to be associated with each cis to trans conversion as described previously. In contrast, if this assumed volume change does not exist, then Equation (4.4-13) predicts that the rotational isomeric contribution ΔU_{rot} will be negligibly small if not zero.

4.4.3.2 Yield Energy and Its Relation to Internal Energy

It is interesting that the yield-energy in Figure 4.3-5 (and also superimposed in Figure 4.4-6) follows closely with the recovered enthalpy (or ΔU). This is probably not simply a coincidence. In fact, another yield parameter known as the Post Yield Stress Drop (or PYSD) has been shown by Hayward et al.[36] to be a measure of the relative "order" in polycarbonate. Yielding is the process of going from elastic deformation to plastic flow (see Matsuoka[24] or Bowden[37] for a discussion of the viscoelastic characteristics of

yielding). Therefore energy is required to break up the glassy structure enough so that long range molecular motions can take place. If the oriented material is already at a lower internal energy state due to better packing, rotational isomerization, etc., then additional energy is required to break up this "structure." This additional energy should be the same as the enthalpy difference ΔH between the oriented and the unoriented state. That this is in fact the case (as seen in Figure 4.3-5) is an indication that yield energy is a good predictor of the degree of structural "ordering" in the system.

On a similar note, Fen[38] has investigated the yield process in polycarbonate using the molecular mechanics method. His results indicate that yielding is the result of the inflection in the Lennard Jones potential which represents the van der Waal's attraction. This is in qualitative agreement with the density and yield energy data. Better packing means the molecules are deeper in the potential energy well. This requires additional energy in order to reach the inflection point, hence higher strain energy at yield.

4.4.4 Dynamic Mechanical Discussion

The previous thermodynamic data have indicated that the localized mobility decreases with orientation, possibly due to the tighter packing and effective chain stiffening. This is also supported by the higher β-transition activation energies for the oriented samples (see Figure 4.3-18). Paradoxically, this decreased mobility seems to contradict the previous physical aging rate data which indicate an *enhanced* mobility in the oriented state. Fortunately, however this discrepancy can be rectified via the DMS data. From the MD loss moduli in Figure 4.3-12, it appears that the process of orientation itself, and not just the degree of orientation, is important. Both the α' and β–relaxation strengths (i.e. the area under the curve) for the isotropic sample are significantly lower as compared to the oriented samples. These trends are also in agreement with the volume relaxation data obtained previously. In addition, both the volume relaxation rate and the relaxation strengths are independent of f for the oriented samples. The increase in MD relaxation

strength with orientation implies that more segments are mobile in the oriented glassy state as compared with the isotropic glass. In fact, Watts and Perry[39] have previously shown using dielectric spectroscopy that, for the β transition, only about 17% of the total chain units are mobile in the glass for isotropic polycarbonate; therefore, there are potentially a large number of dormant segments which are susceptible to "activation" by stretching.

The next step is to relate the relaxation strength data to the kinetics of physical aging. Kinetic processes such as volume relaxation can be modeled with two parameters: the first being the rate at which a single segment/unit relaxes which is multiplied by the second term--the concentration of segments participating in the relaxation. It is this second term which relates to the relaxation strength. For the oriented samples, the first term (which represents localized mobility) is observed to be lower; however, the increased relaxation strength implies that the second term is larger. In fact, this second term must be dominant in the oriented samples since the net effect is an *increase* in volume relaxation rate. Of course, it still remains to answer the question of what exactly is causing the relaxation strength enhancement. It appears as though the act of stretching somehow activates many otherwise dormant segments into motion. This may be the result of residual or internal stresses or it may be connected in some way with the concept of stress induced "rejuvenation" discussed previously in Chapter 2.0. Much of the rest of this discussion will be devoted to discussing possible models for this enhanced relaxation strength.

Although this concept of enhanced relaxation strength appears to correlate nicely with the enhanced volume relaxation data, a paradox arises when the unaged and aged samples are compared. For example, in Figure 4.3-14, it is observed that the β–relaxation strength *increases* in going from an unaged to an aged isotropic sample. Intuition would indicate that fewer segments should be mobile in an aged sample, not more. The α' transition does, however, indicate a decrease in relaxation strength which may resolve this discrepancy. Still, it is uncertain why the β relaxation strength increases with aging.

Because of the anisotropy of the system, it is important to investigate the difference in effective relaxation strength in both the MD and TD directions. Careful inspection of Figure 4.3-16 shows that both the α' and β relaxation strengths are still higher for the oriented samples in the TD direction, yet, are lower compared to the MD values. The exception to this is the β relaxation for the 1.25X sample (f=0.033) which exhibits no relative difference in the MD and TD directions; however, this sample was also shown to undergo slight dilation during stretching as opposed to densification (see Figure 4.3-2). Therefore the anisotropy in chain packing is not expected to be significant. For the higher f samples, the lower relaxation strength in the TD direction indicates that fewer segments are able to relax along the TD (relative to the MD). This anisotropy in relaxation strength also correlates with the anisotropy in linear relaxation rates discussed in Chapter 3.0. Although the relaxation strength is less in the TD, relative to the MD, the activation energy data in Figure 4.3-19 indicate that there is a slightly lower energy barrier to motion in the TD. This implies that the effective local mobility is slightly higher in the TD although still lower than for the isotropic samples. This anisotropy in mobility is probably connected in some way to the anisotropic free volume distribution.

Another approach to analysing the DMS data is to investigate the nature of the frequency-peak temperature data (with accurate data being available for the β–transition only) to see how relaxation times vary with temperature. Because of the shapes of the lines in Figure 4.3-17, this can lead to some very interesting results. Extrapolating the data in Figure 4.3-17 to very low temperatures, the peak frequency is found to decrease monotonically with f. This means that the effective relaxation time is increasing with orientation. This is in qualitative agreement with the trend in conformer molecular weight M, since the tanδ peak frequency is proportional to $(k_s/M)^{1/2}$ where k_s is an effective spring constant. It also agrees with the thermodynamcially obtained mobility data discussed previously. When the data are extrapolated to very high temperatures, however, this trend almost completely reverses. This is shown more clearly in Figure 4.4-7 where the

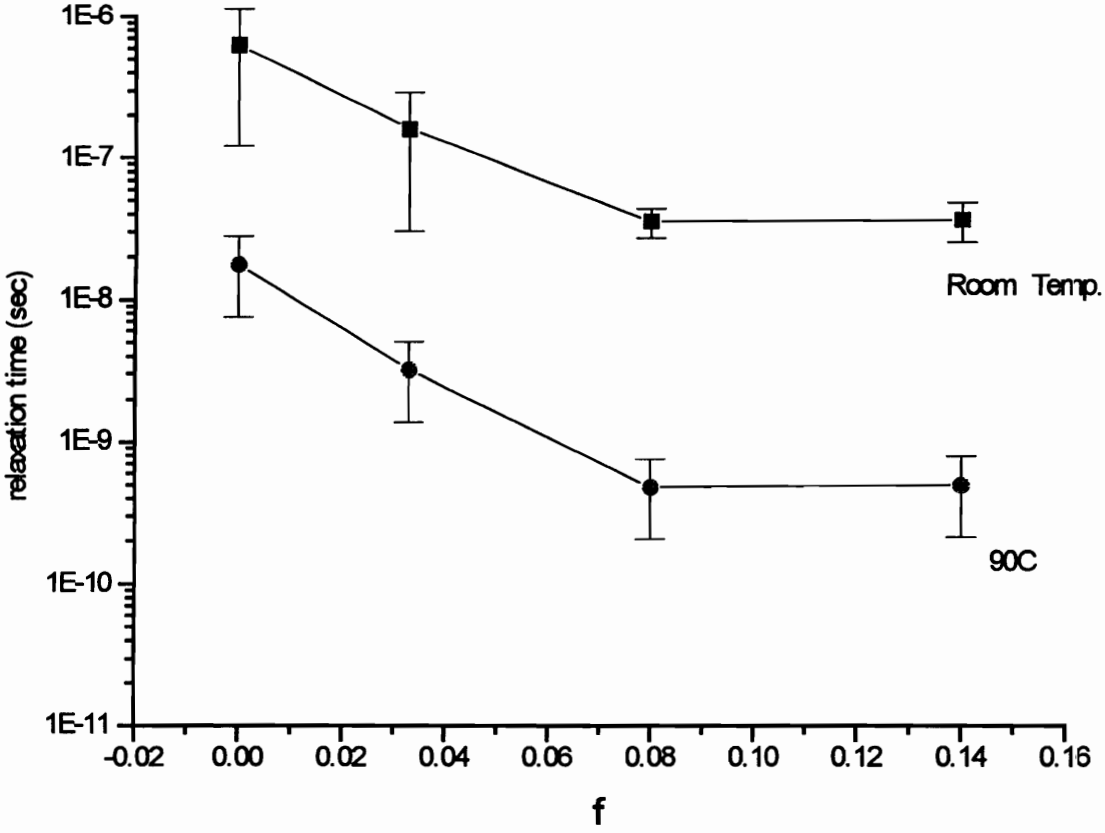

Figure 4.4-7. Calculated relaxation times for beta relaxation at different temperatures.

effective relaxation times at room temperature and 90°C are calculated from the activation energy data. Note that the relaxation time here is simply the reciprocal of the frequency. The calculated data indicate that the oriented systems are able to relax significantly faster in the β–mode relative to the isotropic controls even though the chain packing is higher. These shorter relaxation times are in complete contradiction to the findings of the other experiments which show decreased segmental mobility in the oriented samples. It may be that extrapolation over such a large temperature range has introduced significant error. It's also possible that the combined effect of the β_1 and β_2 transitions are not being adequately modeled by a single peak so the extrapolations are worthless. Nevertheless, it is still possible that the results are indeed valid and may have implications that are yet unknown. Assuming this is the case, a few possible scenarios/explanations are now presented which may help to explain this unusual behavior.

The first approach is to try and explain the trend in the frequency data thermodynamically in terms of an activation entropy (as opposed to simply the activation energy). For this, the rate equation is rewritten as

$$f_p = A \exp\left(\frac{\Delta S_a}{k}\right) \exp\left(-\frac{\Delta H_a}{kT}\right) \qquad (4.4\text{-}14)$$

where ΔS_a and ΔH_a are the activation entropy and enthalpy respectively. The activation enthalpy ΔH_a is the same as E_a in Equation (4.3-4). What differs is the activation entropy which has an effect on the front factor $A\exp(\Delta S_a/k)$. This front factor can be obtained experimentally by extrapolating f_p to infinite temperatures. Since it was shown earlier that f_p increases with f at high temperatures, then this would indicate that ΔS_a must also be increasing (assuming that A remains constant). Is this physically meaningful? If the activated state entropy S* is assumed to be constant, then ΔS_a, which equals (S*- S), should increase since the base configurational entropy S, is decreasing due to stretching. Therefore this trend of increasing ΔS_a is in qualitative agreement with the data. On a

similar note, it is also interesting how the unaged activation energy in Figure 4.3-18 seems to correlate with the hole formation entropy in Figure 4.4-5. Although maybe just a coincidence, it is possible that this correlation is meaningful since the entropy barrier to hole formation is expected to be a function of localized chain mobility.

A more mechanistic explanation for the unusual trends in Figure 4.3-17 may arise from the fact that orientation and thermal shrinkage alter the internal stress state of the polymer. An oriented polymer will see higher chain tension but this force will depend on temperature. This is because chain tension is entropic in nature and requires chain movement in order to exist. As temperature increases, there is more motion of the polymer chains which leads to greater chain tension. This would cause an increase in the effective spring constant k_s and the tanδ peak frequency which could help to explain the reversal in the DMS data. It may also be the reason for the enhanced relaxation strengths observed in the oriented samples since the chain tension might provide enough of an strain energy boost so that otherwise immobile segments can undergo relaxation.

Another mechanistic explanation involves the fact that the β transition can be resolved into two distinguishable sub-transitions as described earlier. Because the experimentally determined values for E_a are in the vicinity of 45-50 kJ/mol at $f = 0$, it is conjectured that one is predominantly measuring β_1. Referring back to the discussion on relaxation mechanisms, the higher temperature of the two β peaks, β_1 (-80°C at 0.01 Hz), has been associated with the movement of strongly dipolar carbonate groups which are restricted by the phenyl groups.[10,12,13] This is interesting since Fen[38] showed by a molecular mechanics approach that the bisphenol moiety more readily orients in the stretch direction as compared with the carbonyl moiety. The orientation function for the bisphenol moiety increased linearly with strain whereas the orientation function for the carbonyl unit plateaued at a strain of 0.2 to 0.3 due to its enhanced mobility. This difference in orientation behavior may be another possible cause for the increase in E_a with orientation

and may also connected with the finding that (MD) relaxation strength is independent of the degree of orientation.

4.5 Conclusions

The compilation of data for unaged, oriented polycarbonate indicates an unusual, transitional behavior which occurs at low *f* followed by a steady change in properties upon further stretching. Surprisingly, the changes that occur with increasing *f* in the unaged film are very similar to the changes observed in isotropic samples during physical aging—i.e. a decrease in free volume, a decrease in enthalpy, an increase in yield stress, etc. One might wonder if the molecular mechanisms responsible are connected in any way. The principle observations are summarized as follows:

1. Upon initial stretching, their is actually a slight decrease in density. This is believed to be due to the standard "Poisson effect" which occurs in most materials. The polymer dilates because the Poisson's ratio is less than the incompressible limit of 1/2. This would continue if it were not for the competing effect in No. 2 below.

2. As stretching is increased further, the chains begin to pack better due to increased alignment. Free volume is reduced as density increases. This causes an upturn in the density-*f* curve. The hole energy increases with *f*, even though free volume is decreasing, and this change correlates with changes in T_g. The resulting increase in conformer size indicates an effective stiffening of the chain and a reduction in localized segmental mobility.

3. Following a trend similar to the density, internal energy decreases with increasing orientation at high values of *f*. The decrease in internal energy/enthalpy is found to be a linear function of the density and is direct result of the change in volume. This reason for this drop in energy is believed to be due to either a decrease in interatomic distance and/or a strain induced changes in the rotational isomeric state although the latter would have to be accompanied by a volume change.

4. Mechanical energy-at-yield is found to correlate directly with the recovered enthalpy. It is believed that this energy difference is the extra energy required to break up the ordered "structure" which forms in the oriented samples. This "structure" may be related either to chain packing, rotational conformations, free volume or cooperative domain size.

5. The act of orientation and molecular alignment somehow alters the relaxation environment for the α' and β-transitions causing the MD activation energy to increase with increasing *f*. This increased barrier to motion also correlates with the decreased segmental mobility predicted by the T_g, ΔC_p and conformer molecular weight data. Interestingly, even though the mobility appears to be reduced in the oriented samples, the number of conformers/segments participating in the relaxations (as determined from the area under the β transition DMS curve) is increased. This would help to explain the enhanced volume relaxation and physical aging rates observed in Chapter 3.0. The TD relaxation strength for the oriented samples, while also larger than the isotropic control, is less than the MD value. This directional dependence of relaxation strength follows the same trend as the linear relaxation rate data and is believed to be due to the anisotropic free volume distribution. As with the physical aging rate data, the increase in the number of relaxing segments is independent of *f* and only depends on whether or not the sample is oriented. It follows that the act of stretching somehow "activates" the segments into a higher energy state making them more likely to undergo relaxation. A number of theories were discussed which may help to explain this unusual relaxation behavior.

6. It is theorized that larger conformers require more localized free volume in order to rotate, thus causing their volume sensitivity to be lower relative to a smaller conformer. The fact that orientation increases the effective conformer size implies that oriented samples should have a lower volume sensitivity, as was found experimentally. Obviously, more work is needed to verify the accuracy of this theory.

4.6 References

1 M.R. Tant and G. L. Wilkes, *Polym. Engr. Sci. 21,* 874 (1981).

2 L.C.E. Struik, *Physical Aging in Amorphous Polymers and Other Materials,* Elsevier, New York, 1978.

3 I. M. Hodge, *J. Non-Crystalline Solids 169,* 211 (1994).

4 G. B. McKenna, *Comprehensive Polymer Science, Vol 2. Polymer Properties,* C. Booth and C. Price, Eds. Pergamon, Oxford, 1990.

5 G. L. Wilkes, "Rheooptical Properties," in *Encyclopedia of Polymer Science and Engineering, Vol 14.,* John Wiley and Sons, New York, 542, 1983.

6 R. S. Stein and G. L. Wilkes, Physico-Chemical Approaches to the Measurement of Anisotropy," in *Structure and Properties of Oriented Polymers,* I. M. Ward, Ed., John Wiley and Sons, New York, 57, 1975.

7 H. J. Biangardi, "Bestimmung der Orientierung und Molekularen Ordnung in Polymeren", *Kunststoff Forschung 1,* H. Kaufer, Ed., Tecn Un. Berlin, 1980.

8 M. Pietralla, H. R. Schubach, H. R. Dettenmaier and B. Heise, *Prog. Colloid Polymer Sci. 71,* 125 (1985).

9 L. C. E. Struik, *Internal Stresses, Dimensional Instabilities and Molecular Orientations in Plastics,* John Wiley and Sons, New York, (1974).

10 D. C. Watts and E. P. Perry, *Polymer 19,* 248 (1978).

11 L. J. Onsager, *J. Am. Chem. Soc. 58,* 1486 (1936).

12 G. Locati and A. V. Tobolsky, *Adv. Mol. Relaxation Processes 1,* 375 (1970).

13 Y. Aoki and J. O. Brittain, *J. Polym. Sci. (A-2), 14,* 1297 (1974).

14 R. A. Davenport and A. J. Manuel, *Polymer 18,* 557 (1977).

15 P.L. Lee, *et al., Macromolecules 28,* 2476 (1995).

16 K. H. Illers and H. Breuer, *J. Colloid Sci. 18,* 1 (1963).

17 *Polymer Handbook,* J. Brandrup and E. H. Immagut, Eds., John Wiley and Sons, New York, 1975.

18 E. Ito, K. Sawamura, and S. Saito, *Colloid and Polymer Sci. 253,* 480 (1975).

19 D. W. Phillips, A. M. North and R. A. Pethrick, *J. Appl. Polym. Sci. 21,* 1859 (1977).

20 E. Ito and T. Hatakeyama, *J. Poly. Sci., Polym. Phys. Ed. 13,* 2313 (1975).

[21] L. C. E. Struik, *Internal Stresses, Dimensional Instabilities and Molecular Orientations in Plastics,* John Wiley and Sons, New York, 411, 1990.

[22] Y. K. Godovsky, "Deformation Calorimetry of Oriented Polymers," in *Oriented Polymer Materials,* S. Fakirov Ed., 184, 1996.

[23] B. Wunderlich, *Thermal Analysis,* Academic Press, Boston, 1990.

[24] S. Matsuoka, *Relaxation Phenomena in Polymers,* Hanser, New York, 1992.

[25] A. C. Lunn and I. V. Yannas, *J. Polym. Sci, Polymer Physics Ed. 10, 2189 (1972).*

[26] E. A. DiMarzio, *J. Res. Natl. Bur. Stand., Sect. A, 68A,*611 (1964).

[27] G. Kanig, *Kolloid-Z. u Z. Polym. 233,* 54 (1969).

[28] C. W. Bunn, *J. Polym. Sci. 16,* 323 (1955).

[29] Y. Abe and P. J. Flory, *J. Chem. Phys. 52,* 2814 (1970).

[30] A. D. Williams and P. J. Flory, *J. Poly. Sci. A-2, 6,* 1945 (1968).

[31] R. Simha and R. F. Boyer, *J. Chem. Phys. 37,* 1003 (1962).

[32] J. J. Aklonis and W. J. MacKnight, *Introduction to Polymer Viscoelasticity,* John Wiley and Sons, New York, 69, 1983.

[33] L. R. G. Treloar, *The Physics of Rubber Elasticity,* Clarendon Press, Oxford, 1958.

[34] J. J. Aklonis and W. J. MacKnight, *Introduction to Polymer Viscoelasticity,* John Wiley and Sons, New York, 102-108, 1983.

[35] D. W. Van Krevelin, *Properties of Polymers: Their Estimation and Correlation with Chemical Structure,* Elsevier, Amsterdam (1976).

[36] R. N. Haward, *et. al., Colloid Polym. Sci. 258,* 643 (1980).

[37] P. B Bowden, "The Yield Behavior of Glassy Polymers" in *The Physics of Glassy Polymers,* R. N. Hayward, Ed. John Wiley and Sons, 1973.

[38] C. F. Fen, *Macromolecules 28,* 5215 (1995).

[39] D. C. Watts and E. P. Perry, *Polymer 19, 248 (1978).*

5.0 PERMEABILITY AND POSITRON ANNIHILATION STUDIES OF UNAGED UNIAXIALLY HOT-DRAWN BISPHENOL-A POLYCARBONATE

5.1 Introduction

Orientation is an important aspect of polymer processing. It can be introduced intentionally to enhance various physical properties as is the case with film blowing, tentering, or blow molding. [1] Or, it may be incidental (and often unwanted) to the process as with residual stresses in injection molded and extruded parts. Because of its prevalence in commercially produced plastic articles, it is important to understand how this orientation affects molecular structure and properties. Although it is clear that orientation can significantly alter certain macroscopic properties—most notably the stiffness—it is somewhat uncertain how orientation affects molecular scale relaxation processes and the corresponding molecular mobility.

Of particular interest to this study is how orientation affects relaxation behavior and mobility in the glassy state. An important characteristic of glasses is that they can undergo time-dependent changes in many physical properties upon cooling through T_g via a process known as physical aging. [2,3,4,5,6] These changes occur because the glassy polymer is not at equilibrium, but is moving, albeit very slowly, toward equilibrium. How fast it approaches equilibrium is determined by the molecular mobility. Some examples of aging-induced property changes include time-dependent loss of ductility, gradual densification, changes in barrier properties, changes in dielectric properties, etc. If not accounted for during the design process, these time dependent property changes can often lead to catastrophic failure.

In Chapter 3.0, it was shown that orientation significantly enhances the rate of volume relaxation (a form of physical aging) in both polycarbonate and atactic polystyrene. In order to further understand why this aging enhancement has occurred, it is important to

determine how orientation affects both the molecular state and mobility of the polymer. Thermodynamic and dynamic mechanical data from Chapter 4.0 indicate that localized segmental mobility decreases with orientation, however the concentration of actively relaxing segments increases. The latter outweighs the former causing the apparent "enhanced mobility" during physical aging for the oriented samples. It is still uncertain how free volume changes correlate with the mobility changes, nor is it clear what causes the increase in relaxation strength. By gaining a better understanding of the free volume distribution and how it changes with orientation, it is hoped that the exact mechanism for the enhanced aging can be better understood. To accomplish this, Positron Annihilation Lifetime Spectroscopy (PALS) has been applied to samples of hot drawn (i.e. stretched above T_g) bisphenol-A polycarbonate (PC). PALS is is one of the few available techniques which can give a quantitative estimate of the free volume. Polystyrene was not included in this study because of findings by Kasbekar[7] that changes in the PALS parameters (in PS) were due to irradiation from the positron source, and not due to changes in free volume. As a complement to the PALS technique, permeability/diffusion measurements were also performed since they too are sensitive to free volume changes and molecular mobility. Finally, some preliminary solid state NMR findings regarding localized chain mobility are also reported at the end of this chapter.

Although the main interest is with aging behavior, *this study focuses primarily on unaged samples*. The first objective is to understand how orientation affects the fundamental molecular structure in the unaged state from which, it is hoped, that the aging behavior can be predicted. A second objective is to further develop both PALS and permeability measurements as viable probes for measuring free volume in oriented samples. Some work has already been performed in which PALS and permeability measurements were made on the oriented samples as a function of aging time. Unfortunately, the data exhibited considerable scatter and will only briefly be mentioned here.

5.1.1 Quantifying the Oriented State in Polymers

For uniaxially oriented, single phase systems, the Herman's orientation function f is defined as[8]

$$f = \frac{3 < \cos^2 \theta > -1}{2} \tag{5.1-1}$$

where θ is the angle between the stretch direction (or machine direction MD) and the chain axis. The angle brackets denote an average over all chains in the system. The orientation function will equal zero for an unoriented system, one in the case of perfect uniaxial orientation, and -1/2 for perfect orientation in the transverse direction (TD). These cases correspond to average values for θ of 54.7°, 0°, and 90° respectively.

The orientation function f can be determined experimentally for single component systems from birefringence measurements,

$$f = \frac{\Delta}{\Delta^o} \tag{5.1-2}$$

Here Δ is the birefringence (i.e. n_{md}-n_{td} where n is the refractive index and the subscripts refer to the material direction) and Δ° is the intrinsic birefringence (i.e. the birefringence for a perfectly oriented chain). The intrinsic birefringence Δ° for polycarbonate was determined to be 0.16 by correlating the birefringence measurements with sonic modulus[9] measurements.

Unlike their crystalline counterparts, purely amorphous polymers rarely show orientation functions above 0.2 to 0.3 (hot drawing). To achieve significant chain alignment during stretching, the amorphous chains must have sufficient mobility to reorient during stretching while, at the same time, have certain points along the chain anchored at various "junction" sites so that the orientation is preserved. Entanglements in an amorphous polymer can serve as the network junctions; however, they also tend to inhibit mobility, thus limiting the chain alignment. Increasing the stretch temperature can enhance chain mobility but it also has the detrimental side effect of reducing the

entanglement effectiveness. Thus, disentangling at high temperatures allows the chains to quickly relax back to the unstretched state even though high sample stretch ratios can be achieved. One exception to this is strain-induced crystallization where crystalline, "network junctions" form in situ (particularly at higher stretch temperatures). These crystalline regions are preferentially aligned in the stretch direction during formation which also helps to anchor the amorphous chains in their highly oriented state.

5.1.2 PALS Measurement Technique

The details behind Positron Annhilation Lifetime Spectroscopy (PALS) measurement in polymers have been outlined by Zipper and Hill[10,11] and Jean.[12] The PALS technique has emerged in the past several years as a valuable nondestructive probe of free volume in polymers due to the localization of the positron species orthoPositronium (oPs) in free volume cavities which range in radius from ca. 0.2 nm to 0.4 nm. This range of cavity radii compares well to non-bonded interatomic distances in polymers and molecular radii of diffusing substances.

The PALS technique typically gives three lifetime components in polymers: τ_1 attributed to paraPositronium (p-Ps) self annihilation, τ_2 attributed to free positron and positron-molecular species annihilation, and τ_3 attributed to o-Ps pickoff annihilation. OrthoPositronium pickoff annihilation is a quenching process wherein the positron in o-Ps, which is localized in the free volume cavity, annihihilates with an electron from the surrounding cavity wall. Each of the τ_i lifetimes above has a corresponding intensity, I_i, indicative of the relative number of annihilations taking place with a particular lifetime. The sum of the I_i's is arbitrarily set to 100%.

It is the third component (τ_3, I_3) that is of interest in polymer work due to its free volume dependence. The mean free volume cavity radius is related to τ_3 because it gives an indication of the local electron density at the oPs annihilation sites. These sites are free volume cavities located between chains and at the chain ends. As these free volume sites become smaller, the local electron density seen by the o-Ps increases and the o-Ps lifetime

τ_3 shortens. In molecular solids, in the absence of chemical inhibition of o-Ps formation, a decrease in the o-Ps pickoff component intensity, I_3, can be interpreted as a decrease in the number of o-Ps annihilation sites (decrease in relative free volume concentration).

The PALS analysis gives parameters indicative of the mean size and relative number of free volume cavities probed by o-Ps, thus the PALS free volume probe can be used to measure a particular fraction of the total static and dynamic free volume. Nakanishi and coworkers[13] have developed a semi-empirical model relating τ_3 to the mean free volume cavity radius, R,

$$\tau_3 = \frac{1}{2}\left[1 - \frac{R}{R + \Delta R} + \frac{1}{2\pi}\sin\left(\frac{2\pi R}{R + \Delta R}\right)\right]^{-1} \qquad (5.1\text{-}3)$$

The parameter ΔR represents an electron layer thickness, assumed to be homogeneous, inside the cavity wall. The value of ΔR is estimated to be 0.166 nm by fitting τ_3 to known vacancy sizes of molecular crystals.[14] Jean and coworkers have also extended the above analysis to obtain a continuous distribution of free volume radii instead of just the mean value.[15]

It is emphasized that the above equation assumes spherical free volume cavities. During orientation, this assumption is expected to be less valid with the cavities most likely being elliptical, or at least anisotropic, in shape. Jean and coworkers[16,17] have determined the eccentricity of the (assumed) elliptical holes in uniaxially cold drawn PEEK using one-dimensional angular correlation (ACAR) spectrometry. The mean ratio of the major axis *a*, to the minor axis *b*, for the elliptical free volume sites was determined to be 2.6 +/- 0.2 for PEEK samples having a stretch ratio of 2.6X (note that their stretch ratio was defined differently as being the ratio of the axial to transverse length after stretching). Jean and coworkers[18] have also shown an *a/b* ratio of 1.65 +/- 0.05 in polycarbonate samples stretched uniaxially to 2X (normal definition for stretch ratio) using 2-D ACAR. The average hole radius in the unoriented control was 2.90 +/- 0.03 Angstroms and for the oriented sample ranged from 2.30 to 3.80 +/- 0.03 Angstroms. The value of *f* for this

sample was 0.19. These polycarbonate samples were stretched using the same procedure as in the present study.

Jean and Shi[16] also showed theoretically that the ratio τ_e/τ_s for a given hole volume—where the subscripts *e* and *s* refer to the elliptical and spherical holes respectively—decreases with increasing eccentricity ε ($\varepsilon = (a^2-b^2)^{1/2}/a$). The relation obtained was[16]

$$\frac{\tau_e}{\tau_s} = (1 + 0.400\varepsilon - 4.16\varepsilon^2 + 2.74\varepsilon^3)(1 + 0.0018a) \qquad (5.1\text{-}4)$$

however the last term with the *a* dependence can often be neglected. This equation is a polynomial best-fit of the results from a more complex eigenvalue problem. Applying (5.1-4) to the PC (f=0.19) data above using $a/2$=3.8 Angstroms and $b/2$=2.3 Angstroms yields a value of 0.79 for ε and a value of 0.065 for τ_e/τ_s. This is a very small ratio and, if accurate, has important implications to the data to be presented later.

5.1.3 Permeability/Diffusion of Gases in Polymers

Permeation and diffusion are significantly affected by the concentration and solubility of the permeant species. For this study, only the case of small, gaseous molecules with low solubilities in the polymer will be considered. If higher concentrations or more active permeants are utilized, then the degree in which the permeant perturbs the internal state of the polymer (i.e. through swelling, plasticization, antiplasticization, etc.) is greatly increased.

Permeation of a species through a polymer film requires multiple steps. First, the permeant must be ad- or absorbed onto one surface of the polymer. Next, it diffuses through the film and finally desorbs into the atmosphere on the other side. If sorption and and desorption occur symmetrically, then the steady-state permeability, *P*, can be related to the apparent solubility coefficient *K*, and the apparent diffusion coefficent *D*, by[19,20]

$$P = KD \qquad (5.1\text{-}5)$$

The solubility, K, is generally concentration dependent (and so is D); however, at low enough concentrations, K becomes approximately concentration independent as per a form of Henry's law.[21] Regardless, the parameters K and D are more accurately termed "apparent" values because of their concentration dependence. This is even more noticeable when higher gas pressures are involved in which case the phenomenon of dual-mode sorption become prevalent.[21]

Maeda and Paul[22] discuss the various parameters and how they relate to different aspects of polymer structure. They point out that K, a thermodynamic parameter, does not vary much from polymer to polymer. For this reason, changes in P can be often be attributed almost solely to changes in D. Peterlin[23] has further suggested that the solubility is directly proportional to the free volume. In contrast, the diffusion coefficient D, is related primarily to the molecular mobility of the system. Interestingly, many theories relate the mobility to the total free volume which should indicate some sort of correlation between K and D although this is rarely seen experimentally. As will be shown in the next section, D can be related to either an activation energy barrier or the free volume depending on which theory is applied.

5.1.3.1 Theories of Diffusion

There are many theories which attempt to explain the diffusion behavior. Some are described in detail by Barker and coworkers[24] and will be discussed here. The first is the (Eyring) transition state theory.[25] This theory assumes that a diffusing molecule is localized in the energy minima of the matrix, while at the same time undergoing rapid thermal vibrations. Occasionally, the diffusant will have sufficient energy to make a jump to a neighboring site. This occurs with an average jump rate Γ. The diffusion coefficient is shown to be

$$D = g\Gamma\lambda^2 \tag{5.1-6}$$

where

$$\Gamma = (kT / h)e^{\Delta S^* / R} e^{-\Delta H^* / RT} \qquad (5.1\text{-}7)$$

The parameter λ is the jump interval, g is a geometrical parameter (2^{nd} order tensor in general which reduces to $g = 1/6$ along the matrix diagonal in the isotropic case), and k and R are the Boltzmann and gas constants respectively. The terms $g\lambda^2(kT/h)exp(\Delta S^*/R)$ can be conveniently lumped together into a front factor D_o. In order for the diffusant to make the jump to the neighboring site, it must overcome an activation enthalpy ΔH^* and activation entropy ΔS^*. These parameters could, in theory, be obtained from statistical mechanics however the calculations would be quite involved, even for an isotropic system. In the oriented state, it is expected that ΔS^* and ΔH^* will be directionally dependent.

Another theory, referred to as the entropy correlation theory, was developed by Barker and coworkers for oriented systems.[24] It assumes that for any process such as orientation which reduces the conformational entropy by an amount ΔS_c, will be accompanied by a equal increase in the activation entropy $\Delta(\Delta S^*)$ (see Equation (5.1-7)). This implies that a certain degree of localized "disordering" is required for a permeant to make a jump to a new location. A highly oriented and structured system will therefore require more rearrangement and thus have a higher entropy barrier. Assuming affine, uniaxial deformation with a stretch ratio of Λ, the conformational entropy change upon stretching is

$$\Delta S_c \approx a_c\left[3 - \Lambda^2 - (2 / \Lambda)\right] \qquad (5.1\text{-}8)$$

where $a_c = \langle r^2 \rangle / 2nl^2$ and r is the end-to-end distance for a chain having n segments with length l. Incorporating this into the diffusion equation yields

$$\ln\left[\frac{D_o(\Lambda)}{D_o(1)}\right] \approx a_c[\Lambda^2 + (2 / \Lambda) - 3] \qquad (5.1\text{-}9)$$

where D_o is the Arrhenius front factor defined previously. It is obtained by extrapolating D versus 1/T data to infinite temperatures. Plotting $\log(D_o)$ versus $[\Lambda^2-(2/\Lambda)-3]$ should produce a straight line with a slope of a_c if the theory is accurate. Tests of the theory by

the authors using oxygen diffusion in various hot-drawn acrylates showed that D_o did indeed increase with stretching in agreement with the theory.[24] It also appears, based on visual inspection of their data, that the activation energy/enthalpy increased slightly with orientation. In contrast, El-Hibri and Paul, applied a similar procedure to oriented PVC and found that both D_o and the activation enthalpy *decreased* with stretching .[33] This is in contradiction to the entropy correlation theory. Interestingly, however, they were still able to obtain a linear correlation between log(D) (the measured diffusion coefficient at one given temperature) and [Λ^2–(2/Λ)–3]. While this still indicates a relationship with the entropy function, the slope of the plot was negative which can not be physically associated with the parameter a_c above. Ito[26] observed a similarly negative slope for CO_2 permeation in polycarbonate.

The last of the theories to be described is the more common free volume theory. The free volume theory assumes that diffusion occurs in and through the free volume sites in a polymer as opposed to across an activated barrier as in the previous theory. One of the most useful free-volume theories for diffusion (and most related to PALS data) is that of Cohen and Turnbull[27] (another is that of Vrentas and Duda which is a modification of the Cohen-Turnbull model and is particularly suited for penetrants with high solubilities[28]). The Cohen-Turnbull theory assumes that a critical free volume hole size v^*, or larger is required for penetrant diffusion, and that diffusion results from the redistribution of free volume such that the penetrant is carried along in a "cage." It takes the general form

$$D = ga^*u \exp\left(\frac{-\gamma v^*}{v_f}\right) \qquad (5.1\text{-}10)$$

where v_f is the average free volume per molecule, γ is an overlap factor (typically close to one) which accounts for multiple permeant molecules trying to enter the same hole, u is a "thermal speed" (having units of length/time), and a^* is the free volume cage diameter. The terms ga^*u and $-\gamma v^*$ are often lumped together into the constants D_o and B respectively.

5.1.3.2 Previous Studies on Oriented Samples

Permeability studies have been performed on oriented samples although few have been directed toward amorphous glasses.[29] Barrie and Platt[30] found that orientation had little effect on either solubility or mobility in a deformed (and externally constrained) natural rubber. Wang and Porter[31] performed one of the most comprehensive studies for amorphous glasses by investigating CO_2 permeation and diffusion in uniaxially oriented atactic polystyrene. Both P and D dropped significantly and monotonically with orientation, however, solubility showed only a slight decrease. With values of f changing from 0 to 0.17, P decreased by 88% and D decreased by 80%. The solubility only dropped by approximately 35% and exhibited more scatter in the data.

Levita and Smith[32] measured P and D in biaxially oriented samples of polystyrene which had a small tensile strain applied. Both parameters increased initially upon application of the strain but decreased over time due to suspected volume recovery. The rate of decrease depended on the strain level and the permeant molecule with small strains showing negligible volume recovery. Using xenon as a permeant at 1.8% strain and 50°C, resulted in decreases in P and D of 13.8 and 11.8% respectively per decade of time. P and D values for CO_2, a much larger permeant, were two to threefold lower than xenon. The authors suggest that these results indicate that the larger free volume holes decrease in size faster than the smaller holes as the volume recovery progresses.

El-Hibri and Paul[33] have performed a comprehensive study of permeation to various gases in uniaxially oriented rigid PVC. This included measuring the effects of draw temperature and above-T_g annealing history on the resulting values of solubility, D and P. Their results also showed a decrease in P, D, and K with orientation however the data was complicated by significant changes in density during annealing/stretching--most likely due to the formation of crystallinity. Crystallinity is known to have a significant impact on permeability which makes it more difficult to analyze purely amorphous orientational effects.

5.1.3.3 Comparison of PALS and Diffusion Studies

PALS data have been successfully compared with diffusion data in a number of papers using the Cohen-Turnbull theory. One question that remains, however, is which of the PALS parameter is best related to v_f, the average free volume per molecule. Kobayashi and coworkers[34] have shown an excellent correlation between log(D) and the inverse of τ_3^3 (i.e. Cohen-Turnbull) for a wide range of polymers. The parameter τ_3^3 is in essence, a measure of the average free volume for a given hole (V_h)--a parameter slightly different than v_f. Presumably, if free volume is responsible for changes in D, then one would expect that both the relative size (τ_3) and number (I_3) would be important.

Okamoto and coworkers[35] have also tested the relationship between V_h and D using the Cohen-Turnbull equation and compared it with the relationship between the fractional free volume, ffv_{pa}, and D where ffv_{pa} is defined as

$$ffv_{pa} = C_1 V_h I_3 = C_2 \tau_3^3 I_3 \qquad (5.1\text{-}11)$$

The subscript "pa" was added to distinguish this measure of fractional free volume obtained from positron annihilation from others to be described later. The scaling constants C_1 and C_2 were added to make the equations exact. The parameter ffv_{pa} is more closely related to v_f than V_h. Nevertheless, Okamoto found that the correlations were slightly better between D and V_h than D and ffv_{pa} although both showed good correlation.

Hill and coworkers[36] have performed permeability studies on blends of PCT and PET while simultaneously conducting PALS measurements. For both oxygen and CO_2 permeants, log(P), τ_3 and I_3 were found to increase approximately linearly with vol% PCT. In contrast, density decreased linearly with wt% PCT. Correlations between P and both V_h and $\tau_3^3 I_3$ showed excellent agreement in both cases.

The fractional free volume can also be calculated using density data and the group contribution method (yielding ffv_{gc}) as performed in the work of Maeda and Paul on blends of polysulfone and poly(phenylene oxide).[22] Their data showed a good correlation

between log(P)--which is approximately log(D) if constant solubility is assumed—and the calculated values of $1/ffv_{gc}$ for a variety of polymers and blends.

Jean and coworkers[37] have shown a linear correlation between ffv_{pa} determined experimentally by PALS and ffv_{gc}, calculated by group contribution methods, for a series of polycarbonate based polymers. Values of D for both O_2 and CO_2 were found to fit ffv_{pa} using a simplified form of the Cohen-Turnbull equation.

5.2 Experimental

Samples of Makrolon 2608 bisphenol-A polycarbonate (Tg= 150°C based on DSC measurements at 20°C/minute heating rate) were stretched uniaxially at 160°C using a T. M. Long film stretcher. The PC had a number average molecular weight M_n =16,500 g/mol obtained from solution viscosity in THF assuming a polydispersity of 2 and applying appropriate correction factors.[38] The crosshead speed for stretching was 12.7 cm/s and the initial gauge length was 10 cm. Samples were typically drawn to stretch ratios of 1.25X, 1.5X, 2X and 2.5X which resulted in orientation functions ranging from 0 to 0.2. After stretching, samples were quenched below T_g with a blast of cold air in order to freeze in orientation. Orientation was determined by way of birefringence measurements using an Abbe refractometer (Na D-line 589.3 nm). For a given sample, the point-to-point variability in f was +/- 0.01. Variability in average f for samples of a given stretch ratio was approximately +/- 0.03 at the higher stretch ratios. The latter was due to fluctuations in temperature, thickness and cooling rate during stretching.

5.2.1 Density Measurement

Densities were measured using a gradient column comprising aqueous solutions of either sodium bromide or potassium bromide and water. Measurements were made at 23°C after the sample was allowed to equilibrate in the column for at least one hour.

5.2.2 Permeability Measurements

Oxygen permeability measurements were performed on 4 inch square films at 23 +/- 0.1 °C and 0% relative humidity using an Oxtran 100[tm] (MOCON) permeability tester. Sample thickness was typically 5 to 10 mils. Samples were allowed to equilibrate in the tester for 24 hours prior to measurement. Upstream oxygen partial pressure was one atmosphere. Downstream consisted of a N_2 carrier gas with trace amounts of H_2 used by the electrochemical detector. Typically 2 to 3 pieces of film were tested for each measurement condition.

In order to determine the diffusion coefficient D, the sample was first treated to an upstream gas flow of pure N_2 for 24 hours. The preconditioning allowed for the removal of any absorbed O_2 in the sample. Next, the upstream gas was switched to pure O_2 and this denoted as time zero. Oxygen transmission was monitored on the downstream side until equilibrium was reached (typically only a few hours). The half-time to steady-state $t_{1/2}$ was then determined and D calculated (assuming Fickian diffusion) as

$$D = \frac{L^2}{7.199 t_{1/2}} \tag{5.2-1}$$

where L is the thickness of the film. Once *P* and *D* have been measured, the solubility coefficient *K* can be determined from Equation (5.1-5). Keep in mind that because K is a calculated value, it encompasses the experimental error from both the P and D measurements and is the least accurate of the three values.

5.2.3 PALS Measurements

PALS measurements were performed by Dr. Anita Hill (CSIRO, Australia) using an automated EG&G Ortec fast-fast coincidence system with a ^{22}Na resolution of 254 psec. The equipment was thermally stabilized to 23 +/- 1.0 °C and also digitally stabilized. Films were stacked parallel to the drawing direction, 5 to 7 films on each side of the $^{22}NaCl$ positron source—a 2mm diameter spot source of 30μCi sandwiched between two

2.54 μm titanium foil sheets—to give a final thickness of 1.2 mm. The source gave a two component best fit (τ_1 = 167 ps, I_1 =99.3%, τ_2 = 700 ps, I_2 =0.97%) to 99.99% pure, annealed, chemically polished aluminum (τ=166 ps). No source correction was used in the analysis of the polymers. Each spectrum contained 30,000 peak counts (approximately one million integrated counts) and took approximately 30 minutes to collect. The spectra could be best modeled as the sum of three decaying exponentials.[39] The shortest lifetime τ_1 was fixed at 0.125 ns characteristic of pPs self annihilation. The third component (τ_3, I_3) is attributed to o-Ps annhilation by pickoff. Only this third component will be reported. Two to five spectra were collected for each sample; the results are the mean values for these spectra. The standard deviations are population standard deviations which ranged from 0.01 - 0.02 ns and 0.12 - 0.35% (absolute %) for τ_3 and I_3 respectively. Conservative values of 0.03 ns and 0.35% are used for error bars in the figures. The PALS results did not vary as a function of contact time with the ^{22}Na source. All measurements were made on samples that had reached a quasi-equilibrium state at room temperature a few months after mechanical and thermal processing.

5.3 Results

Values of f as a function of stretch ratio Λ, are plotted in Figure 5.3-1. The error bars reflect the scatter in f due to differences in temperature and cool down rate during stretching. Room temperature density (ρ) data is shown in Figure 5.3-2 for PC as a function of f. Interestingly, ρ initially decreases slightly, going through a minimum, and then begins to increase with further orientation. This increase in ρ has been seen by other researchers[40,41,42] It is speculated that the process of stretching initially causes a dilation of the material due to the normal Poisson effect. With sufficient molecular alignment, however, the chains begin to pack better which leads to significant densification.

This increase in density should lead to a decrease in free volume. In order to estimate the fractional free volume, ffv_{gc}, one can assume that the unaged, unoriented glass has an

initial occupied volume v_o of 0.694 cc/g based on Bondi's estimate using group contribution methods.[43] If one then defines the total volume as v (where $v = v_o + v_f = 1/\rho$),

$$ffv_{gc} = \frac{v_f}{v} = \frac{v - v_o}{v} = 1 - \rho v_o \qquad (5.3\text{-}1)$$

For a given mass of sample, v_o will remain constant regardless of orientation due to conservation of mass. For the isotropic sample, ffv_{gc} will be equal to 0.17 assuming an isotropic density of 1.1982 g/cc. Values for ffv_{gc} at other values of f are obtained by inserting the corresponding density into Equation (5.3-1) and are plotted in Figure 5.3-3. While this data is rather uninteresting in itself—it is simply the reciprocal of the density data—it will be useful later when correlations are made with the PALS results. It will also be compared with the mobility data (creep/dilatometry) from Chapter 3.0 even though the latter was performed at higher temperatures (90°C). This is because relative differences in free volume for the oriented samples do not change significantly with increasing temperature as long as shrinkage is not significant (little shrinkage occurs below 100°C for PC). This, in turn, follows from the fact that the glassy volume expansion coefficient is approximately independent of f.[44]

5.3.1 Permeability and Diffusion Results

Permeability data for the unaged PC samples are shown as a function of f in Figure 5.3-4. Of interest is the fact that P follows the same trend as the ffv_{gc} data as shown in Figure 5.3-5. Permeabilities normalized to the isotropic value are plotted in Figure 5.3-6 which further serves to illustrate the correlation between free volume and P. Diffusion coefficents along with calculated values for the solubility K are shown in Figure 5.3-7. Values of D, unlike P, are found to decrease monotonically with f. Based on conventional wisdom, this should indicate a decrease in mobility with increasing f although creep and dilatometry data from Chapter 3.0 contradict this finding. On a similar contradictory note, the solubility is found to increase slightly with orientation. This again is surprising since one would expect the decreased density to limit the sites for adsorption.

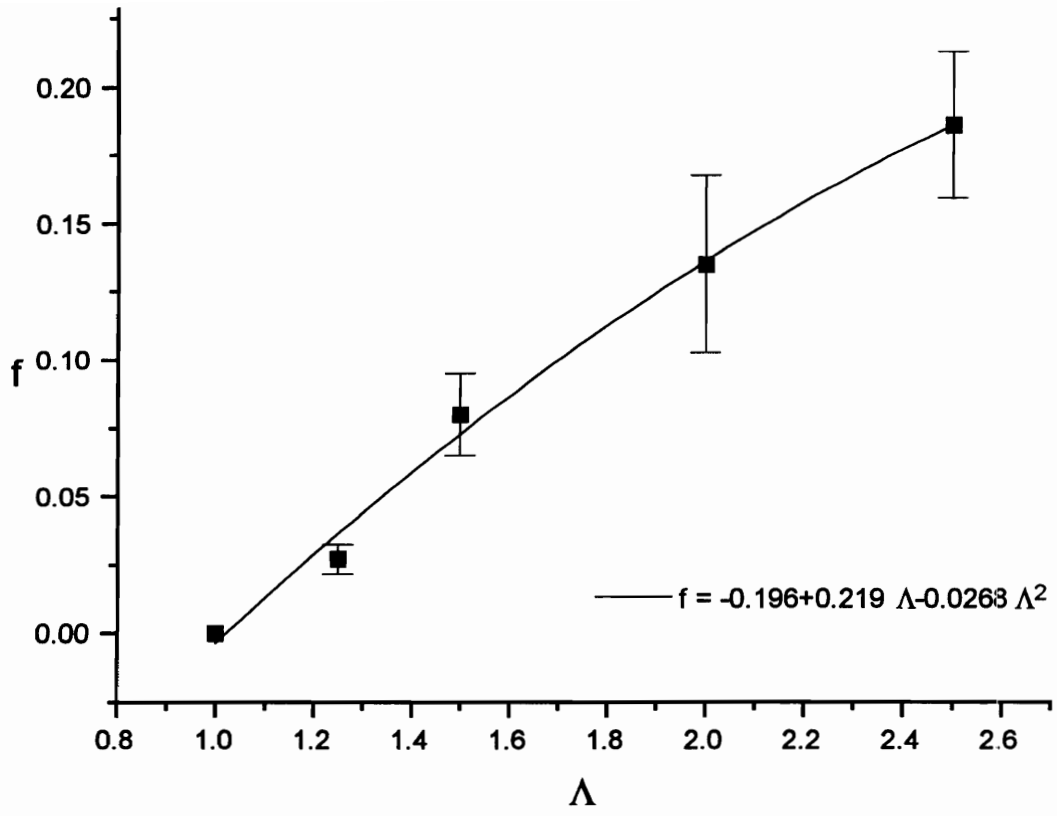

Figure 5.3-1. Orientation function vs. stretch ratio for PC stretched at 160°C .

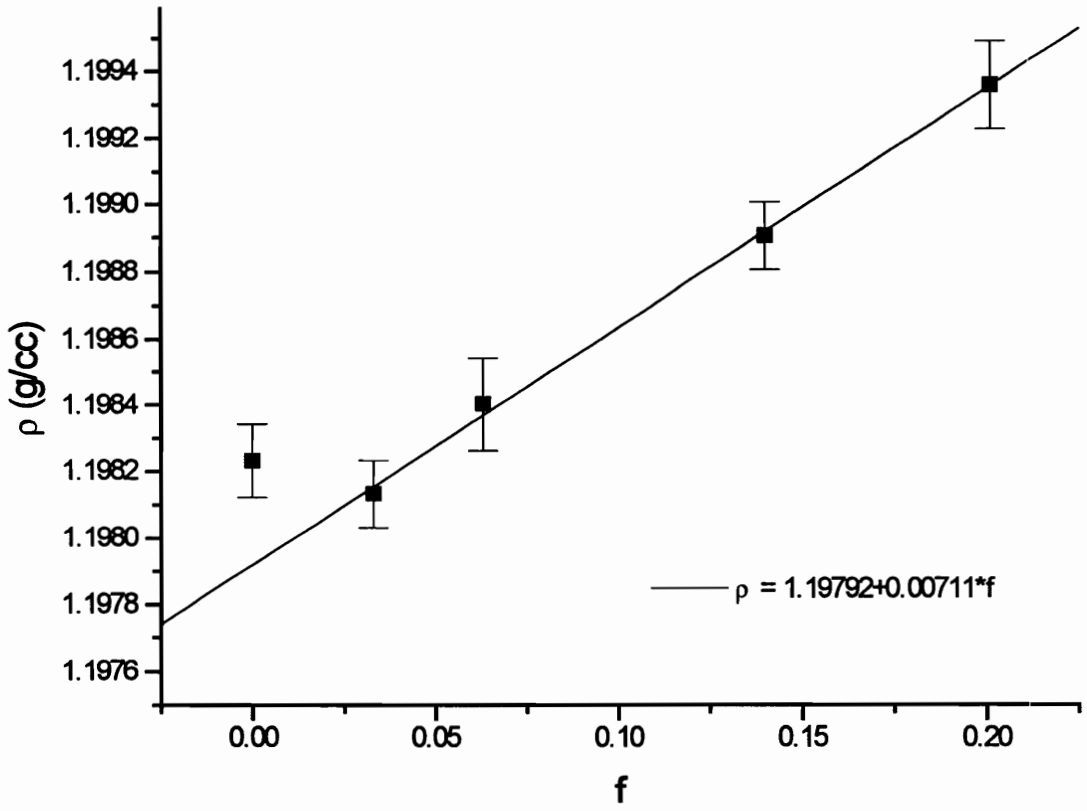

Figure 5.3-2. PC density vs. *f*. Line fit through high *f* points only to illustrate trend in data.

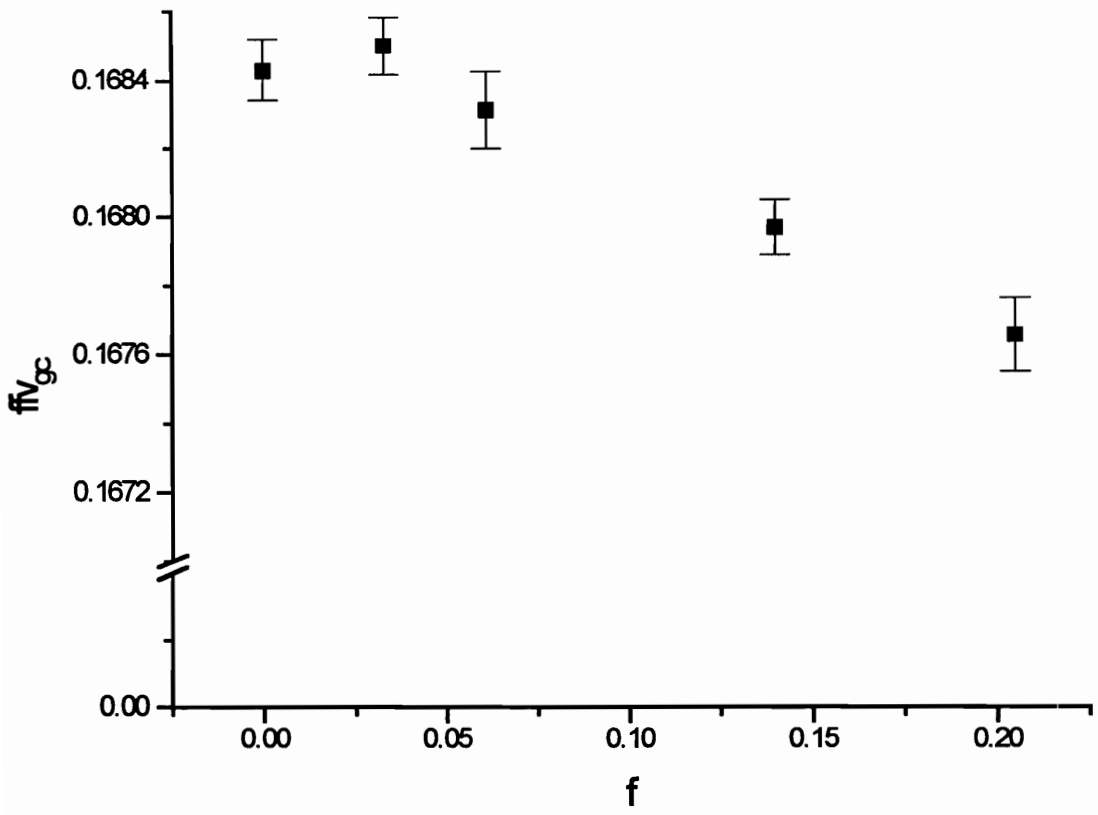

Figure 5.3-3. Fractional free volume (ffv_{gc}) vs. f for unaged PC.

This is also in disagreement with the decrease in solubility seen by other investigators.[31,33] Possible reasons for these discrepancies in the S and D data will be discussed later.

5.3.2 PALS Results

The fundamental PALS results are tabulated in Table 5-1. Values for τ_3 and I_3 are plotted in Figure 5.3-8 as a function of f for the unaged samples. The τ_3 lifetimes show no significant changes with orientation indicating no change in free volume hole size. This also means that, for this study, τ_3^3 is not sufficiently sensitive for use as a measure of free volume. It should be emphasized, however, that the calculations are based on a spherical hole and that orientation most likely produces anisotropic, possibly elliptical voids. Therefore τ_3 may be envisioned as relating to some "effective" spherical hole size. Contrary to the τ_3 results, the I_3 data show a significant drop with f indicating that the number of free volume sites susceptible to the o-Ps probe is decreasing with stretching.

As a measure of the total fractional free volume--as opposed to the hole volume V_h determined from τ_3^3--the parameter $\tau_3^3 I_3$ (related to ffv_{pc} through a scaling constant as per Equation (5.1-11)) was determined and is plotted in Figure 5.3-9. Although the scatter is high, the trend is for a linear decrease in free volume with increasing f. This is compared with ffv_{gc} obtained from density data in Figures 5.3-10 and 11. In Figure 5.3-10, the values of ffv_{gc} and $\tau_3^3 I_3$ are plotted parametrically. Some calculation and extrapolation was required since the data were originally tabulated as a function of f. Except at low values of f, the data show a linear correlation.

In Figure 5.3-10, the free volume functions are plotted together as a function of f. In addition to ffv_{gc} calculated from group contribution methods, the fractional free volume obtained from the WLF method ffv_{wlf}, is also provided.[45] This method assigns the unoriented glassy sample to a fractional free volume of 0.025, the WLF iso-free volume. This yields an occupied volume v_o of 0.814 g/cc based on Equation (5.3-1). Following a similar procedure as before, other values for ffv_{wlf} are determined from the change in density. Note that both measures of ffv along with $\tau_3^3 I_3$ have been normalized with

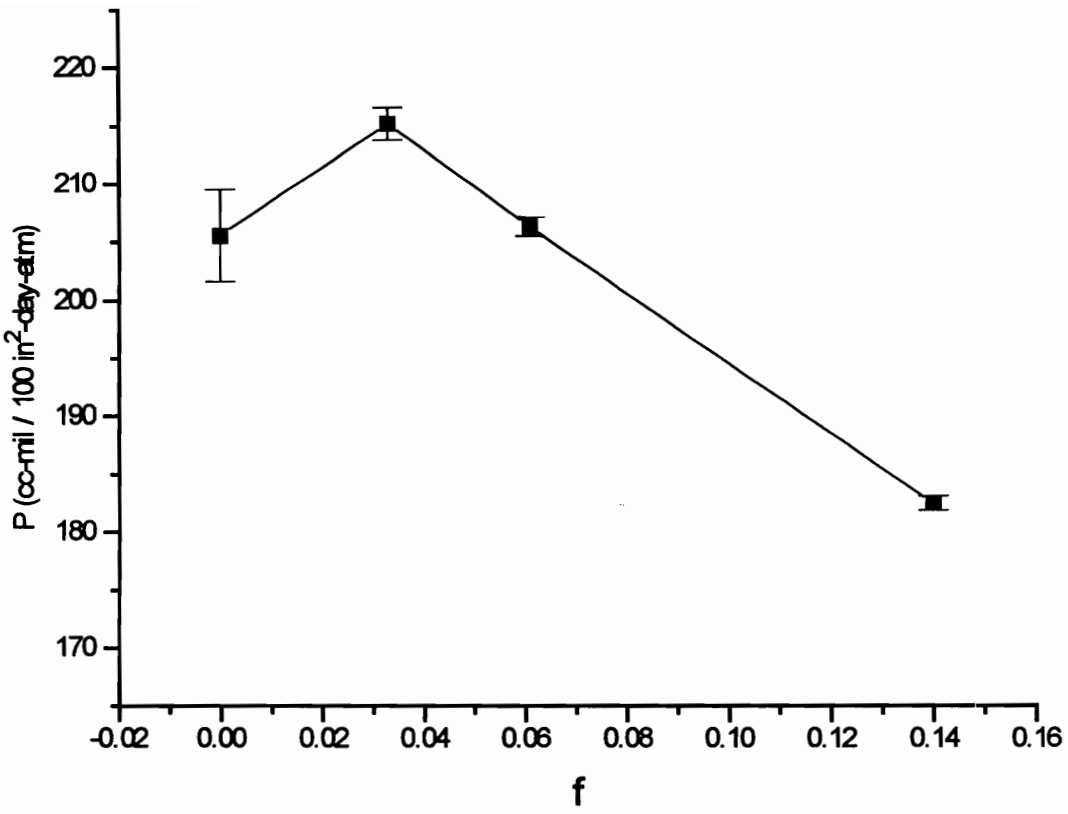

Figure 5.3-4. Permeability vs. f (unaged data at 23C and 0% RH).

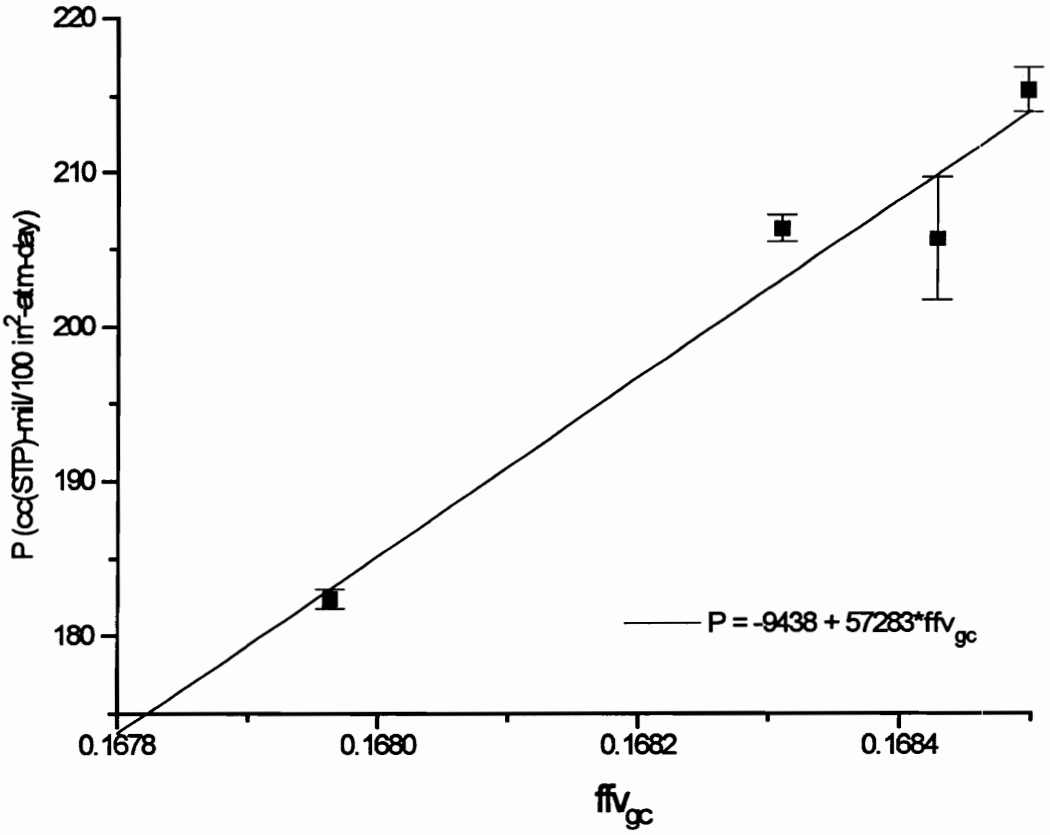

Figure 5.3-5. Permeability vs. ffv_{gc} for unaged PC.

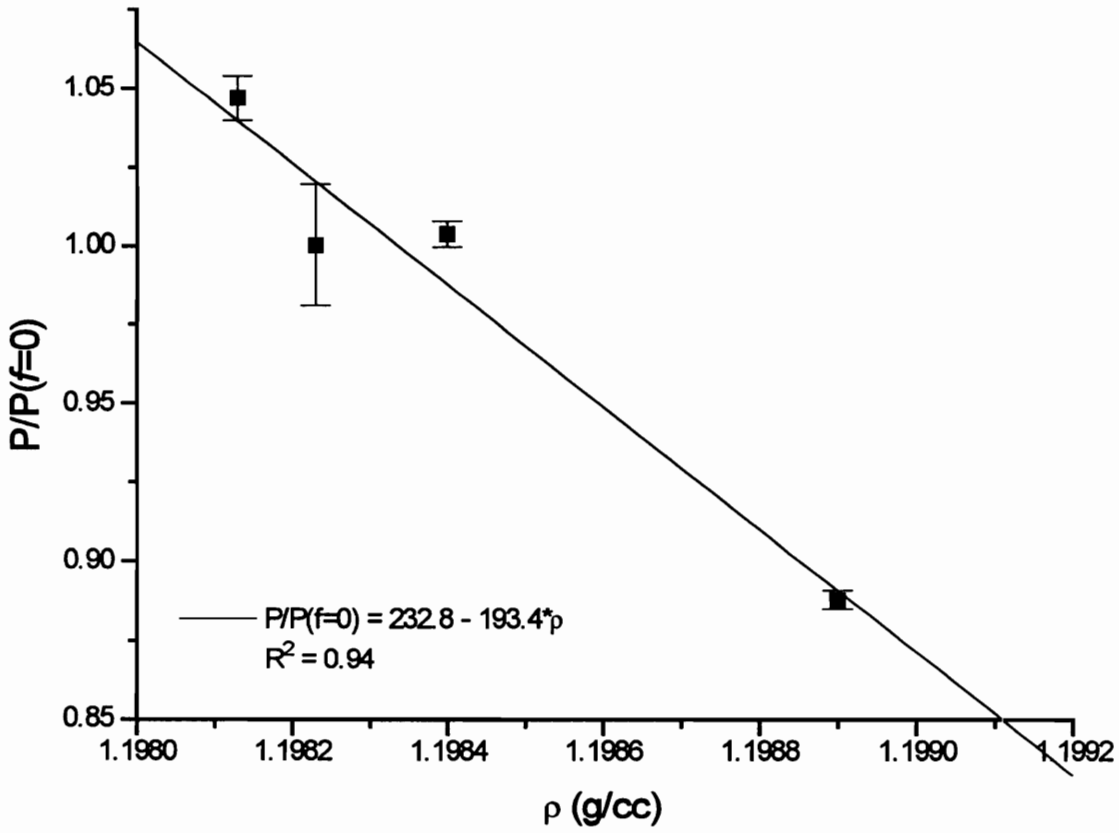

Figure 5.3-6. Normalized P vs. density for PC.

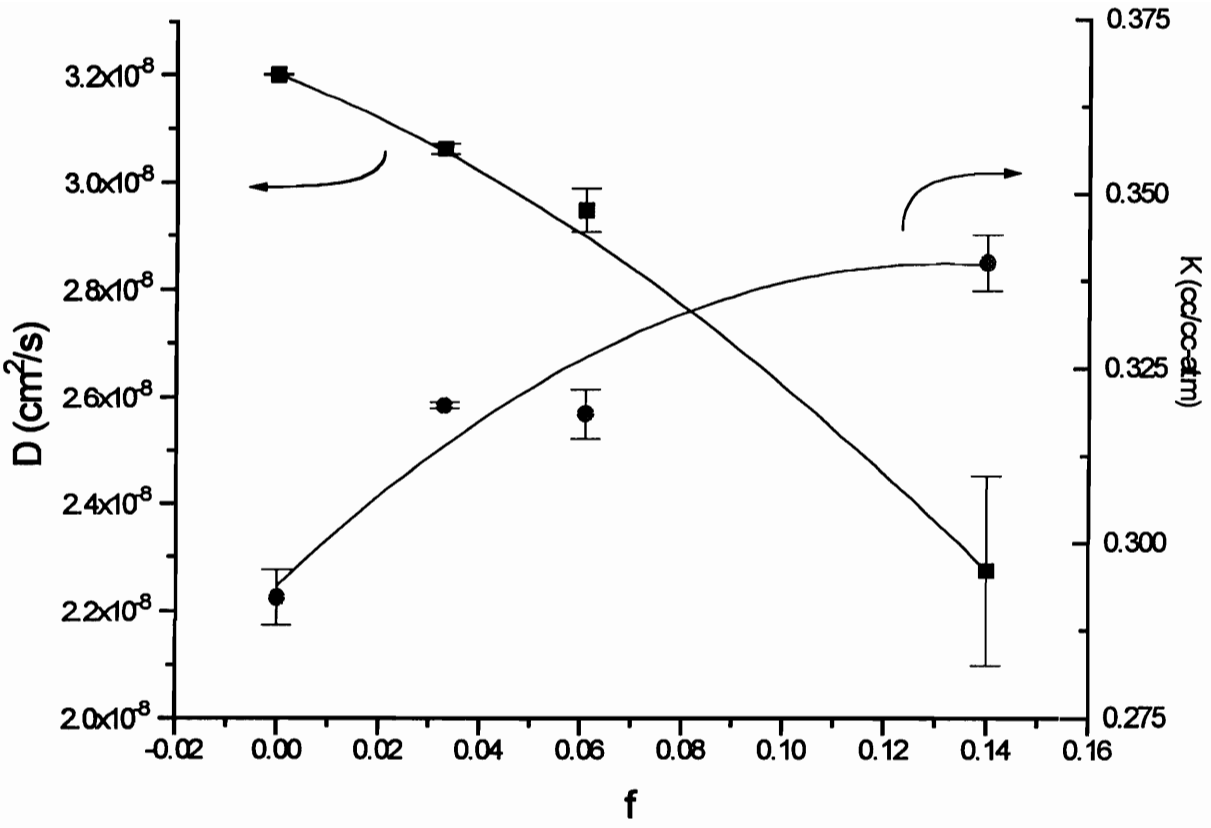

Figure 5.3-7. D and K versus f for unaged PC.

Table 5-1. PALS Parameters for Unaged PC

Draw Ratio	f	τ_3 (ns)	I_3 (%)	$\tau_3^3 * I_3$ (ns^3%)
1	0	1.999	30.376	242.6
1.25	0.024	2.003	29.856	239.9
1.5	0.086	2.005	29.772	239.9
2	0.120	1.994	29.615	234.8
2.5	0.160	1.995	29.536	234.5

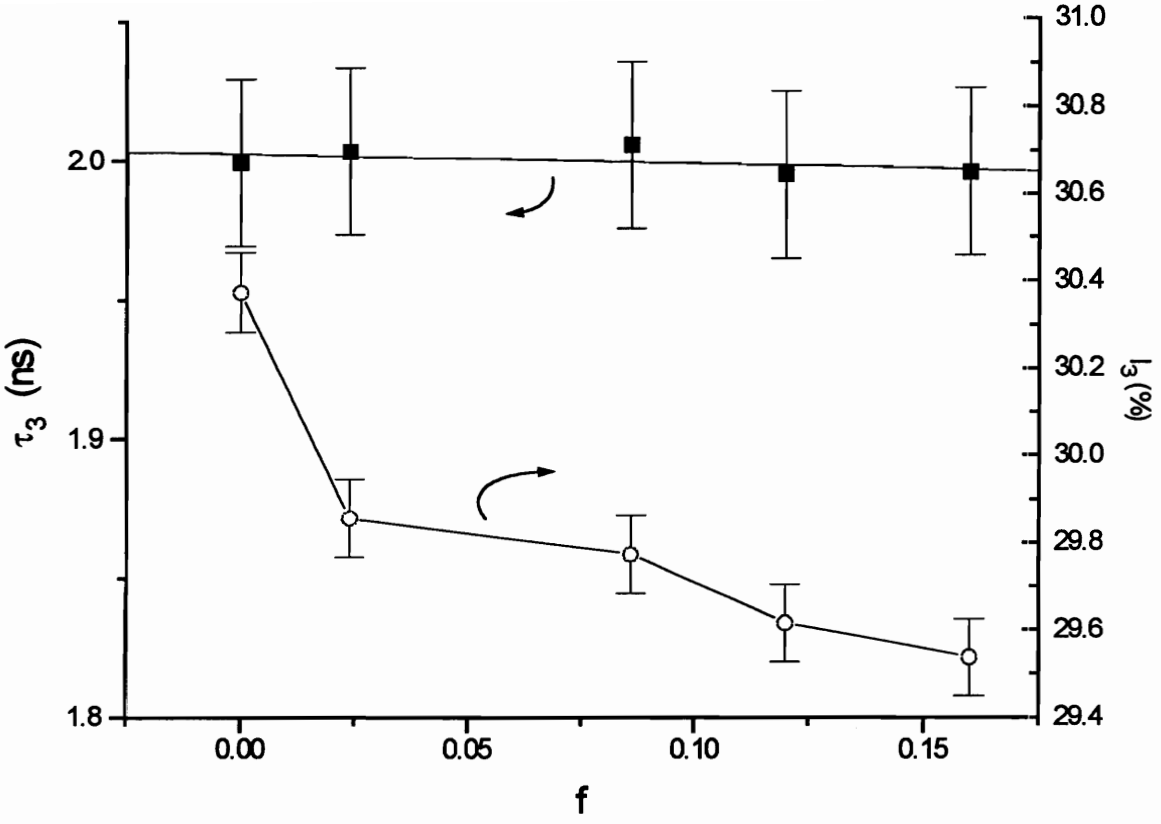

Figure 5.3-8. PALS data as a function of f for unaged PC.

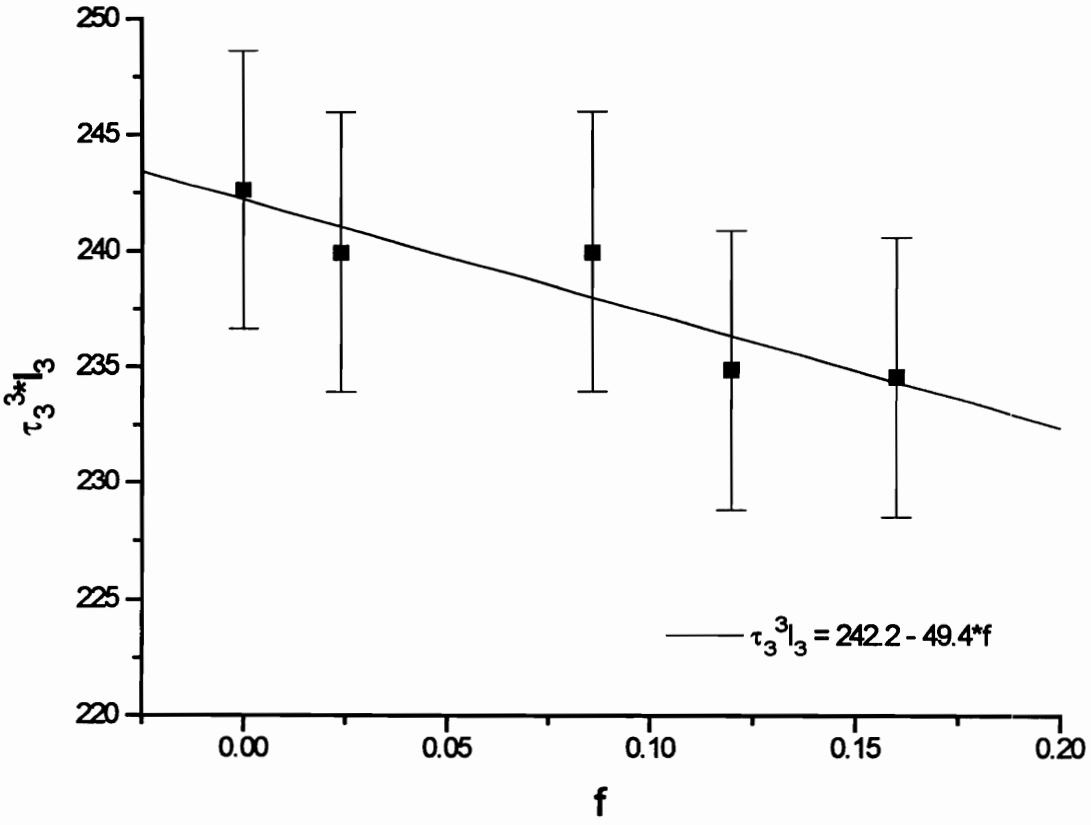

Figure 5.3-9. Effective PALS free volume versus *f* for unaged PC.

respect to the unoriented values. Inspection of the curves shows the same general trend in the data, however ffv_{wlf} is in much better agreement with $\tau_3^3 I_3$. Both decrease approximately 3% upon stretching to an f value of 0.16 (see Table 5-2). In contrast, the parameter ffv_{gc} only shows a decrease of 0.5%. Interestingly, this is close to the decrease observed in τ_3^3, however, the changes in τ_3 were considerably smaller than the error bars which makes this correlation suspect.

5.4 Discussion

Preliminary inspection of the data raises a number of important questions: (a) Which of the free volume functions (ffv_{gc}, ffv_{wlf}, $\tau_3^3 I_3$, τ_3^3) are best at representing the material state as well as correlating with the permeability/diffusion data? (b) How is the orientation affecting the PALS parameters τ_3 and I_3 and their interpretation? (c) Which diffusion theory is the best for describing the oriented systems? and (d) How does orientation affect the mobility and molecular state of the polymer? The last question is obviously the main objective of the study however the second must be answered in order to gain any useful answers from PALS. Each will now be addressed in more detail.

5.4.1.1 Free Volume Functions

There are four fractional free volume functions which have been experimentally determined--the group contribution ffv_{gc}, the WLF free volume ffv_{wlf}, and the PALS based $\tau_3^3 I_3$ and τ_3^3. The parameter τ_3^3 (also referred to as the hole volume V_h), which is widely used in the literature, is of little utility for this study because the magnitude of its change is not statistically significant. Furthermore, although τ_3^3 shows a change at high f approximately equal to that of ffv_{gc} (see Table 5-2), the correlation is not good at low and intermediate values of f.

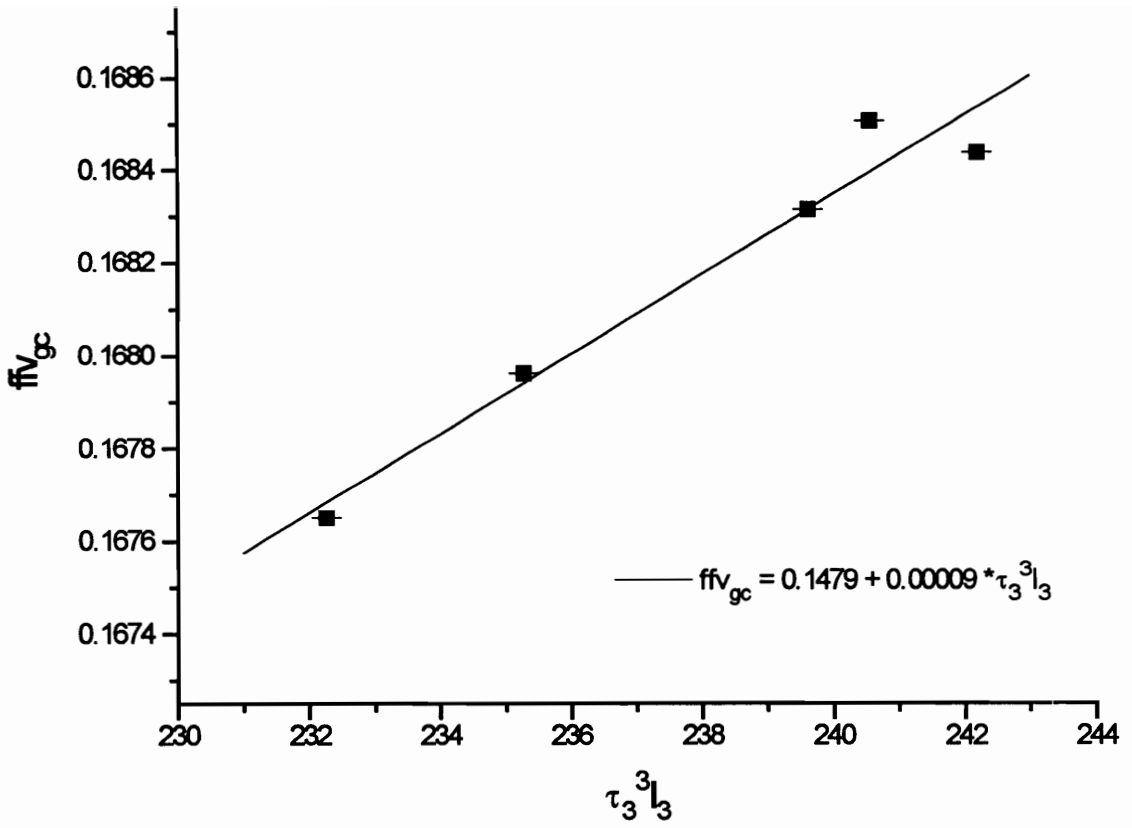

Figure 5.4-10. Correlation between ffv_{gc} and PALS free volume for unaged PC.

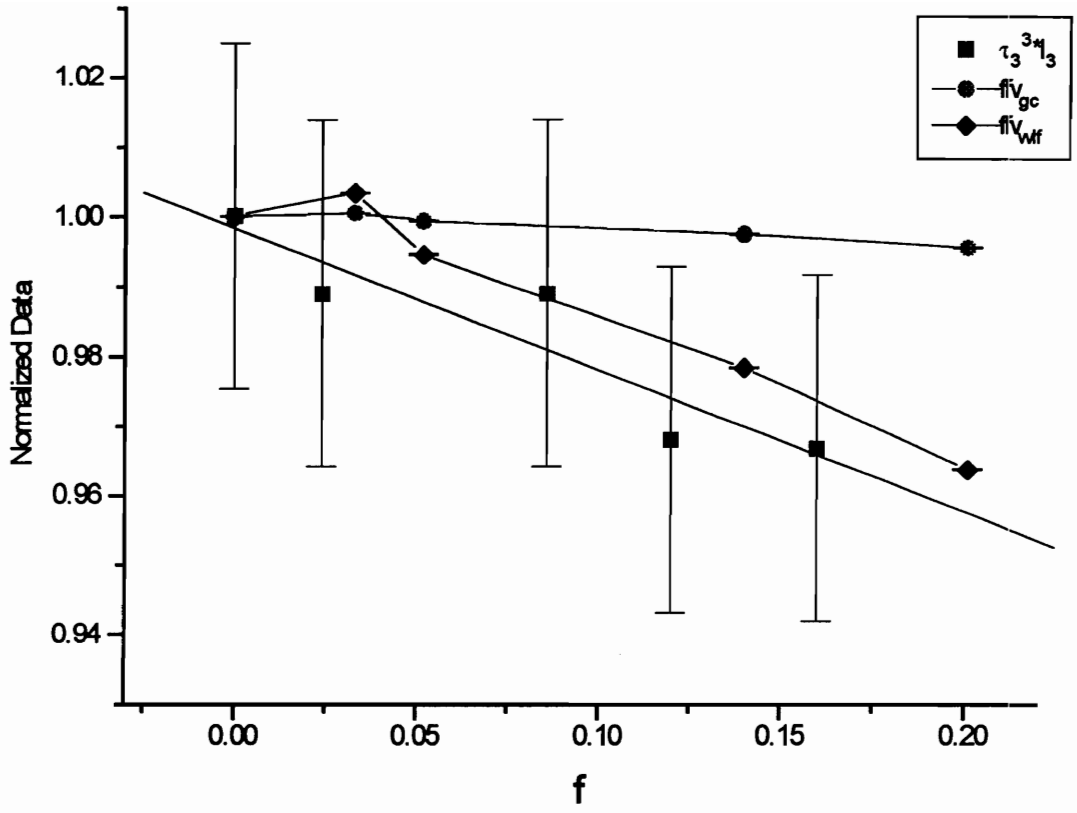

Figure 5.4-11. Normalized free volume measures versus *f* for unaged PC.

Table 5-2. Relative Changes in Parameters for f Changing From 0 to 0.16.

Parameter	% Change
τ_3	-0.2%
I_3	-2.8%
τ_3^3	-0.6%
$\tau_3^3 I_3$	-3.3%
ρ	+0.075%
ffv (group contribution method)	-0.3%
ffv (WLF)	-2.4%
P	-12%
D	-33%
K	+17%

The functions ffv_{gc} and ffv_{wlf} are measures of the static free volume since they both account for all of the void space in the polymer including the very small sites. They account for fluctuations in free volume only in an average sense. The only fundamental difference between the two parameters is in the assumed value for the occupied volume. This means that both undergo the same trends with f however the magnitude of change is much larger with ffv_{wlf} since it starts with a smaller free volume initially.

The PALS based $\tau_3{}^3I_3$ does not sample free volume radii below about 0.1 nm since this is the size of the o-Ps species. This is not necessarily a problem since the O_2 molecule is considerably larger than the o-Ps atom and very small free volume sites are less important to the gas diffusion process. Nevertheless, it is also uncertain how o-Ps interacts with larger holes that are fluctuating rapidly although this dynamic character surely affects the results. As an example, larger holes that open and close in a time frame that is shorter than the average o-Ps lifetime may not be adequately detected by PALS. This would obviously skew the free volume distribution relative to that obtained from density measurements.

Referring back to Figures 5.3-10 and 11, it is apparent that all three measures of free volume change in a similar manner with f, the only difference being a slight jump in ffv_{gc} and ffv_{wlf} at low f. This may indicate that the initial drop in density with stretching is due to the formation or enhancement of very small free volume sites which are not detectable by the positron probe. Another possibility is that these holes are, in fact, not small, but are opening and closing at a rate faster than the PALS probe is able to detect as discussed previously. Another interesting feature is that the P data is also sensitive to this "bump" at low f whereas the diffusivity is not. An understanding of this discrepancy in the transport data may help to explain the difference between the PALS and density-based measures of free volume.

5.4.1.2 Effects of Orientation on PALS Data

The measured changes seen with PALS for oriented systems are real. The uncertainty lies in interpretation of the data. What is unclear is how to model the modified wave functions for the positrons and electrons (already grossly simplified for the isotropic case) so that they can be related to the free volume in the oriented sample. One approach is to assume an elliptical hole geometry for the free volume site for which we can apply Jean and Shi's theory[16] described earlier. Utilizing Equation (5.1-4) and neglecting the polynomial on the far right, one sees that the ratio of $\tau_e/\ \tau_s$ decreases with increasing eccentricity ε (ε is zero for spherical holes but increases with more elliptical holes). The ratio $\tau_e/\ \tau_s$ was already shown earlier to have a value of 0.065 for PC having a value of f equal to 0.19. The value τ_e is the same as the measured value of τ_3 whereas τ_s is what the measured value would be if the hole were spherical and had the same free volume. Since the ratio of $\tau_e/\ \tau_s$ is less than one and decreases with increasing stretch ratio--and the measured τ_e (or τ_3) remains constant with increasing stretch ratio--τ_s and the average hole volume V_h are therefore predicted to increase monotonically with increasing orientation. Intuitively, this seems impossible. The free volume based solely on τ_3^3 would increase significantly with increasing f which is in complete disagreement with both the D and density data. The free volume based on $\tau_3^3 I_3$, however, would be partially offset by the stretch induced decrease in I_3 although this would still not be enough to make the results reasonable.

While it is uncertain whether or not the theory is providing an adequate picture of the oPs decay, it is clear that τ_3^3 is a poor indicator of free volume in the oriented systems. It is also unknown why τ_3^3 provides such a poor measure in this study and such a good measure in the studies described earlier. One hypothesis is that the previous studies involved PALS measurements on different polymers and compositions where τ_3 changed significantly. For this study, the changes were small relative to the error bars so it is possible that PALS lacks the necessary sensitivity.

Although it has already been shown by 2-D ACAR that the anisotropy in free volume hole geometry exists,[18] it is possible that its effect on the PALS parameters is smaller than predicted by Equation (5.1-4). The fact that ffv_{gc} and ffv_{wlf} both follow the same general trend as $\tau_3{}^3I_3$ in Figures 5.3-10 and 11 is one indicator that this may be true. For one reason, the degree of orientation is relatively low. Keep in mind that the maximum f of *ca.* 0.2 corresponds to an average angle θ of only 47° based on Equation (5.1-1). This is far from having perfect orientation and implies that most of the chain segments are only partially aligned in the stretch direction. As a result, it is also possible that free volume sites at different locations, relative to a given chain, may be affected *unequally* by the stretching process. Therefore, some holes might be expected to become more elliptical whereas others will remain nearly isotropic. This would produce a distribution in the hole eccentricity. It is hypothesized that the o-PS probe would more readily sample the nearly spherical holes rather than the highly eccentric ones. This also follows from Jean and Shi's model[16] described earlier where τ_3 decreased significantly with increasing eccentricity. Assuming that a distribution in eccentricity does exist, then the highly eccentric holes would not be adequately sampled by the o-Ps and may even be undetectable by the PALS measurement (particularly in the case of the smaller, highly eccentric holes). The number of highly eccentric, undetectable holes should increase with stretching which might explain the slight drop in I_3 with orientation. Further support for this hypothesis may be provided by some preliminary data (although not discussed in detail here) which shows that I_3 increases with annealing at 90°C in the oriented samples (τ_3 remained approximately constant). It is possible that aging and low-level shrinkage are returning the elliptical holes to a more isotropic shape making them more detectable by the o-Ps probe. Dilatometric data have already shown that free volume decreases significantly with aging (see Chapter 3.0) but this preliminary PALS data would (incorrectly) indicate an increase in ffv with aging.

The fact that τ_3 does not change with f is still puzzling although it may also be due to the distribution in eccentricity. If it turns out that the smaller holes are preferentially

becoming more eccentric relative to the larger holes, then the average value for τ_3 should not change much. This results from the above mentioned hypothesis that the smaller eccentric holes would not be sampled as readily and the fact that the o-Ps probe preferentially samples large holes (regardless of eccentricity). If instead, the larger holes are preferentially becoming more eccentric relative to the smaller holes, then τ_3 should drop significantly which would be in diagreement with the experimental data.

To restate the *proposed* scenario, as the sample is oriented, some of the free volume is lost due to better packing. A distribution in eccentricity occurs with the smaller holes preferentially becoming more elliptical in shape relative to the larger holes. Because the volume of these holes decreases only slightly, then τ_s should also drop only slightly. To correct for the ellipticity, however, the experimentally measured τ_e, will decrease an even greater amount. Nonetheless, this large change in τ_e does not get detected experimentally since the small, highly elliptical holes are virtually undetectable by the o-Ps probe. Therefore, becauses these smaller holes are not sampled, their very low values for τ_e do not decrease the average τ_3 for the system. Where they do become noticed, however, is the decrease in I_3 since this is a measure of the *detected* hole concentration (and the small, highly elliptical holes are not detected).

Assuming that the above hypothesized model is true, the net result is that the changes in τ_3 and I_3 partially offset each other in such a manner that the standard, isotropic free volume measure of $\tau_3^3 I_3$ is still reasonably accurate when applied to unaged, oriented systems. For this reason and, based on the data in Figures 5.3-10 and 11, it will be assumed for the rest of this study that the effect of orientation on the PALS parameters is relatively small and can be neglected. Therefore it is assumed that one can treat $\tau_3^3 I_3$ as a measure of the free volume in a similar manner as is usually done for isotropic samples. Comparison with the rest of the experimental data seems to indicate that this is a reasonable assumption.

5.4.1.3 Interpretation of the Permeability Data

A comparison of the transport parameters shows that the permeability is in better agreement with ffv_{gc} (and density) whereas D is in better agreement with $\tau_3{}^3I_3$. The difference is mainly due to the minimum in the density data at low f which is undetected by $\tau_3{}^3I_3$. The solubility K is somewhere in between although inspection of Figure 5.3-7 would indicate that it is more sensitive to ffv_{gc} due to the slight "bump" in the K data at a value of f equal to 0.033.

The changes in D are similar to those seen by Wang and Porter[31] for polystyrene although not as large. The same hold true for P except for the presence of the maximum at low f. The biggest difference is in the solubility data where an increase is observed with orientation as opposed to a decrease. It is possible that this is due to inherent differences between the two polymers studied. Intuitively one would expect a decrease in K because of the loss of free volume however Vieth and coworkers[46] have found that orientation has little effect on solubility. This increase in K also contradicts Peterlin's assumption that K is proportional to the free volume.[23]

One approach for interpreting the increase in K with orientation is to apply the dual mode sorption theory.[19] It states that the penetrant molecules can occupy two distinct sites in the polymer, namely the matrix (i.e. absorption in interstitial sites between chains), and the free volume holes. The theory treats each of these sites as separate, but at equilibrium, with the hole adsorption being modeled by a Langmuir isotherm and the matrix absorption by Henry's law. At low pressures, as in this study, the two effects occur simultaneously resulting in an equation for the apparent solubility K

$$K = C'_H b_h + k^*_D \qquad (5.4\text{-}1)$$

where k^*_D is the Henry's law constant for dissolution in the amorphous matrix, C'_H is the Langmuir hole saturation constant, and b_h is the Langmuir or hole affinity constant. The increase in K with stretching must be due either to changes in hole adsorption ($C'_H b_h$), matrix absorption (k^*_D), or both occurring simultaneously. It is possible that k^*_D might

change significantly upon stretching due to the higher strain energy of the oriented state and/or the chain alignment. This would account for the fact that K is increasing even though free volume is decreasing. It is also possible that changes in hole geometry might affect $C'_H b_h$. For example, greater hole eccentricity will result in a larger surface area for adsorption, assuming a constant hole volume, and therefore an increase in C'_H. This would be partially offset, however, by the decrease in total free volume since fewer/smaller holes would be available for adsorption. It might also be possible that the higher strain energy state of the oriented chains causes an increase in b_h. This could be thought of as a change in hole "surface tension" causing the diffusant to more readily adsorb on the hole wall. Nevertheless, without knowing more about the free volume distribution, it is difficult to ascertain exactly what is the cause for this increase in K.

The diffusion coefficient is directly related to the molecular mobility although it remains to be determined which theory is best at describing its behavior. Values of $\ln(D)$ are plotted versus the inverse of $\tau_3{}^3 I_3$ in Figure 5.4-1. The best fit straight line, as per the Cohen-Turnbull theory, is also shown. The agreement is reasonably good indicating a correlation between free volume and D, although there does appear to be a small amount of unexplained curvature in the data.

In Figure 5.4-2, the data is compared with a modified form of the entropy correlation theory. Because the temperature dependence of D was not determined experimentally, it is impossible to extract the D_o data needed to compare with the *exact* form of the theory. Instead, as per El Hibri and Paul's method,[33] the log of the room temperature diffusivity D is plotted as a function of the stretching parameter defined in Equation (5.1-8). If the activation enthalpy is assumed to remain constant with stretching, the D_o and D will follow identical trends and the entropy correlation theory would be exact..

The stretch ratio Λ, which really implies the molecular stretch ratio, was assumed to be the macroscopic stretch ratio for the film. This only applies when relaxation during stretching is negligible. To check this, samples of stretched film were immersed in an oil

at 160°C to allow shrinkage to occur. Shrinkage recovery was greater than 99% for most film samples tested which indicates that the the macroscopic and microscopic stretch ratios are approximately the same.

Referring back to Figure 5.4-2, the data were found to follow the predictions of the modified entropy correlation theory as seen by the linear fit of the data. This indicates some form of correlation with the configurational entropy function. Nonetheless, the negative slope does not have a known physical basis. Of course, if one measures permeability along the stretch direction, then D is expected to increase with f and may properly correlate with the entropy correlation function. This directional dependence is an important feature which needs to be clarified further. Also, upon inspection of Equation (5.1-6), it is clear that the other parameters such as the jump interval λ and the geometrical parameter g, will also be changing with orientation and could have a profound impact of D as a function of f even though these parameters were not addressed in this study.

The modified entropy correlation theory provides a slightly better fit than the Cohen-Turnbull theory although both are acceptable. This may be a coincidence or it may be an indication that the two are somehow coupled. Both the entropy and free volume follow a similar trend with stretching which is not unreasonable since chain alignment, which causes the decrease in entropy, also causes the squeezing out of free volume. The fact that the Cohen-Turnbull fits the diffusion data for a wide range of polymers indicates that the importance of free volume cannot be ignored. Nonetheless, it is also possible to relate an increase in free volume to a decrease in activation entropy. For example, in the vicinity of a free volume site, the neighboring chains are able to rearrange in conjunction with the hole such that the number of possible configurations increases with the hole size. This is analogous to the entropy of an ideal gas increasing with the volume of the container. If one then assumes that an entropy barrier of height S_m must be overcome for a permeant molecule to make a jump, then an increase in free volume would increase the nominal entropy S_o. This effectively lowers the relative height of the entropy barrier $\Delta S=S_m-S_o$.

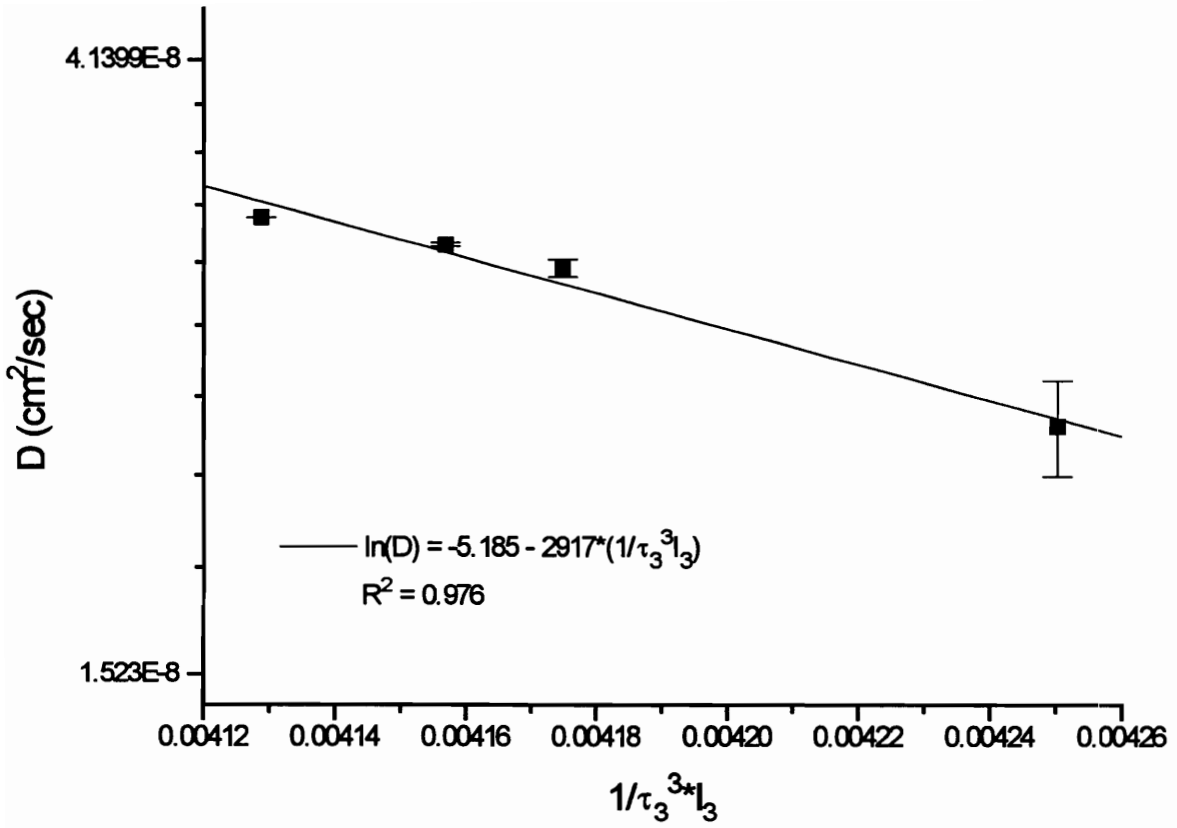

Figure 5.4-1. Ln(D) versus the inverse of the PALS free volume for unaged PC.

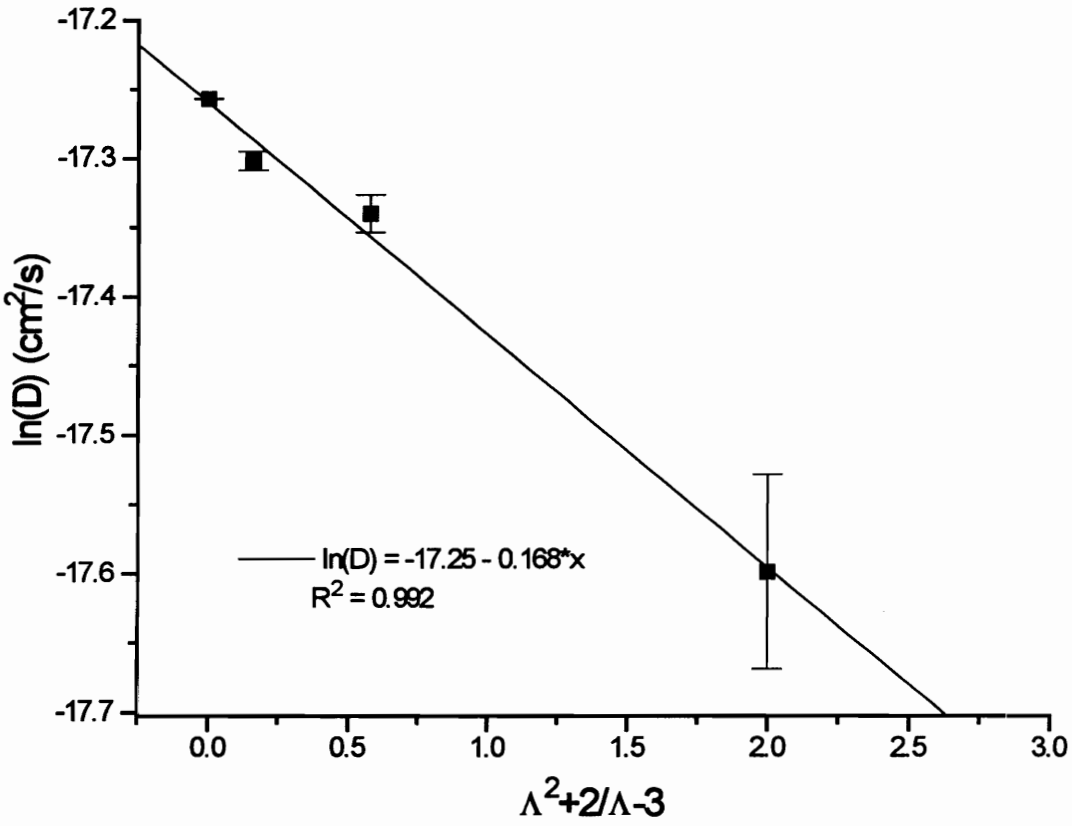

Figure 5.4-2. Ln(D) versus the stretch parameter for unaged PC.

Restated, as the free volume of a polymer increases, the effective entropy barrier will correspondingly decrease.

5.4.1.4 Effects of Orientation on Mobility

The diffusion data—along with the predictions of the Cohen-Turnbull and entropy correlation theory—indicate that mobility should decrease with orientation. This is in contradiction to the volume relaxation data for both PC and PS discussed in Chapter 3.0 but is in agreement with the thermodynamic and dynamic mechanical data in Chapter 4.0. For a truly accurate comparison to be made, however, the tensorial nature of the diffusion coefficient must be explored. The data presented only involves measuring D through the thickness of the film. Because of uniaxial symmetry, there is also an axial value of the diffusion coefficient denoted as D_{md} which will differ from the measured TD or thickness value, D_{td} (which equals D).

It was impossible with the equipment available to measure a value for D_{md}. It is expected that D_{md} will increase with f since the diffusing molecule would be traveling essentially parallel to the oriented chains. This is much less of a barrier than traveling perpendicular to an oriented, well packed set of chains. If values for D_{md} were available, it might be interesting to compare the volume relaxation data to some average or effective value for D. One example might be the first invariant of the diffusivity tensor, simply written as the sum of the diagonals or $D_{md}+2D_{td}$ (the factor of two occurring because the diffusion coefficients in the thickness and transverse directions are the same due to uniaxial symmetry). It would also be interesting to compare the anisotropic D values directly with the linear relaxation rates (from linear dilatometry) since both are tensors. At this point however, the transport data provides little useful information in explaining the enhanced volume relaxation with orientation.

5.4.1.4.1 Solid State NMR Testing

Work is currently in progress by Dr. Anita Hill and Dr. T. J. Bastow of CSIRO (Australia) to probe the molecular mobility as a function of unaged orientation in PC (same sample series as used in the PALS study) using solid-state NMR. At the time of this writing, the analysis was not complete so only preliminary results will be presented here. The details and final summary will be provided in a later report with only the preliminary findings discussed here.[47]

Solid state ^{13}C NMR relaxation time measurements were performed at 23°C using a Bruker 400 MHz spectrometer. Small pieces of the oriented samples were punched out of film stock, checked with crossed polars to verify that orientation was unaffected, and then randomly arranged in the sample test tube. The latter step was performed in order to average out the orientation effects of the sample during magic angle spinning.

The room temperature NMR data indicated a suppressed mobility—as determined from the T_{1_ρ} relaxation times — of the off-axis aromatic carbons with initial draw ratio followed by no further decrease in mobility with further stretching; however, the T_{1_ρ} relaxation times for some of the other carbons were not increased by stretching. In fact, the methyl carbons actually showed a slightly enhanced mobility with orientation. It is apparent that there are distributions of mobility for the individual carbons based on their environments[48] but, overall, the data can be used to suggest a mean reduction in the mobility with stretching. The data suggest that the polymer does not respond homogeneously to the hot-stretching which may also explain why different measurement techniques are indicating different trends in the mobility upon stretching.

5.5 Summary

A combination of PALS, permeability and (preliminary) SS-NMR measurements have been performed on a series of oriented bisphenol-A polycarbonate samples. While the data provided little insight into the enhanced volume relaxation rates with orientation reported in Chapter 3.0, it did help to elucidate changes taking place in the free volume. The PALS data showed no significant change in τ_3 with increasing f however I_3 did decrease montonically. There initially was concern that the formation of anisotropic holes during stretching might alter the PALS results and require a modified interpretation. There seems to be reasonable agreement, however, between the free volume calculated by density measurements using group contribution methods and $\tau_3^3 I_3$ from PALS.

Transport properties went through significant changes with orientation. The solubility was found to increase slightly with f in contrast to the decrease often seen in the literature. This was interpreted in terms of the dual mode sorption theory. The decrease in diffusivity D with orientation was found to correlate with the PALS fractional free volume $\tau_3^3 I_3$ using the Cohen-Turnbull theory. This was not true for the more commonly applied average hole volume determined from τ_3^3. In addition, D was found to correlate with the stretch ratio using the modified entropy correlation theory which indicates that configurational energy changes during stretching are enhancing the activation entropy barrier to diffusion. The fact that both the Cohen-Turnbull theory and the entropy correlation theory provided good fits to the data may indicate a correlation between changes in free volume and changes in the activation entropy barrier.

Limited solid state NMR data indicated that, in general, the localized molecular mobility decreased with stretching although it varies for different carbons in the chain. This variability may explain why different mobility measures used throughout this study provided different trends. It may be that each is probing different effective molecular motions for the PC chain. This is an area that definitely should be investigated further with work already underway to try and address these issues.

5.6 References

[1] L. S. Thomas and K. J. Cleereman, *SPE Journal 28,* 61 (1972).

[2] L. C. E. Struik, Physical Aging in Amorphous Polymers and Other Materials, Elsevier, New York, 1978.

[3] M. R. Tant and G. L. Wilkes, *Polym. Engr. Sci. 21,* 874 (1981).

[4] G. B. McKenna, *Comprehensive Polymer Sci, Vol. 2. Polymer Properties,* C. Booth and C. Price, Eds., Pergamon, Oxford, 1990.

[5] I. M. Hodge, *J. Non-Crystalline Solids 169,* 211 (1994).

[6] J. M. Hutchinson, *Prog. Polym. Sci. 20,* 703 (1995).

[7] A. D. Kasbekar, PhD Thesis, Duke University, Durham (1993).

[8] G. L. Wilkes, "Rheooptical Properties," in *Encyclopedia of Polymer Science and Engineering, Vol 14.,* John Wiley and Sons, New York, 542, 1983.

[9] R. S. Stein and G. L. Wilkes, "Physico-Chemical Approaches to the Measurement of Anisotropy," in *Structure and Properties of Oriented Polymers,* I. M. Ward, Ed., John Wiley and Sons, New York, 150, 1975).

[10] M. D. Zipper and A. J. Hill, *Materials Forum 18,* 215 (1994).

[11] A. J. Hill, *High Temperature Properties and Applications of Polymers and Polymer Composites,* M. R. Tant, H. L. McManus, and J. W. Connell, Eds., ACS Books, Washington, D.C. 1995.

[12] Y. C. Jean, *Advances with Positron Spectroscopy of Solids and Surfaces,* NATO Advanced Research Workshop, Varenna, Italy, July 16-17, 1993, 563.

[13] H. Nakanishi, S. J. Wang, and Y. C. Jean, *Intl. Symposium on Positron Annihilation Studies of Fluids,* S. C. Sharma Ed., World Scientific, Singapore 292, 1987.

[14] Y. C. Jean, *Microchem J. 42,* 72 (1990).

[15] Y. C. Jean and Q. Deng, *J. Polym. Sci. B-30,* 1359 (1992).

[16] Y. C. Jean and H. Shi, *J. Non-Crystalline Solids 172-174,* 806 (1994).

[17] Y. C. Jean, H. Nakanishi, L. Y. Hao, and T. C. Sandreczki., *Physical Review B 42,* 9705 (1990).

[18] Y. C. Jean, Y. Rhee, Y. Lou, D. Shelby and G. L. Wilkes, *J. Polym. Sci. B34,* 2975 (1996).

[19] H. B. Hopfenberg and V. Stannett, in *The Physics of Glassy Polymers,* R. N. Hayward, Ed., Halsted Press, New York, 504, 1973.

[20] *Barrier Polymers and Structures,* W. J. Koros, Ed., ACS Symposium Series, Washington, DC, 1990.

[21] S. A. Stern and S. Trohalaki, in *Barrier Polymers and Structures,* W. J. Koros, Ed., ACS Symposium Series, Washington, DC, 22, 1990.

[22] Y. Maeda and D. R. Paul, *J. Polym. Sci. B 25,* 1005 (1987).

[23] A. Peterlin, *J. Macromol. Sci., Phys. B11.* 57 (1975).

[24] R. E. Barker, R. C. Tsai, and R. A. Willency, *J. Polym. Sci.: Polymer Symposium 63,* 109 (1978).

[25] S. Glasstone, K. J. Laidler, and H. Eyring, *Theory of Rate Processes,* McGraw-Hill, New York, 516, 1941.

[26] Y. Ito, *Kobunshi Kagaku 19,* 412 (1962).

[27] M. H. Cohen and D. Turnbull, *J. Chem. Phys. 31,* 1164 (1959).

[28] J. S. Vrentas and J. L. Duda, *J. Appl. Polym. Sci. 22,* 2325 (1978).

[29] D. H. Weinkauf and D. R. Paul, in *Barrier Polymers and Structures,* W. J. Koros, Ed., ACS Symposium Series, Washington, DC, 1990.

[30] J. A. Barrie and B. Platt, *J. Polym. Sci. 54,* 261 (1961).

[31] L. H. Wang and R. S. Porter, *J. Polym. Sci., Poly. Phys. Ed. 22,* 1645 (1984).

[32] G. Levita and T. L. Smith, *Polym. Eng. Sci. 21,* 936 (1981).

[33] M. J. El-Hibri and D. R. Paul, *J. Appl. Polym. Sci. 30,* 3649 (1985).

[34] Y. Kobayashi, *et al., Polymer 35,* 925 (1994).

[35] K. Okamoto, *et al., Polymer J. 25,* 275, (1993).

[36] A. J. Hill, S. Weinhold, G. M. Stack, and M. R. Tant, *Eur. Polym. J.,* in press, (1996).

[37] Y. C. Jean, *et al., J. Polym. Sci. B33,* 2365 (1995).

[38] *Polymer Handbook,* J. Brandrup and E. H. Immagut, Eds., John Wiley and Sons, New York, 1975.

[39] W. Puff, *Comput. Phys. Commun. 30,* 359 (1983).

[40] E. Ito, K. Sawamura, and S. Saito, *Colloid and Polymer Sci. 253,* 480 (1975).

[41] D. W. Phillips, A. M. North and R. A. Pethrick, *J. Appl. Polym. Sci. 21,* 1859 (1977).

[42] E. Ito and T. Hatakeyama, *J. Poly. Sci., Polym. Phys. Ed. 13,* 2313 (1975).

[43] A. Bondi, *Physical Properties of Molecular Crystals, Liquids and Glasses,* John Wiley and Sons, New York, 1968.

[44] L. C. E. Struik, *Internal Stress, Dimensional Instabilities and Molecular Orientations in Plastics,* John Wiley and Sons, New York, 1990.

[45] M. I. Williams, R. F. Landel, and J. D. Ferry, *J. Am. Chem. Soc. 77*, 3701 (1955).

[46] W. R. Vieth, H. Acalay, and A. Frabetti, *J. Appl. Poly. Sci. 8,* 2125 (1964).

[47] M. D. Shelby, G. L. Wilkes, M. R. Tant, J. Zawada, T. J. Bastow, and A. J. Hill, to appear in *Polym. Prepr.*, April 1997.

[48] A. K. Roy, A. A. Jones, and P. T. Inglefield, *Macromolecules 19,* 1356 (1986).

6.0 SUMMARY AND CONCLUSIONS

6.1 Orientation and Physical Aging Rates

It has been shown that physical aging is significantly affected by the molecular orientation introduced by uniaxial (and biaxial) hot drawing followed by quenching. The magnitude of this effect depends on the method of measurement. For volume relaxation behavior, orientation enhances the volume relaxation rate in both PC and PS by 40 to 60%. This is true even though the oriented samples start at a slightly higher packing density (lower free volume) than the isotropic samples. Normally a lower starting free volume is expected to produce a slower aging rate although, experimentally, this was not the observed. Interestingly, the volume relaxation rate was not affected by the degree of orientation *for the range of f's studied*, but only by the presence or absence of orientation.

Separate measurements on the time dependent relaxation rate in the MD and TD directions showed that, during aging, the volume relaxation occurred almost solely along the MD or stretch direction. In the TD and thickness directions, the sample actually expanded over time. This suggests a scenario where the polymer chains are essentially being "reeled in" during aging while simultaneously being repacked into a denser configuration. However, since changes in f and sample length due to shrinkage were small, it is likely that this reorientation is only occurring on a local scale and is not due to long-range chain reptation.

For creep measurements, the mechanical shift rate dropped slightly with orientation while the effective retardation time decreased significantly. It is possible, although unlikely, that this decrease in μ with orientation is simply an artifact of the shrinkage process. If this were true, however, one would expect a monotonic drop in μ with stretch ratio since the shrinkage effect would increase accordingly. In addition, although the creep curves were corrected for shrinkage, the additional compliance change caused by

shrinkage might alter the characteristic shape of the compliance curve enough to perturb μ slightly. Nevertheless, the change in μ was small. In contrast, the significant drop in retardation time (increase in mobility), which was obtained from the shape of the compliance curves, is in qualitative agreement with the increased volume relaxation rates even though the two probably involve totally different effective relaxation time scales. Faster volume relaxation rates in the oriented samples imply more rapid molecular rearrangement and a shorter effective relaxation time. In the case of PS, the volume relaxation data also showed an induction time in the isotropic sample which dissappeared in the oriented samples. The presence of this induction period is consistent with long relaxation/retardation times.

Finally, the creep and volume relaxation data were combined into a parameter denoted as S, the volume sensitivity, which was found to be significantly lower in the oriented samples. As with the volume relaxation and creep data, it also did not change significantly with further orientation. This drop in S implies that the mechanical properties of an oriented specimen are less sensitive to a slight change in free volume than an isotropic sample. This is in violation of the free volume theory of mobility. A theory was also proposed in which the volume sensitivity is predicted to vary inversely with the conformer size. This follows from the fact that a larger conformer will require a greater amount of localized free volume for a single stress-relieving rearrangement/rotation to occur.

6.2 Orientation and Free Volume

A number of tests were also performed to determine the thermodynamic and free volume structure of the oriented, *unaged* state in order to better explain the unusual aging behavior just described. Except for a slight decrease at low f (i.e. $f = 0.03$-0.05), the density was found to increase linearly with increasing f. This and the fact that orientation has been shown to enhance mobility are also in direct contradiction with the predictions of the free volume theory.

Enthalpy recovery measurements of the unaged samples show that the change in internal energy with stretching is linearly correlated with the change in density (the internal energy decreases with increased stretching) and the energy at yield. This implies that the energy changes are a direct result of changes in free volume and interatomic distance. Comparisons of the data with rubber elasticity theory confirmed this finding.

The stretch-induced change in density was very small but did correlate well with the PALS-based free volume $\tau_3{}^3 I_3$. It is uncertain, however, how the effects of hole anisotropy might have affected the PALS data. The PALS data showed no change in average hole size (τ_3) with stretching but did show a decrease in the concentration (I_3) of free volume sites. This is significant in that utilizing $\tau_3{}^3$ as a measure of the free volume--as is often done in the literature--does not correlate with the free volume changes obtained by density for the oriented samples. This may be a result of the hole anisotropy or it may be because the volume changes occurring are very small. Nevertheless, the estimated level of anisotropy should cause a significant change in the value of τ_3 although this was not observed experimentally. In order to reconcile this difference, a scenario was hypothesized in which there is a distribution of hole eccentricities in the oriented state and where PALS is less sensitive to the more eccentric holes. For the PALS data to agree with the experimental data, however, it is important for the eccentricity to be predominantly in the smaller holes. The smaller, more eccentric holes would then become effectively invisible to the o-Ps probe thereby causing I_3 to decrease while simultaneously leaving τ_3 relatively unchanged. Of course, this scenario is based entirely on conjecture and more work is needed for verification.

6.3 Orientation and Transport Properties

Permeability and diffusion data in unaged PC showed some interesting, if not contradictory, trends as compared with the other measurements. The diffusion coefficient was found to decrease monotonically with increasing f whereas the solubility increased slightly. The permeability was found to correlate with the density, at first increasing slightly and then decreasing upon further stretching.

The increase in solubility is generally assumed to be a result of increased free volume, however, for the oriented samples, the free volume decreased with stretching. This discrepancy may be due to changes in dual-mode sorption behavior with orientation. Changes in the shape (and possibly the number) of free volume holes would affect how penetrant molecules are adsorbed. Similarly, the higher energy state of the oriented chains would affect how penetrant molecules could be adsorbed into interstitial sites (i.e. changes in effective surface tension).

The diffusion coefficient is commonly assumed to be proportional to the mobility which is precisely why it was utilized in this study. The monotonic decrease in D with increasing f indicates that mobility should decrease with stretching. Again, however, this is in contradiction to the experimental data where creep and volume relaxation data show a significant enhancement of the mobility upon stretching. Nevertheless, it is in agreement with the preliminary SS-NMR data which showed an effective decrease in localized segmental mobility. It is important to realize, however, that D is actually one component of a 2nd order tensor. Because of the anisotropy in the sample, there will be different values for D parallel and perpendicular to the stretch direction which has not been accounted for when relating to the mobility. Values for D along the stretch direction (which cannot easily be measured) are surely much higher than the isotropic D and might be the better predictors of the system mobility.

While the measured diffusion coefficients may not correlate with the mobility, they did agree with the predictions of both the Cohen-Turnbull (free volume) and a modified

form of the entropy correlation theories. The latter theory states that the barrier to diffusion for oriented samples is directly related to the stretch-induced change in configurational entropy. The fact that both free volume and entropy correlate with D suggest that the relationship between the two should be investigated further.

6.4 Orientation and Mobility

There is clearly a lot of conflicting data regarding how orientation affects mobility, both for the aged and unaged samples. As previously mentioned, the physical aging rate measurements indicate an enhanced mobility as compared with the isotropic control. In contrast, thermodynamic, activation energy, and solid-state NMR data point to a lower localized mobility. Dynamic mechanical measurements of the α' and β-transitions in unaged PC indicate that the relaxation strength is higher for the oriented samples relative to the isotropic control. As with the volume relaxation data, the relaxation strength was independent of f for the oriented samples. *This indicates that, even though the local mobility might be reduced in the oriented samples, the number of segments actively participating in the relaxation process is greatly increased.* Therefore the effective volume relaxation rate is higher.

Comparison of the dynamic mechanical data in the machine and transverse directions indicates a reduced relaxation strength (i.e. fewer segments participating in the relaxation process) in the TD relative to the MD although both are still higher than the isotropic control. This directional dependence of the relaxation strength also seems to correlate with the linear relaxation data from Chapter 3.0. There it was found that the linear relaxation rate was significantly higher in the MD relative to the TD. It is believed that this anisotropy in relaxation strength (and linear relaxation rate) is due to the anisotropic distribution of free volume. Why the relaxation strength is higher in the first place is still unknown. It is speculated that it is the result of residual stresses or a rejuvenation effect which somehow provides the segments with enough energy so that more of them undergo relaxation.

6.4 Implications of the Results

The results of this study are useful for both the engineer/designer and the polymer scientist. As is often the case, a designer must sometimes make decisions about a polymer long before the scientist completely understands the phenomenon in question. This is particularly true for physical aging. Even though the mechanism for physical aging is still not understood, there is enough data available for the designer to make appropriate decisions, *as long as the sample is isotropic*. Unfortunately, the same does not hold true for oriented samples even though many plastic articles contain some orientation.

While this study has not answered the question of "what causes physical aging?", it has provided a number of useful perspectives on the aging problem. This benefits the scientist. Simultaneously, this dissertation also provides useful data which can benefit the engineer by allowing him/her to properly account for oriented aging in product design. For example, the findings from the previous chapters have shown that the relative changes in mechanical properties during aging should not be significantly different than the isotropic samples (i.e. the change in μ was small) even though oriented samples undergo volume relaxation at a faster rate. Therefore, other than accounting for the inherent differences in properties due to orientation, the designer can treat the oriented samples the same as the isotropic samples in aging conditions where *mechanical* properties are important. In cases where *density related properties* such as refractive index, dielectric properties, etc. are important, the designer should be very careful in determining product lifetimes since properties may change more rapidly with time. Fortunately, oriented polymers are rarely used in these types of applications since thermal shrinkage and point-to-point variation in orientation can result in unacceptable variations in relevant properties (as for example with aberrations in polymeric lenses).

From a scientific standpoint, this study has raised a number of new questions about the nature of glasses while at the same time providing an entirely new perspective on the physical aging problem. It has also brought into question many common aging/mobility correlations commonly applied to isotropic systems. In particular, the mobility-free

volume relationships have been shown to be quite inadequate. Repeatedly, the oriented data have shown that mobility and physical aging rates were higher in stretched samples even though free volume was decreasing. To complicate matters further, the changes in free volume and mobility based on transport properties did not correlate with changes obtained by other measurements such as density, PALS and NMR.

In contrast, what did seem to correlate well was the entropy function. The results indicate that entropy barriers are at least part (if not all) of the cause for the unusual physical aging behavior occurring in the oriented samples. Consequently, if activation entropy barriers are affecting mobility/aging in oriented samples, they must also play a role in isotropic samples. Therefore, it is recommended that attempts to correlate aging behavior with structure be formulated in terms of entropic models (such as Adam-Gibbs or other cooperative motion models), with less emphasis being placed on free volume theories. In fact, the results of these studies suggest that free volume changes are more of an "effect" of the physical aging process rather than a "cause."

7.0 RECOMMENDATIONS FOR FUTURE WORK

While this study has answered many questions, it has also raised a number of new ones. It is clear that orientation affects the relaxation and physical aging behavior of amorphous polymers and this should be investigated further. In particular, future testing should be aimed at determining the mechanism responsible for the aging enhancement. However, because of the significant level of shrinkage that occurs, certain tests are not appropriate. In particular, creep and DSC (enthalpy relaxation) measurements have provided little useful data for the amount of effort required. Instead, testing should focus more on determining the polymer structure and relaxation dynamics via such techniques as NMR and IR spectroscopy. Additional dilatometric work is also in order. Some possible experimental approaches will now be discussed.

7.1 Advanced Dilatometric Studies

Dilatometry proved a very useful tool for studying the aging behavior in oriented systems. Future work should be directed toward a broader range of materials (both amorphous and semicrystalline) and a wider range of aging temperatures. Additionally, more "complicated" aging histories should also be investigated with the possibility of fitting the data to some of the multi-parameter kinetic theories available. Aging to equilibrium at temperatures close to T_g would help to determine if the equilibrium volume for oriented systems is different than for isotropic samples. This would also help to determine how much of a role shrinkage plays in the aging process. Finally, more linear dilatometric experiments--particularly T-jumps--should be performed to further elucidate the anisotropy of the relaxation process.

7.2 Aging at Different Stretch Conditions

This experiment would investigate how various orientation modes such as biaxial stretching and constrained uniaxial stretching would affect the aging behavior. It would

also be useful to compare this data with the PALS technique since the free volume hole geometry is likely to change. Another approach would be to try for even higher values of f in the uniaxial systems, than was obtained in the current study, by optimizing the stretch conditions. Finally, testing in uniaxial systems could be further extended to semicrystalline systems, however, both crystalline and amorphous orientation functions would have to be monitored.

7.3 PALS/Permeability Studies as a Function of Aging Time

These tests were performed in the current study but the data were erratic and should be repeated. The results should be compared with the unaged data to determine the correlation between free volume, aging time, and orientation. Tests at higher pressures as a means of analyzing the dual-mode sorption as a function of orientation and aging would also be beneficial.

7.4 Molecular Modeling Simulations

Molecular modeling simulations may help to explain the unusual relaxation behavior occurring in oriented systems. By simulating an oriented polymer chain, interactions could be studied and the effects on mobility determined. This should help to explain the enhanced mobility in oriented system.

7.5 Solid State NMR and IR Spectroscopic Studies

Additional NMR and IR spectroscopy should be applied to the oriented samples as a function of f and aging time to better understand the relaxation mechanisms in oriented systems. It would also be beneficial to compare hot and cold drawing by these techniques. It is important, however, for the anisotropic relaxation behavior to be taken into account. As with the molecular modeling, understanding the relaxation mechanism may explain the enhanced aging rates.

7.6 *Effects of Stretch Temperature on Aging Behavior*

The objective of this experiment would be to understand the transition between cold and hot drawn aging kinetics. Dilatometric (or other) tests would be performed on samples stretched at different aging temperatures above and below T_g. This could also be accompanied by linear dilatometric measurements to see if there is a difference in relaxation anisotropy between cold and hot drawn samples. Of course, the ultimate goal of this and the previous mentioned experiments is to understand why aging is enhanced in oriented samples.

VITA

Marcus David Shelby, son of Marcus Eugene and Linda (Baskett) Shelby, was born September 18, 1965 in Birmingham, Alabama. He attended Jefferson County Public Schools and was graduated from Shades Valley High School, Birmingham, in 1983. In September, 1983 he entered Auburn University where he studied mechanical engineering. He was awarded the degree of Bachelor of Science (cum laude) in December of 1986. In January, 1987 he began graduate studies in Materials Engineering, also at Auburn University, as a NASA Graduate Research Fellow with the Marshall Space Flight Center in Huntsville, Alabama. He worked in the area of polymeric composites studying new methods for nondestructive testing. He was awarded the degree of Master of Science in Materials Engineering in March, 1989. After graduation, he was employed with Eastman Chemical Company in Kingsport, Tennessee in the Packaging Research Laboratory. There he was involved in polymer processing, new material development, and package/processing design. In August of 1992, he went on an educational sabbatical from Eastman to pursue doctoral studies in chemical engineering at Virginia Tech. Upon completion of his doctoral studies, he will return to Eastman.